

Volume 76 Number 10

25 May 1999

# CURRENT SCIENCE



Optics of heterogeneous films  
Tobacco mosaic virus from tomato  
Archiving manuscripts

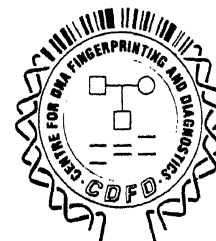
Current Science Association

Indian Academy of Sciences

# **CDFD**

**CENTRE FOR DNA FINGERPRINTING AND DIAGNOSTICS**

CCMB Campus, Uppal Road, Hyderabad 500 007, India



## **INVITES applications for STAFF SCIENTIST positions**

CDFD, an autonomous institution supported by the Department of Biotechnology, Government of India, is India's premier Centre providing services in areas of DNA Fingerprinting, DNA diagnostics and Cytogenetics. The Centre, recognized by the University of Hyderabad as a Centre for pursuing Ph.D. programme in all areas of life sciences, has well-furnished laboratories with strong Bioinformatics back-up and is the India-node for EMBnet. CDFD is now poised to initiate basic research in fields relevant to its objectives. The Centre invites applications from Indian citizens for STAFF SCIENTIST positions to lead independent research groups. Applicants must have an outstanding track record of scientific productivity, as evident from publications in scientific journals of high impact and/or international patents and some indication of independent scientific thinking. Applicants in the areas of Bioinformatics and Instrumentation should be prepared to shoulder primarily 'service' related responsibilities.

The level of appointment, starting from Assistant Professor equivalent, will depend on the length of experience and the quality of scientific productivity. Appointees will be tenured on the basis of their performance after the initial five-year period of contract appointment. CDFD will provide shared laboratory space and initial intra-mural funding. Hyderabad is India's fastest growing metropolis with excellent civic and infrastructural amenities. CDFD is expected to move to its own campus by 2002 where housing would be available for a few scientific personnel. During the interim period, the Centre would assist in providing a leased accommodation to outstation scientists. Applications on plain paper including detailed CV, copies of best publications, a tentative research plan, names, addresses, e-mail, fax/tel. numbers of at least three referees should be sent to the Director, Centre for DNA Fingerprinting and Diagnostics, House No. 12-13-414/1, Sai Nilayam, Street No. 1, Tarnaka, Hyderabad 500 017, India (<http://salarjung.embnet.org.in>). Applicants already working in Government funded institutions in India must send their applications through proper channel.

# CURRENT SCIENCE

## Editors:

Prof. P. Balaram  
Prof. S. Ramaseshan

## Editorial Office:

### *Current Science*

P.B. No. 8001  
Sadashivanagar P.O.  
C.V. Raman Avenue  
Bangalore 560 080  
Phone : 91-80-334 2310  
Fax : 91-80-334 6094  
E-mail : [currsci@ias.ernet.in](mailto:currsci@ias.ernet.in)  
Website : <http://tejas.serc.iisc.ernet.in/~currsci/index.html>  
<http://144.16.79.155/~currsci/index.html>  
<http://ces.iisc.ernet.in/curscinew>  
<http://144.16.65.194/curscinew>

## Subscription

|                                   | <i>Personal</i> | <i>Institutions</i> | <i>Industries</i> |
|-----------------------------------|-----------------|---------------------|-------------------|
| India                             | Rs 200          | Rs 500              | Rs 700            |
| SAARC                             | US \$10         | US \$30             | US \$50           |
| All other countries<br>(Air Mail) | US \$50         | US \$200            | US \$200          |

Single copies other than special issues: Rs 75/US \$15

## Advertisement tariff

|              |   |                 |                    |
|--------------|---|-----------------|--------------------|
| Back cover   | : | B&W Rs 10,000/- | Colour Rs 15,000/- |
| Inside cover | : | B&W Rs 7,000/-  | Colour Rs 12,000/- |
| Inside page  | : | B&W Rs 5,000/-  | Colour Rs 10,000/- |
| Half page    | : | B&W Rs 3,000/-  | —                  |

## Notice to authors

Manuscripts submitted to *Current Science* should adhere to length specified below. Those which do not conform to the length will be returned for condensing.

|                                 |   |
|---------------------------------|---|
| Correspondence                  | Less than 600 words; short letters preferred                                      |
| Commentary/Opinion              | Less than 1500 words  |
| Research News                   | Less than 2000 words; display items should be restricted to 2 Figures and 1 Table |
| Scientific Correspondence       | Less than 1500 words and 2 display items  |
| General Article                 | About 4000 words; 6 display items   |
| Review Article/Research Account | About 6000 words; cited references should be limited to 100                       |
| Research Article                | About 4000 words  |
| Research Communication          | About 2000 words  |
| Book Review                     | Less than 1500 words  |

# CURRENT SCIENCE

Volume 76 Number 10

25 May 1999

1286 In this issue

## EDITORIAL

1288 Peer review, P. Balaram

## CORRESPONDENCE

1290 Nuclear tests, R. Balasubramanian, Rajeeva L. Karandikar and M. S. Raghunathan ■ 1291 *Current Science* – The vital link, Vas Dev ■ 1291 Strategy for promoting science, M. Periasamy ■ 1292 An easy entry to Ramanujan's magnificent mathematical palace, N. R. Ranganathan

## NEWS

1293 IIT Delhi hosts Henry Ford Chair ■ 1293 Seminar on 'science and the media', K. Manjula ■ 1294 Biogeochemistry of the Arabian Sea: Modelling and synthesis, P. S. Swathi

## RESEARCH NEWS

1295 Search for an individual in the midst of a crowd: Tracking a single molecule  
Dipankar Chatterji

## OPINION

1296 Survey of India maps: (Ir)rationality about restricted maps, S. M. Mathur ■ 1297 Futile exercise in thought control, S. R. Valluri

## SCIENTIFIC CORRESPONDENCE

1299 Novel, cost-effective method of archiving manuscripts, Sangeetha Menon and George M. Williams ■ 1301 Why does river Brahmaputra remain untamed? K. S. Valdiya ■ 1305 Avifauna of Mouling National Park, Arunachal Pradesh, India, A. K. Sen and S. K. Mukhopadhyay ■ 1308 Molecular markers for genetic fidelity during micropropagation and germplasm conservation? P. K. Gupta and Rajeev K. Varshney

## SPECIAL SECTION: OPTICS OF HETEROGENEOUS MEDIA

1311 Photonic gap materials  
J. B. Pendry

1317 Nonlinear optics of periodic and quasiperiodic structures  
S. Dutta Gupta

1324 Pearls and shells  
M. S. Giridhar and S. K. Srivatsa

1325 Diffraction in heterogeneous liquid crystals  
K. A. Suresh, G. S. Ranganath and M. S. Giridhar

1330 Life before mean free path  
N. Kumar

1334 Imaging through turbid media  
Hema Ramachandran

1341 Tissue optics  
P. K. Gupta

1348 Moonstones  
M. S. Giridhar and S. K. Srivatsa

- 1349 **Photonic crystals**  
G. S. Ranganath

GENERAL ARTICLE

- 1351 **Turmeric – Nature's precious gift**  
N. M. Khanna

REVIEW ARTICLE

- 1357 **Improvement in nitrogen use efficiency: Physiological and molecular approaches**  
Yash P. Abrol, Sukumar R. Chatterjee, P. Ananda Kumar and Vanita Jain

---

RESEARCH ARTICLE

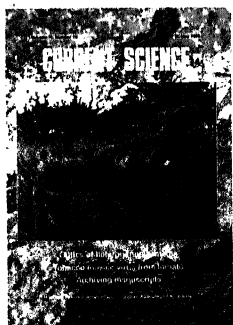
- 1365 **Expression of anthocyanin pigmentation in wheat tissues transformed with anthocyanin regulatory genes**  
H. S. Chawla, Leslie A. Cass and J. A. Simmonds

RESEARCH COMMUNICATIONS

- 1371 **Quantum signature of the classical chaos in the field-induced barrier crossing in a quartic potential**  
P. K. Chattaraj, S. Sengupta and A. Poddar
- 1376 **Multicomponent coordinated defence response of rice to *Rhizoctonia solani* causing sheath blight**  
S. Bera and R. P. Purkayastha
- 1384 **Characterization of tobacco mosaic virus isolated from tomato in India**  
Shoba Cherian, Jomon Joseph, V. Muniyappa and H. S. Savithri
- 1388 **Serotyping of foot-and-mouth disease virus from aerosols in the infected area**  
V. V. S. Suryanarayana, Pradeep Bist, G. R. Reddy and L. D. Misra
- 1391 **Identification of alpha-terthienyl radical *in vitro*: A new aspect in alpha-terthienyl phototoxicity**  
Manish Nivsarkar
- 1393 ***Erratum*: Crystal structure of the peanut lectin–T-antigen complex. Carbohydrate specificity generated by water bridges**, R. Ravishankar, M. Ravindran, K. Suguna, A. Surolia and M. Vijayan [*Curr. Sci.*, 1997, 72, 855–861]

BOOK REVIEWS

- 1394 **The Collected Papers of Albert Einstein – Volume 8 – The Berlin Years: Correspondence, 1914–1918**, reviewed by N. Mukunda
- 1395 **Annual Review of Plant Physiology and Plant Molecular Biology 1998**, reviewed by S. K. Sopory
- 1397 **Annual Review of Immunology 1998**, reviewed by Dipankar Nandi



COVER. IRS-1D image of the Brahmaputra valley and adjoining hills. See page 1301.

Indexed in CURRENT CONTENTS/GEOTitles/Chemical Abstracts

The editors thank Prof. G. S. Ranganath, Raman Research Institute, Bangalore for agreeing to be guest editor for the special section.

Single copy of this issue, Rs 150/US \$20

## In this issue

### Quantum signature of classical chaos

Chaos is considered to be one of the major scientific discoveries in recent times. It is concerned with rather complicated behaviour associated with nonlinear dynamical systems and one of the important features of a chaotic system is a sensitive dependence of its evolution on the initial conditions. While chaos has been studied extensively in classical systems, recently, there has been an upsurge of interest in investigating the quantum dynamics of classically chaotic systems. In this issue, Chattaraj *et al.* (page 1371) present a study of the quantum domain behaviour of a classical double well oscillator (corresponding to a quartic potential) which exhibits chaos in the presence of an external monochromatic field. The study has been based on the hydrodynamical model of quantum mechanics, the so-called quantum fluid dynamics and quantum theory of motion, pioneered by David Bohm and others, which provide a 'classical-like' prescription for the description of a quantum system. The so-called 'Bohemian' trajectories are obtained by integrating the velocity field defined in terms of the gradient of the phase part of the wavefunction. Through the classical as well as quantal phase space portraits based on these trajectories, the authors have arrived at important conclusions about the quantum-classical correspondence of chaotic systems. They demonstrate that while quantum effects suppress the classical stochasticity, classical chaos generally enhances quantum fluctuations.

Swapan K. Ghosh

### Symptom or sequence?

The article on 'The characterization of tobacco mosaic virus isolated

from tomato in India' by Shoba Cherian *et al.* (page 1384), is the first report on the genomic characterization of an Indian isolate of a tobamovirus. The authors have analysed a tobamovirus isolate infecting tomato in Karnataka. This virus was hitherto considered to be tomato mosaic virus (ToMV) and not tobacco mosaic virus (TMV) based on local lesion assay. The virus under study produced local lesions on *Nicotiana sylvestris* like ToMV whereas TMV causes systemic infection on this host. The authors constructed a cDNA library and sequenced a 1 kb fragment from the 3' terminus of the viral genome. Surprisingly, careful alignment of the nucleotide and amino acid sequences with other tobamoviruses, showed greater homology with TMV than with ToMV. Therefore, they concluded that it is a strain of TMV infecting tomato. The question arises as to how this strain of TMV manages to produce local lesion symptoms like ToMV. This paper clearly demonstrates the power of sequencing and sequence alignments to finetune the classification of a virus.

R. Usha

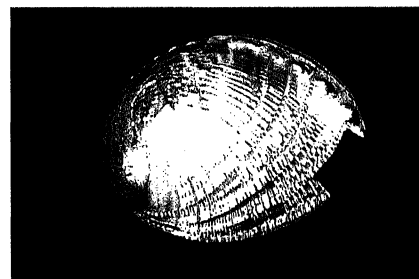
### Optics of heterogeneous media

Nature is spectacular when it comes to colours. Her visible beauty has attracted the attention of not just poets but also of scientists. Surprisingly, more often this coloration is due to an optical heterogeneity present in the system exhibiting the colour. In point of fact, opals, moonstones and the wings of butterflies owe their colours to the structural heterogeneity present in them. Naturally the scale of heterogeneity varies considerably from system to system. It could be either on a scale comparable to the wavelength of light or be very different

from it. In the latter case we have two sub-classes depending upon whether the scale of heterogeneity is very large or very small compared to the wavelength of light. Each of these cases leads to its own special optical effects. To illustrate this point, we mention here that the beautiful iridescence of an opal or the lustre of a pearl is due to a periodic structure on a scale comparable to the wavelength of light. On the



Opal polished



Iridescent shell

other hand, the whiteness of marble is due to a random collection of crystallites of calcium carbonate with a heterogeneity on a scale larger compared to the wavelength of light. As an example of greater relevance to human beings we may mention here that the turbidity of a swollen pathologic cornea or that of cataractous eye lens arises from random variations in refractive index on

a scale comparable to or larger than the wavelength of light.

This rich class of naturally existing optically heterogeneous materials has been enriched further by man-made materials. Also, in recent times, more fascinating optical properties of such systems have been unravelled. The articles appearing in this special section present different facets of this fast growing area of research. Each article highlights the present status, in addition to discussing optical effects associated with the heterogeneous medium under consideration. We have articles covering periodic, quasi-periodic and random media, and this presentation includes all possible situations. Pendry's article discusses photonic gap materials *per se*. This is followed by a review on nonlinear optics in a quasi-periodic structure by Dutta Gupta. Next we have a brief review by Suresh *et al.* dealing with diffraction in periodic and ran-

dom liquid crystals. The paper by Kumar addresses itself to mirror-less lasing in random media. Following this is an article by Ramachandran on transmission in turbid media. To emphasize the medical implications of this subject, we have a paper by Gupta on tissue optics.

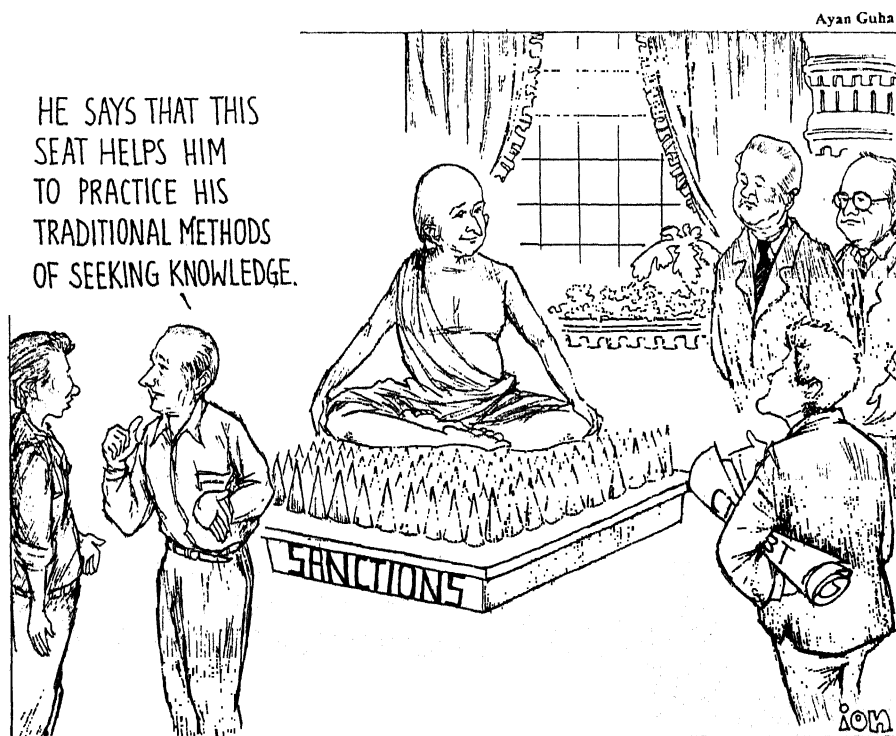
These topics do not exhaust all the important and interesting phenomena seen in heterogeneous media. In this hot topic of research every now and then something new is reported in literature. For example, three years ago it was demonstrated<sup>1</sup> that light propagation in a random medium exhibits an optical analogue of the familiar Hall effect. It was shown that the diffusion of light in a random medium in the presence of an external magnetic field leads to the appearance of light diffusion in a direction perpendicular to both the magnetic field and the direction of incidence of light. The direction of this transverse diffusion is decided

not only by the nature of the particles constituting the medium but also by the direction of the magnetic field. More recently<sup>2</sup> even an optical analogue of magnetoresistance has been demonstrated. On the materials front, in 1998 alone many new photonic crystals were discovered and many more fabricated thus adding to the ever growing list. Since I felt that these new photonic gap materials would be of interest even to a general reader, I have tried to cover some of them in my article 'Photonic crystals'. All in all an attempt has been made to stimulate the reader's interest in this current area of intense research.

Rikken, G. L. J. A. and van Tiggelen, B. A., *Nature*, 1996, **381**, 54-55

Sprenberg, A., Rikken, G. L. J. A. and von Tiggelen, *Phys. Rev. Lett.*, 1997, **79**, 757-760.

G. S. Ranganath



# CURRENT SCIENCE

Volume 76 Number 10

25 May 1999

## EDITORIAL

### Peer review

The noun 'peer' (in the context of science and evaluation) is defined by the *Oxford Dictionary* as 'one equal in civil standing or rank; equal in any respect'. Among scientists the term 'peer review' is often the subject of much discussion. Artists, musicians, authors and poets are evaluated by their public following, who do not usually pretend to any special skills necessary for sitting in judgement. In fact, specialist critics who write in the literary sections of newspapers and magazines can be devastatingly critical, without having the slightest influence on the public perception of an author's work (and most importantly on the sales of a new book). But in science, matters are different. Scientists invariably pride themselves that they are evaluated by their 'peers'; and not by a public mass, ignorant of the subtleties of their craft. Science has become so specialized that many scientists are firmly convinced that anyone who does not belong to a specific sub-discipline is hopelessly incapable of making any meaningful judgement. 'Peer review' is the accepted norm and is a process which permeates every area of scientific activity, including evaluation of papers for publication, grants for funding and decision making on awards and rewards of every kind. In evaluating academic scientists for promotion, their performance is almost always judged by peers; immediate superiors are expected to play only a minimal role. The composition and constitution of peer groups thus, assumes very great significance. An intriguing feature of scientific activity is that many scientists reach a stage where they seem to be on both sides of the fence; one day they are the judges, while on the next they are supplicants. Indeed, the only members of peer groups who do not seem to have a substantial conflict of interest are scientists, who have retired from active science, but are still highly visible on evaluating committees. Since peer decisions impinge on every aspect of a scientist's professional life, it is not surprising that most researchers have a very strong view on the practice of peer review.

The editorial offices at science journals are usually caught in the crossfire between authors and referees. Most authors (probably, rightly) are convinced of the merit of their work and the lucidity of their presentation. Many respond in a positive manner to criticism of their manuscripts by referees and indeed even acknowledge reviewers in their final published work. Some are overly sensitive and often trigger a duel with referees in which the editorial office acts as a passive spectator (and facilitator). Authors who are most sensitive to criticism are often the most critical of referees, themselves. Woe betide the editor who accepts a paper against their recommendation. In discussing Third World science (and publications) there has been some debate on whether the process of peer review (which of course, includes editors) at Western journals is biased against authors from developing countries. Western editors strongly deny any bias and there is ample evidence that the best of Third World research still appears in top ranking Western journals, suggesting that geography and national origin may not unduly influence the peer review process.

The peer review process in our journals (*Current Science* is a prime example) is also the target of sniping. A recent (unfortunately, anonymous) letter is from a disgruntled reader (fellow scientist and presumably sometime author) who criticizes a published paper, charging editors with using 'mediocre referees' who allow poor papers to appear in print. He attacks referees and charges them with prejudice: *'It is well known to the whole world that many referees of Indian journals are a prejudiced, lazy lot who often do not bother to read critically the manuscript sent to them spending time and energy, but pass a manuscript as suitable for publication merely on the basis of the institution from where it comes. For instance, if a paper is from one of the Central government supported institutes, then even without reading the article carefully, it is passed for publication. ... But the same hypocritical referee may retain a*

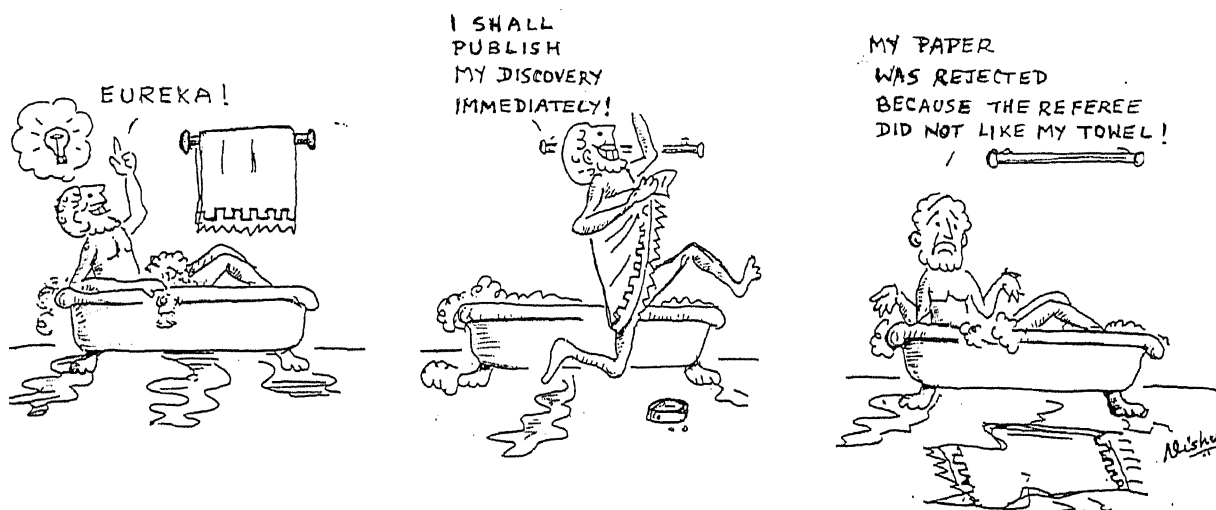
*well written article of international standing coming from a less known institution or student of science, for months and years together without commenting and finally under pressure from the author (routed through the editor of the journal of course, because the referee is kept anonymous), sends back the manuscript after making some silly comments, concluding that it is not fit for publication.'* Harsh words, indeed, but have not the same thoughts crossed our minds when manuscripts are returned after apparently superficial and frivolous review. Our anonymous correspondent offers to reveal his name, provided the veil of anonymity is lifted from referees also. Journals the world over have debated the issue of anonymous reviewing, but the vast majority of the most prestigious publications have not come up with a superior alternative.

In the case of grants (and many awards) peer review procedures are often more transparent. Even though anonymous referees reports are sought, most often the

decision making is done by committees, whose membership is no secret. Here the 'peers' are out in the open, but the rumbles of discontent with the system are no less. The problem of course, is that even collective decision making is subjective and for every winner there are several losers.

The peer review process is unique to scientific activity and sometimes the 'peer groups' can be separated by continents. Citation analyses can often reveal transnational groups; clusters of geographically separated scientists who work in the same area and are fully aware of each others work. Indeed, editors often choose referees by scanning reference lists, although this primitive practice is being replaced by computerized databases of potential 'peers'. Despite all its obvious imperfections it is unlikely that peer evaluations are likely to be replaced by a radically new system.

P. Balaram



## Nuclear tests

Ever since India carried out the Shakti series of nuclear tests in May 1998, several letters appeared in various newspapers, magazines and journals including *Current Science* expressing criticism. These perhaps give the impression that the scientific community as a whole is opposed to the tests. We do not think that this is really the case: in fact we believe that there is a substantial body of scientists who subscribe to the views we express below.

In an ideal world, no one would have any nuclear weapons, and any nation that initiates the process of nuclear weaponization can rightly be condemned as a 'rogue nation'. However, given that five nations have arrogated to themselves the right in perpetuity to remain as the only nuclear nations, it seems to us somewhat strange that people from this country should join the chorus of hypocritical condemnation by the West and the Chinese of India's nuclear tests; the more so when these voices were far from heard when tests were carried out by France and China before they acceded to CTBT. Some of the more objective criticisms directed against the Indian tests stem from one or more of the following premises.

**Premise No. 1.** Before May 1998, India was in a strong moral position by refusing to sign the NPT and CTBT, and at the same time, refraining from carrying out any more tests in spite of its 'proven' nuclear capability. By conducting the second round of tests in 1998, India has forfeited its position of moral superiority.

There is little evidence that our earlier non-testing had the kind of impact suggested in this argument. The so-called moral superiority of India seems to us at best an Indian perception, perhaps no more than a comforting myth. In any case, this moral superiority does not translate into any ability to influence the world at large: we lost out to Japan, a G7 nation, in our bid to get a non-permanent seat in the Security Council before the nuclear tests. While many of us in India may pride ourselves on our restraint after the test in 1974, as an outcome of a principled policy, it is

far from clear that such a view is shared by the international community. Our restraint has been, more often than not, perceived as the result of weaknesses – economic, scientific, technological, as well as political. We should also not read too much into the fact that various nations voted along with the USA and UK in condemning our tests. The same countries were earlier coerced into signing the NPT and CTBT, whose discriminatory aspects they were well aware of; thus it is not surprising that these countries voted to censure India, a vote which costs relatively nothing. Need we be overly sensitive to moral pronouncements made at international fora that have virtually endorsed the recent Anglo-American actions in Iraq.

**Premise No. 2.** India's relations with its two major neighbours, namely, Pakistan and China were slowly improving. However, ever since the tests, the relations have become strained, and any chance of a permanent lasting peace has been lost.

In the immediate aftermath of the tests our relations with Pakistan no doubt suffered a set-back, but after the recent initiatives it would appear that any lost ground has essentially been retrieved. The fact that the two countries have to deal with each other now as nuclear weapon states need not affect adversely any move towards a more friendly relationship. China has actively contributed to the deterioration of our security environment even if there may be some merit in suggesting that this need not have been emphasized as the reason for our nuclear tests. There seems to be an exaggerated concern among some of our more articulate compatriots about Chinese sensitivities, but they do not seem to be unduly worried about Chinese disdain for Indian perceptions and interests. Improvement in relations cannot be on the basis of unilateral concessions. In any event things definitely seem to be improving (see *The Hindu*, 3 March 1999 or *India Today*, 8 March 1999).

**Premise No. 3.** To facilitate the efficient and deliverable deployment or/and

to prevent any accidental deployment of nuclear weapons, we need to have an extremely efficient Command, Control, Communication, and Intelligence system.

If we need 'an extremely efficient C<sup>3</sup>I system', we will develop one. Moreover, such a C<sup>3</sup>I system is needed in any case, whether the weapons of our armed forces are nuclear or non-nuclear. Thus the need to develop a C<sup>3</sup>I system cannot be used as an argument against the induction of nuclear weapons.

**Premise No 4.** A poor country like India cannot afford the huge expenditure. The cost of weaponizing our nuclear capability has been put at Rs 50,000 crores over 10 years invested in weaponization.

Two points need to be made here. (i) The estimate of Rs 50,000 crores includes Rs 20,000 crores for four nuclear-powered submarines, which are a side issue to nuclear weaponization. In other words, India will have to opt for nuclear-powered submarines, even if they carry only conventional, non-nuclear weaponry. (ii) Rs 50,000 crores over ten years is Rs 5,000 crores per year, or a 10% increase in the defence expenditure, assuming no matching reductions in conventional forces. An important reason why US, Russia and other P5 nations went in for nuclear weapons in a big way is the perception that nuclear weapons are cheaper than conventional weapons for the same level of deterrence. Even if one were to assume that no money will be saved otherwise, an increase of 10% of our defence budget, which translates into an additional 1.5% increase in the overall budget, or 0.1% of the GDP, is easily justifiable in the context of national security. The US spends 4% of its GDP on defence, though it has two oceans on the east and west, and two weak neighbours to the north and the south. China and Pakistan spend even more on defence, as a percentage of the GDP.

Summarizing, we would like to say that nuclear testing and weaponization are the realistic responses that this country needed to make in the context

of our security environment and the self-seeking totally discriminatory nuclear weapons regime that the P5 nations seek to impose on the world. If deterrence is good enough reason for the five to expand and improve their already elaborate nuclear arsenal, it is an

equally good reason for India to test and weaponize.

R. BALASUBRAMANIAN\*  
RAJEEVA L. KARANDIKAR\*\*  
M. S. RAGHUNATHAN†

\**Institute of Mathematical Sciences,  
Chennai 600 113, India*

\*\**Indian Statistical Institute,  
Delhi 110 016, India*

†*Tata Institute of Fundamental  
Research,  
Mumbai 400 005, India*

## Strategy for promoting science

This is with reference to the editorial 'Strategic follies' (*Curr. Sci.*, 1999, **76**, 712), referring to the Government of India's decision to give higher pay to DRDO scientists and institute a set of handsome annual awards for development of defence-related technologies. The editor discussed the 'wilful neglect' of other sectors and also the decline (and fall) of science departments in Universities and concluded, 'while there appears to be some limited appreciation of what constitutes "strategic science" there is in fact no clear strategy for promoting science'.

Unfortunately, no one seems to know the strategy to promote science. Perhaps, one can deduce something from the demand of the society. The demand for engineering college admissions nowadays is due to the belief that one can earn a decent living if he/she becomes an engineer. Also, the interest in degree courses in biotechnology, organic chemistry, etc. indicates that the public is more interested in

job-oriented courses. Hence, the science administrators and educationists should devise strategies so that the degree courses in traditional science subjects (physics, chemistry, and biology) are oriented more towards application and technology development.

The scientists working in the DRDO, DAE and ISRO demonstrated that they could do good work to benefit the country and the government instituted handsome reward schemes for them. However, research in basic sciences is somewhat individualistic in nature and hence more diffused. Therefore, the achievements of basic scientists are not that spectacular, especially in India where the support for basic research is meagre. However, it is always refreshing to hear statements from the basic scientists to the effect 'scientific research is at its best when it is useful' and 'it is a great satisfaction to a scientist when the society finds his work useful'. So, instead of having a pessi-

mistic outlook that their research efforts do not have social relevance, senior basic scientists in India should come forward to orient their research work more towards solving problems faced by the industries/society. This is not a very difficult proposition. For instance, in the 1980s, a retired basic scientist was running from pillar to post to set up a silicon manufacturing unit based on his research work. Surely, having such scientists in our midst should boost the morale of young scientists. Perhaps, the strategy to promote science in India should be to institute handsome reward schemes to appreciate the efforts of such scientists so that all basic scientists will come forward to orient their research towards problems of interest to industries/society.

M. PERIASAMY

*School of Chemistry,  
University of Hyderabad,  
Central University P.O.,  
Hyderabad 500 046, India*

## Current Science – The vital link

Information, education and communication (IEC) are the key elements for human resource development and its optimal utilization. In this very context, *Current Science* is rendering yeoman's service to the scientific fraternity. This very periodical has come a long way in its metamorphosis to its present form. Yet education is a continuing process and there is further scope for its development to cater to the need of younger

generations at the turn of the century. I have been personally subscribing for this journal for over a decade and have immensely benefitted being located in a tribal pocket of Assam. I take pride to congratulate the editorial board for their painstaking job in keeping pace with the flow of manuscripts and maintaining its periodicity intact. In response to the editorial by P. Balaram (*Curr. Sci.*, 1999, **76**, 615–616), I suggest that in

keeping with the truly multidisciplinary nature of the journal, efforts should be made to solicit articles from disciplines other than Biological Sciences (most contributions being from this field), viz. Chemical Sciences, Engineering Sciences, Physical Sciences, etc.

Further, select news/articles may be reproduced from leading international journals. There is a definite need to improve the quality of reproduction of

B/W figures and its spacing in the text. Long-winded articles are indeed a distraction and should be clearly avoided.

A drive should be launched for advertisements, particularly placements/scholarships in India/abroad for fresh

graduates. This would increase readership among younger generations and elicit interest in basic sciences.

Lastly, I personally feel much comfortable reading a page printed in tri-columns than bi-column pattern.

VAS DEV

*Malaria Research Centre (ICMR),  
P.O. Sonapur, Kamrup District,  
Assam 782 402, India*

## An easy entry to Ramanujan's magnificent mathematical palace

Two revelations struck me after reading carefully K. Murugesapillai's review of the book *Srinivasa Ramanujan: A Mathematical Genius* (*Curr. Sci.*, 1999, **76**, 697). The first is that he holds the view that too much importance is given to the role played by G. H. Hardy and others in enabling Ramanujan to become a great mathematician. This view is certainly unorthodox and even original. Murugesapillai has gone one step further (see *Curr. Sci.*, 1998, **75**, 326–327) by writing that all the available biographical literature on Ramanujan does not do justice to the greatness of Ramanujan as a mathematician, who appears only once in a while and he feels that since Ramanujan was born with a 'mathematical spoon', his genius would have flowered even in India. However, I feel that he should substantiate his views by writing perhaps a long essay on how Ramanujan would have developed as a mathematician since he was living in grinding poverty, in contrast to C. V. Raman, Satyendra Nath Bose and others. In the life of every genius, certain apparently trivial incidents do tend to trigger a sequence of events which enable him to realize his full potential. In my view, Hardy's response to Ramanujan's letter is one such incident. It is for Murugesapillai to prove otherwise. It is worth remarking here that we live our lives only once and despite infinite possibilities, our lives trace out particular paths. If Ramanujan had not gone to Cambridge, he would have led a life of misery and poverty and one may even conjecture that he

would have ended his life by committing suicide!

The second revelation is that the author of this book, Srinivasa Rao, has done a remarkable job in writing it despite his lack of training as a pure mathematician. His researches on the relation between hypergeometric functions and quantum theory of angular momentum led him to get acquainted with some aspects of Ramanujan's work. This aroused his curiosity to know more about Ramanujan. The advent of the birth centenary of Ramanujan (in 1987) and the worldwide celebrations of the event in the form of symposia exposed Srinivasa Rao to the immense contributions Ramanujan had made to the world of mathematics. This book is the result of a labour of love over a decade. Since the birth centenary, numerous books, conference proceedings, and even a journal called the *Ramanujan Journal* have appeared satiating all except the serious mathematicians who are involved in the topics related to Ramanujan's conjectures and results and often one is engulfed in a feeling of *deja vu*.

Stirred by the harsh remarks of Murugesapillai on Srinivasa Rao's book on Ramanujan, I read the book carefully. In my opinion, the book provides an easy access to all the known source materials relating to Ramanujan's life as well as to his enormous achievements. One should remember that Srinivasa Rao's aim is to convey and share his joy of discovering the incredible mathematical achievements of Ramanujan to the

coming generations. None can deny that Srinivasa Rao has succeeded in this. One of the attractive features of the book is that it contains all the struggles of Ramanujan in becoming a mathematician. The book contains even a list of websites relating to Ramanujan. For those interested in getting to know more about Ramanujan, these will be really useful. Another noteworthy aspect of this book is that Srinivasa Rao has taken great pains to give credit to all those who have struggled to keep the memory of Ramanujan alive despite severe lack of financial and administrative support. In my opinion, there is nothing wrong in retelling the story of Ramanujan at several levels – from the profound to the popular – just like our epics, the *Ramayana* and the *Mahabharatha*. Ramanujan is indeed an epic mathematician and so also the story of his life. Though the lack of an index, both subject-wise and author-wise, cannot be compensated for, the appendices and the notes at the end of the book are very valuable additional material. I have no doubt in my mind, that this book does provide an easy entry to the magnificent palace full of mathematical riches which Ramanujan has bequeathed to the mathematicians of the 20th and even the 21st century.

N. R. RANGANATHAN

*'Srisuswara'  
S-5, Adyar Apartments,  
HIG Flats, Kotturpuram,  
Chennai 600 085, India*

## IIT Delhi hosts Henry Ford Chair

IIT Delhi signed an MOU on 18 March this year with the US-based Ford Motor Company to establish the 'Henry Ford Chair for Biomechanics and Transportation Safety'. The Ford Motor Company has made a grant of US \$140,000 for establishing this Chair. The grant will be invested in the corpus fund of IIT Delhi. The interest from the grant will support the Chair and will meet

academic and research expenses.

The Transportation Research and Injury Prevention Programme (TRIPP) at IIT Delhi is already actively involved in a programme which it runs in close collaboration with government agencies and industry leaders. This programme focuses on issues specific to the conditions prevailing in India for enabling people to travel safely; and also to do so

without causing injury or health hazards to users and others.

Through this alliance with IIT Delhi, Ford sees a partner with considerable experience in transport safety. The Ford Chair will strengthen work in the area of vehicle crash modelling with special emphasis on crashes with pedestrians, motorcyclists and bicyclists and biomechanical analysis of injuries to road users.

## Seminar on 'science and the media'

How much of the intriguing research that goes on behind gleaming ivory towers of our scientific institutions has really managed to percolate into the minds of the public at large? When a senior scientist was confronted with these questions, he replied, 'Sure, we'd love to communicate our research findings to the layman but who has the time to decode the technical jargon into simple terms? And those "pesky journalists" simply can't tell the difference between 'terminal differentiation and terminator genes....'. For their part, several honourable members of the fourth estate frown upon the reluctance of scientists to assist the former in translating 'scientific gobbledegook' into simpler terms. And so there continues to be a mysterious generation gap between scientists, the press and the man on the street. That is, his failure to 'generate' interest among the public towards good science. Something clearly needs to be done to mitigate this yawning gap.

On 1st and 2nd March 1999, a seminar on 'science and the media', was held at the Inter University Centre for Astronomy and Astrophysics (IUCAA), Pune, to address this very issue. Several eminent scientists and media persons graced the occasion bringing forth a vivid collage of thoughts through the lively interactive sessions.

At the inaugural session of the seminar, Jayant V. Narlikar (Director, IUCAA), one of the country's most dedicated communicators of science, alluded to the interactive 'triangle model', that held science at its apex and with scientists and the society teamed up at the base. He further related that science, through its technological in-

ventions, controlled society. Society, on the other hand, controlled science through politics and commerce. Since each was inter-dependent on the other, there was a pressing need for scientists to communicate science to the public. However, he warned, in the all pervading atmosphere where scientists needed to 'publish or perish', publicizing their science should be done with caution and without hype.

In his hard-hitting lecture punctuated with wry humour, Rajesh Kochhar (Indian Institute of Astrophysics, Bangalore) said '... In India, it is relatively easy to get research grants from the government. And yet the irony is that many scientists feel that they do not owe anything to the average tax-paying citizen...'. On its part, was the media upholding the right kind of objectives, and sending socially relevant messages to the public? M. M. Chaudhuri, a scientist-turned-science communicator on TV, opined that it certainly was not doing so. He was quick to add that in a country where illiteracy was a major problem, there was a need to change the attitudes of the public by ushering in an era of 'education through entertainment' ('edu-tainment').

Several participants in the seminar were sceptical over the role of science in mass communication. B. Ramachandran, a scientist-turned-science writer from *The Hindu* group of publications, wondered out loud 'Who needs science journalism?' 'After all', he said, 'when the total R&D investment in the country remains less than 1% GDP, and a mere 3 to 4% of Indian newspapers cater to science journalism, who needs science anyway?'

While bouquets and brickbats were generously being exchanged between

everyone and no one in particular, Dilip Salwi (freelance science writer) suggested the idea of starting 'Science Media Centres' in the country. Media consultants employed by the centres could decode scientific data passed on by scientists into simple terms understandable by journalists. This would reduce any error that could seep in while communicating complex scientific phenomena to the public. In this manner, communication between scientists and the public could be polished and further streamlined to perfection.

Many scientists fervently believe that science is universal, and scientists in India and abroad are one large happy family. While that may be a pleasant thought in itself, it is sad to note that there is an increasing trend among Indian newspapers to simply lift articles from as many foreign-based science publications as possible. Does this mean that Indian science is a dying profession? In the failure to project Indian science in a proper and responsible manner among the public and the media, with whom does the fault lie? So can we (as Ramachandran suggested), simply press 'control-alt-delete' and start all over again?

The seminar on 'science and the media' succeeded in creating a 'big bang' of ideas, mooted by both scientists as well as science communicators all over India. But unless concrete measures are taken to improve channels of communication, all our collective efforts in educating the public about scientific endeavours carried out within these shores will merely end with a 'small sigh'.

**K. Manjula, Deccan Herald, 75, M. G. Road, Bangalore 560 001, India**

## Biogeochemistry of the Arabian Sea: Modelling and synthesis

The CSIR Centre for Mathematical Modelling and Computer Simulation (C-MMACS) hosted a 3-day International Scientific Symposium on the Biogeochemistry of the Arabian Sea (18–20 January 1999) followed by a training course on modelling and synthesis (21–29 January 1999) intended to impart state-of-the-art knowledge to young researchers. The symposium and training course were sponsored by C-MMACS, System for Analysis, Research and Training in Global Change Studies (START), Inter-governmental Oceanographic Commission (IOC), International Ocean Colour Coordinating Group (IOCGG), Joint Global Ocean Flux Study (JGOFS), the US JGOFS Project Office and the Scientific Committee for Oceanic Research (SCOR).

The past decade has seen an intense observational programme in the Arabian Sea as a part of the JGOFS programme to study the physics, biology and chemistry of the region. The western Arabian Sea, off the Arabian Coast and Somalia was covered by American, Dutch, French, German and British expeditions while the northern and eastern sectors were covered under the Pakistani and Indian JGOFS programmes, respectively. All countries covered some sections in the central Arabian Sea. The main goal of the symposium was to bring all the main researchers involved in these cruises together to exchange ideas and knowledge to broaden the scope of understanding. The symposium would evolve strategies to synthesize the data so far collected into comprehensive models which would elucidate the mechanisms of the processes on much wider temporal and spatial scales than afforded by measurements.

Eighty-seven participants from 23 countries attended the symposium. The programme began with the inaugural address by V. K. Gaur, C-MMACS, on the importance of the JGOFS programme in the Arabian Sea in answering many of the questions related to climate change. It was followed by a keynote address by S. Krishnaswami, Physical Research Laboratory, Ahmedabad, in which he gave a broad overview of the Indian JGOFS programme. The other keynote address by K. Banse, University

of Washington, provided a comprehensive review of the reanalysis of the Coastal Zone Colour Scanner (CZCS) to yield a synoptic picture of primary production in the Arabian Sea. A review of the physical and biological measurements of the Indian JGOFS programme was given by S. Prasanna Kumar, National Institute of Oceanography, while a similar review of the US programme was made by Sharon Smith, University of Miami. The scientific programme comprised sessions on air–sea exchange, remote sensing, hydrography and nutrients, phytoplankton, bacteria, zooplankton, export from surface to deep waters, oxygen minimum zone, ocean colour algorithms and modelling of primary productivity and biogeochemical cycles. A total of 33 papers were presented orally and a poster session consisting of nearly 20 papers was also organized.

Peter Burkill chaired the final session on 'what was learnt at the symposium'. Several points which arose in the symposium, such as the importance of remote sensing, the level of complexity needed to model the ecosystem, inconsistencies between different kinds of measurements, etc. were debated. One issue that attracted attention was whether the Arabian Sea was a source or a sink of CO<sub>2</sub>. Experimental measurements and modelling studies presented at the symposium seemed to indicate that the Arabian Sea was a perennial source. A final draft of this discussion will be circulated shortly by Burkill after the ideas are consolidated.

The symposium was followed by a training course attended by 51 students from 19 countries including a third from India. Keeping in view the need to synthesize several types of observations and modelling methodologies, Karl Banse of the University of Washington gave an overview of the biological aspects of the JGOFS programme including a review of recent attempts to reanalyse CZCS data. K. Denman of the Institute of Ocean Sciences, Canada provided an exposition of mixed layer modelling using advanced turbulence mixing theories. A. Oschlies from University of Kiel, Germany made a presentation of data assimilation methods in complex ocean models. J. Kindle of

Naval Research Lab, USA provided a study of a coupled physical–biological model to simulate the conditions that prevailed off the Arabian and Omani coasts during the 1995 cruises. Trevor Platt provided a review of biological processes in the ocean. Shubha Satyendranath reviewed the bio-optical algorithms used in retrieving biological parameters from ocean colour measurements. V. Garçon of CNES, France reviewed her recent results from the JGOFS programme in the Atlantic where she had employed a complex three-dimensional coupling between physics and biology. A review of each term that appeared in marine ecosystem models along with its significance was provided by G. Evans of the Department of Fisheries and Oceans, Canada. Diana Ruiz-Pino of CNRS, France provided a review of box models of biology, chemistry and physics which yielded quick but reliable estimates of fluxes and standing stocks in ecosystem modelling. Alain Vezina of Institut Maurice Lamontagne, Canada gave a review of food-web models from the point of view of the application of inverse methods, especially singular value decomposition, linear and quadratic programming. K. S. Yajnik, former Head of C-MMACS and Andy Edwards of Dalhousie University gave an exposition of recent studies on the stability of marine ecosystem models.

Besides lectures, computer demonstrations of models and software, along with hands-on training of students also formed a major part of the course. Some of the demonstrations included: (a) processing of Sea Wifs data to obtain biological parameters; (b) inverse modelling and data assimilation using MATLAB; (c) complex coupled ecosystem modelling using software from Plymouth Marine Laboratory; (d) mixed layer modelling; (e) use of box models like STELLA for the marine ecosystem; and (f) a coupled physical–biological–chemical model of the Arabian Sea. In addition, Internet access was provided for the instructors and the participants.

---

**P. S. Swathi**, CSIR Centre for Mathematical Modelling and Computer Simulation, Bangalore 560 037, India.

# Search for an individual in the midst of a crowd: Tracking a single molecule

*Dipankar Chatterji*

Many of us started science at school with test tubes, solutions, concept of moles, Avogadro number, etc. Till today we describe a reaction, be it chemical or biological, as an interaction between groups of organized molecules all behaving in a similar fashion in one group, any aberration from this organized behaviour is not allowed or not detectable at the most. Thus, when we follow a ligand-receptor interaction, we believe that all the ligands in the ensemble (roughly about  $10^{17}$  molecules in a micromolar solution) have exactly the same affinity and the same rate of interaction with the receptor. In a radioactive tracer technique, used by biologists, only one single molecule on an average is labelled with a radioactive probe within a million molecules. Yet its behaviour represents the behaviour of the million. Or in other words, the concept of equilibrium thermodynamics guides the study of the interacting species.

Now, however, the picture is changing and a new area has started emerging, which in the opinion of the many may dominate research in chemical and biological sciences for at least the next twenty years. Molecules are not happy to be treated in such a democratic fashion! They want to exert their individual identity and scientists have taken up this challenge. It is now possible to study how a single molecule or a reacting species finds the other molecule with which it should react, how the bond is formed, what is the strength of a single covalent bond, and finally how much force is necessary to tear out a single bond. An amazing experiment has been performed where the two strands of a DNA double helix have been forced open with an optical tweezer breaking one hydrogen bond at a time and scientists have tried to listen to the 'unzipping' sound of the helix resulting due to this breakage of hydrogen bonds (melting?).

There are several difficulties in studying a single molecule. The first is to create a heterogeneous environment so

that a molecule can be detected among many such molecules and then follow its behaviour with a sensitive technique. Optical probing seems to be the choice in most of the cases where a probe can be attached to a molecule and then traced microscopically<sup>1</sup>. This detection of the signal is complicated by the interference from surrounding materials, like the crystal or solvent. Minimizing the background interference from impurities and Raman scattering now seems to be possible and this has enhanced the detection limit of the fluorescent signal from a single molecule.

Thus, to follow the chemistry of a single molecular species we need: (i) a sensitive probe, mostly fluorescent; (ii) a sensitive device to excite the fluorophore, mostly laser source; and (iii) an optical microscope to monitor the signal emitted from the fluorophore. When a reaction between two molecular species needs to be followed, sometime it is advantageous to fix one molecule over a glass surface and follow the movement of the other towards the fixed one under steady flow. A few years ago, a DNA fragment was fixed in this way over a glass surface and the movement of RNA polymerase suitably labelled with a fluorophore was monitored. One could visualize in video imaging the movement of the enzyme towards the promoter sequence in real-time<sup>2</sup>. Recently this experiment has been further improved. A group from Princeton<sup>3,4</sup> has developed the 'world's tiniest tug-of-war' machine, where the DNA at its downstream end is attached with a microscopic bead and the bead is visualized by a fixed optical trap. The RNA polymerase molecule is fixed on a glass surface and placed at the opposite end (upstream) of the DNA molecule. If this system is charged with all the nucleotides, Mg(II), etc. transcription would proceed. The RNA polymerase will exert pressure on the DNA to move and the bead will be pulled from the optical trap. An optical resorting force builds up until it just balances the force ex-

erted by RNA polymerase and transcription stops. The force with which the enzyme pulls the DNA is 25 piconewton, four times that exerted by myosin, the protein that contracts the muscles. Similar experiments performed by fixing two ends of a DNA showed that new conformations could be achieved by exerting an awkward twist within a DNA. A series of experiments are now being performed to monitor how much twisting force is generated when endonuclease or topoisomerase are attached to one end of a DNA.

Fluorescence resonance energy transfer (FRET) studies have been used to map the distances between a donor and an acceptor fluorophore conveniently located on a macromolecule. The very rapid and remarkable development of fluorescence single molecule detection (SMD) and single molecule spectroscopy have made it possible to use FRET to measure intermediates and follow time-dependent pathways of chemical reactions that are difficult to synchronize at the ensemble level<sup>5</sup>. A major advance in the SMD field came with room temperature microscopy and spectroscopy of immobilized single fluorophore (as described before in the case of RNA polymerase) by near field scanning optical microscopy, confocal microscopy, improved charge-coupled device (CCD) cameras and atomic force microscopy (AFM). Techniques of immobilization with improved chemistry help to track emitting photons continuously and improve the signal to noise ratio. Such SMD applications on immobilized molecules have seen their remarkable application when turnover of ATP molecules could be seen by a single myosin molecule<sup>6</sup>. In all these cases, attachment of a fluorophore to a molecule of protein is necessary for detection, which, however, creates perturbation in the system that is unwarranted. This problem can be handled by using native fluorescence of the protein by fusing it with GFP (green fluorescent protein).

**Table 1.** Types of motors employed by the cell

| Type of motor | Direction of movement | Example from biology           |
|---------------|-----------------------|--------------------------------|
| Rotary        | Anticlockwise         | Flageller movement in bacteria |
| Rotary        | Anticlockwise         | ATP synthase                   |
| Linear        | Bidirectional         | Actin/myosin                   |
| Linear        | Bidirectional         | Kinesin (dyanin)/microtubule   |
| Linear        | Unidirectional        | RNA polymerase/DNA             |

Recently, Noji *et al.*<sup>7</sup> have identified the first molecular motor,  $F^1$ -ATPase. Cells employ a variety of linear motors (Table 1) which exert forces as they move along. We know of one rotary motor, the bacterial flagellum which propels bacteria by a circular motion and comprises 100 different proteins. Single molecule measurements have shown that  $F^1$ -ATPase acts as a rotary motor, the smallest known so far.  $F^1$ -ATPase is known to contain three  $\alpha$ - and three  $\beta$ -subunits and one  $\gamma$ -subunit.  $F^1$ -ATPase, together with the membrane embedded  $F_0$  unit forms  $H^+$ -ATP synthase that reversibly couples transmembrane proton flow to ATP synthesis/hydrolysis in respiring and photosynthetic cells. Various structural and biochemical studies suggested that the  $\gamma$ -subunit rotates within the hexamer of  $\alpha_3\beta_3$ . Noji *et al.* have now fixed the  $\alpha_3\beta_3$  hexamer on a glass coverslip coated with Ni(II) complex with the help of His-tag. Then  $\gamma$ -subunit was attached with a fluorescent actin filament and in the presence of ATP the anticlockwise rotation was noticed from

the coverslip (membrane) side. The speed of revolution was measured to be 4 Hz and the torque produced reached up to 40 piconewton per nm.

However, the most novel conclusion which has come at the beginning of this year<sup>8</sup> would force all of us to look again at the ligand-receptor interaction. A report showed that the ligand-receptor interaction strength is not fixed. At least in the single molecule level, the strength of interaction can be tuned to be weak or strong by varying the retracting force, which is known as 'loading rate'. Patrick Stayton wrote 'Nature might regulate bioadhesive strengths through activation barriers engineered by evolution'.<sup>9</sup> The affinity between streptavidin and biotin is the strongest non-covalent interaction in biology ( $10^{13}$  to  $10^{15}$  M<sup>-1</sup>). However, the authors probed bond formation over six orders of magnitude in the loading rate and observed that the stability of the bond varies from 1 min to 0.0001 s, with increasing loading rate. They attached streptavidin to a surface (immobilization) and biotin to a probe. They were allowed to interact and

form a bond and were then pulled apart. Upon measuring the force necessary to pull them apart, the authors found that the interaction strength depends on how fast they were pulled! It may be impossible to arrive at such conclusions from bulk measurements.

One of the major drawbacks of single molecule measurements is the technological limitations, cost and maintenance of such a facility. As one can understand, signal to noise is extremely weak and therefore requires very clean measurements for reproducibility. Cost is not the rate-determining step; the better the probe having strong signals, less is the cost. So, the chemistry for probe selection, and attachments, will diversify further. However, it requires participation of many experts in various disciplines to start such an activity.

1. Uppenbrink, J. and Clery, D., *Science*, 1999, **283**, 1667.
2. Kabata, H. *et al.*, *Science*, 1993, **262**, 1561.
3. Yin, H. *et al.*, *Science*, 1995, **270**, 1653-.
4. Wang, M. D. *et al.*, *Science*, 1998, **282**, 902.
5. Weiss, S., *Science*, 1999, **283**, 1676.
6. Funatsu, T. *et al.*, *Nature*, 1995, **374**, 555.
7. Noji, H. *et al.*, *Nature*, 1997, **386**, 299.
8. Merkel, R. *et al.*, *Nature*, 1999, **397**, 50.
9. Stayton, P. S., *Nature*, 1999, **397**, 20.

Dipankar Chatterji is in the Molecular Biophysics Unit, Indian Institute of Science, Bangalore 560 012, India.

## OPINION

### Survey of India maps: (Ir)rationale about restricted maps

S. M. Mathur

Restricted maps are such topographic sheets of the Survey of India (SoI) that are not sold freely and require permission from certain government departments (in some cases even the Ministry of Defence) for sale. The buyer is bound to observe stringent conditions, violations of which are liable to attract penal action. The categories of maps that have been declared restricted are all topog-

raphical and geographical maps which cover about 80 km wide strip of the land along the coasts and along the international boundaries, the whole of Jammu & Kashmir (J&K), and the islands of Andaman & Nicobar and Lakshadweep on scales 1:1 million and larger as depicted on an index map. Gridded topographic sheets of unrestricted areas are also not for open sale. There are restric-

tions on depiction of contours and heights as also of several types of installations and lines of latitudes and longitudes. Even the map catalogue of SoI is restricted.

However, 1:1 million World aeronautical charts and International maps of the world (Carte Internationale du Monde), including that of J&K, sold by SoI are exempted. Is it because such

maps are freely available abroad and form part of a global system? For example, the US Army Map Service has covered the whole of India, including the mountainous regions, on maps on a scale as large as 1:25,000. Detailed maps of the western Karakoram glaciers have been published in Italy (1:500,000 scale) and Germany (1:450,000 scale).

These restrictions hamper the efforts of many people, agencies and institutions engaged in developmental work and scientific research. Earth scientists are specially hampered because numerous regions in the restricted zone happen to be geologically important. They cannot easily obtain the standard 1:50,000 scale topographic sheets – not to speak of sheets on a larger scale – that are normal for geological mapping and other investigations.

Another arm of the Government of India, the National Remote Sensing Agency (NRSA), freely sells detailed imageries not only covering India but also adjoining territories; these include areas that fall under Sol 'restricted' categories. These imageries have a resolution of 5.2 to 5.8 m. This means that objects even as small as a truck on the ground can be identified. Also, the height of any topographic feature or object can be calculated therefrom, making the prohibition of depicting contours on maps of certain domains redundant. On the other hand, the large-

est standard topographic sheet produced by Sol is on the 1:250,000 scale with contour interval of 10 m. This shows only broad topographic features, and even a small village is depicted not larger than a dot. Then, what is the rationale of Sol to restrict sale of numerous maps on scales larger than 1:1 million?

The policies of Sol and NRSA contradict each other though both are Central Government organizations. Is Sol, carrying the burden of its hoary old age of 232 years (established in the year of grace 1767) so hidebound that it is unable to shake off its antediluvian outlook?

The geological maps of the 'restricted' areas published by the Geological Survey of India (GSI) are also restricted because they are based on Sol maps.

Also in Sol, all topographic sheets on scales larger than one-fourth inch or more equal to a mile come stamped with the injunction 'not for export'. The obvious intention is that the maps should not be taken out of India. The rationale behind this rule is also questionable, when foreign agencies have published maps of these areas for open distribution.

While Sol will not allow its maps to go out of the country, NRSA sells freely the imageries, tapes and maps the world over, earning valuable foreign ex-

change. As a global player in this field, it offers quite a competition to NASA, America, in providing satellite photographs and data.

Foreign agencies publish maps of India without obtaining the permission of the Surveyor General of India. For example, bathymetric Admiralty maps of the seas surrounding the Indian coast for navigation purposes, are available from a firm in Calcutta (possibly from other sources as well in India) issued by a foreign organization, obviously without the mandatory approval of the coastal features by the Survey.

In the interest of not only geological investigations but of scientific research and overall development as well, it is urged that the Government remove the irrational classification of restricted maps, and make available freely all maps issued by Sol.

Quite a few laws and rules on the statute books are hopelessly outdated having no relevance now, but the Government has taken no action to repeal them. The Ministry of Science and Technology should advise the Government about the absurd restrictions enumerated above and urge for their removal.

*S. M. Mathur lives at B-15, Alokपुरी, रावन्द्रापल्ली, Lucknow 226 016, India.*

## Futile exercise in thought control

*S. R. Valluri*

*The Hindu* of 17 December 1998, reporting on a parliament proceeding stated that 'A formal warning has been issued to a scientist at the Institute of Mathematical Sciences (IMSc) for writing an article specifically criticizing the present nuclear tests' and that 'Action has been initiated against T. Jayaraman under the provision of the Institute conduct rules and that some scientists wrote to the IMSc Director, opposing any disciplinary action'. Since the issue has attracted parliament attention, it has assumed political overtones and raises some issues of wider impor-

ance. Jayaraman discussed some very important policy issues. To argue his viewpoint he quoted statements publicly reported to have been made by the secretaries to the Department of Atomic Energy (DAE) and DRDO. In a democracy, it is not a crime to base ones argument on public statements of politicians or government officials. In fact, in a similar situation, the scientists in United States started publishing the *Bulletin of Atomic Scientists* to give an opportunity to 'non establishment scientists' to freely express their viewpoint on the US nuclear policies. It is within

the right of citizens in a democracy with many political parties to hold 'politically partisan views', such as they are on issues of vital importance that can affect all of us.

This action of the Director of IMSc has apparently been prompted by the unhappiness expressed by the Secretary to the DAE which is the grant-in-aid funding agency for IMSc. This precipitated the present anomalous situation. It has attracted more attention than the original article of Jayaraman among the scientific community. One wonders, if this was what the Secretary, DAE

and the Director, IMSc had really decided.

It is not clear what the situation would have been, if IMSc had been under the authority of the HRD Ministry, which has a moral obligation to protect the concept of academic freedom in the institutions supported by it. One wonders if the government cannot tolerate any criticism of its nuclear policy and is therefore not keen for any public debate in the scientific community on this issue of profound importance to humanity. The memories of censorship and excesses during 'Emergency' in 1975-77 are not yet forgotten. It is not easy to take lightly any constraints on rights of people to think and express their thoughts freely.

Many of us in our administrative careers, running academic and research institutions, had occasions to invoke conduct and service rules. It is also a fact that when such powers have been used rather arbitrarily, some of us got our knuckles rapped by public opinion or higher appellate authorities, if not by courts. It is not that such rules should not be used, but that their application should not grossly violate some general conventions and rights bestowed upon different cross-sections of our society.

However, we must also be clear, how far this freedom of expression of a citizen extends in a democracy. A person directly employed by the government, surrenders this right to question government policies publicly. He is governed by the Central Conduct Service (CCS) Rules. He may not publicly dissociate himself with any official policy of the government. The elected leaders may change their views and even reverse policies. In public, the government employees however are obliged to dance to the tune of their political masters. Had Jayaraman been directly an employee of DAE, which he is not, the Secretary, DAE would have been within his rights to take action against him for publicly disagreeing with a government policy.

IMSc however, is a grant-in-aid institution unfortunate enough to receive its funds from DAE, and with its Secretary, as the Chairman of its Council. By general convention, the Chairman is the appellate authority on matters of discipline, when a staff member disagrees with a decision of his Director. It would

appear that the Chairman of the Council, who triggered off this action has unwittingly compromised the integrity of the appellate authority by expressing his unhappiness, which apparently motivated the Director of IMSc to take action. It would appear that no distinction has been made between the rights and responsibilities of appellate authority on the one hand and those of the disciplinary authority on the other.

Rules and regulations (other than General Financial Rules) are enabling clauses to be exercised with discretion, bearing particularly in mind, the precedents they set. The essence of a functioning democracy is not to discourage free public debate out of which policies could and should normally be evolved by the elected leaders. The government does have the last word in the decision making, but they do not have the luxury of curtailing free debate in a free society.

One wonders if this is not a case of intrusion into the right of inquiry and expression of the staff in grant-in-aid institutions. Should grant-in-aid institutions be obliged to incorporate into their bylaws, as a precondition and without any right of discretion, aspects of conduct and service rules which prohibit the right to differ with any government policy? To carry the argument further should these institutions in turn be also required tomorrow to stipulate similar conditions on others while dealing with them? Where does one draw the line?

Nuclear power in any form, leave alone the development of nuclear bombs, had been a controversial issue all over the world, with some countries even giving up nuclear energy as a source for generation of electrical power, because of the inherent dangers it involves, even for its own people. It behoves the government to encourage and to listen to the debate and to review and temper our nuclear policy, if deemed necessary, instead of getting the 'establishment scientists' exercise 'thought control' on issues of profound importance to all of us.

It should not come as a big surprise that the public sympathy is wholly with Jayaraman. The general feeling is that it was unworthy of scientist bureaucrats to exercise their authority in this manner. In any case, Jayaraman's comments

have nothing to do with the functioning of IMSc to attract strictures, but everything to do with developments that could affect all of us. Let it again be understood that in such a debate personal criticism of individuals involved can only dilute and distract the arguments and not strengthen them. The arguments should carry conviction in their own right.

This incident reminds this writer of an event that took place after Morarji Desai came to power in the elections held after the lifting of the emergency in 1977. Morarji wanted to take action against this writer who was then the Director of the National Aerospace Laboratories of the CSIR. What was the crime? Morarji wanted to substantially dismantle the CSIR structure and transfer the bulk of its laboratories to other government departments. A PTI reporter from Delhi asked this writer for comments. At that time PTI was still being run essentially as a government arm. In all innocence, this writer therefore took the query to mean that the government really wanted to know the opinions of people directly familiar with the matter. This writer told the reporter, that while the government would be well within its rights to do what it pleased, it would not cost the government much to ascertain from CSIR directors, the pros and cons of such a decision. The comment was widely reported in the press. Morarji considered this as a criticism of the government and wanted to take disciplinary action. Fortunately better sense prevailed and the matter was dropped.

If the Prime Minister could change his mind and reverse his judgment, and refrain from taking a punitive action against a scientist, would it be too much to hope that the Secretary, DAE, the scientist that he is, would be gracious enough to receive from Jayaraman an appeal to rescind the note of warning from the Director and put this unpleasant incident behind. As it stands, the Secretary, DAE and the Director, IMSc have lost more than Jayaraman, in the eyes of the disinterestedly interested scientific community.

---

*S. R. Valluri lives at 'Prashanthi', 659, 100 Feet Road, Indiranagar, Bangalore 560 038, India.*

## Novel, cost-effective method of archiving manuscripts

Physical preservation of manuscripts is a difficult task, even under the best of conditions. Indian paper manuscripts may last four hundred years while palm leaf manuscripts may, under the best of conditions, last seven hundred years. And many of India's ancient manuscripts are now in a bad condition. In the past, scribes would have been called in and would have meticulously copied them (perhaps adding scribal mistakes to those that might already be there).

Photography, especially microfilming, and photocopying (xeroxing) have sometimes damaged the originals but have always been costly – and offer only a few decades of preservation. Manuscripts could also get lost during microfilming. Scanners have been used by a few centers but are relatively slow and can damage the manuscripts, especially ones that are deteriorating. A far more expensive approach has been first to microfilm the manuscript, and then to use a medical or high-definition film

scanner to digitize the manuscript as images. This expensive method can be used only by the best-subsidized archives in the world.

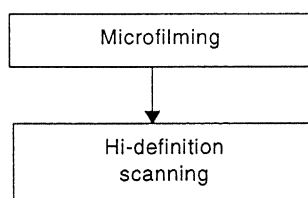
Another option that was rejected prior to 1998 was digital still cameras which were both expensive and could copy only a few pages before their images had to be downloaded into a computer. Their flash-card memory was much too expensive and limiting for travel to an archive and copying for days at a time. Hence, an experiment was done in June 1998, when the first manuscripts were digitized directly with a DV format camcorder. But, in 1999 a new generation of digital still cameras was introduced which met the needs for in-house digital copying. The procedure is even simpler and can be taught easily. Two new digitizing procedures have been successfully tested at archives in South India by the National Institute of Advanced Studies (NIAS). The technology is far cheaper than conventional methods and the learning time is minimal

(Figure 1). But there are some expensive mistakes that can be avoided.

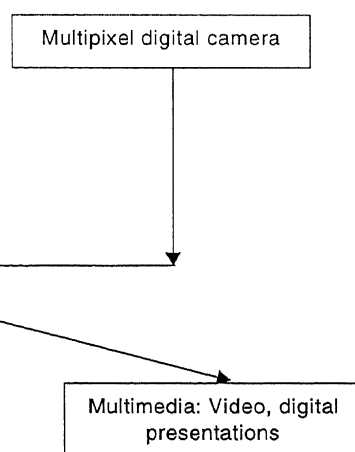
A few archives in South India were visited for our tests. The *Bhagavad Gita* (a critical edition, two CD ROMs, myriad translations into the languages of the world) was chosen as the text (Figures 2, 3). The main reason for the selection of *Gita* arose from its very innocence. It was the most likely manuscript that archivists and librarians would allow to be copied with a new technology (note 1).

The initiative began with two goals: (1) to test digitization of manuscripts; and (2) to digitally copy manuscripts of the *Bhagavad Gita* for inclusion in a computer database open to the nation and the world. The equipment and digital capture procedures worked superbly. Where access was permitted a greater range of textual variants and variables were discovered than hypothesized (note 2). There was a great cause for alarm that the rare cultural treasures of India were being rapidly lost due to

Conventional preservation of MSS



Digital preservation



**Cost:** The digital process requires an initial equipment investment of 1/20 to 1/30 of the conventional microfilm lab. Few libraries and archives can afford the Rs 10 lakh investment, and so have the work done outside.

**Secondary cost:** There are no film or processing costs in digital copying.

**Time:** Since there is one step less, the work is done in-house and the process is simpler. It requires less photographic skills. The digital process is estimated to take a time of 1/4 to 1/3 that of the conventional method.

Once the data reaches the computer, the time and cost are relatively the same.

The major disadvantage of less resolution is rapidly disappearing with new megapixel cameras. However, most of the high-definition, colour information is not needed and is even discarded in most manuscript usage.

Figure 1. Cost, time and process comparison.

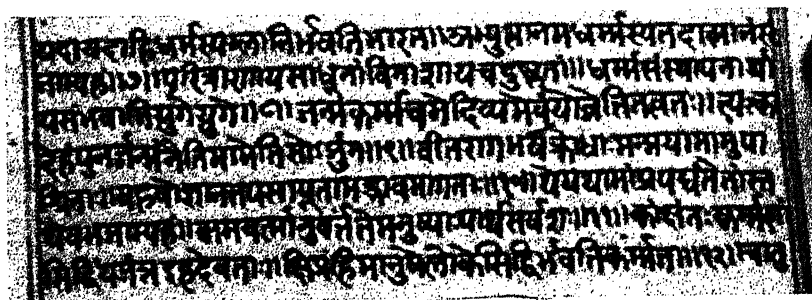


Figure 2. Selection from the paper manuscript on *Bhagavad Gita* in Devanagari, from Manuscripts Division, Osmania University Central Library, Hyderabad.

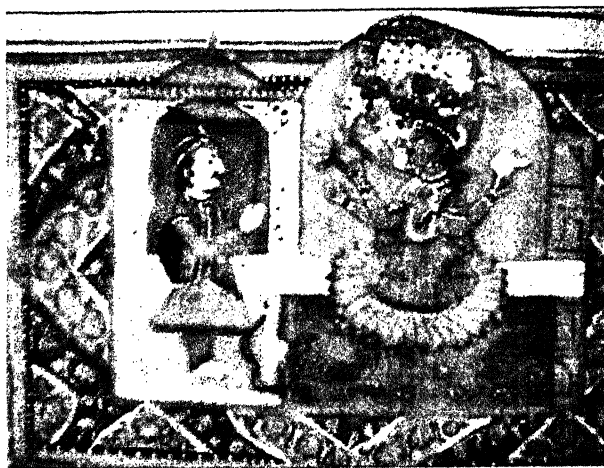


Figure 3. Selection from the paper manuscript on *Bhagavad Gita* (in Sarada script), from Adyar Library, Chennai.

neglect, damage, etc. But there is enough hope that this can be reversed with this initiative from NIAS.

What was needed was a method that was less expensive, more permanent, capable of full colour, faster, in-house, and extensible (capable of being used with master books, CDs, databases and share over the internet). NIAS has tested one such method. The NiDAC procedure should be used with a notion of sharing these rare manuscripts with others as freely and widely as possible. The archive or library can still secure copyright for the manuscripts that they own, so that others cannot publish or exploit them commercially. Their use can be licensed (especially manuscript graphics), and they can be shared via the Internet or by CDs. The philosophy of sharing information is as important as any archiving and computerization technique. Low cost educational and research materials should be the result of the NiDAC procedure.

Instead of using a scanner to digitize each page of a manuscript as a computer graphic, the NiDAC procedure begins with the new DV video format. The DV camcorder that was chosen was the third generation of a technology that is advancing in about three months. The DV video format simply records everything as binary code onto a mini DV tape. The camcorder weighs less than two kg even with an eight-hour battery. The camcorder connects to higher end computers via an IEEE 1394 cable and card. Thus, there is no composite video to digital conversion. The digital image can be manipulated as a graphic or converted into alphanumeric (text). Images before compression are quite large but become small files when compressed into image formats like JPEG (depending on quality and detail required). Computerization is completed with various forms of storage (re-writable media like hard drives are quite fragile but CDs have at least a half-century life

rather than a few decades like the microfilm).

The second method is to use a megapixel digital still camera with extra large memory cards. The memory cards are then removed from the camera, put into a disk-like device, and then downloaded via the floppy drive port into the computer. This method is at least ten times faster than downloading via a parallel or serial cable. Again, if the camera is well-chosen, the image enters as a JPEG file and is instantly manipulable for storage and distribution. This method is far superior to the DV digitization when the work is in-house. It will also work for extended field trips to archives if a lap top or a computer with adequate storage is available. The DV digitizing method can however be utilized for work in remote archives for extended times with no computer access and uncertain or fluctuating electrical power supply, etc.

The NiDAC procedures allow in-house copying of acid paper books (most of those published in the last fifty years in India). Such books are characteristically yellowed and crumble in hand as one reads or photocopies them and may disappear without a trace unless there is inexpensive digitization (note 3). NiDAC methods also include the direct copying of microfilm and microfiche into the computer, reducing the expense of current methods.

India should adopt a two-fold step to preserve its ancient manuscript treasures: (1) immediately begin a ten-year project of digitally copying all ancient manuscripts with new and relatively inexpensive technology, and (2) develop and use speech recognition technology (note 4).

## Notes

1. Pre-information age philosophies still govern most archives and libraries in India (they fear losing control of their manuscripts – otherwise, what else would explain meticulous procedures to limit access and copying of manuscripts). Consequently many manuscripts have no backup at a given library or archive. Some cannot be discovered by a published list, record or catalogue. (Current computer access of an archive's holdings via the Internet seems decades away.)

2. Most of the archives and libraries were poorly funded and supported. The procedures at more than 75% of the institutions

visited were highly protective, bureaucratic (requiring long forms and longer waiting periods), and often disappointing (manuscripts catalogued could not be found, manuscripts listed in the catalogue as 'in good condition' were highly damaged by worms or silverfish, even microfilms were often missing or found in a deteriorating condition).

3. Digitizing will come sooner or later to every library and archive in the world. It is the future. Librarians and archivists should know that these methods might pose a threat to their holdings. Rather than attempting to stop digital copying, a far more positive approach would be to institute procedures where scholars and scholarly organizations, or even commercial companies, will enter into agreement with the archive. Licenses and agreements can predetermine use, profit sharing with private companies and procedures that encourage mutual cooperation.

4. Sanskrit, like any language, is both spoken and written. Sanskrit as an oral language is one of the most regular in grammar and pronunciation. It is in fact, so rigid that

it has been called 'artificial' – great for finished literature but poor for conservation. Oral Sanskrit is perfect for computerization. Written Sanskrit has a clear and precise relationship with oral Sanskrit and consequently is also a perfect candidate for computerization. Already projects around India have begun this process. But other priorities have actually thwarted Sanskrit's computerization. Some are clearly political. No living language, even those derived from Sanskrit, meet these criteria – their irregularity, flexibility and colloquial inventiveness are precisely at fault. Written Sanskrit can be represented with any script – but since the Roman script or alphabet has only 26 letters, this representation is incomplete and less than adequate. (Alphabetic, written languages also have important differences from syllabic, written languages. This need not be a concern at this stage but might suggest the need for another type of keyboard or data entry system instead of just copying the Qwerty keyboard.) Diacritical marks are added to make up for this deficiency in a Roman alphabet representing Sanskrit syl-

lables. This should be standardized in 2-bit code, also recognizing the differences between alphabetic and syllabic languages. Using a standardized, universal 2-bit code would allow instant switching by computer from any world script (Roman to Devanagari to Kannada) to any other script.

**ACKNOWLEDGEMENTS.** We thank the Manuscripts Division of Osmania University Central Library and Adyar Library, Chennai. We also thank Prof. B.V. Sreekantan, Chief Advisor of this project, and Prof. Roddam Narasimha, the Director of IAS, for their encouragement. The initial phase of this project is supported by INFOSYS Ltd. Bangalore.

SANGEETHA MENON  
GEORGE M. WILLIAMS

*National Institute of Advanced Studies,  
Indian Institute of Science Campus,  
Bangalore 560 012, India*

## Why does river Brahmaputra remain untamed?

Come May and the wild river of the east is seized with spells of unrelenting spate, attendant deluge, sediment deposition and erosion. The flood hazard has been ravaging upper Assam unabatedly since time immemorial. Explorers of ancient times – those who established Praagjyotishpur in Kamrup province – must have discerned in this river something very different from all other rivers of the subcontinent, as evident from the singularly masculine name they gave it – 'Brahmaputra' or 'the son of Brahma'. Despite gigantic efforts and colossal expenditure (> Rs 15,000 million) in building 3647 km of embankments, 599 km of drainage channels and 431 km<sup>2</sup> area of soil conservation<sup>1</sup>, Brahmaputra continues to wreck havoc by uncontrollable floods year after year. Records show that catastrophic floods occurred in 1954, 1962, 1966, 1972, 1973, 1977, 1978, 1983, 1984, 1987, 1988, 1991, 1993, 1995, 1996 and 1998. Upwards of 9600 km<sup>2</sup> land, that is 12.21% of the geographic area of Assam, is annually affected by floods. In 1998, the flood which came in 4 frightening waves, deluged 38,200 km<sup>2</sup> or 48.65% geographic area of the state,

putting in peril the lives and properties of 12.5 million people<sup>1</sup>.

Why are we so helpless in containing the spates of Brahmaputra and coping with its flood hazard? Why do our efforts go awry and all civil engineering measures end up in shambles? The answer, in my opinion, lies in our failure to recognize the reality of active faults and continuing crustal movements in this geodynamically restless region. Understandably, the flood coping measures have never been designed to accord with this recognition.

Girdled as it is, by the arms of the Eastern Himalayan Syntaxis – the knee-bend of the mountain ranges – the Assam terrane is underthrusting northwards under the Arunachal Himalaya and, less energetically, eastwards beneath the Indo-Myanmarese ranges<sup>2,3</sup>. There is, therefore, very severe deformation and attendant faulting and thrusting in the terrane caught between the Himalaya-Patkai Naga ranges and the Meghalaya massif (Figure 1). The drastic reduction of the width of the alluvial plains from 350 to 300 km, respectively, in the flood plains of Sindhu and Ganga to less than 100 km

in the Brahmaputra basin is not without significance. Coming of the Meghalaya-Mikir blocks of the Peninsular Indian Shield closer to the Himalaya explains this attenuation of the alluvial domain of the Quaternary foreland basins.

The severe deformation of the Assam region is eloquently expressed in its much faulted framework<sup>4,5</sup>. The E-W trending faults (Dauki Fault, Brahmaputra-Mikir Fault), and the transverse tear faults (Kopili Lineament, Dhubri Fault, Dudhnoi Fault, Chidrang Fault, Um Nagot Lineament) and thrusts (Dapsi Thrust, Barapani Thrust) are among the many that dissect the terrane of the Meghalaya-Mikir blocks (Figure 2). The E-W Dauki and Brahmaputra-Mikir Faults roughly demarcate the southern and northern physiographic limits of the Meghalaya Plateau which is a horst of sorts. The plateau stands as a ~ 2000 m high physiographic eminence against the sunken 3–4 m high (above sea level) Sylhet Plains in Bangladesh.

Most of these faults are seismically quite active<sup>4</sup> as borne out by the distribution of epicentres in the fault zones (Figure 2), such as the locations of 7 earthquakes of  $M \geq 4.5$  along the 26.5°



**Figure 1a.** Girdled by the mountain arc which makes a pronounced knee-bend, the Brahmaputra valley in Assam is a terrane under severe deformation, and the Meghalaya massif in the south is faulted in the E-W and transverse directions. (Drawn by Shampa Sikdar after an illustration in *National Geographic*, 1988, 175).

parallel – the line of the Brahmaputra–Mikir Fault; and in the NNW–SSE trending belt of the Kopili Lineament (Figure 2).

The catalogue of earthquakes of magnitude 4.5 and above in the period 1897–1992 shows the higher (87%) seismicity in the Meghalaya–Mikir blocks and adjoining Indo-Myanmarese range and northern Bangladesh plains (Figure 2), compared to near absence in upper Assam and lower seismicity in Arunachal Himalaya<sup>6</sup>. In the Meghalaya block, the western part (Tura region) riven with faults exhibits greater

seismicity as testified by major earthquakes of 1897, 1923, 1930 and 1943 (Figure 2).

Gowd *et al.*<sup>6</sup>, Molnar<sup>7</sup> and Gahlaud and Chander<sup>8</sup> attribute the higher seismicity of the Meghalaya–Mikir blocks to reactivation of what has been postulated as a gently dipping shallow thrust or midcrustal detachment. I believe that many E–W and transverse faults that dissect the block (Figure 2) are active. Compared to the N3°E orientation of  $S_{H_{max}}$  in the Meghalaya–Mikir blocks, it is N26°E in upper Assam (and N23°E in Peninsular Indian Shield)<sup>6</sup>. The NNW–

SSE trending Kopili Lineament of high seismicity thus constitutes the tectonic boundary between the two stress domains. Significantly, it was in the belt of this Kopili Lineament that earthquakes have occurred recurrently – one of  $M$  7.2, three of  $6.0 \leq M < 7.0$  and several of  $4.5 \leq M < 6$ . Doubtless, tectonic movements have been taking place time and again on the faults of the Kopili Lineament. This seismically active Kopili lineament cuts across the Brahmaputra about 35 km NW of Navagaon between Mikir Hills and the prolongation of Meghalaya massif (Figure 2).

Levelling observations<sup>9</sup> made three times during 1910–1976 indicated that the blocks of the Guwahati–Dergaon section have been consistently rising – the vertical velocity increasing progressively from 0.3 mm/yr to 4.5 to 31 mm/yr at Dergaon (approximately 30 km west of Jorhat) implying faster rise of the Mikir block. In the Guwahati–Goalpara sector, the eastern side moved in the NNE direction and the western part shifted SSW-ward during 1856–1938 (ref. 9). North of the Dauki Fault, the Meghalaya block has been rising at the rate of 0.3 to 0.4 mm/yr (ref. 10).

It is obvious that the block delimited by seismically active faults has been rising perceptibly though variably in space and time. The uplift of the Meghalaya block is evident in the gorge that the otherwise wide Brahmaputra has cut near Guwahati (Figure 3) – in the place where a N–S lineament traverses the river.

The uplift of the Meghalaya block – through the prolongation of which the Brahmaputra has cut its channel – must have caused ponding of the river. The continuing movements must be impeding its flow with resultant accumulation of sediments in the upstream channel (Figure 4). The deposition of great volumes of sediments – occurring as islands and bars – in the channel has phenomenally reduced the carrying capacity of the Brahmaputra. Flood waters are bound to spill over and spread far and wide. The 1897 earthquake of  $M$  8.7 had caused not only the ponding of streams but also blockade of the Brahmaputra. According to Oldham<sup>11</sup>, there was a deluge unrelated to rains as a result of a barrier formation across the



Date of Image : 03-March-1998

Scale

100

0

100

Kilometers

Figure 1b. IRS-1D image of the Brahmaputra valley and adjoining hills (Photo courtesy: D. P. Rao, NRSA, Hyderabad).

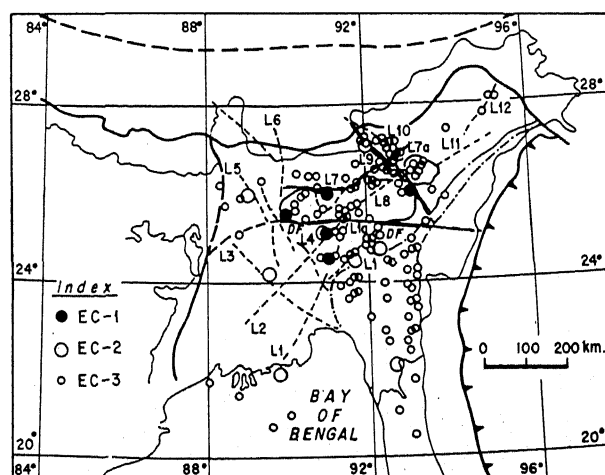


Figure 2. Seismicity of north-eastern India is related to continuing tectonic activities on faults, as borne out by the locations of epicentres. Note in particular the epicentral distribution in the belts of Kopili Lineament (L-9), Brahmaputra-Mikir Lineament (L7-L8) and Dauki Fault (DF) (From Gowd *et al.*<sup>6</sup>).

Brahmaputra, downstream of Hathi-mura, accompanied possibly by subsidence of the floor under the river. The 15 August 1950 earthquake ( $M$  8.7) had likewise drastically affected the gradient of this river, stopping the flow temporarily and bringing about flooding and rapid accumulation of enormous volume of sediments in the channel. The lowest water level rose by 3 m as a result of the earthquake, and near Dibrugarh and downstream the channel was silted up 2.5 to 3 m. The scarp<sup>13</sup> that one sees north-east of Dibrugarh (Figure 5) is probably the surface expression of the fault that lifted up the downstream block and caused ponding of the Brahmaputra.

Imagine a similar development overtaking the Brahmaputra valley in the event of a major earthquake! Taking

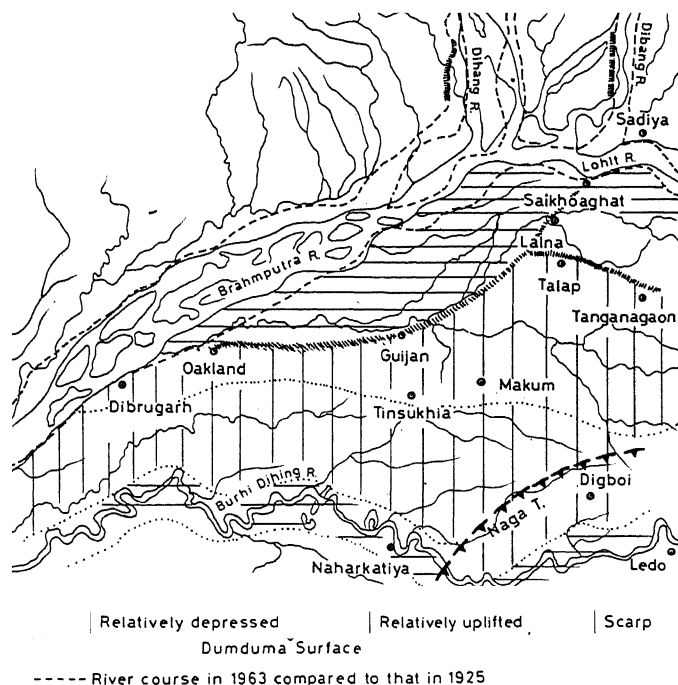


Figure 3. The wide Brahmaputra, choked with sediments, suddenly narrows down as it cuts a gorge to get through the rising block of the Meghalaya Plateau. The block is defined by N-S trending lineaments (presumably tear faults near Guwahati). (Satellite photo of Guwahati and its environs as viewed by IRS-1B on 29 January 1993, NRSA, Hyderabad.)



Figure 4. Slackening of the flow and probable partial ponding of the Brahmaputra evident from its sediment choked channel and the wide stretch of the flood plain characterized by marshy conditions (coloured indigo) as seen in the Kaziranga National Park area. (Digitally classified landuse photo, IRS-1C on 8 January 1996, NRSA, Hyderabad.)

into consideration the reality of the continuing tectonic movements on active faults, it should be evident that building of embankments and drainage channels in upper Assam would not bring lasting relief from flood hazards. The solution lies in channelizing discharge of the order of  $48,160 \text{ m}^3/\text{s}$  (ref. 12) of the Brahmaputra through canals, aqueducts, tunnels, etc. across the northward prolongation of the Meghalaya block, particularly between Guwahati and Hathimura and other places (west of Mikir Hills) where identified active faults cross its channel. The canals would have to be deepened periodically in order to keep pace with the rate of uplift of the block. Absence of channelization of the Brahmaputra in spate would always cause ponding, leading to deposition of sediments, reduction in carrying capacity and



**Figure 5.** The 15 August 1950 earthquake of magnitude 8.7 drastically affected the gradient of the Brahmaputra in upper Assam. The Talap–Gujjan–Oakland scarp is an expression of the uplift of the downstream block. This must have temporarily ponded the Brahmaputra<sup>13</sup>.

inundation of the flood plain. In my opinion, this is what is happening today. It will therefore be advisable to embark on a comprehensive multidisci-

plinary investigation of the Brahmaputra valley in Assam to provide a rational knowledge-based perspective for the design of flood resilient mitigation measures.

1. Goswami, S., *Souvenir: National Workshop on Geodynamics of North-eastern India*, Dibrugarh University, Dibrugarh, 1998, pp. 36–41.
2. Mukhopadhyay, M. and DasGupta, S., *Technophysics*, 1988, **149**, 299–322.
3. Acharyya, S. K., *Indian J. Geol.*, 1997, **69**, 211–234.
4. Nandy, D. R. and DasGupta, S., *Phys. Chem. Earth.*, 1991, **18**, 1147–1163.
5. Kayal, J. R. and De, R., *Bull. Seismol. Soc. Am.*, 1991, **81**, 131–138.
6. Gowd, T. N., Srirama Rao, S. V. and Chary, K. B., *Curr. Sci.*, 1998, **74**, 75–80.
7. Molnar, P., *J. Geol. Soc. India*, 1987, **30**, 13–27.
8. Gahalaut, V. K. and Chander, R., *Tectonophysics*, 1992, **204**, 163–174.
9. Rajal, B. S. and Madhwal, H. B., *Himalayan Geol.*, 1996, **17**, 17–32.
10. Chugh, R. S. and Valdiya, K. S., *Indian J. Geol.*, 1989, **61**, 1–13.
11. Oldham, R. D., *Memoir Geol. Surv. India*, 1899, **29**, 1–379.
12. Goswami, Dulal, C., in *Flood Studies in India*, Geol. Soc. India, Bangalore 1998, pp. 53–75.
13. *Proc. Intern. Symp. Neotectonics of South Asia*, Survey of India, Dehradun, 1986.

K. S. VALDIYA

*Geodynamics Unit,  
Jawaharlal Nehru Centre for  
Advanced Scientific Research,  
Bangalore 560 064, India*

## Avifauna of Mouling National Park, Arunachal Pradesh, India

Arunachal Pradesh includes a major portion of the eastern Himalayas, which has been recognized as one of the 18 biodiversity hotspots of the world<sup>1</sup>. Climatic features of this region have created a natural boundary making it an abode for a number of endemic species both flora and fauna<sup>2</sup>. Earlier works<sup>3–6</sup> on the avifauna of Arunachal Pradesh mainly covered Pakhui Wildlife Sanctuary, D'Ering Memorial Wildlife Sanctuary, Mehao Wildlife Sanctuary and its adjacent Mishmi Hills and Namdapha National Park. This is the first attempt to make a check-list of birds of Mouling National Park from the birdwatchers'

viewpoint. The long list indicates physical as well as biological richness of the habitat; such diverse avian species assemblages have also been recorded from the Western Ghats, another biodiversity hotspot<sup>5,6</sup>. The Mouling Hills harbour varied forest types; there are tropical wet evergreen, semievergreen subtropical broad-leaved hill forests, montane wet temperate forests while the wet hollows are occupied by cane brakes and the wet ground along the margins of the streams and rapids are covered with wet bamboo brakes. Such a variation in the vegetation of the locality has attracted a variety of bird species; a num-

ber of lotic habitats and chain pools are an added advantage to study the water-dependent birds of this region.

Mouling was declared a National Park in 1986 but little is known about its floral and faunal diversity. This park (lat. 28°33'N, long. 94°46'E) covers an area of 483 sq km and the configuration is gentle to very steep and rugged mountainous land. Steep slopes of these mountains are covered with dense evergreen and semi-evergreen vegetation. The whole national park is irrigated by a number of perennial brooks and streams. Thirteen major perennial streams flow down the slopes of Moul-

ing ranges and all voids in the mighty Siang River. This fast-flowing river system gives a special local topographical feature with much higher rainfall; greater atmospheric humidity and a reduced temperature range prevail in the lower elevations which give the area a climate different from that of other lowland tracts. Such a special condition is distinguished as 'montane climate', a class by itself. Very thick cane and bamboo brakes along the wet banks of the streams at lower altitudes and high water current and unpredictable drainage load in these lotic situations are a source of major hindrance in approaching the park. Notable plant species in the areas surveyed are *Terminalia myriocarpa*, *T. bellirica*, *T. citrina*, *Altingia excelsa*, *Canarium strictum*, *Castanopsis indica*, *C. hystrix*, *Albizia sapium*, *Amoora wallichii*, *Chukrasia tabularis*, *Toona ciliata*, *Duabanga grandiflora*, *Cinnamomum glanduliferum*, *Michelia excelsa*, *M. montana*, *M. kisopa*, *Musa* spp., *Dillenia pentagyna*, *Quercus* spp., *Betula alnoides*, *Arundinaria maling*, *Dendrocalamus hamiltoni*, *Bambusa pallida*, *Calamus erectus* and *C. floribunda*. Luxuriant growth and high density of tree ferns and screw pines are also noted. Thick growth of epiphytic plants is mainly constituted by a variety of mosses, ferns and orchids. Creepers, climbers and herbaceous flora are also abundant; at places different herbaceous species of the families Rosaceae, Acanthaceae, and Hypericaceae are densely grown.

Month-long expeditions with short visits were organized during winter (October to end of January) from 1995 to 1998. Due to hostile climatic conditions, it is very difficult to approach this forest with limited infrastructure except between November and March. This period maintains a uniform weather condition and appears to be excellent to study the passage migrants and winter visitors along with the resident bird species of the region. Observations were made in the altitude range of 460–1620 m. Lower altitudes (460–650 m) were selected for observation in 1995–1996 while higher elevations (840–1620 m) were studied in 1997–1998 to record the diversity and abundance of the avian species. Species were recorded during extensive trekking (about 65 km)

through the difficult terrain, covering all the salient forest types of this region. Nine different locations were selected and at each of these locations keeping the camp at the centre, an area encompassing 1 km radius was surveyed. Three to five survey treks (numbers varied with the approachability/ruggedness of the terrain) were made at each location towards different directions (selected randomly) from the camp between 4.00 and 16.00 h. At normal strolling speed the linear treks from the camp and back were performed to cover a 2 km (up and down) trail within a two-hour period. A Barigo (Germany) walking pedometer measured trekking distance. Results of independent observations following belt transect method<sup>7</sup> were later compared, consolidated and averaged, where necessary, to comment on the abundance and status of the species. Belt transects involved noting of the avian species sighted within 50 m on either side, both in front and above. Mist-net was also employed for closer observation and identification of smaller bird species. Species abundance is categorized by numbers in the text as follows: (1) Rare – Observed (singly or in pair or in party/groupings for gregarious species) or call heard only once during the study period; (2) Uncommon – Seen or call heard not more than thrice during the study period; (3) Regular – Seen or call heard not more than five times during the study period; and (4) Common – Seen and/or call heard more than five times during the study period.

Birds were observed in the field using NIKON (9 × 25) field binoculars. Information on their microhabitat and floral-avian affinity, if any, were also noted. Description of the study sites and the codes used in the text for the study locations are follows: RmC – Ramsingh Forest Rest House camp; altitude 680 m; 55 km drive from Jenging Divisional Forest Office; montane semi-evergreen biotope, SiC – Siyor camp; altitude 460 m; 5 km south-west of Ramsingh tribal village; montane semi-evergreen biotope, NgC – Nguri camp; altitude 500 m; 3 km trek to south of Siyor camp; montane climate semievergreen forests; Siring rivulet sides bordered by sparingly distributed bamboo brakes, KeC – Kebung camp; altitude 560 m; 6 km south of Nguri camp; montane climate evergreen forests; thick bamboo

brakes alongside Siring rivulet, KuC – Kubsef camp; altitude 650 m; 4 km farther south of Kebung camp; Siring rivulet gorge with steep rise of the walls on either side; right bank with thick growth of bamboo and cane brakes while the left wall was completely denuded by heavy landslips, BvC – Bomdo village camp; altitude 840 m; 30 km from Ramsingh FRH; a small *adi* tribal hamlet, lightly inhabited; montane subtropical broadleaved hill forest, EpR – Epong ridge; altitude 1450 m; 2.5 km south-west of Bomdo village; montane wet temperate broadleaved forest with predominant evergreen species, EgC – Egong camp; altitude 1400 m; 2 km east of Epong ridge site; on the bank of fast flowing Sidi rivulet; montane wet evergreen biotope, and AnR – Angong ridge; altitude 1620 m; 5 km west of Egong camp; wet temperate broadleaved forest with predominant evergreen species.

For scientific nomenclature and arrangement order of the bird species, the book by King *et al.*<sup>8</sup>, was followed in general. However, where we differed, especially for scientific names of the species, Ali<sup>5,9</sup> and Schavense<sup>10</sup> were followed. Different indices to comment on the community structure were calculated following Odum<sup>11</sup>.

One hundred and fourteen bird species under 38 families were recorded from 9 different study locations and are listed below along with location and abundance codex.

*Phalacrocorax carbo* 1SiC; *Mergus mergan* 1SiC; *Pernis ptilorhynchus* 3BvC; 2EpR; *Accipiter nisus* 2BvC; 1NgC; 2AnR; *Circus melanoleucos* 1SiC; *Spizaetus nipalensis* 1BvC; 1EpR; *Microhierax melanoleucos* 1KeC; *Falco tinnunculus* 1NgC; *Treron bicincta* 2EpR; 1AnR; *Ducula badi* 1EpR; 1AnR; *Columba hodgsonii* 1RmC; 1AnR; *Streptopelia orientalis* 1RmC; 2BvC; 1EpR; *Psittacula finschii* 1BvC; 2AnR; *Otus spilocephalus* 1RmC; 2EgC; *Athene brama* 3RmC; 2BvC; *Stryx aluco* 2EgC; *Harpactes erythrocephalus* 1SiC; *H. wardi* 1EgC; *Ceryle lugubris* 3SiC; 3NgC; 2KeC; 3KuC; *Halcyon coromanda* 1EgC; *Ceyx erithacus* 1KeC; *Megalaima virens* 3BvC; 2NgC; 2KeC; *M. franklinii* 2AnR; *M. australis (duvauceli)* 1NgC; 1KeC; BvC; EpR; *Sasia ochracea* 1RmC; 1BvC; *Picus canus* 1RmC;

1EgC; 1AnR; *P. flavinucha* 2EpR; 2AnR; *Picoides cathpharius* 1BvC; 2EgC; *Psarisomus dalhousiae* 2EpR; *Delichon urbica* 3RmC; 2SiC; 2NgC; 2KeC; 2KuC; 2BvC; *Hemipus picatus* 2SiC; 3AnR; *Tephrodornis virgatus* (gularis) 2BvC; 1EpR; 2EgC; *Coracina novaehollandiae* (javensis) 2EpR; *Pericrocotus flammeus* (speciosus) 4NgC; 2BvC; 2EpR; 2AnR; *P. ethologus* 1EpR; 2EgC; *Aegithina tiphia* 2RmC; 2BvC; 2EpR; *Chloropsis hardwickii* 1BvC; 1EpR; 2EgC; 2AnR; *Irena puella* 2EgC; *Pycnonotus jacosus* 2RmC; 3SiC; 3NgC; 1BvC; *P. leucogenys* 2RmC; 3BvC; *Dicrurus leuphaeus* 1BvC; 1EpR; 2AnR; *D. aeneus* 1SiC; 1NgC; 1KeC; 2EpR; 3AnR; *D. remifer* 1KeC; 1BvC; 2EgC; *D. hotten-tottus* 3EgC; *Oriolus trailii* 1EgC; *Urocissa erythrorhyncha* 2EgC; *Corvus macrorhynchos tibetosinensis* 2RmC; BvC; *Aegithalos concinnus* (anna-mensis) 2RmC; BvC; 1EpR; *Parus dichorus* 3AnR; *P. monticolus* 2RmC; 3BvC; 2EgC; *P. spilonotus* 1RmC; 2EpR; 2AnR; *Melanochlora sultanea* 2BvC; 2EgC; *Sitta formosa* 1EpR; 3AnR; *Cinclus pallasi* 4SiC; 4NgC; 4KeC; 4KuC; *Troglodytes troglodytes* 4SiC; 2EgC; *Pomatorhinus hypoleucos* 2EgC; *P. ochraceiceps* 1EgC; 1AnR; *Turdoides striatus* 2BvC; 2EpR; *Napothera brevicaudata* 1SiC; 1NgC; 1KeC; 1KuC; 2EpR; 2EgC; *Spelaornis badeigularis* 3KeC; 3KuC; 2EgC; 3AnR; *Garrulax leucolophus* 3NgC; 3KeC; 3KuC; 3BvC; 4EpR; 2AnR; *G. monileger* 2RmC; 3SiC; 2NgC; 2KeC; 2KuC; 4EpR; 2AnR; *G. Pectoralis* 2SiC; 2KeC; 3BvC; 2EpR; 2AnR; *Cutia nipalensis* 1EpR; 3EgC; *Actinodura egertoni* 2EpR; 2EgC; *A. waldeni* (nipalensis) 2AnR; *Yuhina bakeri* 3SiC; 3NgC; 2EgC; *flavicollis* 2SiC; 2NgC; 1AnR; *Y. zantholeuca* 3EgC; *Paradoxornis atosupercillari* 1KeC; 1EgC; *Erithacus pectoralis* 1BvC; *Phoenicurus aureus* 2SiC; 2NgC; *Rhyacornis fuliginosus* 2SiC; 2NgC; 2KeC; 2KuC; *Chaimarrornis leucocephalus* 3SiC; 3NgC; 3KeC; 3KuC; *Enicurus scouleri* 4RmC; 3SiC; 1NgC; 1KeC; 2KuC; 2BvC; *E. schistaceus* 2NgC; 1KeC; 1KuC; 2BvC; *Monticola cinclorhynchus* 2RmC; 3BvC; *Myiophonus caeruleus* (temminckii) 2RmC; 2SiC; 1EgC; *Seicercus affinis* (burkii) 2BvC; 2EpR; *S. castaneiceps* 2RmC; 2BvC; 3EpR; *Phylloscopus ricketti* 3EgC; *P. fuscatus*

2EgC; 3AnR; *Phragmaticola aedon* 3EgC; 2AnR; *Orthotomus cuculatus* (cucullatus) 1EgC; *Tesia castaneocoronata* 4EgC; 1AnR; *Muscicapa thalassina* 1BvC; 2EpR; 2EgC; 3AnR; *Niltava macgrigoriae* 2RmC; 3EpR; *Cyornis banyumas* 1EpR; 1EgC; 2AnR; *Rhipidura hypoxantha* 2EpR; *Prunella fulvescens* 2AnR; *P. immaculata* 1EpR; 1EgC; *Motacilla alba alboides* 3RmC; 2BvC; *M. cinerea* (caspica) 2NgC; 2KeC; 2KuC; *M. flava* 2NgC; 2KeC; 2KuC; *M. maderaspatensis* 1SiC; 1NgC; 1KeC; 1KuC; *Dendronanthus indicus* 1SiC; 1NgC; 1KeC; 1KuC; 2LpR; *Lanius cristatus* 1EgC; 2AnR; *L. tephronotus* (schach) 2SiC; 2KeC; 1BvC; 1EpR; *Gracula religiosa intermedia* 3RmC; 2BvC; 1AnR; *Aethopyga nipalensis* (ezrai) 1KeC; 1KuC; 1EpR; 3AnR; *A. saturata* (johnsi) 3EgC; 2AnR; *A. siparaja* 2RmC; 2BvC; 2EpR; *Arachnothera longirostra* 1SiC; 1NgC; 3EgC; *Dicaeum ignipectus* 2EgC; *Zosterops palpebrosa* 2RmC; 2BvC; 2EpR; *Passer montanus* 3RmC; 3BvC; *P. rutilans* 2RmC; *Lonchura striata* 2EpR; 3AnR; *L. punctulata* 3RmC; 3SiC; 2NgC; 2KeC; *L. malacca* 1RmC; 2EpR; *Serinus thibetanus* 1BvC; *Coccothraustes melanozanthos* 1EgC; *Emberiza rutila* 1BvC; *Melophus lathamii* (melanicterus) 2RmC; 2SiC; 3AnR.

Table 1 depicts some of the useful indices to comment on the species structure in the avian communities of different localities. From the beginning, eastern Himalayas was considered to be one of the biodiversity hotspot, with 39% endemism<sup>12</sup>. The large number of bird species recorded in this study amply speak for the niche diversity and richness of the Mouling Forests. In the present study, 78 species were observed between 450 and 850 m, while 83 species between 850 and 1650 m. Of these, 47 were identified as common species, observed to occur at both lower and higher reaches of the forest (similarity index 0.58). Shannon-Weaver index of general diversity calculated to comment on the overall diversity, as it is reasonably independent of sample size<sup>11</sup>, varied from 3.94 to 5.75 (mean 5.15; SD 0.58). However, this index of general diversity was observed to be marginally higher for the avian community of the higher reaches (diversity index 4.70) than for the lower elevations (diversity index 4.56). Such was the

case for evenness and species richness indices too.

Index of dominance (range 0.09–0.30; mean 0.126; SD 0.005) was fairly low at all study sites, except for KuC at 650 m altitude, where the index of dominance was calculated as 0.3. This could possibly be attributed to the physical feature of the site and the abundance of water-dependent birds here. The KuC site exhibited lowest diversity index of 3.94. This site also showed minimum species richness (richness index 4.34) and evenness (evenness index 1.14) when compared to the avian community structure of the locations of the adjacent locations at the lower reaches. For example, RmC at 680 m and SiC at 460 m exhibited higher richness (6.87 and 6.46, respectively) and evenness (1.29 and 1.55, respectively). It is felt that heavy land-slips had affected the vegetation and avian community at KuC while relatively undisturbed locations supported a comparatively rich avian community showing more diversity and little dominance. BvC at 840 m altitude exhibited the highest species diversity (richness index 5.75) and very low dominance (dominance index 0.11). In locations at further lower elevations, diversity index varied between 3.94 and 5.26 while it varied between 5.49 and 5.70 at locations with even higher elevations. Among the locations in higher altitudes, EpR at 1450 m showed minimum species dominance (dominance index 0.09) and maximum species richness (richness index 9.50).

Montane wet evergreen biotope extends an intricate microclimate of its own, characterized by its special set of physico-chemical and biological features. These conditions have encouraged its own avian assemblage, which is calculated as over 31.5% in the present investigation. It may be pointed out that only a few selected patches of Mouling Forests were studied; a more intensive study would surely result in identifying many more species from the eastern Himalayan wet evergreen biotope. In the present study, Sulfur-breasted Warbler (*Phylloscopus ricketti*) is being recorded for the first time in the Indian subcontinent. However, as the commoner species of leaf warblers were not recorded from the areas under study, confirmation of the occurrence of *P. ricketti* needs

**Table 1.** Different indices to comment on the species structure of the study sites

| Study sites    | Birds site | Species site | Richness index | Diversity index | Evenness index | Dominance index |
|----------------|------------|--------------|----------------|-----------------|----------------|-----------------|
| RmC            | 59         | 29           | 6.87           | 5.26            | 1.29           | 0.16            |
| SiC            | 56         | 27           | 6.46           | 5.11            | 1.55           | 0.19            |
| NgC            | 52         | 26           | 6.34           | 4.95            | 1.52           | 0.18            |
| KeC            | 43         | 25           | 6.38           | 4.42            | 1.37           | 0.15            |
| KuC            | 32         | 16           | 4.34           | 3.94            | 1.14           | 0.30            |
| BvC            | 78         | 40           | 8.95           | 5.75            | 1.56           | 0.11            |
| EpR            | 75         | 42           | 9.50           | 5.49            | 1.47           | 0.09            |
| EgC            | 77         | 40           | 8.98           | 5.69            | 1.54           | 0.10            |
| AnR            | 73         | 36           | 8.16           | 5.70            | 1.59           | 0.13            |
| mean           | 60.5       | 31.2         | 7.33           | 5.15            | 1.40           | 0.126           |
| SD             | 15.4       | 8.25         | 1.58           | 0.58            | 0.15           | 0.05            |
| Lower reaches  | 320        | 78           | 13.35          | 4.56            | 1.05           | 0.007           |
| Higher reaches | 225        | 83           | 15.14          | 4.70            | 1.06           | 0.009           |

further observational support. Absence of relatively common species of foothills, peripheral jungles and around habitations in the study sites and alongside the occurrence of very rare Mishmi Wren-babbler and many other less common species also demands further confirmation and more intensive studies. Some of the species, though recorded as rare in the present study, might appear regularly during other seasons or if the study was more intensive. The short list of species under the families, Sylviidae, Prunellidae and Dicaeidae was due to the limitations in study duration. However, the present effort records, for the first time, the avian assemblage of Mouling National Park with comments on their community

structure. This study would help in the initiation of more detailed studies to enrich the list of species and to record the nature and extent of passage and local migration with the resident spe-

1. Mayers, N., *Environmentalist*, 1990, **10**, 243–256.
2. Mukhopadhyay, S. K. and Mukhopadhyay, D., *Sanctuary Asia*, 1998, **18**, 34–37.
3. Singh, P., *Arunachal Forest News*, 1991, **9**, 1–10; *ibid*, 1995, **13**, 17–23.
4. Chowdhury, A., *ibid*, 1992, **10**, 39–42.
5. Ali, S., in *Field Guide to the Birds of the Eastern Himalayas*, Oxford Univ. Press, Delhi, 1977.
6. Mukhopadhyay, S. K., Khan, T. N., Banerjee, K. K. and Banerjee, H.,

*J. Bengal Nat. Hist. Soc.*, 1996, **15**, 37–48.

7. Southwood, T. R. E., *Ecological Methods*, ELBS, Cambridge, 1978, 2nd edn.
8. King, B., Woodcock, M. and Dickinson, E. C., in *A Field Guide to the Birds of South-East Asia*, Collins, London, 1991.
9. Ali, S., in *The Birds of Sikkim*, Oxford Univ. Press, Delhi, 1962.
10. Schavense, De M. R., in *The Birds of China*, Smithsonian Inst. Press, Washington DC, 1984.
11. Odum, E. P., in *Fundamentals of Ecology*, W. B. Saunders Co. Philadelphia, 1971, 3rd edn.
12. McNeely, J. A., Miller, K. R., Reid, W. V., Mittermeier, R. A. and Warner, T. B., in *Conserving the World's Biological Diversity*, IUCN Publ. Service, Switzerland, 1990.
13. Pramod, P., Joshi, N. V., Ghatge, Utkarsh and Gadgil, M., *Curr. Sci.*, 1997, **73**, 122–127.

**ACKNOWLEDGEMENTS.** We are grateful to Mr B. A. Mathews, IFS, the Chief Conservator of Forests (Wildlife), Govt. of Arunachal Pradesh, Itanagar, for encouragement and help. S.K.M. thanks the Director of Public Instructions, Govt. of West Bengal, for laboratory facilities.

A. K. SEN\*

S. K. MUKHOPADHYAY\*\*

\*Divisional Forest Office,  
Mouling National Park,  
Jenging 791 002, India

\*\*Department of Zoology,  
Hooghly Mohsin Government College,  
Chinsurah 712 101, India

## Molecular markers for genetic fidelity during micropropagation and germplasm conservation?

In recent years, with the advent of recombinant DNA technology and PCR, molecular markers are being used for a variety of studies. The molecular markers include Restriction Fragment Length Polymorphisms (RFLPs), Random Amplified Polymorphic DNAs (RAPDs), Amplified Fragment Length Polymorphisms (AFLPs), Simple Sequence Repeats (SSRs) or Sequence Tagged Microsatellite Sites (STMS),

Sequence Tagged Sites (STS), DNA Amplification Fingerprinting (DAF) and Microsatellite Primed-PCR (MP-PCR) (ref. 1). More recently, molecular markers have also been used for testing the genetic fidelity during micropropagation/*ex situ* conservation on the one hand, and for characterization of plant genetic resources on the other. This aspect of the use of molecular markers has received attention in recent years

due to the significance that is being attached to micropropagation of elite genotypes and to the *in situ* and *ex situ* conservation of plant genetic resources (PGRs). Molecular markers have particularly been suggested to be useful for confirmation of genetic fidelity in micropropagated tree species, where life span is quite long and performance of micropropagated plants could only be ascertained after their long

juvenile stage in field conditions. In India also, studies have been conducted and research projects funded for research where lack of polymorphism shown through the use of molecular markers has been used to infer genetic fidelity<sup>2,3</sup>.

In commercial industry, where micropropagation technology has been developed, their foremost concern is the maintenance of true-to-type nature of the micropropagated plants *vis-à-vis* explant source. This can be achieved by developing the micropropagation protocols based either upon axillary branching or somatic embryogenesis. These two methods are believed to give rise to genetically uniform and true-to-type plants, since the organized meristems do not undergo genetic changes that might arise during cell division or differentiation from callus cultures<sup>4,5</sup>. Although a number of reports support this view<sup>6-8</sup>, there are some other reports also which document the occurrence of somaclonal variation even among plants derived either through somatic embryogenesis or through enhanced axillary branching cultures. It has, therefore, been suggested that commercial application of tissue culture to perennial crops must await adequate quality check under field conditions irrespective of the method used for micropropagation<sup>9</sup>. However, if the analysis is carried out during various cultural passages, it would establish genetic variation (if any) very early in the cultural systems, so that one may like to suitably modify the micropropagation protocols to avoid the above variation.

Several cytological, isozyme and molecular markers have been used to detect the variation and/or confirm the genetic fidelity in micropropagated plants<sup>3</sup>. A large number of RFLPs were recorded in regenerated maize, rice, wheat, barley, triticale, potato<sup>3</sup> and some tree species including populus, eucalyptus and coffee<sup>1</sup> for studying the variation and genetic fidelity during micropropagation. Brown *et al.*<sup>10</sup> also suggested the use of PCR in the analysis of tissue culture-derived plants, so that PCR has been used specially in the form of RAPDs in onion<sup>11</sup>, *Picea*<sup>12</sup>, populus and eucalyptus species<sup>2,3</sup> and in the form of MP-PCR in eucalyptus, populus and coffee species<sup>3</sup>.

In several reports, variations have been observed through molecular mark-

ers and characterized as somaclonal variation. For instance in rice, doubling the time of *in vitro* culture resulted in quadruplicating the detected DNA polymorphisms in regenerants<sup>13</sup>. However, in some other studies, the lack of polymorphism in micropropagated plants screened through molecular markers was used to suggest genetic fidelity. For instance, in a study on *Picea* the genetic integrity during somatic embryogenesis has been studied using RAPDs<sup>12</sup>. In India also, an extensive study on genetic fidelity and molecular diagnostics in micropropagation systems was carried out where several molecular markers including RFLPs (using rDNA probes and mtDNA probes), RAPDs, MP-PCR and oligonucleotide in-gel hybridization were used in micropropagated clones of 4 tree species namely *Populus deltoides*, *Eucalyptus tereticornis*, *E. camaldulensis* and *Coffea arabica*<sup>3</sup>. In this study, the authors inferred genetic fidelity in those micropropagated clones where molecular markers failed to detect any polymorphism. In their study, the micropropagated clones of *P. deltoides*, when examined for RFLPs, using three heterologous rDNA probes, showed uniformity in combination with 6 base cutter enzymes but the same clones revealed distinct variation using 4 base cutter enzymes. A reverse situation was observed in *Coffea arabica*. It is apparent thus, that sometimes, the same clones may show uniformity with one molecular marker and variation with another marker. In further studies, while using a set of 25 RAPD primers, 4 out of 5 clones of *P. deltoides* and all the clones of *E. tereticornis* and *E. camaldulensis* showed uniformity. The use of 5 oligonucleotides complementary to microsatellites namely (GATA)<sub>4</sub>, (GACA)<sub>4</sub>, (GTG)<sub>5</sub>, and (TCC)<sub>5</sub> in MP-PCR and in-gel hybridization also showed uniformity. We, however, believe that the use of a larger number of RAPD primers, additional microsatellites and other molecular marker systems could detect the variation in those clones also where uniformity was observed with a limited number of primers or oligonucleotides/enzyme combinations as above. Such a belief is based on our own experience in bread wheat, where failure of the detection of polymorphism by a molecular marker system

indicated the inadequacy of the molecular marker for detecting polymorphism, so that relatively more powerful molecular markers need to be used to detect polymorphism. In our own studies, different molecular markers, namely oligonucleotide in-gel hybridization, RAPDs, MP-PCR, DAF, STS and STMS, have been used in 10 bread wheat genotypes. The use of as many as 23 SSR probes in combination with 14 restriction enzymes (a total of 142 probe-enzyme combinations) failed to detect the polymorphism in these genotypes<sup>14</sup>. Our unpublished preliminary results on RAPDs, MP-PCR and AFLPs also showed lack of polymorphism in these genotypes. But this does not mean absence of polymorphism in the material studied but instead suggested inadequacy of these marker systems, since other molecular markers (e.g. DAF, STS and STMS) did detect adequate and reproducible polymorphism in the same material<sup>15-17</sup>. We, therefore, are of the opinion that any failure to detect polymorphism should not be used to infer genetic fidelity. We also like to emphasize that each marker system screens only a fraction of the genome and not the whole genome and that different markers may screen different fractions of the genome. The entire genome cannot be studied on the basis of only one type of molecular marker. For instance, the oligonucleotide in-gel hybridization is only suitable for studying the repetitive DNA<sup>18</sup>; RFLPs are suitable only for the study of variation in restriction sites of a particular restriction enzyme. In view of this, any molecular marker system needs to be first assessed for its suitability for DNA fingerprinting and for ascertaining genetic fidelity.

Molecular markers have also been used to find out whether or not additional variation originates during storage and conservation, (i.e. detect duplications, seed mixtures, inadvertent outcrossing and genetic drift). For this purpose, our experience suggests that DNA fingerprinting using microsatellites, DAF and AFLP markers may be relatively more suitable. Microsatellite markers have been used successfully to determine the degree of relatedness among individuals or groups of accessions, to clarify the genetic structure, or partitioning of variation among individuals, accessions, population and

## SCIENTIFIC CORRESPONDENCE

species of rice<sup>18</sup>. RFLPs (using nDNA and cpDNA probes) and RAPDs were also used for characterization and identification of genetic resources of perennial crops like *Musa* and to solve problems related to plant genetic diversity conservation<sup>19</sup>. The potential of molecular markers have also been shown in other crops for characterization and identification of core collection for germplasm conservation<sup>20</sup>. For germplasm conservation also, we believe that individual molecular markers, unless proved to be suitable for DNA fingerprinting, should not be used to study the genetic fidelity but only for detection of genetic variation arising during storage and conservation.

1. Mohan, M., Nair, S., Bhagwat, A., Krishna, T. G., Yano, M., Bhatia, C. R. and Sasaki, T., *Mol. Breeding*, 1997, **3**, 87-103.
2. Rani, V., Parida, A. and Raina, S. N., *Plant Cell Rep.*, 1995, **14**, 459-462.
3. Rani, V. and Raina, S. N., in *Genetics and Biotechnology in Crop Improvement* (eds Gupta, P. K., Singh, S. P., Balyan, H. S., Sharma, P. C. and Ramesh, B.), Rastogi Publications, Meerut, 1998, pp. 370-380.
4. Vasil, I. K., in *Tissue Culture in Forestry and Agriculture* (eds Henke, R., Hughes, K., Constanin, M. and Hol-laender, A.), Plenum Press, New York, 1985, pp. 31-47.
5. Shenoy, V. B. and Vasil, I. K., *Theor. Appl. Genet.*, 1991, **83**, 947-955.
6. Hanna, W. W., Lu, C. and Vasil, I. K., *Theor. Appl. Genet.*, 1984, **67**, 155-159.
7. Swedlund, B. and Vasil, I. K., *Theor. Appl. Genet.*, 1985, **69**, 575-581.
8. Armstrong, C. L. and Green, C. E., *Planta*, 1985, **164**, 207-214.
9. Dunstan, D. I. and Thorpe, T. A., in *Cell Culture and Somatic Cell Genetics of Plants vol. 3, Plant Regeneration and Genetic Variability* (ed. Vasil, I. K.), Academy Press, Orlando, 1986, pp. 223-241.
10. Brown, P. T. H., Lange, F. D., Kranz, E. and Lorz, H., *Mol. Gen. Genet.*, 1993, **237**, 311-317.
11. Bohanec, B., Jakse, M., Ihan, A. and Juornik, B., *Plant Sci.*, 1995, **104**, 215-224.
12. Isabel, N., Temblay, L., Michaud, M., Tremblay, F. M. and Bonsquet, J., *Theor. Appl. Genet.*, 1993, **86**, 81-87.
13. Muller, E., Brown, P. T. H. and Hartke, S., *Theor. Appl. Genet.*, 1990, **80**, 673-679.
14. Varshney, R. K., Sharma, P. C., Gupta, P. K., Balyan, H. S., Ramesh, B., Roy, J. K., Kumar, A. and Sen, A., *Plant Breeding*, 1998, **117**, 182-184.
15. Sen, A., Balyan, H. S., Sharma, P. C., Ramesh, B., Kumar, A., Roy, J. K., Varshney, R. K. and Gupta, P. K., *Wheat Inf. Ser.*, 1997, **85**, 35-42.
16. Prasad, M., Varshney, R. K., Kumar, A., Balyan, H. S., Sharma, P. C., Edwards, K. J., Singh, H., Dhaliwal, H. S., Roy, J. K. and Gupta, P. K., *Theor. Appl. Genet.*, 1999, **98** (in press).
17. Roy, J. K., Prasad, M., Varshney, R. K., Balyan, H. S., Blake, T. K., Dhaliwal, H. S., Singh, H., Edwards, K. J. and Gupta, P. K., *Theor. Appl. Genet.*, 1998 (accepted).
18. Gupta, P. K. and Varshney, R. K., *Euphytica*, 1999 (submitted after revision).
19. Bhat, K. V., Lakhnapaul, S., Chandel, K. P. S. and Jarret, R. L., in *Molecular Genetic Techniques for Plant Genetic Resources* (eds. Ayad, W. G., Hodgkin, T., Jaradat, A. and Rao, V. R.), IPGRI, 1997, pp. 107-117.
20. Ayad, W. G., Hodgkin, T., Jaradat, A. and Rao, V. R., in *Molecular Genetic Techniques for Plant Genetic Resources*, IPGRI, Rome, 1997.

ACKNOWLEDGEMENTS. Thanks are due to the Department of Biotechnology and the Council of Scientific & Industrial Research, New Delhi, for financial assistance.

P. K. GUPTA  
RAJEEV K. VARSHNEY

*Molecular Biology Laboratory,  
Department of Agricultural Botany,  
Ch. Charan Singh University,  
Meerut 250 005, India*

# Photonic gap materials

J. B. Pendry

Department of Physics, The Blackett Laboratory, Imperial College, Prince Consort Road, London SW7 2BZ, UK.

**The concept of a photonic material is explained in terms of Bragg diffraction. Analogies are also made with electrons in semiconductors. Possible routes to manufacture of these structures are explored as some naturally occurring micro-periodic structures. The article concludes by giving some background to computational modelling of these materials.**

## The concept of a photonic crystal

As the world demands more computers and communication we turn increasingly to optical devices whose bandwidth and speed of execution offer great potential. However materials science has lagged behind in this rush into the optical domain. Optical properties of materials are not always well-matched to the functions we seek. This is in contrast to the vast range of electronic properties available to us. In the electronic domain we can almost make materials to order. The main cause of this richness in electronic properties is the interaction of electrons with the periodic structure of the materials. It is this interaction that decides whether a material will be a metal, a semiconductor, or an insulator, and can be further exploited to fine-tune the detailed electronic properties. Change the structure change the properties.

It was this concept that led Yablonovitch<sup>1</sup> to propose that we try the same trick with light. Interaction of electromagnetic waves with periodic structures goes back to Bragg and his observation that planes of atoms can act like perfect mirrors to X-rays when the Bragg condition is met (Figure 1):

$$\lambda = 2d\sin(\theta \pm \delta).$$

In fact the perfect mirror behaviour holds over a range of angles,  $\pm\delta$ , determined by how strongly the atoms scatter the X-rays. Any given arrangement of atoms will contain many possible Bragg planes reflecting X-rays from different directions. As a crystal is turned in a beam of X-rays it will briefly 'glint' as each Bragg condition is met. Figure 2 illustrates the point.

Thus we know that a crystal rejects X-rays for certain limited angles of incidence. The concept of Bragg reflection applies equally well to visible radiation except that we cannot rely on atoms to do the work for us. The material must have some periodic structure on the scale of the wavelength of light – a fraction of a micron. In fact, nature has made this arrangement for us in the case

of gemstone opal. Some years ago, using an electron microscope it was shown that the brilliant colours observed in precious opal were due to mesoscale structure within the mineral. The structure had eluded previous workers because the scale was too fine to be seen with optical instruments, and too coarse to be observed by X-rays. However, it is now possible to make beautiful electron micrographs that reveal the face-centred cubic close-packed arrangement of the microscopic silica spheres that constitute opal. Figure 3 shows such a micrograph.

Nearly all of biology is 'engineered' on the micron scale and with the help of DNA very complex structures are manufactured. Not surprisingly the optical properties are frequently exploited, nowhere with more spectacular effect than in the butterfly. Many species show iridescent green or blue patches and these owe their colouring to diffraction from periodic materials in the scales of the wing. Figure 4 shows a photograph of a Peacock butterfly where the 'eyes' exhibit the characteristic blue metallic sheen of a photonic material. Figure 5 shows a somewhat enlarged section of an almost entirely blue butterfly, the Adonis Blue, in which the tiny sub-millimetric scales are visible, and in Figure 6 we see an electron micrograph of a scale, the entity responsible for the colour. Diffraction from a three-dimensional array of holes in the scale gives rise to its characteristic colour. Man has not yet completely mastered the art of manufacturing three-dimensional optical structures which nature produces with such ease.

So, just like electrons, photons can be pushed around by the structure of a material. Yablonovitch wanted to find out if just as a semiconductor has a forbidden band of energies within which no electron could enter the crystal, is it possible to make a periodic dielectric such that in a forbidden range of frequencies no photon could enter the crystal. What we need to do is find a periodic material in which the scattering of light is so strong that the rejection windows of the different Bragg planes overlap (Figure 7). When this happens photons will be rejected whatever direction they attempt to penetrate the material. In fact, such a material could truly be called a 'photonic insulator'.

## Realizing the concept

Although the *concept* is a simple one, *realizing* a material structured on a sub-micron scale in three-dimensions

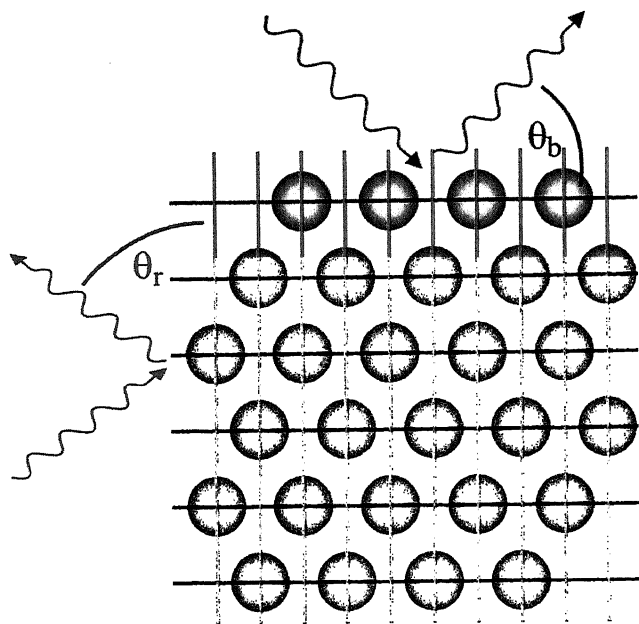


**Figure 1.** A regular array of atoms diffracts X-rays when the Bragg condition is met. For incident X-rays of a given wavelength different planes reflect at different Bragg angles.

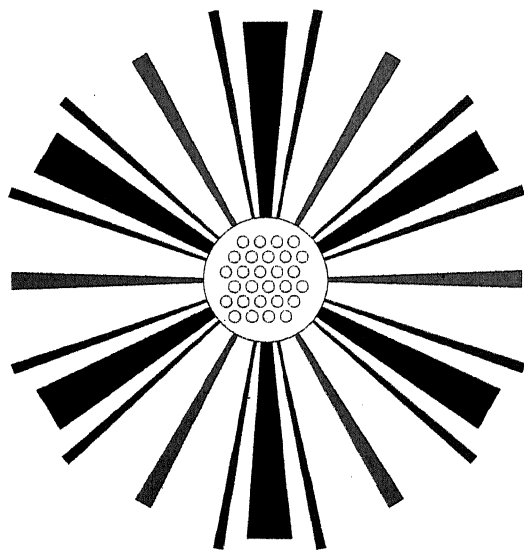


**Figure 2.** Bragg scattering for X-rays. Each set of planes acts like a mirror in a *small* range of angles which scarcely overlap.

is a highly non-trivial exercise. In opals, nature does the work for us by close packing spheres. Unfortunately this material, although beautiful, falls short of perfection – it is not a photonic insulator. The dielectric contrast between silica and air is too small, and the structure consisting of close-packed spheres is not sufficiently favourable. However Yablonovitch has shown<sup>2,3</sup> that there is a structure manufactured by drilling holes that does behave as a photonic insulator. This structure has

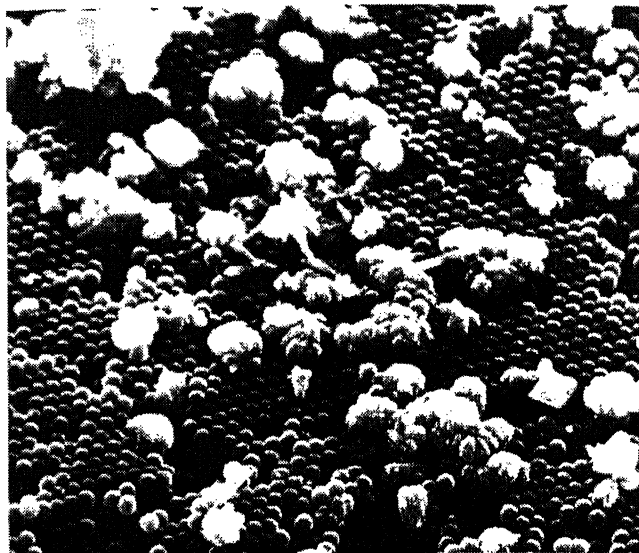


**Figure 3.** An electron micrograph of precious opal comprising sub-micron-sized silica spheres arranged in a face-centred cubic close-packed structure. The individual spheres are clearly visible under a layer of surface clutter.



**Figure 4.** Many butterflies owe their colour to diffraction by three-dimensional micro-structures within the wings. This is particularly true of blues or greens which exhibit a metallic sheen, as in the 'eyes' of this Peacock (*Inachis io*).

been christened 'Yablonovite' in honour of its inventor, and its construction is given in Figure 8.

If the refractive index of the host material is of the order of 3.6 or greater, this material is a photonic insulator. This was demonstrated in an elegant manner by observing that all structured materials obey a very general scaling law – if a given structure is a photonic insulator for incident light of wavelength  $\lambda$ , then another



**Figure 5.** The wing of a butterfly consists of a series of scales each a fraction of a millimetre long. In this photograph of an Adonis Blue (*Lysandra bellargus*) the small scales are visible as striations of the blue section of the wing. The black spots are caused by the occasional missing scale.

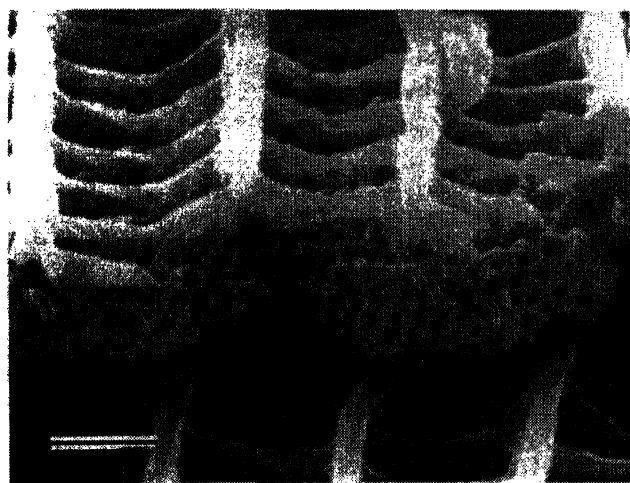


**Figure 6.** Electron micrograph of a broken scale taken from the butterfly *Mitoura grynea* revealing a periodic array of holes responsible for the colour. The bar in the bottom left is one micron long. (Taken from ref. 10).

material structured on double the length scale of the first, will also be a photonic insulator, but at incident wavelength  $2\lambda$ . This is true provided that the dielectric function does not depend on frequency. Therefore, it should be possible to make a proof of principle experiment on a much larger structure, active in the microwave range, and much more easily constructed, than to invoke

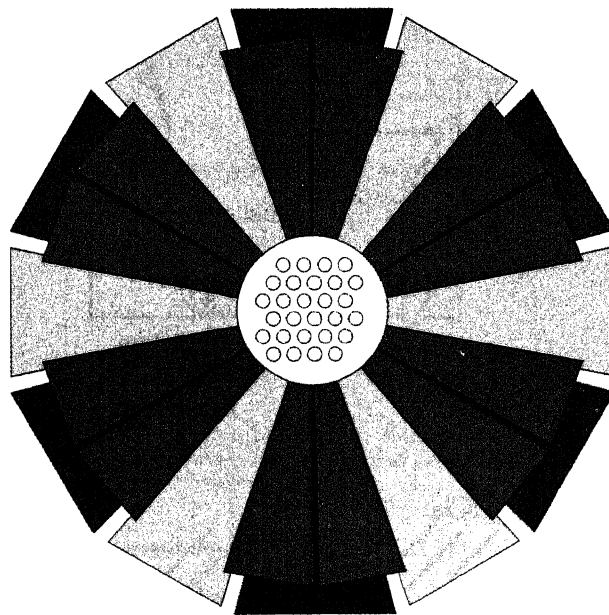


**Figure 7.** Bragg scattering for a photonic material. Each set of planes acts like a mirror in a large range of angles which overlap completely. Under these circumstances no radiation can penetrate into the material which is a *photonic insulator*. For a limit range of frequencies, the band gap, radiation is rejected whatever the incident angle.

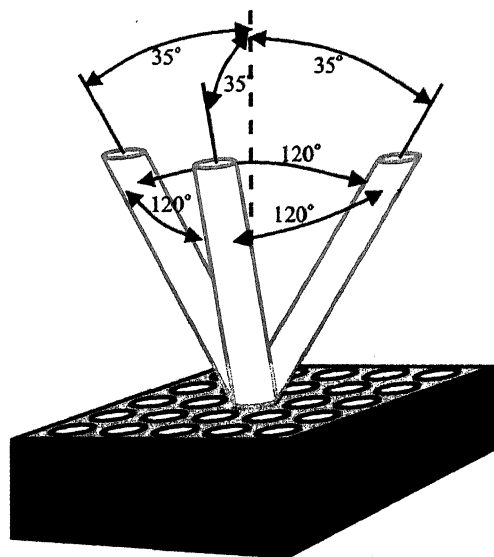


**Figure 8.** 'Yablonovite': a slab of material is covered by a mask consisting of a triangular array of holes. Each hole is drilled through three times, at an angle  $35.26^\circ$  away from normal, and spread out  $120^\circ$  on the azimuth. The resulting criss-cross of holes below the surface of the slab produces a fully three-dimensionally periodic *fcc* structure.

the scaling theorem to prove that if only a small structure could be manufactured, it would function as an insulator in the visible.

Figure 9 shows Yablonovitch's measurements for a sample of Yablonovite made with unit cell dimensions of a few millimetres and the band gap is clearly visible.

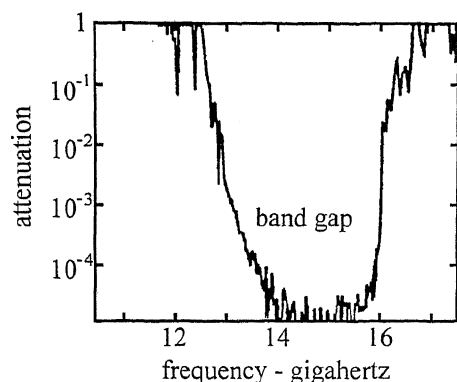


Figure 9. The transmission coefficient to microwaves of a sample of Yablonovite that shows a large band gap at frequencies around 14 GHz.

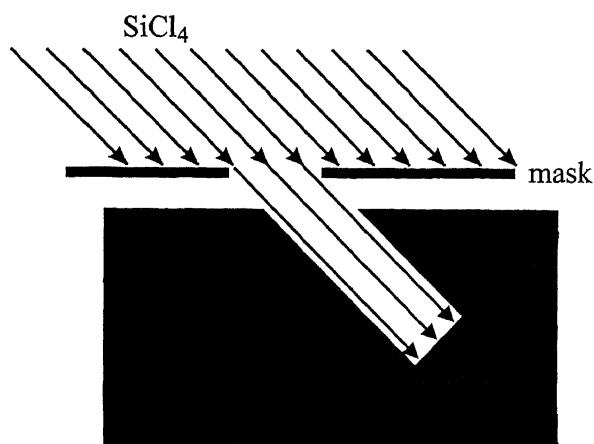


Figure 10. Hole drilling by reactive ion etching. Reactive ions,  $\text{SiCl}_4$  in this case, erode a surface at the point where they strike. A mask selectively protects the surface from unwanted erosion. Holes as small as 100 nm in diameter can be drilled.

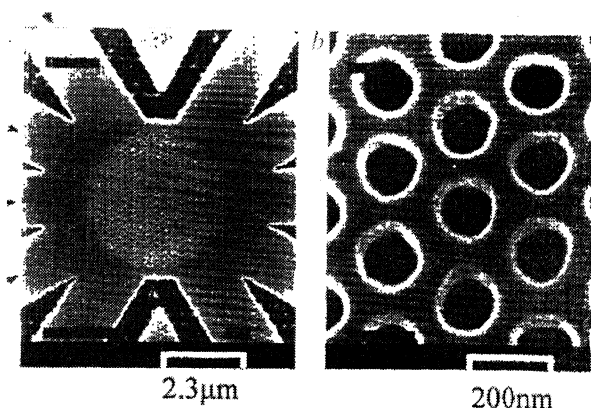


Figure 11. A photonic structure after Krauss *et al.*<sup>14</sup>, drilled into a 0.4 μm thick sample of AlGaAs. On the left an overview is given with the photonic structure in the centre surrounded by connecting waveguides. On the right we see a 10x enlargement of the central photonic region.

There still remains the challenge of sub-micron engineering which is currently being addressed in laboratories

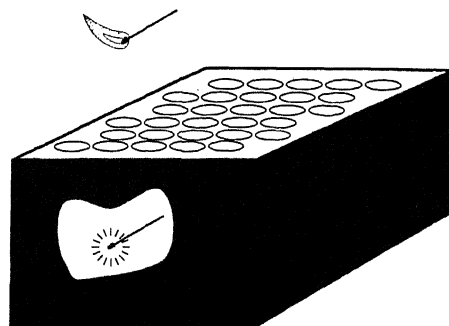


Figure 12. Trying to make light inside a photonic insulator by striking a match. The match will not light because photons are rejected by the photonic insulator. It is so dark that not even the quantum zero point fluctuations are present. We can exploit this effect to preserve atoms in their excited state to make lasers more efficient.

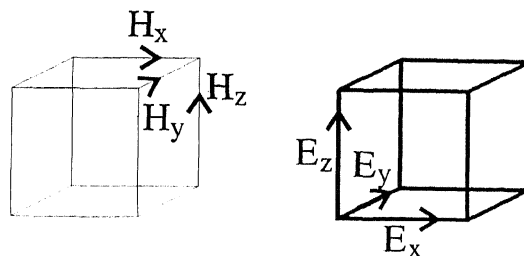


Figure 13. The unit cells of the  $\mathbf{H}$  and  $\mathbf{E}$  lattices. Note that the origin is different in each case: at the top right of the cell of the  $\mathbf{H}$ -field, and at the bottom left for the  $\mathbf{E}$ -field.

around the world. One tool that has shown great promise is reactive ion etching. Ions incident on a sample will react with the first surface atom they meet and carry it away into the vacuum. Thus, shaping the beam by passing it through a shadow mask, and choosing its orientation, we can drill holes of a chosen cross-section in any direction we choose. Figure 10 illustrates the principle of this technique. Krauss *et al.*<sup>4</sup> have employed this technique to make the structures shown in Figure 11.

In fact the Glasgow structure, though a technical *tour de force*, is still only a two-dimensional material, and therefore is not a true photonic insulator. Nevertheless, technical progress is sufficiently encouraging that we can expect these structures to be part of a materials scientist's resources in future.

### Why photonic materials are special

Why should a material that excludes all light in a given frequency range be special? After all there are other ways of excluding light – a metal box is quite dark inside! I want to emphasize how very special a photonic material is – it rejects light not because light cannot penetrate through the surface, but because there is just no place for the light to go once it is inside. There are

no electromagnetic states available inside the material. Take a practical illustration of this fact. The interior of a sealed metal box is dark, but can be illuminated by, say, striking a match inside. However, if we introduced a suitably miniature match down one of the excavated cylinders in Yablonovite and attempted to strike it, we could not do so. The structure would return the photons to the reacting atoms refusing to accept the energy (Figure 12).

Although no one is interested in striking matches inside these structures, they are interested in manufacturing lasers from them where similar principles may help the efficiency of the laser. In most lasers there is a power threshold for lasing action, because there are other ways of emitting light than into the desired lasing mode. The demands of these spurious modes must be met before the critical amplitude can be established in the lasing mode. Encasing the laser in a suitably structured photonic material can forbid the power sapping modes and increase the laser efficiency moving us further towards thresholdless lasers.

### The contribution of the theorist

At this challenging time when the photonic concept is established, but practical realization remains so difficult, it is extremely valuable to have computer programs that can predict the properties of these materials, avoiding costly experimentation with difficult new technology. Perhaps the most successful approach to computation has been the discrete sampling of the electric and magnetic fields on a fine lattice of points. Maxwell's equations present particular difficulties in that they are concerned with vector fields and geometry is an ever present subtlety. However one successful approach<sup>5,6</sup> is to define two simple cubic lattices – unit cells shown in Figure 13. Along the edges of one are arranged the **E** fields, and along the edges of the other, the **H** fields. Next arrange the two lattices so that they interpenetrate – one lattice centres the other as we see in Figure 14. Note that each *face* of the **H** lattice is pierced by a *line of force* of the **E** lattice.

Applying Stokes theorem around the edges of the face and using Maxwell's equation,

$$\frac{\partial}{\partial t} \epsilon_0 \epsilon \cdot \mathbf{E} = +\nabla \times \mathbf{H}$$

gives the discrete form of the first Maxwell equation. Similarly, the second equation can be obtained by considering faces of the **E** lattice and applying,

$$\frac{\partial}{\partial t} \mu_0 \mu \cdot \mathbf{H} = -\nabla \times \mathbf{E}.$$

The resulting difference equations have been much exploited to calculate photonic properties and to publish

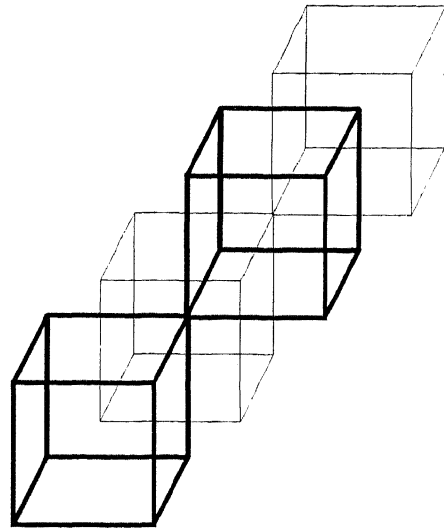


**Figure 14.** The **H** and **E** fields comprise two interpenetrating simple cubic lattices: the origin of the **H**-lattice is displaced by  $(a + b + c)/2$  relative to the origin of the **E**-lattice. Note that each bond carrying a component of the **E**-field is encircled by four bonds defining the side of one of the **H**-field cells, and correspondingly for each bond of the **H**-field.

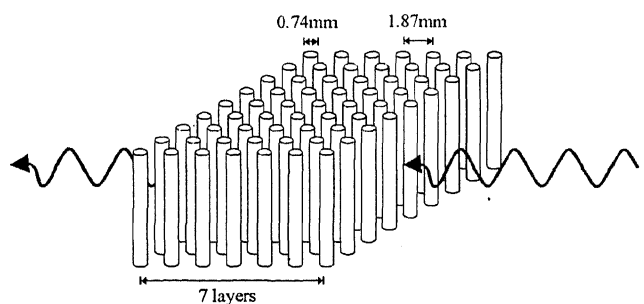


**Figure 15.** Schematic version of the microwave experiment by Robertson *et al.*<sup>8</sup> Microwaves are incident on a simple cubic array of cylinders,  $\epsilon = 8.9$ , 7 layers deep but effectively infinite in the directions perpendicular to the beam. The amplitude of the transmitted beam is measured.

computer codes that are freely available<sup>7</sup>. One of the first such calculations was a 'proof of principle' for an array of dielectric cylinders shown in Figure 15. The calculations<sup>6</sup> shown in Figure 16 are in good agreement with experiment<sup>8</sup>.

Even if the lattice is distorted, we can still apply Stokes theorem and get some equations. These can be transformed back to the original Maxwell's equations on the *undistorted* lattice provided that we modify  $\epsilon$  and  $\mu$  and the fields<sup>9</sup>,

$$\frac{\partial}{\partial t} \epsilon_0 \hat{\epsilon} \cdot \hat{\mathbf{E}} = +\nabla \times \hat{\mathbf{H}},$$

$$\frac{\partial}{\partial t} \mu_0 \hat{\mu} \cdot \hat{\mathbf{H}} = -\nabla \times \hat{\mathbf{E}}.$$

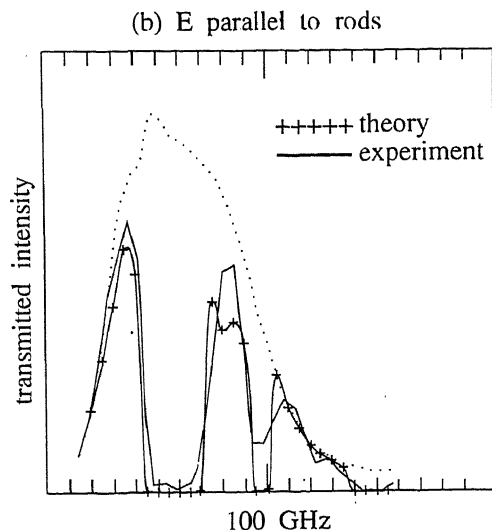


**Figure 16.** Transmitted power for an array of seven rows of dielectric cylinders. The dotted curve shows the instrument response in the absence of the cylinders.  $E$  is parallel to the cylinders.

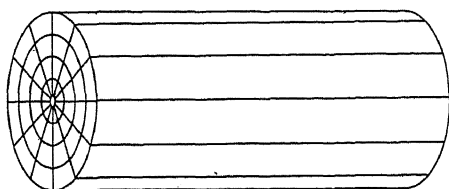


**Figure 17.** An adaptation of the simple cubic mesh to the geometry of a fibre. The  $z$ -component of the mesh can be taken to be uniform.

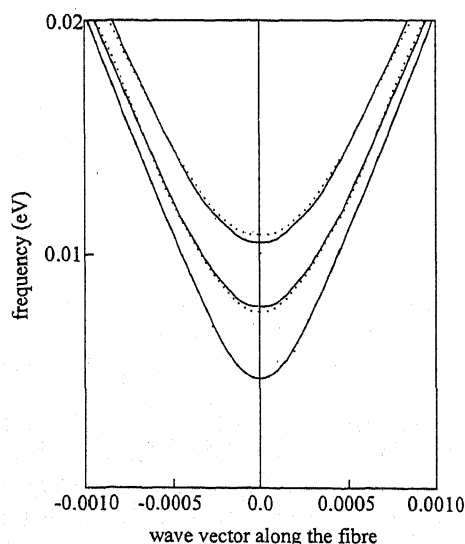


**Figure 18.** The lowest three modes of a  $10^{-4}$  m radius cylindrical metal waveguide for angular momentum  $m = 0$ , plotted against wave vector. The full lines are the results of a numerical calculation using a cylindrical mesh; the dotted lines are the exact results of analytic theory.

Remarkably, we find that the *form* of Maxwell's equations is invariant to coordinate transformations. We can choose any coordinate system, adapted to the particular geometry in which we are working, and the only effect on the equations we solve is to modify  $\epsilon$  and  $\mu$ . This is a remarkable and valuable simplification. It means that once we have written our computer codes for one coordinate system, all we have to do to work with another system is to plug in different values of  $\epsilon$  and  $\mu$ . For example, suppose that we are examining structured optical fibres, we can choose a cylindrical coordinate system compatible with the cylindrical symmetry of the fibres, rather than try to fit a square peg in a round hole which is what the original cubic lattice would require us to do. Figure 17 shows the new coordinate system.

Finally we show this scheme in action for a cylindrical wave guide with perfect metal boundaries. One advantage of the cylindrical mesh is that angular momentum is now a good quantum number in the computation, and in addition cylindrical symmetry can be exploited to speed up the calculation. The computations taken from Ward and Pendry<sup>9</sup> and presented in Figure 18 are compared to the analytic result demonstrating that the distorted mesh shows the same excellent convergence as the original uniform version.

## Conclusions

The idea of photonic materials is at an exciting stage – the concept is well established and at the same time powerful numerical techniques enable us to foresee many new applications. However we have still to meet the challenge of manufacturing these structures. Existing sub-micron technology is well-developed for two-dimensional objects, but photonic materials demand a fully three-dimensional facility. When it arrives we can expect the rapid incorporation of this new technology into optical devices. In the meantime, we can draw inspiration from the manner in which nature structures her works on exactly the scale we seek.

1. Yablonovitch, E., *Phys. Rev. Lett.*, 1987, **58**, 2059.
2. Yablonovitch, E., Gmitter, T. J. and Leung, K. M., *Phys. Rev. Lett.*, 1991, **67**, 2295.
3. Yablonovitch, E., *J. Phys.* 1993, **5**, 2443.
4. Krauss, T. F., De La Rue, R. M. and Brand, S., *Nature*, 1996, **383**, 699.
5. Pendry, J. B. and MacKinnon, A., *Phys. Rev. Lett.*, 1992, **69**, 2772.
6. Pendry, J. B., *J. Mod. Opt.*, 1994, **41**, 209.
7. Bell, P. M., Pendry, J. B., Martín-Moreno, L. and Ward, A. J., *Comput. Phys. Commun.*, 1995, **85**, 306.
8. Robertson, W. M., Arjavalingam, G., Meade, R. D., Brommer, K. D., Rappe, A. M. and Joannopoulos, J. D., *Phys. Rev. Lett.*, 1992, **68**, 2023.
9. Ward, A. J. and Pendry, J. B., *J. Mod. Opt.*, 1996, **43**, 773.
10. Ghiradella, H., *Appl. Opt.*, 1991, **30**, 3492–3500.

# Nonlinear optics of periodic and quasiperiodic structures

S. Dutta Gupta

School of Physics, University of Hyderabad, Hyderabad 500 046, India

**Periodic and quasiperiodic structures are known to possess some very special properties. Recent technological breakthrough in poling techniques in nonlinear materials has rendered nonlinear variants of such structures realizable. We review some of the latest developments in nonlinear optics of these systems. We show that the use of such structures leads to several major advantages like lowering of threshold, increase in efficiency of nonlinear mixing, fabrication of media with better characteristics, etc.**

RECENT years have witnessed an intense development of nonlinear optics of periodic and quasiperiodic media<sup>1</sup>. Even the linear counterpart of such structures are interesting because of their very special properties<sup>2,3</sup>. The simplest possible example of such systems can be a periodic or quasiperiodic arrangement of dielectric slabs. Optical properties of such systems can be quite distinct from those of the bulk constituents because of 'structural' dispersion. In fact, the transmission through such structures becomes frequency selective though the constituent layers do not have material dispersion. The most distinct property of periodic structures is the existence of stop gaps<sup>2</sup>, while quasiperiodic systems are known to exhibit exotic properties like self-similarity, scaling and multifractal spectra<sup>3</sup>. The other important feature is the ability of such structures to support modes with very high quality factors and large local field enhancement. For example, for finite periodic structures, such modes are located near the edge of the stop gap. These high  $Q$  resonances play a very important role in lowering the threshold of various nonlinear optical processes. In fact, diode lasers with sub-watt power levels can now be used to observe most of the nonlinear optical effects.

In the context of layered media (both periodic and quasiperiodic) one needs to distinguish the case of normal incidence from that of oblique incidence<sup>1</sup>. In the former, the system is equivalent to coupled Fabry-Perot cavities, while in the latter, one needs to take into account the possible surface and guided modes of the structure. The case of oblique incidence is more

complicated because of the necessary distinction of  $s$ - and  $p$ -polarizations. It should be noted here that guided mode structures are of tremendous technological value since they offer large power densities over longer propagation distances compared to what can be achieved in bulk samples. Besides, they offer the possibility of integrating various functionalities on the same optical 'chip'.

Till recent times most of the development in nonlinear optics of periodic and quasiperiodic media has been in the theory front, largely due to the lack of proper and comparatively cheap fabrication techniques. A real technological breakthrough has been the domain reversal technique<sup>4</sup> in ferroelectric materials like LiNbO<sub>3</sub>, LiTaO<sub>3</sub>, KTP, etc. The most important application of this technique has been in quasi phase matched<sup>5</sup> nonlinear mixing in second order materials<sup>4,6</sup>.

Periodicity/quasiperiodicity henceforth needs to be understood in a much broader perspective. For example, the system can be composed of periodic (quasiperiodic) arrangement of dielectric slabs with given optical properties and widths or can be a medium with the corresponding variation of, perhaps, refractive index. It can also be a layered medium with one or more interfaces with a periodic (quasiperiodic) profile. Irrespective of the details, these structures possess interesting spectral features. In what follows we treat the cases of periodic and quasiperiodic structures separately to bring out the manifestations of various nonlinear effects.

## Nonlinear periodic structures

Linear optical properties of periodic media are now well understood<sup>2</sup>. As mentioned earlier, irrespective of the details, these structures possess forbidden frequency gaps or stop gaps as a direct consequence of Floquet-Bloch theory. These gaps are located around Bragg frequencies, which are determined by the modulation period and the average refractive index. Waves with frequencies in the stop gap of an infinite structure are reflected and the gaps are perfect. For finite structures sharp transmission resonances occur at the gap edges. The location of the gap and such resonances has critical dependence on the refractive index. It is in this context

email: sdgsp@uohyd.ernet.in.

that Kerr nonlinearity (leading to intensity-dependent refractive index) plays a crucial role. A periodic structure made of alternating Kerr nonlinear slabs exhibits transmission, which has very strong power dependence. In fact, one can tailor both the transmission resonances and the gaps by changing input power levels. This suggests tremendous and diverse potentials for all-optical devices. Some potential applications of nonlinear periodic structures were earlier reviewed by Winful and Stegeman<sup>7</sup>. These include optical bistability, nonlinear coupling and tuning of surface and guided modes, tunable filters, pulse compression, etc. Other important applications such as power limiting<sup>8</sup>, all-optical logic gating<sup>9</sup>, VLSI compatible switching devices<sup>10</sup> and diode action have also been demonstrated.

The exact analytical treatment of nonlinear periodic structures even with the simplest possible nonlinearity (viz. Kerr nonlinearity) can be quite complicated. As of now exact solutions for a single nonlinear slab are known only for normal incidence, which were later generalized to the case of a lossless nonlinear periodic medium<sup>11</sup>. For oblique incidence, the case of *s*-polarized light was dealt with by Leung<sup>12</sup>. However, the solutions for *p*-polarization even for a single nonlinear layer are yet to be worked out. In view of the complexity of the exact solutions, and sometimes their unavailability, various numerical and approximate schemes were developed. A particularly simple and general method has been the nonlinear characteristic matrix method<sup>13</sup>, which has been applied to various layered media, including periodic<sup>14</sup> and quasiperiodic media<sup>15–17</sup>. The method can incorporate the effects of losses though it is limited only to the case of weakly nonlinear systems. There have been other approximate and exact matrix methods, which rely heavily on computation<sup>18</sup>. In the context of nonlinear periodic media the coupled mode theory<sup>19</sup> as well as the envelope function approach<sup>20</sup> have been quite popular.

The major outcome of the studies on Kerr nonlinear periodic media has been the prediction of solitary wave profiles with the frequency in the stop gap of the structure. The static (immobile) profiles, termed as 'gap solitons' were first discovered in numerical experiments carried out by Chen and Mills<sup>11</sup>. The exact method was applied to calculate the transmission from a finite superlattice with alternating linear and nonlinear slabs. The superlattice was illuminated with normally incident plane waves with frequency in the stop gap but close to the edge. Multivalued output in transmission was noted. The intensity distribution corresponding to the total transmission state exhibited *sech* profile. Thus, it was interpreted that the total transmission through the nonlinear structure is mediated by these gap solitons. Existence of analogous solitons in other contexts were reported by several authors<sup>21</sup>.

There have been several experiments on periodic structures with intensity-dependent refractive index. One of the preferred realizations of such structures is the corrugated waveguide. Sankey *et al.*<sup>22</sup> studied a silicon on insulator waveguide with the top surface of the Si layer corrugated. Two surface gratings were used to couple in and out the radiation from the waveguide. A similar structure (Figure 1) was studied to demonstrate the possibility of VLSI compatible switching<sup>10</sup>. The major experimental result is given in Figure 2, where the typical incident and reflected pulse shapes are shown. At the leading edge of the pulse the reflected signal mimics the incident signal. With an increase in the incident energy, the shift of the stop gap can be sufficient for the incident field to tune itself out of the stop gap, which leads to a sudden drop of the reflection and corresponding decrease in the peak amplitude of the reflected signal. As the incident intensity decreases, a sudden rise occurs in the reflected amplitude, after which there is a steady decrease following the incident pulse. Along with other applications<sup>23</sup> power limiting has been a major goal. Power limiting using periodic structures has been demonstrated by several groups<sup>8,24</sup>. The origin of power limiting in periodic structures is simple. The intensity-dependent refractive index has two major effects on the stop gap. For a defocusing nonlinearity the gap shifts to the lower wavelengths because of decrease in the average refractive index, and at the same time a broadening of the gap occurs due to an increase in the refractive index contrast (assuming the nonlinear layers having lower index). For the red edge there is a competition between these two effects. On the other hand, for the blue edge a decrease in transmission will occur leading to power limiting.

An important class of problems in nonlinear optics has been wave-mixing phenomena. The high *Q* modes of periodic structures can play a very important role in en-

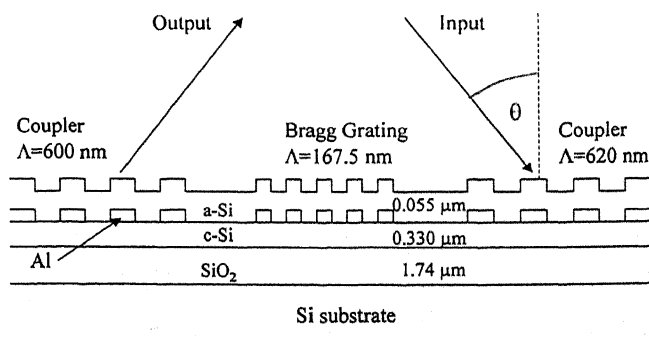
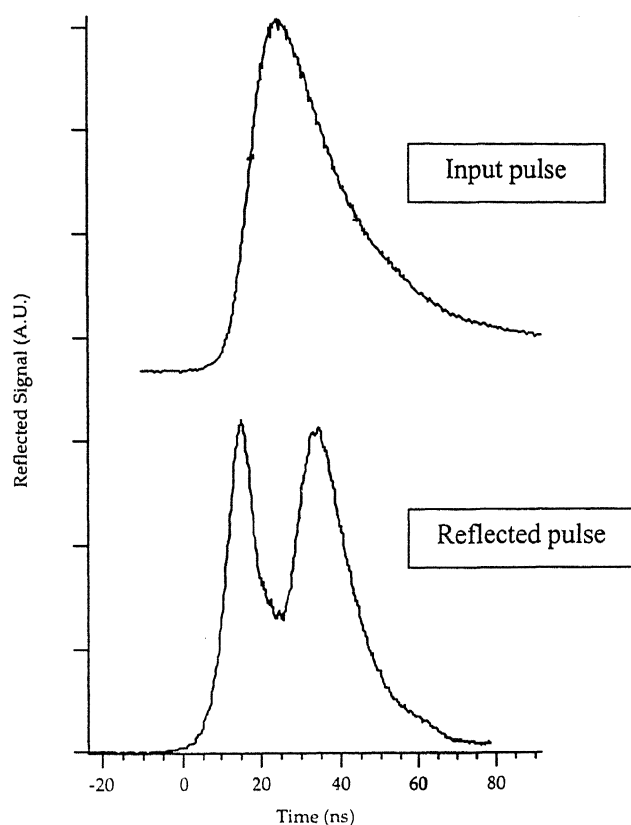


Figure 1. Schematic view of the experimental set-up of Bieher *et al.*<sup>10</sup>. The waveguide with 55 nm thick a-Si layer has end couplers for input and output radiation. The separation between the couplers and the Bragg grating is 0.5 nm. Second order backward coupling is used to excite the  $TM_0$  guided mode.



**Figure 2.** Incident and reflected pulse profiles for the structure of Figure 1 (ref. 10).

hancing the mixing efficiency. In the context of harmonic generation the advantages of such resonances can be easily understood. Fundamental distribution in the layered sample will be enhanced if its frequency coincides with one of the mode frequencies of the periodic structure. Since the fundamental distribution along the periodic structure acts as the source for the generated harmonic, there will be an increase in the output of the harmonic wave<sup>25</sup>. The general theory of wave-mixing in layered media, in particular, in periodic media, albeit under undepleted pump approximation, has been developed by Bethune<sup>26</sup> and by Hashizume *et al.*<sup>27</sup>. Bethune's approach is a straightforward extension of the earlier work of Bloembergen for a single slab, adding further the elegance of transfer matrices, while the other group uses Green's function technique to arrive at the harmonic output and, in our opinion, gives a better understanding of the underlying physics. The work of Hashizume *et al.* contains also the experimental results, which show excellent agreement with theoretical predictions.

Perhaps the most important application of periodic structures in the context of harmonic generation and

three-wave-mixing has been in quasi phase matching (QPM) in waveguide geometries. The major advantage of wave-mixing in guided wave structures stems from the fact that in addition to conventional phase matching techniques (using birefringence) one has the option of QPM which can make use of the largest  $d$ -coefficient of the nonlinear crystals. The principle of QPM has been known for quite sometime since the classic work by Armstrong *et al.*<sup>5</sup>. However, the actual realization has been achieved only recently using the periodic domain reversal techniques in ferroelectric crystals leading to a layered media with opposite signs of nonlinear coefficient in alternate layers<sup>4,6</sup>. In principle, in order to achieve QPM, any relevant waveguide parameter (e.g. refractive index or the nonlinear coefficient) can be spatially modulated with modulation vector  $K(= 2\pi/\Lambda, \Lambda$  is the period). The second harmonic (SH) effective index  $n_{\text{eff}}^{2\omega}$  can then be matched with a Bragg scattered fundamental effective index  $n_{\text{eff}}^{\omega}$  as follows

$$n_{\text{eff}}^{\omega} \pm (mK) \frac{c}{2\omega} = n_{\text{eff}}^{2\omega}, \quad (1)$$

where  $m$  is an integer.

Note that in guided wave structures both the fundamental and the SH need to be the modes of the waveguide with distinctive transverse field distributions. A large overlap of the transverse profiles is crucial for efficient harmonic output. Note also that we used effective indices in eq. (1) to characterize the modes of the waveguide. Though there is an option to use refractive index modulation for achieving QPM, one never exploits the possibility in reality. Rather one patterns the nonlinear susceptibility by means of suitable masks. The method of patterning in ferroelectric materials depends on the specifics of the crystal, especially their Curie temperature<sup>4</sup>. The most feasible method has been the patterned dopant technique involving patterned in- or out-diffusion of certain dopants leading to a corresponding distribution of reversed domains. For example, in lithium niobate, periodic domain reversal can be achieved by in-diffusion of a Ti film patterned into a grating of a desirable period by standard photolithographic technique at temperatures close to the Curie temperature.

Blue light generation by up-converting diode laser output is in demand for purposes of optical storage and xerography because of the compact nature of such devices. QPM has played an important role in such devices. QPM has been used in LiTaO<sub>3</sub>, LiNbO<sub>3</sub> and KTP to obtain such blue sources. A domain inverted LiTaO<sub>3</sub> channel wave-guide was shown to lead to a 2.4 mW of SH at 424 nm wavelength<sup>28</sup>. Gain switching and locking of the oscillation wavelength by grating feedback were shown to lead to a better efficiency. A 4.5 mW of aver-

age blue light power with 13% conversion efficiency was achieved later. Other efficient designs using a continuous wave Nd-YAG laser and exploiting an array of channels and a fan-patterned domain inverted grating were tested resulting in an efficiency of 17% (ref. 29). Another interesting geometry leading to surface emitting SH corresponds to the case of counter-propagating fundamental waves that belong to the same waveguide mode<sup>30</sup>. Since the resulting nonlinear polarization does not have any surface component, the generated SH is radiated normal to the surface. GaAs based waveguides, where some form of QPM in multilayered geometry could be used, show a lot of promise. Novel proposals have been put forth for phase matching in periodically corrugated waveguides for surface emitted SH. One such proposal makes use of higher order spatial harmonics for both the fundamental and the SH in the guiding layer. Recently the proposal has been tested using a corrugated polymer waveguide on a glass substrate<sup>31</sup>. There have been other interesting suggestions for combining counter-propagating geometry with the QPM. Results based on coupled mode theory for such structures were compared with the case of co-propagating fundamental waves. In most situations the counter-propagating geometry turns out to be more advantageous.

Cascaded second order nonlinearity has been at the focus of some of the recent studies. A major goal of these studies was to achieve nonlinear phase shift, much like in third order materials. The principle behind the intensity-dependent phase shift in cascaded second order nonlinear processes is as follows: a fundamental is up-converted to, say, the SH, which is then down-converted back to the fundamental. The resulting fundamental wave can have a phase, which is distinct from that of the original wave. Since second order nonlinear coefficients are much larger than the third order counterparts, the effective 'third order' effect due to cascading can be orders of magnitude larger than conventional Kerr phase shifts. The first experimental demonstration of cascading in guided wave geometry was given by Sundheimer *et al.*<sup>32</sup>, who used a QPM KTP waveguide to measure the self-phase modulation, where the phase information was inferred from spectral data. A direct interferometric measurement was carried out only recently by the same group. A proposal for a novel type of frequency shifter was presented by Gorbunova *et al.*<sup>33</sup>. The proposed structure involves SH generation in a waveguide by counter-propagating fundamentals at frequency  $\omega$ , followed by difference frequency generation in a second waveguide on top with an input wave at  $\omega_s$ . Recall that the counter-propagating geometry leads to SH emitted normal to the surface of the waveguide. This SH can then interact with the probe at  $\omega_s$  leading to an idler at frequency  $\omega_i = 2\omega - \omega_s$ , which propagates in the opposite direction of the signal. A multilayered QPM struc-

ture between the waveguides with additional mirrors was shown to lead to conversion efficiency much larger than that of typical waveguide shifters made of GaAs/AlGaAs multilayers.

A very interesting consequence of self-phase modulation due to cascaded processes in periodic structures has been the emergence of solitary wave profiles in such systems. Clausen *et al.*<sup>34</sup> considered the propagation of a cw beam at both fundamental and its SH frequencies in a QPM second order nonlinear slab waveguide, where only the nonlinear susceptibility was modulated. Existence of rapidly oscillating solitary waves was demonstrated. Analogous problems have also been considered by Torner and Stegeman<sup>35</sup> who investigated numerically the formation and evolution of spatial solitons with allowance for the fluctuations of the domain lengths to bring out the effects of the randomness.

A major area of activity in nonlinear optics has been the search for new nonlinear materials with better characteristics. Synthesis of new materials with higher nonlinear coefficients, faster response times and higher damage thresholds is one such direction. An alternate scheme to enhance the nonlinear susceptibility with existing materials was proposed by Sipe and Boyd<sup>36</sup>, exploiting the local field effects in composite materials. A composite consists of two or more constituents as 'grains'. Grain size or the linear dimension of each constituent must be large enough so that they may be represented by their bulk properties. At the same time, they should be small enough (much less than the wavelength) so that an effective medium description holds. In order to understand the scope of such materials let us consider a composite consisting of spherical inclusions with dielectric constant  $\epsilon_i$  embedded in a host with dielectric constant  $\epsilon_h$ . A single spherical inclusion in the composite experiences the local field  $\vec{E}_{loc}$  (and not the applied field  $\vec{E}$ ) which is given by:

$$\vec{E}_{loc} = \vec{E} + \frac{4\pi}{3\epsilon_h} \vec{P}. \quad (2)$$

The field inside the spherical inclusion  $\vec{E}_{loc,i}$  is given by:

$$\vec{E}_{loc,i} = \frac{3\epsilon_h}{\epsilon_i + 2\epsilon_h} \vec{E}_{loc}. \quad (3)$$

If, for example, the inclusion is made of a metal with  $\text{Re}(\epsilon_i) < 0$ , one may choose the host and inclusion such that  $\text{Re}(\epsilon_i + 2\epsilon_h) = 0$ . This corresponds to the plasmon resonance and there is the possibility of resonant enhancement of the field, which can be exploited for low threshold nonlinear phenomena. For several such inclusions Maxwell-Garnett calculations along with other approaches exist to arrive at the effective index. Similar

approaches can be extended to nonlinear composites in order to derive the higher order effective nonlinear susceptibilities<sup>37</sup>. While considering a general problem of nonlinear inclusion in a nonlinear host, Sipe and Boyd<sup>36</sup> demonstrated that a careful choice of the linear properties of the constituents and their volume fraction can lead to an effective medium with nonlinear susceptibilities larger than those of the constituents. The enhanced effective nonlinear susceptibility of the composite results as a consequence of the local field corrections and does not necessarily need some of the constituents to be metals. Despite the elegance of the theoretical predictions involving spherical inclusions, the realization of such composites turned out to be a formidable job because of stringent and unachievable conditions. Again periodic layered media with layer widths much less than the wavelength came to the rescue. The theory of layered composites was presented by Boyd and Sipe<sup>38</sup>, who calculated the effective nonlinear susceptibilities for various nonlinear processes. For example, for SH generation and for electric field polarized perpendicular to the layers, the effective second order nonlinearity is given by:

$$\chi_{\text{eff}}^{(2)}(2\omega = \omega + \omega) = f_1 \chi_1^{(2)} \frac{\varepsilon_1^2(\omega) \varepsilon_{\perp}(2\omega)}{\varepsilon_1^2(\omega) \varepsilon_1(2\omega)} +$$

$$f_2 \chi_2^{(2)} \frac{\varepsilon_2^2(\omega) \varepsilon_{\perp}(2\omega)}{\varepsilon_2^2(\omega) \varepsilon_2(2\omega)},$$

with

$$\frac{1}{\varepsilon_{\perp}} = \frac{f_1}{\varepsilon_1} + \frac{f_2}{\varepsilon_2}, \quad (5)$$

where  $f_i$ ,  $\chi_i^{(2)}$  and  $\varepsilon_i$  are the volume fraction, second order susceptibility and the linear dielectric constant of the  $i$ th constituent, respectively. The results for nonlinearity only in one component ( $\chi_1^{(2)} \neq 0$ ,  $\chi_2^{(2)} = 0$ ) are shown in Figure 3. It is clear from the figure that an enhancement of three can be achieved for an optimal choice of parameters. Though we cited the results for SH generation, the experiments on enhancement of the effective nonlinear susceptibility exploiting local field corrections were carried out for the third order process leading to nonlinear phase shifts<sup>39</sup>. A z-scan technique was used to measure the nonlinear phase shift in the composite made of alternating linear (titanium dioxide) and nonlinear (PBZT) layers with layer thickness of about 500 Å. It was shown that the predictions of the effective medium theory match the experimental results well.

### Nonlinear quasiperiodic structures

Quasiperiodicity implies the presence of two or more incommensurate periods. Thus quasiperiodic structures are intermediate between periodic and random media.

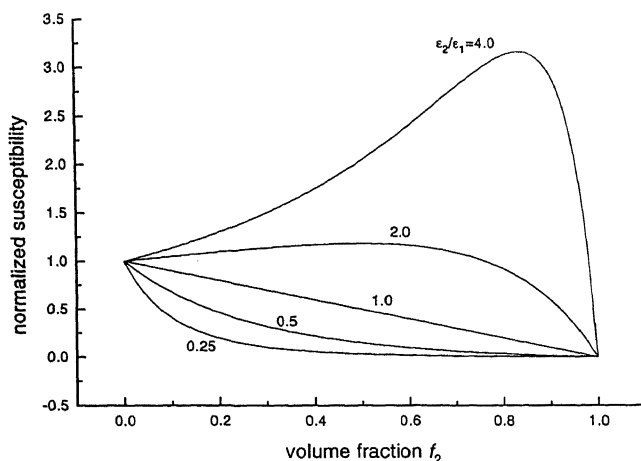


Figure 3. Effective second order nonlinear susceptibility  $\chi_{\text{eff}}^{(2)}$  normalized to  $\chi_1^{(2)}$  as a function of the volume fraction of the second component  $f_2$  for a layered composite<sup>35</sup>. Different curves are labelled by the corresponding values of the ratio of the linear dielectric constants  $\varepsilon_2/\varepsilon_1$ .

The interest in quasiperiodic structures stems from the realization that such structures can be ideal candidates for weak localization. In fact, localization in solid state systems has been a very 'hot' field ever since the discovery of Anderson localization. Weak localization in quasiperiodic solid state systems has been studied by several groups<sup>3</sup>. The theoretical studies received an impetus with the experimental realization of quasiperiodic superlattice by Merlin *et al.*<sup>40</sup>. The first ever proposal for weak localization in optical systems was presented by Kohmoto *et al.*<sup>41</sup>. The optical systems in general have several advantages over their solid state counterparts. Optical experiments are purer since the photons are noninteracting. On the other hand, in solid state systems electron-electron and electron-phonon interactions are unavoidable and can pose a real threat for direct observation of theoretical predictions. Besides, the polarization of light adds a new dimension to the problem of localization. Kohmoto *et al.*<sup>41</sup> considered the transmission of a plane wave through a Fibonacci optical multilayer. A Fibonacci multilayer can be constructed recursively, for example, by dielectric slabs A and B (with distinct refractive indices) as

$$S_{j+1} = S_j - 1 S_j, \text{ with } S_0 = (B) \text{ and } S_1 = (A). \quad (6)$$

Thus second generation  $S_2$  is given by (BA),  $S_3$  by (ABA),  $S_4$  by (BAABA), etc. Assuming the same optical width for both slabs, it was shown that the system can be described by a  $(2 \times 2)$  map, which can be further reduced to a trace map. The most interesting property of such structures is the self-similarity of the transmission coefficient as a function of optical width for various

generations. Another interesting feature is the fact that allowed states (characterized by total transmission) form a Cantor set with Lebesgue measure zero<sup>41</sup>. Sendler and Steel<sup>42</sup> presented a detailed treatment of the system and a comparison with a periodic structure. The Landauer resistivity defined by  $R_L = R/(1 - R)$ , where  $R$  is the reflectivity of the total structure, was studied. It is well-known from solid state results that  $R_L$  as a function of system length becomes exponential or power law bounded for localized and critical states, respectively. An extended state is characterized by a constant or a bounded function of system length. A major finding was the following: for a very large number of layers, all the observable states are exponentially localized surface states. For a smaller number of layers some states appear to be critical, but cross over to exponentially localized states as the system size (number of layers) increases. The above conclusions were reached at by looking directly at the field distribution along the length of the system and noting the dependence of  $R_L$  on the number of layers  $j$  or  $\log(j)$ . Experimental demonstration of the scaling behaviour and the self-similarity was achieved much later using a  $\text{SiO}_2$  and  $\text{TiO}_2$  multilayer<sup>43</sup>.

Perhaps the first ever study of nonlinear quasiperiodic structure was carried out by Dutta Gupta and Ray, who considered a Fibonacci multilayer with one or both the constituent layers with Kerr type non-linearity<sup>15-17</sup>. The nonlinear characteristic matrix approach was applied to calculate the transmission through such structures. It was shown that nonlinearity coupled with the richness of Fibonacci spectra can lead to a wide variety of bistability and multistability<sup>15</sup>. A very important observation was the existence of bulk localized states (described by a *sech* distribution)<sup>16</sup>. In fact, the total transmission of the structure was shown to be mediated by these bulk localized states. The situation is quite analogous to the gap solitons of nonlinear periodic structures. The symmetric (with respect to the center of the structure) distribution in the quasiperiodic system (lacking any such symmetry) results from a delicate interplay between dispersion and nonlinearity. A detailed numerical study of the effects of nonlinearity on localized, extended and critical states was carried out by the same authors<sup>17</sup>. It was shown that strong surface localized states in linear theory spread over the whole structure as the power is increased. Thus nonlinearity leads to delocalization. However, the extended states corresponding to  $R \sim 0$  in the linear regime do not change their character under the influence of nonlinearity. There was also evidence of critical-like states. As mentioned earlier, the most important result was the emergence of bulk localized states without any linear counterpart, which persisted even for large system sizes. In fact, these states exhibited a direct scaling with the system size.

A significant achievement in the field of nonlinear optics of quasiperiodic media was the report of SH generation in QPM quasiperiodic structures<sup>44</sup>. QPM in a quasiperiodic structure has its own specifics due to the presence of incommensurate periods. The relevant phase matching condition, for example, for two incommensurate periods can be written as follows:

$$\Delta k = k_{2\omega} - k_{\omega} - K_{m,n} = 0, \quad (7)$$

where  $m, n$  are integers,  $K_{m,n}$  is the reciprocal vector. The reciprocal vector in eq. (7) needs two integers for labelling because of the two incommensurate periods of the structure. Note that for periodic structures the reciprocal vector  $K_m (= mK)$  is indexed with only one integer. In view of the much broader options for  $K_{m,n}$ , QPM in quasiperiodic structures can cover a large number of harmonic frequencies. The nonlinear quasiperiodic structure in the experiment of Zhu *et al.*<sup>44</sup> was fabricated using the pulse field poling technique in a  $\text{LiTaO}_3$  wafer at room temperature. Each of the building blocks  $A$  and  $B$  of the structure had one positive and one negative ferroelectric domain and they were arranged in a Fibonacci sequence with the starting generations given by  $A$  and  $AB$ . The tunable output of a parametric oscillator was used to record an efficiency of 5 to 20% as the input wavelength was tuned to 0.9726, 1.0846, 1.2834, 1.3650 and 1.5699  $\mu\text{m}$ . Self-similarity feature was shown to be destroyed because of dispersion in constituent layers.

There have been studies of quasiperiodic structures other than that given by a Fibonacci sequence. A self-similar Fabry-Perot resonator consisting of dielectric slabs of two different refractive indices, with the high index slabs forming a Cantor set was studied. Along with the waveguide realization of the above structure these authors studied the nonlinear Cantor corrugated waveguide to show bistability with the narrow transmission resonances<sup>45</sup>.

In conclusion, we presented some of the new directions in research involving nonlinear periodic and quasiperiodic structures. Avoiding mathematical derivations (interested readers may find them in ref. 1) we tried to reveal the immense scope of such structures for device applications. It is perhaps because of the theoretical achievements and technological progress in such fields that Bloembergen<sup>46</sup>, father of nonlinear optics, commented that nonlinear optics has entered a technology phase. The problem now is not in having high power lasers, but in fabricating nonlinear materials with sufficiently high damage thresholds. Hence, some of the very interesting predictions of theory are yet to be tested. The search for such materials is on and success in this regard will lead to ever more exciting results in this field.

1. For a detailed review, see for example, Dutta Gupta, S., in *Progress in Optics* (ed. Wolf, E.), North Holland, Amsterdam, 1998, vol. 38, pp. 1–84.
2. Linear properties of periodic media are discussed in Yeh, P., *Optical Waves in Layered Media*, Wiley, New York, 1998, ch. 6.
3. For linear properties of quasiperiodic media see, for example, Kohmoto, M., Kadanoff, L. P. and Tang, C., *Phys. Rev. Lett.*, 1983, **50**, 1870–1872; Kohmoto, Sutherland, B. and Tang, C., *Phys. Rev. B*, 1987, **36**, 1020–1030.
4. Fejer, M. M., in *Guided Wave Non-linear Optics* (eds Ostrowsky, D. B. and Reinisch, R.), Kluwer Academic, Dordrecht, 1992, pp. 133–145.
5. Armstrong, J. A., Bloembergen, N., Ducuing, J. and Pershan, P. S., *Phys. Rev.*, 1962, **127**, 1918–1939.
6. Bierlein, J. D., in *Guided Wave Nonlinear Optics* (eds Ostrowsky, D. B. and Reinisch, R.), Kluwer Academic, Dordrecht, 1992, pp. 49–65.
7. Winful, H. G. and Stegeman, G. I., *SPIE*, 1984, **517**, 214–218.
8. Herbert, C. J., Capinski, W. S. and Malcuit, M. S., *Opt. Lett.*, 1992, **17**, 1037–1039.
9. Cada, M., He, J., Acklin, B., Proctor, M., Martin, D., Morier-Genoud, F., Dupertuis, M. A. and Glinski, J. M., *Appl. Phys. Lett.*, 1992, **60**, 404–406.
10. Bieber, A. E., Prelewitz, D. F., Brown, T. G. and Tiberio, R. C., *J. Opt. Soc. Am. B*, 1996, **13**, 34–40.
11. Chen, W. and Mills, D. L., *Phys. Rev. Lett.*, 1987, **58**, 160–163.
12. Leung, K. M., *Phys. Rev. B*, 1989, **39**, 3590–3598.
13. Dutta Gupta, S. and Agarwal, G. S., *J. Opt. Soc. Am. B*, 1987, **4**, 691–695; Agarwal, G. S. and Dutta Gupta, S., *Opt. Lett.*, 1987, **12**, 829–831.
14. Dutta Gupta, S., *J. Opt. Soc. Am. B*, 1989, **6**, 1927–1931.
15. Dutta Gupta, S. and Ray, D. S., *Phys. Rev. B*, 1988, **38**, 3628–3631.
16. Dutta Gupta, S. and Ray, D. S., *Phys. Rev. B*, 1989, **40**, 10604–10606.
17. Dutta Gupta, S. and Ray, D. S., *Phys. Rev. B*, 1990, **41**, 8047–8053.
18. He, J. and Cada, M., *Appl. Phys. Lett.*, 1992, **61**, 2150–2152; Trutschel, U., Lederer, F. and Golz, M., *IEEE J. Quantum Electron.*, 1989, **25**, 194–200; Langbein, U., Lederer, F., Peschel, T., Trutschel, U. and Mihalache, D., *Phys. Rep.*, 1990, **194**, 325–342.
19. Coupled mode theory has been applied to nonlinear periodic structures by many. See, for example, Mills, D. L. and Trullinger, S. E., *Phys. Rev. B*, 1987, **36**, 947–952; Christodoulides, D. N. and Joseph, R. I., *Phys. Rev. Lett.*, 1989, **62**, 1746–1749; de Sterke, C. M. and Sipe, J. E., *Phys. Rev. A*, 1990, **42**, 2858–2869.
20. Sipe, J. E. and Winful, H. G., *Opt. Lett.*, 1988, **13**, 132–133; de Sterke, C. M. and Sipe, J. E., *Phys. Rev. A*, 1988, **38**, 5149–5165; de Sterke, C. M. and Sipe, J. E., *J. Opt. Soc. Am. B*, 1989, **6**, 1722–1725; de Sterke, C. M. and Sipe, J. E., *Phys. Rev. A*, 1989, **39**, 5163–5177.
21. For a review of gap solitons, see, for example, Sipe, J. E., in *Guided Wave Nonlinear Optics* (eds Ostrowsky, D. B. and Reinisch, R.), Kluwer Academic, Dordrecht, 1992, pp. 305–318.
22. Sankey, N. D., Prelewitz, D. F. and Brown, T. G., *Appl. Phys. Lett.*, 1992, **60**, 1427–1429.
23. Assanto, G., in *Guided Wave Nonlinear Optics* (eds Ostrowsky, D. B. and Reinisch, R.), Kluwer Academic, Dordrecht, 1992, pp. 257–284.
24. Prelewitz, D. F. and Brown, T. G., *J. Opt. Soc. Am. B*, 1994, **11**, 304–311.
25. Mahalakshmi, V., Jose, J. and Dutta Gupta, S., *Pramana-J. Phys.*, 1996, **47**, 317–324.
26. Bethune, D. S., *J. Opt. Soc. Am. B*, 1989, **6**, 910–916.
27. Hashizume, N., Ohashi, M., Kondo, T. and Ito, R., *J. Opt. Soc. Am. B*, 1995, **12**, 1894–1904.
28. Yamamoto, K., Mizuuchi, K. and Taniuchi, T., *Opt. Lett.*, 1991, **16**, 1156–1158.
29. Ishigame, Y., Suhara, T. and Nishihara, H., *Opt. Lett.*, 1991, **16**, 375–377.
30. Normandin, R., Letourneau, S., Chatenoud, F. and Williams, R. L., *J. Quantum Electron.*, 1991, **27**, 1520–1530.
31. Blau, G., Popov, E., Kajzar, F., Raimond, A., Roux, J. F. and Coutaz, J. L., *Opt. Lett.*, 1995, **20**, 1101–1103.
32. Sundheimer, M. L., Bosshard, C., Van Stryland, E. W., Stegeman, G. I. and Bierlein, J. D., *Opt. Lett.*, 1993, **18**, 1397–1399.
33. Gorbounova, O., Ding, Y. J., Khurgin, J. B., Lee, S. J. and Craig, A. E., *Opt. Lett.*, 1996, **21**, 558–560.
34. Clausen, C. B., Bang, O. and Kivshar, Y., *Phys. Rev. Lett.*, 1997, **78**, 4749–4752.
35. Torner, L. and Stegeman, G. I., *J. Opt. Soc. Am. B*, 1997, **14**, 3127–3133.
36. Sipe, J. E. and Boyd, R. W., *Phys. Rev. A*, 1992, **46**, 1614–1629.
37. Agarwal, G. S. and Dutta Gupta, S., *Phys. Rev. A*, 1988, **38**, 5678–5687.
38. Boyd, R. W. and Sipe, J. E., *J. Opt. Soc. Am. B*, 1994, **11**, 297–303.
39. Fischer, G. L., Boyd, R. W., Gehr, R. J., Jenekhe, S. A., Osaheni, J. A., Sipe, J. E. and Weller-Brophy, L. A., *Phys. Rev. Lett.*, 1995, **74**, 1871–1874.
40. Merlin, Bajema, R. K., Clarke, R., Juang, F. T. and Bhattacharya, P. K., *Phys. Rev. Lett.*, 1986, **55**, 1768–1770.
41. Kohmoto, Sutherland, B. and Iguchi, K., *Phys. Rev. Lett.*, 1987, **58**, 2436–2438.
42. Sessler, E. and Steel, D. G., *J. Opt. Soc. Am. B*, 1988, **5**, 1636–1639.
43. Gellermann, W., Kohmoto, M., Sutherland, B. and Taylor, P. C., *Phys. Rev. Lett.*, 1994, **72**, 633–636.
44. Zhu, S., Zhu, Y., Qin, Y., Wang, H., Ge, C. and Ming, N., *Phys. Rev. Lett.*, 1997, **78**, 2752–2755.
45. Bertolotti, M., Masciulli, P., Ranieri, P. and Sibilio, C., *J. Opt. Soc. Am. B*, 1996, **13**, 1517–1525.
46. Bloembergen, N., in *Guided Wave Nonlinear Optics*, (eds Ostrowsky, D. B. and Reinisch, R.), Kluwer Academic, Dordrecht, 1992, pp. 1–9.

ACKNOWLEDGEMENTS. I thank the Department of Science and Technology and National Laser Programme, Government of India for supporting this work.

# Pearls and shells

M. S. Giridhar and S. K. Srivatsa

Raman Research Institute, C. V. Raman Avenue, Sadashivanagar, Bangalore 560 080, India

## Pearls

Pearls are formed inside aquatic organisms called oysters when a solid foreign body like a grain of sand gets lodged inside its shell. The organism secretes concentric layers of organic material around this object resulting in a pearl. The exquisite beauty of a pearl is due to this layered structure. It is a near spherical multilayer stack with alternating layers of aragonite and conchyolin, an organic material. Each layer of the pearl is an aggregation of aragonite crystallites packed invariably with their *c*-axis more or less normal to the layers and their *a* and *b* axes having fairly well-defined orientations in the plane of the layers. The small imperfections in the orientation of these axes lead to optical diffusion.

Optical reflection at the successive layers is accompanied by a strong scattering or diffusion spreading the reflected light over a range of solid angles (Figure 1). Thus sharp mirror reflections do not exist. On the other hand, an illusion is created that the pearl itself is a lustrous brilliant object. Thus one of the most admired optical features of a pearl is due to an admixture of multilayer reflection accompanied by scattering due to weak randomness in the alignment of crystallites in each layer. A closer examination of the light reflected by the pearl reveals more information about its optical behaviour. In a majority of pearls, the reflected foggy image of the source of light is saddled on either side by two diffuse spots of the same colour. These spots arise from the inner layers meeting the external surface of the pearl resulting in periodic surface irregularities as in an echelon. The spots will not occur in pearls that are perfectly spherical. The light reflected by the layers gets diffracted at the surface by these external corrugations, thus leading to diffracted images of the source. The different diffraction orders are generally not well separated and are visible only under a magnifying lens. In a perfectly spherical pearl with its layers parallel to the outer spherical surface this diffraction accompanying reflection is totally absent.

Observation of a pearl with a point source of light shows that the reflected image of the source is always surrounded by a chromatic diffusion halo. In the case of a perfectly spherical pearl this halo appears in the form of a diffuse circle. The dominant colour of the halo is complementary to that of the reflected light. This arises from the fact that light which is not reflected by the lay-

ers goes through the body of the pearl and in the process gets diffracted by the individual crystallites of aragonite embedded in a network of conchyolin.

Another beautiful optical effect that enhances the appearance of a pearl occurs when a pearl is illuminated over a very narrow region and is observed from a direction nearly perpendicular to the direction of illumination. The entire pearl then becomes visible because any light that gets scattered parallel to the layers gets transported along the layers illuminating the pearl on the way. This is the optical counterpart of the acoustic whispering gallery effect.

## Shells

The most commonly encountered shells are hard structures built by molluscs (of which oysters are a type)

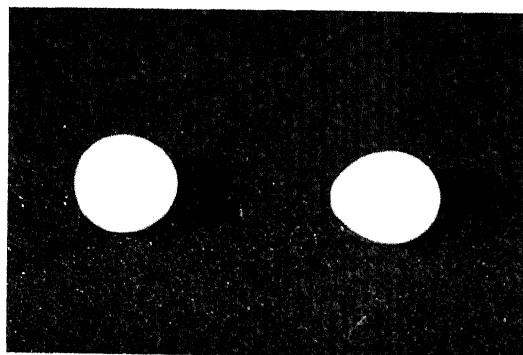


Figure 1. Two natural pearls with a bright lustrous glow caused by diffusion of light illuminating the pearls.

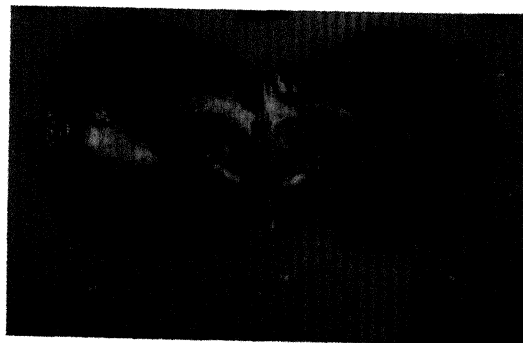


Figure 2. Typical bright metallic sheen seen on the inner surface of an opened up oyster shell.

around themselves primarily for protection from predators. Shells are mainly made up of aragonite and small amounts of other minerals found in the molluscs' environment.

Shells have again a layered structure that is very similar to the pearls and thus exhibit almost all the optical features that we find in pearls. The important structural difference between a pearl and a shell is that the layers of a shell do not close upon themselves as in a perfect pearl. They always meet the external surface of the shell. As a result the shell surface is locally corrugated on a fine scale. Hence, we always get surface dif-

fraction accompanying multilayer reflection. The reflection results in a metallic sheen of the shell and the diffraction orders are well separated from the specular reflections (Figure 2).

As in pearls, here also we find diffusion haloes. While in pearls they are seen in the reflection mode, in shells since they are thin, we can see them in the transmission mode. The halo arises from the diffraction of light by the crystallites of aragonite present in the different layers. Further all the optical properties exhibit marked polarization features.

## Diffraction in heterogeneous liquid crystals

K. A. Suresh\*, G. S. Ranganath and M. S. Giridhar

Raman Research Institute, C. V. Raman Avenue, Sadashivanagar, Bangalore 560 080, India

**We review briefly optical diffraction exhibited by periodically and non-periodically heterogeneous liquid crystals. Some of the novel features of the diffraction phenomena have been highlighted. We also discuss non-linear optics in such media. Attention has been paid to the present status in this area.**

LIQUID crystals are states of matter with a molecular order between that of crystals and liquids. Many of them are optically heterogeneous. The heterogeneity arises from the fact that the index tensor varies from point to point inside the medium. For example, in the cholesterics, chiral smectic C and the twist grain boundary smectics (TGB), the index tensor periodically varies along the twist axis and remains a constant in an orthogonal direction. On the other hand, in the cubic blue phases, the index tensor is a three-dimensional periodic function of space. Further, in polymer dispersed liquid crystals (PDLC), it randomly varies in space. It is therefore to be expected that in all these media, light undergoes scattering, diffraction or both. In this article we briefly review diffraction from such liquid crystals.

### Periodic liquid crystals

#### *Cholesterics*

The cholesteric liquid crystals (cholesterics) are made up of molecules that are locally aligned preferentially in

a particular direction represented by the director, which twists uniformly about an orthogonal direction. This results in a helical structure of a definite pitch. We consider a plane wavefront of linearly polarized light incident along a direction normal to the twist axis. When its electric vector is parallel to the twist axis it emerges as a plane wavefront while for the electric vector in the orthogonal state it emerges as a periodically corrugated wavefront. The latter case leads to diffraction of light as in a phase grating<sup>1</sup>. In general, it is seen<sup>2</sup> that the various diffraction orders are mainly polarized with the electric vector perpendicular to the twist axis whereas the central or the zeroth order is mainly polarized with the electric vector parallel to the twist axis. Further, intensities of the different orders can be such that higher orders are more intense than the lower orders. The intensities are also a sensitive function of sample thickness. These are characteristic features of a phase grating.

Raman and Nath (RN) were the first to solve an equivalent optical problem<sup>3</sup> in the context of ultrasonic diffraction of light in isotropic liquids. In the RN theory, the diffraction pattern is obtained by Fourier transforming the corrugated wave front emerging from the medium. That is, the amplitude  $F(q)$  of the diffracted light is given by:

$$F(q) = \int_{-\infty}^{\infty} U(y) \exp(-iqy) dy,$$

where  $q$  is the scattering vector and  $U(y)$  represents the corrugated wavefront described by:

\*For correspondence. (e-mail: suresh@rri.ernet.in)

$$U(y) = A_0 \exp[i2\pi n(y)d/\lambda].$$

Here,  $A_0$  is the amplitude of the incident plane wavefront,  $d$  is the thickness of the sample,  $\lambda$  is the wavelength of the incident light,  $y$  is the direction of phase variation and  $n(y)$  the local refractive index of the medium.

In cholesterics, the diffraction pattern can be analysed in an analogous manner<sup>4,5</sup>. However, RN theory ignores the internal diffraction of light in the medium. Therefore, it is valid only for samples where the phase fluctuations inside the medium are very weak. Rokushima and Yamakita<sup>6</sup> have worked out a theory of phase gratings incorporating internal diffractions. In this approach, the sample is divided into thin sections, each contributing to the diffraction pattern. When a plane wavefront encounters the first section of the sample, the diffraction is similar to that described by the RN theory. Here each diffracted beam represents a plane wavefront. When these diffracted beams encounter the next section, they again get diffracted individually according to the RN theory. This process continues for each section throughout the sample resulting in a cascade of diffractions. This leads to a coupled wave theory<sup>7,8</sup> of diffraction. It may be mentioned that in absorbing heterogeneous media the RY theory in its present form is not applicable.

### Chiral smectic C

The chiral smectic C (Sc\*) liquid crystalline phase is essentially similar to cholesterics excepting that the director precesses about the twist axis at a constant angle which is between zero and  $\pi/2$ . Further, the structure is locally biaxial. Here also, for propagation of light perpendicular to the twist axis, the medium acts as a phase grating resulting in diffraction. A typical diffraction pattern obtained in such a structure is shown in Figure 1. In view of the local biaxiality, a Sc\* behaves very differently from a cholesteric. For example, in Sc\*, the medium diffracts light for any azimuth of the linearly polarized incident light. The diffraction experiments in Sc\* are usually carried out to determine the structural pitch and there have not been many studies on the optical features of the diffraction pattern. Recent experiments<sup>9</sup>, on a particular Sc\* liquid crystal, have led to the elucidation of some very interesting features associated with the diffraction pattern. Some of these have been depicted in Figure 2. Here, one finds that irrespective of the state of polarization of the incident light, the diffracted light in the different orders are nearly linearly polarized parallel to the twist axis. However, in thick samples, the polarization features of the diffraction pattern are sensitive to the temperature dependent optical parameters. Further, in all the samples studied, the

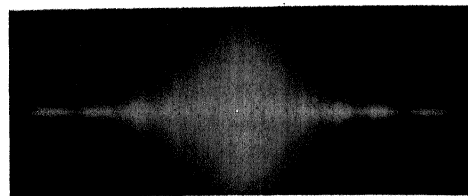


Figure 1. The diffraction pattern in a Sc\* sample for a laser beam (He-Ne,  $\lambda = 633$  nm). One can clearly see five orders of diffraction.

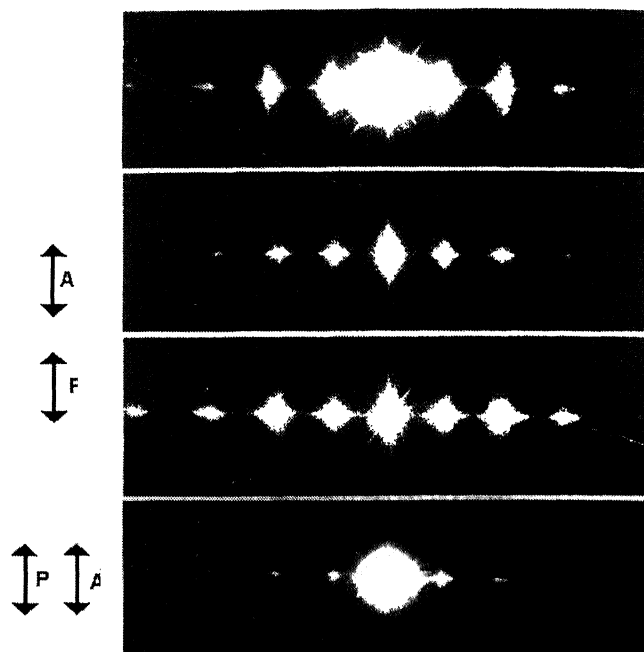


Figure 2. The diffraction patterns of a 50  $\mu\text{m}$  Sc\* sample at room temperature ( $\approx 25^\circ$ ). In each pattern, the first symbol denotes the setting of the polarizer P and the second symbol denotes the setting of the analyser A with respect to the twist axis of the Sc\*.

zeroth order has nearly the same state of polarization as that of the incident light.

The problem of optical diffraction in a Sc\* can be solved either by a generalization of the RN theory of phase gratings<sup>5</sup> or by using the RY theory of anisotropic dielectric gratings<sup>6,7</sup>. Many of the observed features<sup>9</sup> can be accounted for by the RY theory.

### Twist grain boundary smectics

The twist grain boundary smectic phases are endowed with many interesting optical properties. In this phase, thick smectic blocks are helically stacked with intermediate twist grain boundaries. The important feature of the structure is the possibility of incommensuration between the pitch of the helix and the thickness of the

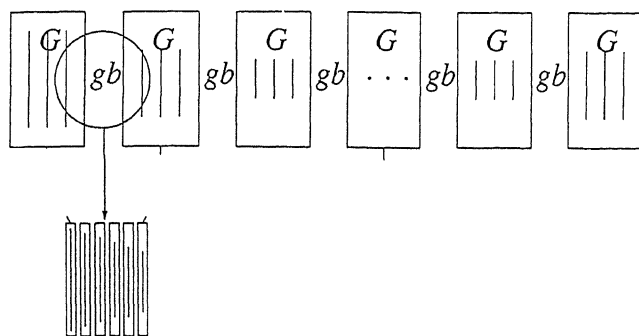


**Figure 3.** A model of  $TGB_A$ .  $G$  represents a smectic block and  $gb$  represents a grain boundary. The vertical line represents the projection of the local director.

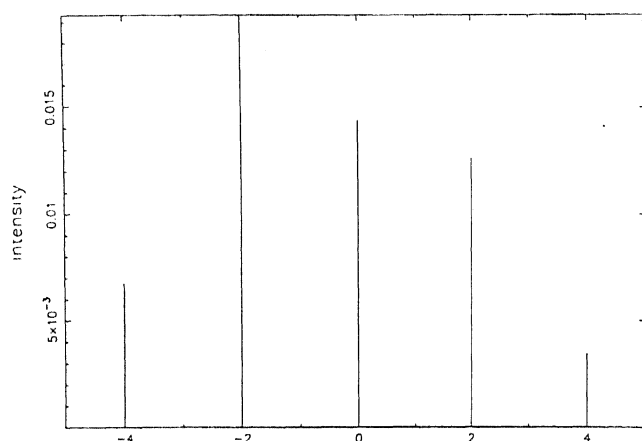


**Figure 4.** Computed diffraction pattern of an absorbing  $TGB_{C_1}$ . The numbers on the abscissa represent the orders of diffraction.

smectic blocks. Optically, the smectic blocks can be thought of as thick birefringent plates. Similarly, one can consider a grain boundary as a helical stack of thin birefringent plates. These thin plates smoothly rotate and connect the adjacent smectic blocks (see Figure 3). The smectic blocks could be of either smectic A or smectic C structure. Then they are designated respectively as  $TGB_A$  and  $TGB_C$ . Also the diffraction features of  $TGB_C$  are in general sensitive to the orientation of the local 2-fold axis with respect to the twist axis. For example, it can have its 2-fold local axis either parallel ( $TGB_{C_1}$ ) or perpendicular ( $TGB_{C_2}$ ) to the twist axis.

In the case of  $TGB_A$  or  $TGB_{C_1}$  the diffraction pattern is similar to that of cholesterics whereas for  $TGB_{C_2}$  the diffraction pattern is rather similar to that of  $Sc^*$ . From the diffraction pattern of  $TGB_A$  or  $TGB_{C_1}$  one can evaluate<sup>10</sup> the sizes of smectic blocks and the grain boundaries. In the absorbing case, the diffraction patterns of  $TGB_A$  and  $TGB_{C_1}$ , obtained using the RN theory, continue to be symmetric. However, interestingly, in absorbing  $TGB_{C_2}$  the pattern becomes asymmetric due to

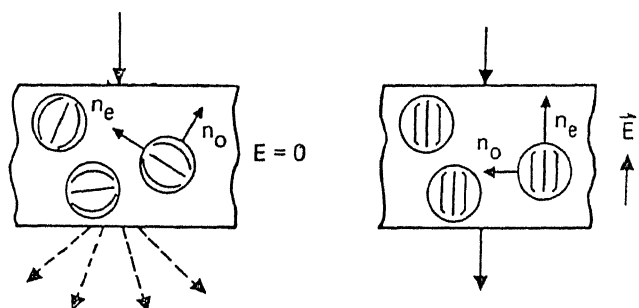


**Figure 5.** The director configuration in the nematic droplets of PDLC. In each droplet the director is tangential to the droplet surface.  $n_o$  and  $n_e$  are the ordinary and the extraordinary refractive indices of the nematic.  $E$  represents the direction of the externally applied electric field.

local biaxiality. This is obvious in the computed diffraction pattern shown in Figure 4.

## Non-periodic liquid crystals

### Quasi-periodic blue phases

The blue phases are optically isotropic. They appear in some cholesterics over a narrow range of temperatures close to the cholesteric–isotropic phase transition. In general, there are three blue phases, viz. BPI, BP II and BP III. The phases BPI and BP II have cubic symmetry. On the other hand, the structure of BP III is still not well-established. There are some indications that the BP III is a quasiperiodic structure<sup>11</sup>. As a consequence, the optical diffraction in one-dimensional quasi-periodic cholesteric<sup>12</sup> is of relevance to the analysis of optical diffraction in BP III.

We consider one particular model of a quasi-periodic cholesteric. It is twisted in a particular direction according to a Fibonacci sequence<sup>13</sup>, i.e. two incommensurate but uniformly twisted regions of thicknesses  $l_1$  and  $l_2$  occurring in a Fibonacci sequence. Within each unit there is a uniform helical stack of birefringent layers, with a total twist of  $2\pi$ . Also  $l_1 = (1 + h)l_2$  where  $1/h = (\sqrt{5} + 1)/2$ . Here, the dielectric tensor is locally uniaxial and gradually rotates along the twist axis but with two incommensurate periods. In the diffraction mode, for light incident with its electric vector perpendicular to the twist axis, the emergent wavefront has corrugations due to phase fluctuations. It may be mentioned that in a periodic cholesteric<sup>5</sup>, in the same geometry, the diffraction peaks will occur at the wave vectors  $q = 2\pi(N/l)$ ,  $N$  being an integer. However, the diffraction pattern of this quasi-periodic cholesteric has peaks at

$$q = \frac{2\pi}{l(1+h^2)} (r+hs),$$

where  $r$  and  $s$  are integers and  $h$  is an irrational number. Further, it is well known that in a quasi-periodic amplitude grating, the intense diffraction peaks occur when  $r$  and  $s$  are in the ratio of successive Fibonacci numbers<sup>13</sup>. Interestingly, in this quasi-periodic phase grating such a result is not found. The intensity in any given order is a function of the birefringence of the medium, sample thickness and wavelength. We may expect similar diffraction features in BPIII.

### *Inhomogeneous cholesterics*

In cholesterics, one assumes that the director rotates uniformly in space giving rise to a uniform pitch in the medium. In practice, the sample is generally sandwiched between two substrates. The surface effects due to the substrates usually create inhomogeneities in the structure. We have investigated cholesterics with pitch distortion. We find that even a distortion of the order of two per cent can alter the diffraction features considerably<sup>14</sup>. For instance, each diffraction order becomes a broad top-hat intensity profile instead of being narrow and sharp.

### *Polymer dispersed liquid crystals*

In recent times, polymer dispersed liquid crystals have attracted considerable attention since they have gained a lot of importance in display devices. Here, we highlight the interesting optical properties associated with such heterogeneous media. The simplest of the PDLCs are obtained in the two-phase region of a binary mixture of a nematic and a polymer. Here we have droplets of a nematic liquid crystal suspended in an optically isotropic polymer matrix. In a normal polymer matrix, the different droplets will have different orientations as shown in Figure 5. In the case of droplets that are very large compared to the wavelength of light, one is in the regime of geometrical optics. Even in this case, an incident beam of light gets scattered due to random phase corrugations of the incident plane wavefront. This results in a poor transmission. Surprisingly, the system can be brought to a near transmission state by the application of an electric field. Beyond a threshold electric field, the different droplets are brought into the same orientation with the director in each droplet aligned in the direction of the external field. Invariably the materials are so chosen that the refractive index of the isotropic polymer matches with the ordinary refractive index of the nematic liquid crystal. Then it is easy to see that for an incident light beam propagating along or opposite the direction of the external field there is a good transmission irrespective of the polarization state of light while for the orthogonal direction of propagation the ordinary wave is transmitted and the extraordinary wave is diffracted.

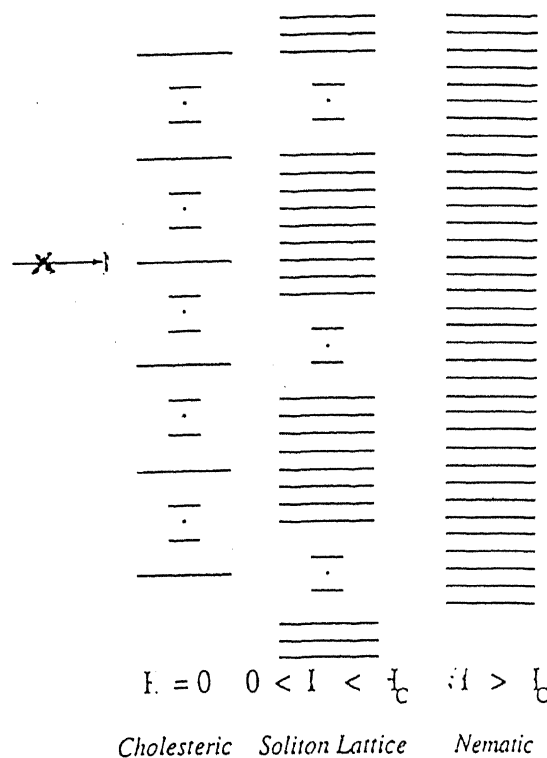


**Figure 6.** Transformations of a cholesteric structure due to the nonlinear optical effects in the phase grating mode.  $I_c$  represents the threshold intensity for the cholesteric to nematic transition.

### **Nonlinear optics in liquid crystals**

Now we describe briefly nonlinear optics in heterogeneous liquid crystals. We consider a cholesteric in the phase grating mode. If the light intensity is high enough then the electric field of the light wave couples to the director resulting in a mechanical torque on the director. This torque will distort the uniformly twisted cholesteric. In fact, the effect of the light beam will be similar to that of an external electric or a magnetic field acting perpendicular to the twist axis. The uniform cholesteric will become non-uniform with walls of  $180^\circ$  twist separated by large, nearly untwisted regions. In other words, this is akin to a soliton lattice. With increase of light intensity, the width of the untwisted region increases and at a particular threshold intensity the structure gets completely unwound. The associated structural transformations are depicted in Figure 6. The light beam will also suffer diffraction in this mode. Hence, as the structure begins to unwind, the diffraction pattern continuously gets altered and disappears altogether at the threshold intensity.

We now end with a brief note on the generation of a second harmonic wave in PDLC's. Though both the polymer matrix and the suspended nematic droplets do

not on their own exhibit second harmonic generation (SHG), the composite structure leads to a SHG. This arises at the interface of the droplets and the matrix. The effect has been experimentally established though indirectly. In this context, an interesting possibility of optical diffraction of SHG is worth mentioning. Even when all the droplets are aligned such that the ordinary wave emerges without diffraction, the second harmonic wave will suffer diffraction. Hence, we can expect the main beam of the fundamental to be surrounded by a diffraction halo of its second harmonic.

1. Rayleigh, J. W. S., *Theory of Sound*, New York, Dover, 1945, vol. 2, p. 89.
2. Sackmann, E., Meiboom, S., Snyder, L. C., Meixner, A. E. and Dietz, R. E., *J. Am. Chem. Soc.*, 1968, **90**, 3567–3569.
3. Raman, C. V. and Nagendra Nath, N. S., *Proc. Indian Acad. Sci. A*, 1935, **2**, 406–412.
4. Chandrasekhar, S. and Prasad, J. S., *Physics of Solid State* (eds Balakrishna, S., Krishnamurthi, M. and Ramachandra Rao, B.), Academic Press, 1969, p. 77–82.
5. Suresh, K. A., Sunil Kumar, P. B. and Ranganath, G. S., *Liq. Cryst.*, 1992, **11**, 73–82.
6. Rokushima, K. and Yamakita, J., *J. Opt. Soc. Am.*, 1983, **73**, 901–908.
7. Galatola, P., Oldano, C. and Sunil Kumar, P. B., *J. Opt. Soc. Am. A*, 1994, **11**, 1332–1341.
8. Sunil Kumar, P. B., Ph D thesis, Bangalore University, 1994.
9. Suresh, K. A., Yuvaraj Sah, Sunil Kumar, P. B. and Ranganath, G. S., *Phys. Rev. Lett.*, 1994, **72**, 2863–2866.
10. Andal, N. and Ranganath, G. S., *J. Phys. II France*, 1995, **5**, 1193–1207.
11. Rokhsar, D. S. and Sethna, J. P., *Phys. Rev. Lett.*, 1986, **56**, 1727–1730.
12. Yuvaraj Sah and Ranganath, G. S., *Opt. Commun.*, 1995, **114**, 18–24.
13. Levine, D. and Steinhardt, P. J., *Phys. Rev. B*, 1986, **34**, 596–615.
14. Giridhar, M. S., Suresh, K. A. and Ranganath, G. S., to be published.

## We'll help you get there

If you're selling science books/journals or laboratory products, or wish to recruit scientists in your establishment, then

**you're sure to benefit by  
advertising here.**

Because *Current Science* reaches nearly every university, scientific institution and industrial R&D unit in India. What's more, it's read by hundreds of individual subscribers—students, doctoral scientists and professionals in virtually every field of scientific activity in India.

*Current Science* has the largest circulation among scientific journals in India.

And to give you more impact, we're now bigger, and better.

Write now, or send your copy to

**CURRENT SCIENCE**

C. V. Raman Avenue, P. B. No. 8001,  
Bangalore 560 080

# Life before mean free path

N. Kumar

Raman Research Institute, C. V. Raman Avenue, Sadashivanagar, Bangalore 560 080, India

**A coherently amplifying medium containing dense random weak scatterers can exhibit mirror-less lasing beyond a threshold of optical pumping even when the active medium has linear dimensions much smaller than the estimated transport mean free path. The threshold pump power decreases with decreasing mean free path. This mirror-less lasing can be understood in terms of the sub-mean free path scatterings which are normally statistically rare, but are now made effective by the coherent amplification that more than offsets their otherwise low probability of occurrence.**

WAVE propagation through a spatially random scattering medium holds many surprises of condensed matter physics, of which the best known example is Anderson localization<sup>1</sup> – weak as well as strong. The wave in question may be a complex scalar (e.g. the quantum mechanical probability amplitude as in the case of electrons moving in a disordered solid), or a real scalar (e.g. the sound wave propagating in an elastically disordered medium), or a real vector (e.g. the light wave propagating through a disordered dielectric, which is of interest here). It may, however, even be a real tensor (e.g. the gravitational wave scattering on a random background metric, as perhaps in the early universe!). A closely related phenomenon here is that of the large statistical fluctuations of the wave transmission/reflection coefficient – over an ensemble of macroscopically controllably identical but microscopically uncontrollably distinct realizations of the spatial (quenched) randomness, making the system non-self-averaging. The strong as well as the weak localization, and the sample-to-sample statistical fluctuations (or the *reproducible noise*) are all diverse manifestations of the common phenomenon of intermittency which is favoured by randomness. Here intermittency refers to the occurrence of rare events that are nevertheless intense enough to affect the statistics drastically. For the wave motion in a random medium it is due generally to the coherent multiple scattering, and more specifically to the Coherent Back Scattering (CBS)<sup>2</sup>, i.e. the partial wave-amplitudes counter-propagating along the same return path acquire identical phase-shifts (see Figure 1). The amplitude doubling resulting from these time-reversed partial waves returned in phase refocuses the scattered wave in a direction opposite to that of incidence. This sharp feature persists no

matter how strong the disorder is so long as the medium is time-reversal symmetric, e.g. no external magnetic field. (Caustics and Glory are the common examples of intermittency known from optics.) The CBS refocussing, in fact, defines a cone of finite opening angle which is typically a few milli-radians for light, and increases with disorder.

Now, the disordered medium referred to above has been so far assumed to be passive, which is the only kind of spatial randomness relevant to the case of electrons (fermions). But, photons are bosons admitting the possibility of coherent amplification by stimulated emission beyond a threshold of optical pumping. This has led to a novel development, namely that of light propagation in a Random Amplifying Medium (RAM)<sup>3-11</sup>. Such a random amplifying medium is readily realized as a colloidal suspension of dielectric microspheres in the solution of a laser-active dye, optically pumped by an appropriate pulsed laser. Thus, for example<sup>4</sup>, the random scatterers could be micron-sized spheres of rutile ( $\text{TiO}_2$ ) dispersed in methanol giving a high refractive index contrast. The dye solution could be rhodamine 640 perchlorate in methanol with an emission peak at  $\sim 617$  nm. The pump could be a frequency-doubled pulsed Nd:YAG laser operating at  $1.064 \mu\text{m}$ . The main point to note here is that the coherent amplification

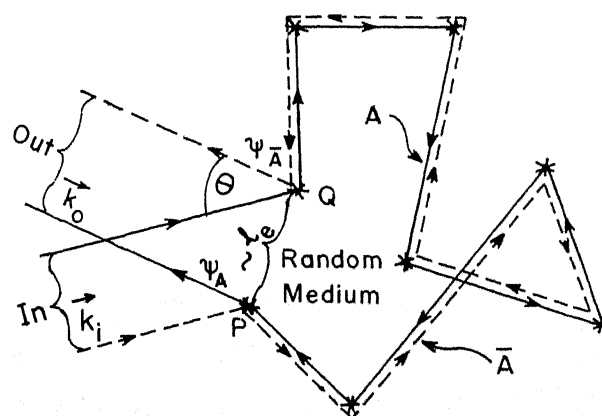


Figure 1. Coherent back-scattering. The path A (solid line) and its time reversed path  $\bar{A}$  (dashed line) visit the same scatterers but in the reversed sequence, giving identical phase shifts, for  $\theta = 0$ .

maintains the condition for coherent back-scattering, and, indeed, it enhances the various intermittency effects noted above, e.g. the higher the amplification the narrower the CBS cone angle; also greater is the tendency to localization inasmuch as the longer return paths now contribute more effectively to CBS.

Mirror-less lasing in such a RAM has been reported by several experimental groups<sup>4,7,11</sup>. Fundamentally, it may involve one of the two distinct mechanisms – the Anderson localization that provides a virtual high- $Q$  cavity giving a resonant positive feedback<sup>3</sup>; or it may result from diffusion, a non-resonant distributed feedback from the enhanced path lengths traversed by the diffusing photon<sup>12</sup>. Such a randomly folded optics in a RAM subtends a high gain. We are concerned here with this latter case. However, it raises an interesting question, namely, what if the medium has linear dimensions much smaller than the transport mean free path  $l^*$ ? Such a sub-mean free path medium can hardly be expected to subtend diffusively the prolonged path lengths, much less localization; and hence no mirror-less lasing is to be expected. But, there is now experimental evidence of and theoretical support for mirror-less lasing in this case too<sup>11</sup>. This can be physically understood in terms of the statistically rare scattering events occurring before the mean free path, which become effective because of the high-gain RAM. A RAM with Dense Random Weak Scattering (DRWS), indeed, provides an interesting example of what is known in a game of chance as the St. Petersburg paradox, where orders of magnitude lower probability odds have orders of magnitude higher gains, upping thereby the *ante*.

### Mirror-less lasing in sub-mean free path RAM: Experimental

Recent experimental results on lasing in a RAM in the limit of sub-mean free path sample size suggest that a novel mechanism is at work. The random amplifying medium studied by us<sup>11</sup> was an aqueous suspension of polystyrene microspheres containing the rhodamine 590 dye. The RAM parameters were:

Dye concentration:  $5 \times 10^{-5} \text{ M} - 5 \times 10^{-2} \text{ M}$  (mole/litre); polystyrene microspheres:  $0.12 \mu\text{m}$  diameter; polystyrene microsphere concentration  $n_s = 10 \text{ cm}^{-3} - 10^{13} \text{ cm}^{-3}$ ; pump ( $p$ ) frequency-doubled Nd:YAG; pump wavelength  $\lambda_p = 532 \text{ nm}$ ; pump pulses duration:  $10 \text{ ns}$ ; pump repetition rate:  $10 \text{ pps}$ ; energy deposited per pulse ( $E$ ):  $50 \mu\text{J} - 13 \text{ mJ}$ ; active medium size  $\approx 1 \text{ mm}$ ; estimated transport mean free path  $l^* (\mu\text{m}) = [(4.35 \times 10^{15})/n_s]$  ( $4.35 \times 10^{14} \mu\text{m} - 4.35 \times 10^2 \mu\text{m}$ ); gain narrowing was observed for  $n_s > 10^9 \text{ cm}^{-3}$ .

Figure 2 shows a typical plot of gain narrowing enhancement by random scattering. The surprise, however, is that the effect persists even for the sample size  $L \ll l^*$ , the photon transport mean free path when the normal diffusion can hardly be expected to dominate.

Thus, for  $n_s = 1.24 \times 10^9 \text{ cm}^{-3}$ ,  $l^* = 350 \text{ cm}$ , and for  $n_s = 1.24 \times 10^{11} \text{ cm}^{-3}$ ,  $l^* = 3.5 \text{ cm}$  while  $L \sim 0.1 \text{ cm}$ . And for proper diffusion, we need to have the sample size  $\geq 6l^*$ . Thus there seems to be unexpected life *before* the mean free path !

### Mirror-less lasing in sub-mean free path RAM: Theoretical

Consider a random amplifying medium characterized by a scattering length  $l_s$ , and a gain length  $l_g$  in the absence of scattering. (We assume the scatterers to be isotropic so that  $l_s = l^*$ , the transport mean free path given by  $n_s l_s \sigma_s = 1$ , where  $n_s$  is the number density of the scatterer of scattering cross-section  $\sigma_s$ .) For diffusive motion in a RAM with uniformly excited medium, optical energy-density  $\rho$  can be described by the diffusive-reactive equation:

$$\frac{\partial \rho}{\partial t} = D \nabla^2 \rho + \frac{1}{\tau_g} \rho, \quad (1)$$

where the diffusion constant  $D = (1/3)cl_s$  and the gain time  $\tau_g^{-1} = c/l_g$ , with  $c$  the speed of light in the averaged

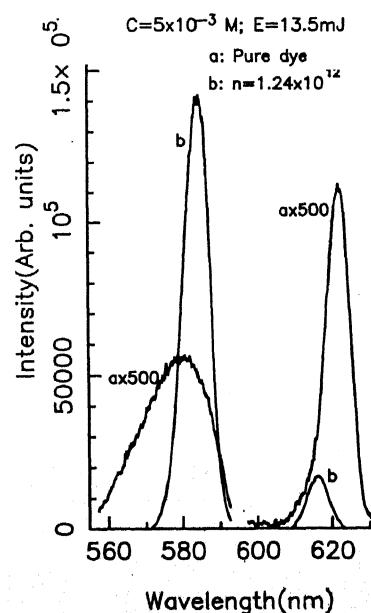


Figure 2. Emission spectrum from a RAM as function of the scatterer density at a fixed pump power. Gain narrowing for higher scatterer density is clearly seen even with the sample size less than transport mean free path (ref. 11).

refractive index medium. Physically this diffusive description is valid over length scales  $L \gg l_s$ . (Formally, eq. (1) is valid on all length scales in the limit  $l_s \rightarrow 0$ ,  $c \rightarrow \infty$ , and  $l_g \rightarrow \infty$ , keeping  $D$  and  $\tau_g$  constant.) This diffusion-reaction equation describes the threshold condition for lasing in much the same way as the corresponding equation for neutrons describes the criticality of chain reaction in a nuclear reactor. The gain length  $l_g$  decreases with increasing optical pumping.

Equation (1) is, of course, not valid under the sub-mean free path condition  $l_s \gg L \equiv$  the linear dimension of the active medium, as is the case in the experiment discussed above for a RAM with dense random weak scatterers. For the DRWS, we have  $(\frac{4\pi}{3} \cdot l_s^3) n_s \gg 1$  (dense),  $1/kl_s \equiv$  disorder parameter  $\ll 1$  (weakly scattering) with  $\lambda = 2\pi/k$  = the wavelength of light and  $L \ll l_s$  (sub-mean free path). We will now work out the contribution of the rare sub-mean free path scatterings to lasing in a RAM. First, let us note that for an arc length  $s$  traversed by a diffusing photon in a passive DRWS medium, the mean number  $s$  of scatterings is  $s/l^* \equiv \mu$ . Now, for a Poissonian distribution of the discrete scattering events in a continuum, the probability for  $m$  events in the arc length  $s$  will be  $P_s(m) = e^{-\mu} \mu^m / m!$ . Thus there is a non-zero, albeit small, probability of undergoing scattering even for  $\mu \ll 1$  (i.e.  $s \ll l^*$ ). Normally these rare events are ignorable in any reckoning. For a RAM, however, this statistical rarity may be offset by the medium gain. As a rough estimate of this effect, consider the probability of undergoing at least one scattering back into the finite RAM of size  $L$ . It is  $\sim (1 - \exp(-L/l^*))$ , in one-dimension. The associated gain factor is  $\exp(L/l_g)$ . Now, for high enough gain (pumping), i.e. for small enough  $l_g$ , one can have the product  $(1 - \exp(-L/l^*)) \exp(L/l_g) > 1$ . For sub-mean free path-sized medium,  $L \ll l^*$ , we get the threshold condition  $(L/l^*) \exp(L/l_g) \geq 1$ , which is indeed realizable. We expect this result to hold qualitatively even in higher dimensions.

An essentially exact analytic treatment of the lasing threshold is possible for a model RAM in one-dimension as outlined here. This treatment covers the localization as well as the diffusion limit noted above. The Maxwell wave equation for a time-harmonic electric field vector  $= \text{Re}E(x)\exp(i\omega t)$  propagating in a RAM is:

$$-\nabla^2 \mathbf{E} + \nabla(\nabla \cdot \mathbf{E}) - \left[ \frac{\omega^2}{c^2} \right] \epsilon_r(x) \mathbf{E} = \epsilon_0 \left[ \frac{\omega^2}{c_0^2} \right] \mathbf{E}, \quad (2)$$

with  $\omega$  = circular frequency, and  $c_0$  = the speed of light in vacuum. Disorder in the medium is introduced here phenomenologically through a dielectric constant  $\epsilon(x) = \epsilon_0 + \epsilon_r(x)$ , where  $\epsilon_r(x)$  is the spatially random part of it modelling quenched disorder and fluctuating about  $\epsilon_0$ , the mean dielectric constant. It is now possible to

simulate coherent amplification (gain) by adding a negative imaginary part to the dielectric constant. Thus we consider  $\epsilon_0 \rightarrow \epsilon_0' - i\epsilon_0''$ , and take  $\epsilon_0'' (> 0)$  to be constant. With this,  $\epsilon(x) = \epsilon_0' - i\epsilon_0'' + \epsilon_r(x)$ , where  $-i\epsilon_0''$  amplifies the wave while  $\epsilon_r(x)$  scatters it, both without causing decoherence. We have assumed here local isotropy of the dielectric tensor.

It is readily seen that, but for the second depolarization term on the left hand side of eq. (2), we have a Helmholtz equation well-known in the electronic context. Further simplification results by noting that  $(\nabla \cdot \mathbf{E}) = -(\nabla \ln \epsilon(x)) \cdot \mathbf{E}(x) + (1/\epsilon(x)) \nabla \cdot \mathbf{D}(x)$ , where  $\mathbf{D}(x)$  = displacement field. Assuming no free charges, we have  $\nabla \cdot \mathbf{D}(x) = 0$ , and hence  $\nabla \cdot \mathbf{E} = -(\nabla \ln \epsilon(x)) \cdot \mathbf{E}(x)$ . Now, for a transverse electromagnetic mode propagating along an optical fibre (for a 1-dimensional propagation) with the dielectric constant varying randomly along the propagation direction, this quantity vanishes identically, and the wave equation (eq. (2)) reduces to the Helmholtz equation:

$$\frac{\partial^2 \mathbf{E}}{\partial x^2} + k^2 (1 + \eta_r(x) + i\eta_a) \mathbf{E} = 0, \quad (3)$$

with  $k^2 = \frac{\omega^2}{c^2} \cdot \epsilon_0'$ ,  $\eta_r(x) = \frac{\epsilon_r(x)}{\epsilon_0'}$  and  $\eta_a = -\frac{\epsilon_0''}{\epsilon_0'}$ .

Despite the formal similarity, eq. (3) differs from its electronic counterpart in an important respect even in the absence of the amplification factor ( $i\eta_a$ ). The scattering term  $k^2 \eta_r(x) \equiv (\epsilon_r \omega^2 / c_0^2)$  involves the eigenvalue  $\omega^2$  multiplicatively. Indeed, this term is responsible for the famous  $1/\lambda^{(1+d)}$  Rayleigh scattering (in  $d$  dimensions in the first Born approximation). Here it becomes small and ineffective in the limit of low frequency/long wavelength. This is not so for the electronic case. Thus, localization of light is suppressed in the low frequency limit, while for the electron the low energy tail is easily localized. In the high frequency limit, of course, the problem is no different from the electronic case and we have the geometrical-optical limit that again makes localization difficult. Indeed, localization for photons is most demanding and requires a combination of strong single-particle resonance scattering (high dielectric contrast for the scatterers) and a pseudo-gap providing a Bragg reflection-resonance condition  $\mathbf{k} \cdot \mathbf{G} = \frac{1}{2} \mathbf{G} \cdot \mathbf{G}$ . This helps satisfy the Mott-Ioffe-Bragg condition for localization. One-dimensionality is, however, an exception and arbitrarily small disorder can cause exponential localization.

The Helmholtz equation will now be studied for super-radiant reflection of an incident wave of unit amplitude. This should reveal the synergetic enhancement of amplification due to the localization effect of the dielectric disorder, as also due to the lengthening of the path

due to diffusion. The imbedding equation for the amplitude reflection coefficient  $R(L)$  is now<sup>13</sup>:

$$\frac{dR(L)}{dL} = 2ikR(L) + \frac{ik}{2}(1 + \eta_r(L) + i\eta_a)(1 + R(L))^2, \quad (4)$$

with  $R(L) = (r(L))^{1/2} e^{i\theta(L)}$  and  $R(L=0) = 0$ . Here  $r(L)$  is the intensity reflection coefficient.

We take the disorder to be a gaussian white noise

$$\langle \eta_r(L) \rangle = 0,$$

$$\langle \eta_r(L) \eta_r(L') \rangle = \eta_0^2 \delta(L - L'). \quad (5)$$

In the random phase approximation, where we assume the joint probability density  $p(r, \theta, L)$  to factorize and  $\theta$  to be uniformly distributed over  $2\pi$ , the Fokker-Planck equation for the marginal distribution  $p(r, L)$  is obtained as:

$$\begin{aligned} \frac{\partial p(r, l)}{\partial l} = & r(1-r)^2 \frac{\partial^2 p(r, l)}{\partial r^2} + [1 + (-6 - D_s)r + 5r^2] \\ & \times \frac{\partial p(r, l)}{\partial r} + [(-2 + D_s) + 4r] p(r, l). \end{aligned} \quad (6)$$

Here  $l = L/l_s$ , the dimensionless sample length,  $l_s = 2\eta_0^2 k^2 =$  the localization length ( $\xi$ ), and the gain parameter  $D_s = 4\eta_a/\eta_0^2 k = l_s/l_a$ , with the amplification length  $l_a = 1/2\eta_a k \equiv$  gain length  $l_g$ . (In 3-D we can relate the transport mean free path  $l_g$ , the gain length  $l_g$  and the speed of light  $c$  in the medium to the parameters  $\eta_0^2$ ,  $\epsilon_0''$  and  $\epsilon_0'$  characterizing scattering, amplification, and the mean dielectric constant of the medium as:

$$l_s = \frac{4\pi}{\eta_0^2 k^4} \quad l_g = \frac{1}{|\epsilon_0'| k} = c\sqrt{\epsilon_0'},$$

(Dimensionality is important).

Equation (6) has been solved<sup>3</sup> analytically in the asymptotic limit  $l \rightarrow \infty$ . We are, however, interested here in the sub-mean free path limit  $l \ll 1$ . Numerical solution in this limit confirms super-reflection with  $\langle r(l) \rangle \gg 1$  for sufficiently large gain. Such a treatment is directly applicable to a single mode polarization maintaining optical fibre doped with the rare-earth laser-

active ion  $\text{Er}^{3+}$ , pumped optically, and having some refractive index randomness along its length. Recently, a generalization of the above treatment of RAM to the case of N-channels (modes) has been achieved by Beenakker *et al.*<sup>8</sup>. Their treatment is based on the DMPK equation<sup>14</sup> and contains a number of new results.

## Conclusions

Lasing observed in a sub-mean free path-sized random amplifying medium can be understood in terms of the statistically rare scatterings over length scales  $< l^*$ , which become effective due to the high gain in the optically pumped medium beyond a threshold. It will be interesting to analyse what determines the emission wavelength and its line-width as also the effect of non-linearity, e.g. saturation, which is particularly important beyond the threshold for the onset of lasing.

1. For a review, see Lee, P. A. and Ramakrishnan, T. V., *Rev. Mod. Phys.*, 1985, **57**, 287-337.
2. Bergmann, G., *Phys. Rep.*, 1984, **107**, 1-58.
3. Pradhan, P. and Kumar, N., *Phys. Rev. B*, 1994, **50**, R9644-R9647.
4. Lawandy, M. N., Balachandran, R. M., Gomes, A. S. L. and Sauvain, E., *Nature*, 1994, **368**, 436-438; and Genack, A. Z. and Drake, J. M., *ibid*, 1994, **368**, 400-401.
5. Zhang, Z. Q., *Phys. Rev. B*, 1995, **52**, 7960-7964.
6. Zyuzin, A. Yu., *Phys. Rev. E*, 1995, **51**, 5274-5278.
7. Wiersma, D. S., van Albada, M. P. and Lagendijk, A., *Nature*, 1995, **373**, 203-204; also Wiersma, D. S., van Albada, M. P. and Lagendijk, A., *Phys. Rev. Lett.*, 1995, **75**, 1739-1742.
8. Beenakker, C. W. J., Paasschens, J. C. J. and Brouwer, P. W., *Phys. Rev. Lett.*, 1996, **76**, 1368-1371.
9. Misirpashaev, T. Sh., Paasschens, J. C. J. and Beenakker, C. W. J., *Phys. Rev. B*, 1996, **54**, 11887.
10. Burkov, A. A. and Zyuzin, A. Yu., *Phys. Rev. B*, 1997, **55**, 5736-5741.
11. Prasad, B. R., Ramachandran, H., Sood, A. K., Subramanian, C. K. and Kumar, N., *Appl. Opt.*, 1997, **36**, 7718.
12. Letokhov, V. S., *Sov. Phys. JETP*, 1968, **26**, 835-840.
13. Kumar, N., *Phys. Rev. B*, 1985, **31**, 5513-5515; See also Heinrichs, J., *Phys. Rev. B*, 1986, **33**, 5261-5270; For generalization to higher dimensions, see Kumar, N. and Jayannavar, A. M., *J. Phys. C*, 1986, **19**, L85-L89; For a review of invariant imbedding, see Rammal, R. and Doucot, B., *J. Phys. (Paris)*, 1987, **48**, 509-526.
14. Mello, P. A., Pereyra, P. and Kumar, N., *Ann. Phys. (N.Y.)*, 1988, **181**, 290-317. For a comprehensive review of DMPK equation, see Beenakker, C. W. J., *Rev. Mod. Phys.*, 1997, **69**, 731-808.

# Imaging through turbid media

Hema Ramachandran

Raman Research Institute, C. V. Raman Avenue, Sadashivanagar, Bangalore 560 080, India

**In recent years, there has been rapid advance in the field of imaging through turbid media. The technological advances have made possible feats that some years ago would have been thought to be impossible – like looking through flesh with visible light. Some of the techniques developed, and applications of these will be reviewed.**

IMAGING through turbid media has, in recent years, become a field of immense research, for its great potential for diverse applications like observing objects through fog, sighting aircraft through clouds, or searching for objects in murky waters. Aviation, defence, astrophysics, marine science and many industries are some of the areas which would benefit from advances in imaging through turbid media. Currently emphasis has mostly been laid on medical applications using infrared or visible light instead of harmful X-rays for imaging through tissues and flesh. Clinical studies have shown that the absorption characteristics at some wavelengths by normal tissues differ significantly from some tumours<sup>1</sup> and this behaviour has been adapted for discriminating or locating tumours in the human body. This article will briefly discuss propagation of light in turbid media, and will concentrate on the various techniques devised to image through such media.

## Light propagation in turbid media

Fog, milk and other random inhomogeneous media render imaging difficult due to the random multiple scattering of light. Inhomogeneities in the media cause scattering which may alter the direction of propagation, polarization and phase of light. While the propagation of light through such media may be analysed either by means of the wave picture or the photon picture, the latter is more appealing. Photons travel in straight line paths until they encounter an inhomogeneity, when they are scattered in random directions. The scattering is said to be in the Rayleigh regime when the radius,  $a$ , of the scatterer, is less than  $\lambda$ , the wavelength of light. In this case, the intensity of scattered light is equal in both the forward and backward directions (Figure 1 a). As the size of the particle increases, the scattering is more peaked in the forward direction (Figure 1 b). The case of  $a > \lambda$ , known as the Mie regime, shows peaking in some angles (Figure 1 c).

In a turbid medium made up of a random aggregate of scatterers, the photons undergo repeated scattering. The turbid medium is characterized by the scattering mean free path,  $l_s$ , which is the mean distance the photons travel before getting scattered, and the transport mean free path,  $l^*$ , which is the mean distance photons travel before the direction of propagation is randomized. Since it is quite possible that photons are forward scattered (and continue to travel in the same direction),  $l^* > l_s$ . The transport mean free path depends upon the number density of scatterers, refractive index contrast between the medium and the scatterers, and the anisotropy factor, i.e. a factor quantifying the directional distribution of scattering. Typical values<sup>2</sup> of  $l^*$  for infrared light in tissues are 1–2 mm.

The light emerging from a turbid medium consists of three components – the ballistic, the diffusive and the snake photons. These differ in their paths through the medium, and consequently in their imaging properties. The unscattered or forward scattered photons travel undeviated and emerge the first, having travelled the shortest distance through the medium (Figure 2). These preserve the characteristics of the incident light, namely direction of propagation, polarization and are

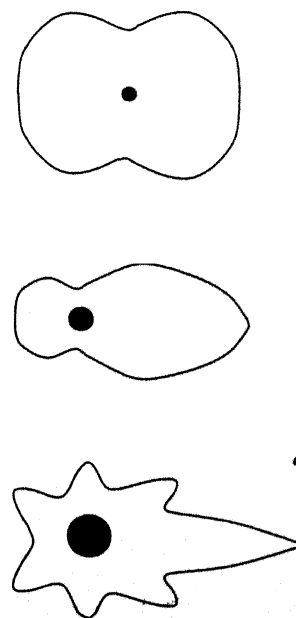


**Figure 1.** Intensity distribution of scattered light of wavelength  $\lambda$  from a spherical particle of radius  $a$ . a,  $a \ll \lambda$ ; b,  $a = \lambda/4$ ; and c,  $a \gg \lambda$ .

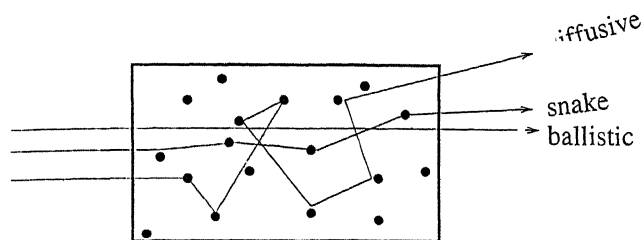


**Figure 2.** Trajectories of photons in a random medium, showing the ballistic, diffusive and snake components.

hence best for imaging. However, they are few in number, their intensity falling off as  $I = I_0 \exp(-x/l^*)$  where  $I_0$  is the input intensity, and  $x$  is the distance travelled. The diffuse component, which forms the bulk of the emergent light in turbid media is made up of photons that have undergone random multiple scattering, and these emerge later than the ballistic photons because of their increased path lengths. Their polarization, direction of propagation and phase are completely randomized. For most techniques of imaging, these form the unwanted, incoherent, diffuse background. Snake photons are those that travel in near-forward paths, having undergone few scattering events, all of which are in the forward or near-forward direction. Consequently, they retain the image bearing characteristics to some extent. Due to the varying path lengths the different photons have in the medium, a pulse of light incident on a turbid medium emerges elongated. Typically, a femtosecond pulse is stretched to a picosecond or a nanosecond pulse on travelling through a turbid medium.

All methods of imaging attempt to separate the undeviated ballistic photons from the multiply scattered diffused photons; however, they differ in the method used to achieve this discrimination. While most methods use the ballistic photons to form shadowgrams of objects hidden in turbid media, a few others make use of the diffuse photons to infer about the objects. The rapid advance in this field over the last few years has been possible due to the technological advances, like the availability of femtosecond lasers, fast electronics and very sensitive detectors.

### Principles of imaging

The ballistic photons, having travelled a straight, undeviated path in the medium, can form shadows of objects in their path. Thus, if the ballistic photons could be separated from the diffusive, one could obtain shadowgrams of hidden objects. While there are several means of discriminating the ballistic photons in the presence of the diffusive, the most obvious technique appears to be

time-gating, which exploits the fact that the diffusive photons arrive later than the ballistic photons. A short, femtosecond pulse is incident on the sample, and the emergent pulse is sliced; the first femtosecond slice would form the shadowgram of the object hidden in the turbid medium. As this required fast electronics that were not available in the early 70's, an alternate ingenious method was proposed involving a nonlinear interaction between two beams. One of these is derived from the input femtosecond pulse, while the other is the elongated pulse that has emerged from the turbid medium. Since the nonlinear interaction takes place only in the presence of both pulses, this interaction offers a means for time-gating. A typical set-up employing this technique is shown in Figure 3, where the input pulse is amplitude-divided into two parts. One of these travels through the turbid medium, and falls on the nonlinear medium, while the other follows an alternate route, and reaches the nonlinear medium at the same time as the first one. In the nonlinear medium, the mixing takes place only for the overlap period of the two pulses, which is just the duration of the input pulse. One of the earliest experimental realizations of this was by Duguay and Mattick<sup>3</sup>, where picosecond time-gating was achieved using Kerr effect. An ultra-fast Kerr shutter was formed by birefringence induced by the ultra-short infrared pulses. The shutter consists of a glass cell containing CS<sub>2</sub> placed between crossed polars (Figure 4). In the absence of any infrared pulse, no light is transmitted. The presence of an infrared pulse induces birefringence, which then permits the input signal light to pass through. Thus, ultra-short infrared pulses can be used to open the shutter for small durations, to permit just the ballistic component of the signal light to pass through. By this technique objects behind scattering media like tissue paper were imaged. Duguay and Mattick also suggested gated ranging in order to estimate the distance of

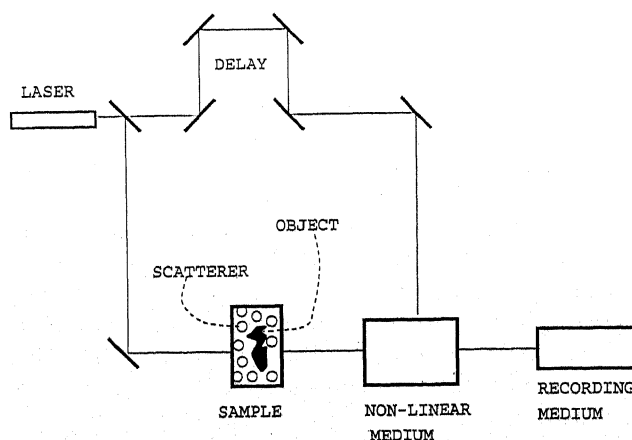


**Figure 3.** Schematic diagram of an experiment to image through turbid media using a nonlinear process for discrimination.

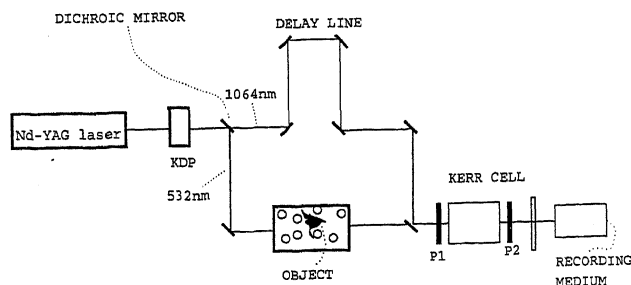


Figure 4. Schematic diagram for imaging using Kerr effect.

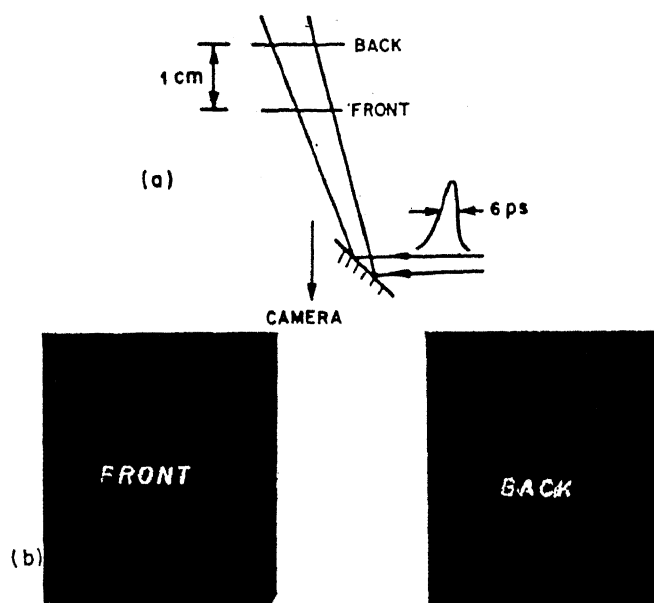


Figure 5. Experimental results of gated imaging of a transparent glass cell with the words 'FRONT' and 'BACK' written on the front and back faces, respectively. The top portion shows the schematic arrangement, where a 6-picosecond pulse is incident on the glass cell. The back-scattered light is directed towards a camera, with a Kerr shutter. The lower portion of the figure shows the gated images of the front and back faces of the cell (from ref. 3).

objects enveloped in scattering media like fog. Short pulses of light may be sent through the fog, and the back-reflected light from the obstacles be recorded by Kerr time-gating. Since just the ballistic part is passed through the Kerr shutter, an image of the scattering object is formed. The opening of the Kerr shutter may be delayed by various times so that the distance to the scattering object may be estimated from the delay time which gives the best image, this being the time taken by the input pulse to travel to the object and back. In a demonstration of gated ranging, they have imaged a glass cell which has the words 'FRONT' and 'BACK' written on the front and back faces respectively. The delay between the light arriving from the front and back

faces was calculated, and the shutter opened for picoseconds, after each of the two delays. The resulting images are shown in Figure 5. Thus, nonlinear time-gating appeared to be a very powerful tool for discriminating the ballistic photons from the diffusive. The first medical application of the ultra-fast Kerr shutter is the imaging of an isolated mammalian heart using backscattered light, by Martin and coworkers<sup>4</sup>.

Much more progress has been made in Kerr gating. Wang *et al.*<sup>5</sup> have obtained sub-millimeter resolution for two-dimensional imaging of objects placed behind human and chicken tissue, and colloidal suspensions of polystyrene microspheres. They have also reported improvement of signal-to-noise ratio by a factor of 500, and a 3-fold improvement in shutter speed by the use of a double-stage Kerr shutter<sup>6</sup>.

In a similar fashion, several other nonlinear processes have been adapted to obtain discrimination of photons. Fujimoto *et al.*<sup>7</sup> employed second harmonic generation to achieve cross-correlation of the reference and the ballistic photons, and have reported femtosecond optical ranging, with 15  $\mu\text{m}$  resolution. This technique was applied in investigating the cornea in a rabbit's eye *in vivo*, and to study the epidermal structure of the human skin *in vitro*. Yoo *et al.*<sup>8</sup> have used second harmonic generation in KDP to achieve 100 femtosecond time-gating.

The nonlinear methods discussed above merely permit transmission or frequency conversion of the ballistic signal, without amplification, often with intensity loss. Duncan *et al.*<sup>9</sup> have demonstrated a technique based on stimulated Raman amplification, where the ballistic photons were amplified by six orders of magnitude in a Raman amplifier, with the long wavelength Stokes beam being amplified by a shorter wavelength pump. The difference in the two wavelengths coincides with a fundamental vibration of the Raman amplifier medium, which in this case was hydrogen gas at 30 atm. The input pulse at the Stokes wavelength was amplitude-divided into the signal and pump pulses. The signal pulse that emerged elongated in time on traversing the turbid medium, was incident on the Raman amplifier, which was strongly pumped by an ultra-short pulse, with an appropriate delay to provide time-gating of the ballistic light. The output of the Raman amplifier had the Stokes signal amplified, resulting in a sensitivity and resolution higher than would have been possible otherwise. A similar technique was employed by Devaux *et al.*<sup>10</sup> where parametric amplification was used for time-gating as well as improvement of the ballistic signal strength.

Meanwhile, by the late 80's fast nanosecond and picosecond detection devices became available, throwing open a vast new area for development of imaging techniques. Delpy *et al.*<sup>11</sup>, using a streak camera, studied the propagation of near-infrared light through the head of a

rat. In another study, Das *et al.*<sup>12</sup> employed a high repetition rate 100 fs laser pulse for illumination, and a streak camera for scanning, and imaged a translucent piece of chicken fat embedded in 40 mm thick chicken breast tissue. Another technique of imaging using fast electronics, developed by Andersen-Engels *et al.*<sup>13</sup>, adapts delayed coincidence photon counting, where a part of the input pulse was fed to the photon counter, the remaining being incident on the sample. The pulse emerging from the sample was fed to the coincidence counter, and the number of photons arriving after a pre-set delay time was monitored. In this manner, the ballistic signal could be recorded. In both the streak camera method and the delayed coincidence method, two-dimensional imaging requires a step scan, where at each step the ballistic signal is measured.

The methods discussed so far employ time-gating which selects the ballistic light by virtue of the time of travel in the turbid medium. An alternate approach uses the fact that the input light is coherent, and the ballistic part retains the coherence. Some of the methods which make use of this feature are optical coherence tomography, holography, and coherent anti-Stokes Raman scattering (CARS). Optical coherence tomography is based on the low coherence interferometry, and may be implemented both in retro-reflection and trans-illumination modes. While the former can yield images of microstructures in tissues, the latter may be used to obtain shadows of opaque objects embedded in turbid media. The method uses a broadband light source, and a Michelson interferometer, with the sample in one arm and a mirror in the other (Figure 6). Fringes with good visibility are obtained when the path lengths in the two arms differ to within the coherence length of the source; thus smaller the coherence length of the source, the better the resolution of imaging. By sweeping one arm and simultaneously recording the interference fringes,

one can obtain a map of the reflecting surface. In this manner, Izatt *et al.*<sup>14</sup> have imaged *in vitro* the anterior segment of a human eye with micron resolution. Optical coherence tomography has found applications in ophthalmology in the study of the corneal and retinal structure<sup>15,16</sup>. This technique has been further developed<sup>17</sup>, whereby the dynamic, motion-artifact free *in vivo* image of a beating heart was obtained. This was achieved by forming a Michelson interferometer with fibres, and using a piezo-electric fibre-stretcher to vary the reference arm delay.

Another method based on optical coherence is the holographic technique, where an ultra-short pulse is split into the object and the reference beams. The object beam traverses the turbid medium and reaches the recording device at the same time as the appropriately delayed reference beam. The interference pattern is recorded, with a meaningful pattern being formed during the overlap period of the two beams. Thus, the ballistic component contributes to the holographic recording, while the later arriving diffuse light forms incoherent noise, exposing the recording medium and reducing the fringe visibility. Considerable work in this field has been carried out by Abramsons and Spears<sup>18</sup> and Leith *et al.*<sup>19,20</sup>. In the initial investigations, photographic media were used, which have now been replaced by CCD cameras, giving rise to the term 'electronic holography'.

As work in this field grew in volume, several other results were established. It was recognized that spatial filtering, to some extent, was equivalent to time-gating<sup>19-21</sup>. A spatial filter is formed by a lens-aperture system, with a lens of focal length  $f$  which collects light and focuses it onto an aperture of radius  $a$  placed at its focus (Figure 7). Since light travelling along the axis is focussed onto the aperture and transmitted, while light travelling in other directions is focussed off the aperture, and is blocked, the spatial filter may be used to cut off, to some extent, the diffuse light that travels in all directions, while transmitting the on-axis ballistic light. Similarly, attention was also focused on the polarization characteristics of the diffusive light, and it was conclusively established that discrimination could be carried out based on polarization. Several schemes have been devised that utilize the fact that the ballistic light preserves the initial direction of propagation and polarization. Implementation of spatial filtering and polarization discrimination was found to aid in the sensitivity and resolution<sup>22-24</sup>.

Almost all work has concentrated on the use of a pulsed source of light, and in contrast, there has been very little work using continuous wave sources. This is because the diffusive part of an earlier portion of the input light would overlap with the ballistic photons from a later part of the input light, making the separation

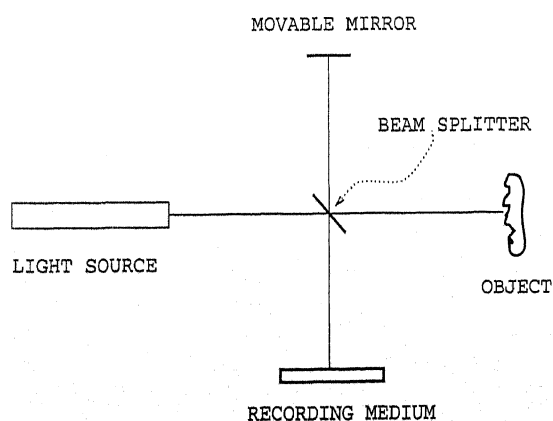
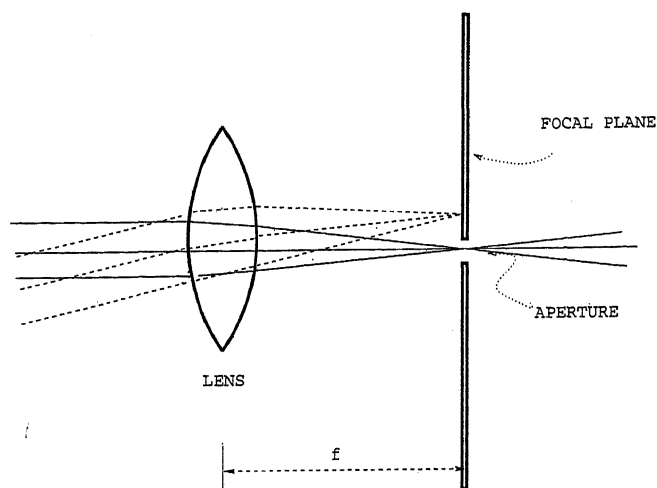


Figure 6. Schematic diagram for optical coherence tomography.



**Figure 7.** A spatial filter formed by a lens and an aperture at its focal point.

impossible by the methods discussed so far. Early work on continuous wave sources used intensity-modulated continuous wave light<sup>25</sup>, which gives rise to a diffuse photon density wave that has a well-defined wavelength, amplitude and phase at all points in the medium. The scattering of these waves by hidden objects is measured by detectors placed all around the sample, and imaging is considered an inverse source problem.

Horinaka *et al.*<sup>23</sup> have shown that ballistic and snake photons can be extracted by continuous wave sources using light polarization. They established the equivalence of temporal gating using pulsed sources and polarization discrimination using continuous wave polarization-modulated sources. While Demos and Alfano<sup>24,26</sup> have used polarization discrimination to obtain images using pulsed sources, Emile *et al.*<sup>27</sup> have obtained images using continuous wave light from a 30 mW dye laser. Their scheme (Figure 8) uses a linearly polarized source, with the plane of polarization rotating at some angular frequency. Two pinholes, one in front of the sample, and one behind, define the direction of propagation. Light emerging from the exit pinhole passed through a fixed analyser, and was detected by a photomultiplier tube, the output of which was passed to a lock-in amplifier that locked onto the frequency corresponding to that of the input polarization rotation frequency, thus picking out the ballistic component (and to some extent the snake) in the presence of the diffusive. By a synchronized step-scan of the two pinholes, they have obtained images of a millimeter-sized object immersed in milk. This was a significant achievement, as it used easily available continuous wave sources, and did not require very sophisticated electronic devices.

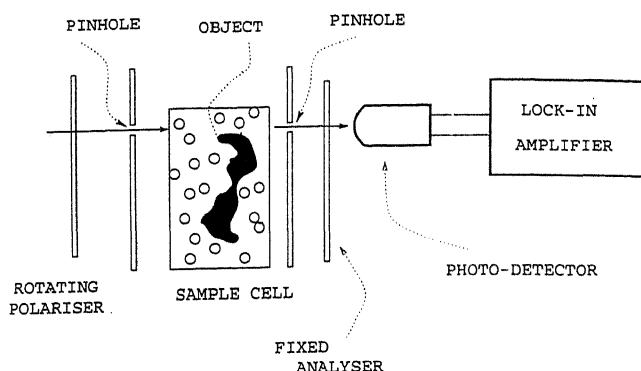


**Figure 8.** Imaging scheme using a continuous wave light source, with polarization discrimination and step scan.

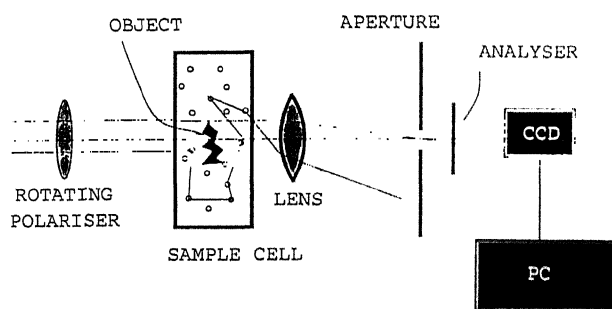


**Figure 9.** An imaging scheme for two-dimensional imaging through turbid media using a continuous wave source.

Recently, we have devised a method<sup>28</sup> of rapid two-dimensional imaging using low power continuous wave sources. The technique uses a combination of spatial filtering and polarization discrimination, separating out the ballistic photons by virtue of the fact that these have retained their polarization, and direction of propagation, while the diffusive photons have not. Light from a continuous wave source like a low-power HeNe laser or a diode laser is polarization-modulated by a rotating linear polarizer, or half wave plate, and is incident on the sample (Figure 9). The light emerging from the sample is spatially filtered and passed through a fixed analyser onto a CCD camera that rapidly acquires a sequence of frames. These frames are two-dimensional intensity data, with the successive frames differing in that the direction of input polarization was different. The polarization discrimination is achieved by Fourier transforming the time sequence of images to extract the component that has the same frequency of variation as the input polarization modulation. This is the ballistic component (and to some extent the snake). By this

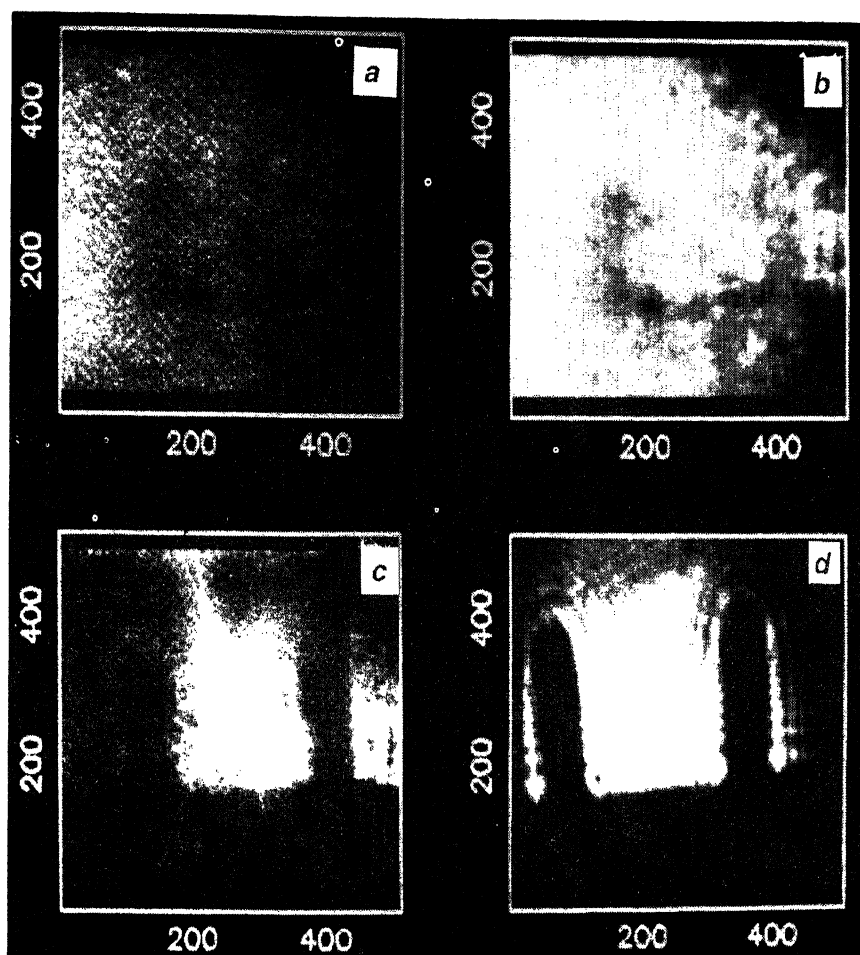


Figure 10. Experimental realization of imaging using a HeNe laser<sup>28</sup>. *a*, A typical frame recorded by the CCD camera. No object is visible; *b*, The zero-frequency component after Fourier transform. The hexagonal structures are the cells on the face plate of the CCD camera. The dark spot is a defective region on the face plate of the CCD; *c*, The image of the object (a portion of an IC) obtained at the frequency  $2\omega$ . Note that even some diffraction lines are seen; and *d*, The bare object, with no scattering medium.

technique, using a 1 mW HeNe laser, we have obtained better than 100  $\mu\text{m}$  resolution imaging of millimeter-sized objects immersed in turbid media that are more than 30 transport mean free paths thick (Figure 10). Direct formation of two-dimensional images, the absence of synchronized stepping parts and polarization discrimination by software in post-processing contribute to the speed and ease of data collection. The use of diode lasers makes the equipment compact and portable, an advantage in medical and field applications.

## Conclusions

Imaging through turbid media has become a field of intense activity, and rapid progress has been made using different techniques which have demonstrated numerous applications. Although the basic physics in this field was

known for a long time, practical implementation had to wait for technology to provide suitable devices like femtosecond lasers, fast detection devices, and two-dimensional array cameras. Intense efforts are currently being directed towards improving detection capability and resolution.

1. Ertefai, S. and Profio, A. E., *Med. Phys.*, 1985, **12**, 393.
2. Peters, V. G. *et al.*, *Phys. Med. Biol.*, 1990, **35**, 1317.
3. Duguay, M. A. and Mattick, A. T., *Appl. Opt.*, 1971, **10**, 2162–2170.
4. Martin, J. L., Lecarpentier, Y., Antonetti, A. and Grillon, G., *Med. Biol. Eng. Comput.*, 1980, **18**, 250.
5. Wang, L., Ho, P. P., Liu, C., Zhang, G. and Alfano, R. R., *Science*, 1991, **253**, 769–771.
6. Wang, L. M., Ho, P. P. and Alfano, R. R., *Appl. Opt.*, 1993, **32**, 535–539.
7. Fujimoto, J. G., de Silvestri, S., Ippen, E. P., Puliafito, C. A., Margolis, R. and Oseroff, A., *Opt. Lett.*, 1986, **11**, 150–152.

## SPECIAL SECTION: OPTICS OF HETEROGENEOUS MEDIA

8. Yoo, K. M., Xing, Q. and Alfano, R. R., *Opt. Lett.*, 1991, **16**, 1019.
9. Duncan, M. D., Mahon, R., Tankersley, L. L. and Reintjes, J., *Opt. Lett.*, 1991, **16**, 1868-1870.
10. Devaux, F., Lantz, E. and Malliotte, H., *Opt. Commun.*, 1995, **114**, 295.
11. Delpy, D., Cope, M., van der Zee, P., Arridge, S., Wray, S. and Wyatt, J., *Phys. Med. Biol.*, 1988, **33**, 1433.
12. Das, B. B., Yoo, K. M., Alfano, R. R., *Opt. Lett.*, 1993, **18**, 1092-1094.
13. Andersen-Engels, S., Berg, R., Svanberg, S. and Jarlman, O., *Opt. Lett.*, 1990, **15**, 1179-1181.
14. Izatt, J. A., Hee, M. R., Huang, D., Swanson, E. A., Lin, C. P., Schuman, J. S., Puliafito, C. A. and Fujimoto, J. G., *Optics and Photonics News*, October 1993, p. 14.
15. Hee, M. R., Izatt, J. A., Swanson, E. A., Huang, D. Lin, C. P., Schuman, J. S., Puliafito, C. A. and Fujimoto, J. G., *Arch. Ophthalmol.*, 1995, **113**, 325.
16. Puliafito, C. A., Hee, M. R., Lin, C. P., Reichel, E., Schuman, J. S., Duker, J. S., Izatt, J. A., Swanson, E. A. and Fujimoto, J. G., *Ophthalmology*, 1993, **102**, 217.
17. Tearney, G. J., Bouma, B. E., Boppart, S. A., Golubovic, B., Swanson, E. A. and Fujimoto, J. G., *Opt. Lett.*, 1996, **21**, 1408-1410.
18. Abramson, N. H. and Spears, K. G., *Appl. Opt.*, 1989, **28**, 1834.
19. Leith, E., Arons, E., Chen, H., Chen, Y., Dilworth, D., Lopez, J., Shih, M., Sun, P. C. and Vossler, G., *Optics and Photonics News*, Oct. 1993, 19-23.
20. Chen, H., Chen, Y., Dilworth, D., Leith, E., Lopez, J. and Valdmans, J., *Opt. Lett.*, 1991, **16**, 487-489.
21. Wang, Q. Z., Liang, X., Wang, L., Ho, P. P. and Alfano, R. R., *Opt. Lett.*, 1995, **20**, 1498-1500.
22. Wang, L., Ho, P. P. and Alfano, R. R., *Appl. Opt.* 1989, **28**, 2304.
23. Horinaka, H., Hashimoto, K., Wada, K. and Cho, Y., *Opt. Lett.*, 1995, **20**, 1501-1503.
24. Demos, S. G. and Alfano, R. R., *Opt. Lett.*, 1996, **21**, 161-163.
25. O'Leary, M. A., Boas, D. A., Chance, B. and Yodh, A. G., *Phys. Rev. Lett.*, 1992, **69**, 2658.
26. Demos, S. G. and Alfano, R. R., *Appl. Opt.*, 1997, **36**, 150-155.
27. Emile, O., Bretenaker F. and le Floch, A., *Opt. Lett.*, 1996, **21**, 1706-1708.
28. Hema Ramachandran and Andal Narayanan, *Opt. Commun.*, 1998, **154**, 255-260.

ACKNOWLEDGEMENTS. I am indebted to Prof. N. Kumar, who introduced me to this subject, and to Prof. Rajaram Nityananda, with whom I had many useful discussions. I also wish to thank Dr Andal Narayanan with whom I worked on the imaging experiment.

# Copies of articles from this publication are now available from the UMI Article Clearinghouse.

For more information about the Clearinghouse, please fill out and mail back the coupon below.

**UMI** Article  
Clearinghouse

Yes! I would like to know more about UMI Article Clearinghouse. I am interested in electronic ordering through the following system(s):

- ☐ DIALOG Dialorder      ☐ ITT Dialcom  
☐ OnTyme                      ☐ OCTC III Subsystem  
☐ Other (please specify) \_\_\_\_\_  
☐ I am interested in sending my order by mail.  
☐ Please send me your current catalog and user instructions for the system(s) I checked above.

Name \_\_\_\_\_  
 Title \_\_\_\_\_  
 Institution/Company \_\_\_\_\_  
 Department \_\_\_\_\_  
 Address \_\_\_\_\_  
 City \_\_\_\_\_ State \_\_\_\_\_ Zip \_\_\_\_\_  
 Phone (\_\_\_\_\_) \_\_\_\_\_

Mail to: University Microfilms International  
 300 North Zeeb Road, Box 91, Ann Arbor, MI 48106

# Tissue optics

P. K. Gupta

Laser Biomedical Applications Laboratory, Centre for Advanced Technology, Indore 452 013, India

**The article provides a brief overview of light propagation in tissue. The application of tissue optics for medical diagnosis and phototherapy is also discussed.**

THERE exists considerable current interest in the use of optical methods for medical imaging, diagnosis and therapy<sup>1</sup>. This is motivated by the growing maturity of lasers, fiber optics and associated technologies because of which practical realization of the considerable potential of the optical approaches has now become feasible. Encouraging results have already been obtained for use of optical techniques for *in situ* monitoring of tissue parameters, discrimination of diseased tissue from normal, mammography, and several therapeutic applications. For most of these applications, in particular for the use of light in therapy, it is important to be able to predict the spatial distribution of light in the target tissue. This is rather involved because the biological tissue is inhomogeneous and the presence of microscopic inhomogeneities (macromolecules, cell organelles, organized cell structure, interstitial layers etc.) makes it turbid. Multiple scattering within a turbid medium leads to spreading of a light beam and loss of directionality. Therefore, much of the results of the optics of homogeneous, nonscattering media (like the Beer Lambert's law, used widely to work out the spatial variation of light in a nonscattering medium) are not applicable to light propagation in tissue. A rigorous, electromagnetic theory based approach for analysing light propagation in tissue will need to identify and incorporate the spatial/temporal distribution and the size distribution of tissue structures and their absorption and scattering properties. Clearly this is a formidable task. Therefore, heuristic approaches with different levels of approximations have been developed to model light transport in tissues. An effort for modelling light transport also requires accurate values for the optical transport parameters of the tissue. Measurement techniques, different from those used for homogeneous nonscattering media are required for this purpose.

The term tissue optics encompasses modelling of the light transport in tissues, measurement of tissue optical transport parameters, and development of models which can explain the optical properties of tissue and their

dependence on the number, size and arrangement of the tissue elements. In this article we provide a brief overview of these aspects and also discuss some representative applications of tissue optics for biomedical applications.

## Tissue optical parameters

An exact modelling of the inhomogeneous and turbid tissue is not presently feasible. The tissue is therefore generally represented as an absorbing bulk material with scatterers randomly distributed over the volume. Further, it is usually assumed to be homogenous, even though this is not a true representation. The parameters used to characterize the optical properties of the tissue are, the absorption coefficient ( $\mu_a$ ), single scattering coefficient ( $\mu_s$ ), the transport coefficient ( $\mu_t = \mu_a + \mu_s$ ) and the phase function  $p(s, s')$  (refs 2, 3). The linear optical coefficients  $\mu_i$  are defined so that  $l_a = \mu_a^{-1}$ ,  $l_s = \mu_s^{-1}$ , and  $l_t = \mu_t^{-1}$  give the absorption, scattering, and transport mean free paths, respectively. The function  $p(s, s')$  is the probability density function giving the probability of photon scatter from an initial propagation direction  $s$  to a final direction  $s'$ . The linear optical coefficients are related to the absorption and scattering cross-sections ( $\sigma_a$  and  $\sigma_s$  respectively) by  $\mu_a = \rho\sigma_a$  and  $\mu_s = \rho\sigma_s$ . Here  $\rho$  is the particle density and independent scatterer approximation is implicit. The integral of phase function (or the differential cross-section) over  $4\pi sr$  may be normalized to one or more frequently to the ratio  $\mu_s/(\mu_a + \mu_s)$ . This quantity is the transport albedo ( $a$ ) and will be unity for a nonabsorbing scattering material. The first moment of the phase function is the average cosine of the scattering angle, denoted by  $g$ . It is also referred to as the anisotropy parameter. The value of  $g$  ranges from  $-1$  to  $+1$ , where  $g = 0$  corresponds to isotropic scattering,  $g = +1$  corresponds to ideal forward scattering and  $g = -1$  corresponds to ideal backward scattering. A photon acquires random direction after about  $1/(1 - g)$  scattering events, which is only five for  $g = 0.8$ . Typical values of  $g$  for biological tissues vary from 0.7 to 0.99. Another parameter frequently used is  $\mu_s' = \mu_s(1 - g)$ . This is referred to as the reduced scattering coefficient. It defines the probability of photon to be scattered in path length  $z$  when the scattering is described by an isotropic function. The use of  $\mu_s'$  assumes that the reflection and transmission for a slab of tissue with optical parameters  $\mu_a$ ,  $\mu_s$  and  $g \neq 0$  are the same as those for the

e-mail: pkgupta@cat.ernet.in

same slab with optical parameters  $\mu_a$ ,  $\mu'_s$  and  $g = 0$ . This so called similarity principle, is not exact and holds if  $\mu'_s \gg \mu_a$  and if the light distribution is studied far enough away from the light source and boundaries, typically at a distance greater than the effective mean free path  $(\mu'_s + \mu_a)^{-1}$ . An exact calculation of the cross-sections for the poorly characterized absorbing and scattering centers located in a biological tissue is not feasible. The average optical constants of relatively homogeneous tissues can be calculated from experimental data by fitting the experimental results with appropriate models. This will be discussed later in the article.

Development of optical models that explain the observed scattering properties of soft biological tissues is also of considerable interest<sup>4</sup>. Such modelling can provide insight into how the scattering properties are influenced by the numbers, sizes and arrangements of the tissue elements. Single scattering of collimated light is used widely to study cells and subcellular structures in suspensions. This approach is not directly applicable for tissues due to multiple scattering. Nevertheless, diffusely scattered light from tissue contains information about its underlying structures. Measurements on the diffusely scattered light have recently been used to get estimates for scatterer size in tissues<sup>5</sup>. Further, the extrapolation of the results obtained from cell suspensions to tissues suggest that a majority of scattering from a tissue takes place from organelles within the cell<sup>6</sup> and that the cell shape has little effect. Therefore, scattering from tissue should contain information on changes in organelle structure and number. Recently<sup>7</sup> the density and size distribution of the epithelial cell nuclei have been estimated by analysis of the reflectance from a mucosal tissue. This could have valuable application in clinical diagnosis since these quantities are important indicators of neoplastic precancerous changes in biological tissues.

### Tissue optic theories

Theoretical formulations based on the electromagnetic theory, though rigorous, in that it is possible to include all the multiple scattering, diffraction and interference effects, do not lead to solvable equations for any case of practical interest in tissue optics. The heuristic radiative transfer (RT) theory has been the most successful in modelling light transport in tissues<sup>2,3,8</sup>. In this approach, originally developed by Chandrasekhar<sup>9</sup> to explain light propagation in stellar atmosphere, light propagation in a tissue is described by transport of energy by the motion of photons through a medium containing discrete scattering and absorption centres. The time-independent equation for the net change of radiance  $L(\mathbf{r}, \mathbf{s})$  at position  $\mathbf{r}$  in the direction of unit vector  $\mathbf{s}$  can be written as:

$$(\mathbf{s} \cdot \nabla_{\mathbf{r}})L(\mathbf{r}, \mathbf{s}) = -\rho\sigma_t L(\mathbf{r}, \mathbf{s}) + \frac{\rho\sigma_t}{4\pi} \int_{4\pi} p(\mathbf{s}, \mathbf{s}') L(\mathbf{r}, \mathbf{s}') d\Omega' + \epsilon(\mathbf{r}, \mathbf{s}). \quad (1)$$

The first and the second term on the right hand side represent the depletion and increase of  $L(\mathbf{r}, \mathbf{s})$  respectively. The last term specifies the contribution to  $L(\mathbf{r}, \mathbf{s})$  of sources located within the medium. This equation called the equation of transfer is equivalent to the Boltzman equation used in the kinetic theory of gases and in neutron transport theory.

There are no exact general solutions to the transport equations in a tissue. For tissues, tenuous scattering approximation (volume density of scattering particles  $< 10^{-3}$ ) rarely applies. Tissues are therefore usually modelled either as intermediate scattering media or dense media (volume density  $> 10^{-2}$ ). The intermediate scattering case is the most difficult to handle rigorously. Several approaches like the Kubelka-Munk model have been employed<sup>2,3</sup>. The range of validity of these models is not well established and the formulation cannot be generalized to most cases of practical interest. For weakly absorbing, dense media, in which scattering predominates ( $(1-g)\mu_s \gg \mu_a$ ), the integro-differential equation of radiation transfer reduces to a simpler photon diffusion equation<sup>2,3,8</sup> whose time-independent form can be expressed as<sup>2,3</sup>.

$$\nabla^2 \phi_d(\mathbf{r}) - \frac{\mu_a}{D} \phi_d(\mathbf{r}) = -\frac{S(\mathbf{r})}{D}, \quad (2)$$

where  $D$  is the diffusion constant, given by  $D = 1/3[\mu_a + \mu_s(1-g)]$ ,  $S(\mathbf{r})$  is the 'source' term and  $\phi$  is the radiant energy fluence rate or 'space irradiance'. It is defined as the radiant flux incident from all directions on a small sphere divided by the cross-sectional area of the sphere. When the medium does not contain actual light sources, the 'apparent' source consists of unscattered photons. In order to solve the diffusion equation for a given problem an appropriate choice of the phase function and the boundary condition are required. The choice of phase function is arbitrary due to the diversity and the unknown nature of the inhomogeneities. Several approximations have therefore been used<sup>2,3,8</sup>. The exact boundary condition for diffuse intensity is that at the surface there should be no diffuse intensity entering the medium from outside because the diffuse intensity is generated only within the medium. In the diffusion approximation this cannot be satisfied exactly and approximate boundary conditions are used<sup>2,8,10</sup>. One such approximation, valid for matched boundaries, is that at the surface the total diffuse flux directed inwards be zero. For unmatched boundaries this will be the part of the outwardly directed flux reflected

by the surface. A typical tissue-air boundary reflects more than 50% of the outwardly directed isotropic diffuse fluence<sup>10</sup>. Therefore, boundary reflections have a significant influence on the distribution of light, particularly near the surface. It is pertinent to note that the diffusion approximation itself holds only for the region far from the boundary and the source, where the incident photons have lost all of their initial directionality. Time resolved measurements on the transport of photons<sup>11</sup> through a slab of random media (with thickness  $l$ ) have confirmed that the prediction of the time-dependent diffusion approximation deviates monotonically from the measured scattered pulse as the value of  $l/l_t$  decreases or the anisotropic scattering increases. For  $l/l_t = 6$  and  $l = 10$  mm, the average time of arrival was about 0.9 times that predicted by diffusion theory<sup>11</sup>. For a uniformly illuminated optically dense slab, far away from boundary so that  $S(\mathbf{r}) = 0$ , eq. (2) can be integrated to give the following expression for the diffuse flux density  $\phi_d(z)$ :

$$\phi_d(z) = \phi_d(z=0) \exp(-\mu_{\text{eff}} z). \quad (3)$$

Here,  $\mu_{\text{eff}}$  is the effective attenuation coefficient for diffuse flux deep into the tissue, and is related to the optical constants by:

$$\mu_{\text{eff}}^2 = 3\mu_a[\mu_a + \mu_s(1-g)]. \quad (4)$$

The diffusion approximation is a fair representation for light transport, in a soft tissue, in the visible and near-infrared spectral region and has therefore been applied to many cases of interest for laser applications in medicine. The other widely used method for modelling light transport in tissues is the Monte-Carlo simulation. In this statistical approach to radiative transfer, the multiple scattering trajectories of individual photons are determined using random numbers to predict the probability of each microscopic event. The superposition of many photon paths approaches the actual photon distribution in time and space. Although Monte-Carlo simulations may require lengthy computation time they can be performed for any experimental geometry and are considered the 'gold standard' of tissue optics calculations.

### Measurement of tissue optical parameters

Measurements of tissue optical parameters are made complicated by multiple scattering. In this section we provide a brief overview of the techniques developed for *in vitro* and *in vivo* measurements. For details the reader is referred to the excellent review provided by Wilson<sup>12</sup>.

#### *Direct measurement of optical parameters of a resected tissue*

An obvious approach to eliminate multiple scattering effects is to use tissue sample with thickness  $d \ll 1/\mu_s$ . The absorption coefficient can then be determined by measuring all the photons transmitted or scattered by the sample, so that the only loss is due to absorption. Similarly, for the typical situation, where  $\mu_a \ll \mu_s$ , the scattering coefficient can be determined by filtering out the collimated photons using a suitable aperture and detecting all the scattered photons. Measurement of phase function requires determination of the angular distribution of the scattered photons. All the three measurements are most conveniently done using an integrating sphere. This approach, however, has a fundamental limitation. Because the typical value of  $\mu_s$  for soft tissues is in the range  $100\text{--}1000\text{ cm}^{-1}$ , the samples thickness must be less than about  $10\text{ }\mu\text{m}$ . The methods used for the preparation of these thin sections may alter the tissue optical properties. Further, the signals are weak. For example, for soft tissues in the visible wavelength range,  $\mu_a \sim \mu_s/100$ . Therefore, the loss of photons due to absorption in sample thickness  $d \ll 1/\mu_s$  is very small. The weak signal may easily be swamped by several artifacts like unavoidable fluctuations in incident light flux, nonuniformity of response of the integrating spheres etc. Although methods have been developed to minimize these effects this approach may not provide very accurate measurements.

#### *Indirect measurements on a resected tissue*

A more practical approach for determining tissue optical parameters is to work with an optically thick tissue section and measure its optical characteristics like the diffuse reflectance ( $R_d$ ), the diffuse transmittance ( $T_d$ ), the transmitted collimated light ( $T_c$ ), spatial distribution of fluence, etc. Approximate analytical models or the Monte-Carlo simulation can then be used to determine the tissue optical parameters through their relationship with the measured parameters. It is pertinent to note that for measurement of  $T_c$ , the tissue has to be thin and therefore measured  $R_d$  and  $T_d$  may not correspond to the completely diffused light. If only  $R_d$  and  $T_d$  are measured, then it is not possible to determine all the three parameters ( $\mu_a$ ,  $\mu_s$  and  $g$ ). With these measurements one can estimate  $\mu_a$  and the reduced scattering coefficient  $\mu'_s$  under the assumption that the similarity principle holds.

The analytical models, even where applicable, have not yet provided a closed form equation for the tissue optical parameters in terms of the measured parameters. Therefore, for both the analytical and Monte-Carlo methods it is necessary to either (i) forward calculate the

measured parameters over the expected range of values for the tissue optical parameters and interpolate or (ii) use an iterative procedure. The right choice of model to derive the optical properties involves a trade off between accuracy, speed and flexibility.

Several other approaches have also been developed. In the 'added absorber' method,  $\mu_{\text{eff}}$  for the tissue is measured as a function of the concentration of a dye of known extinction coefficient which is uniformly distributed in the tissue. From these measurements,  $\mu_a$  and  $\mu_s'$  can be worked out using a suitable theoretical model under the assumption that the tissue scattering remains unchanged with the addition of dye. The angular peak shape of the coherently backscattered light has also been used for estimating the optical parameters of a tissue<sup>13-15</sup>. Photothermal and photoacoustic techniques can also be used. However, very little published information exists in this regard. We had used photoacoustic spectroscopy to estimate the wavelength dependence of breast tissue absorption<sup>16</sup>. The values for  $\mu_a$  measured at several wavelengths were in reasonable agreement with the values reported using other techniques.

#### *In vivo measurements*

Some of the techniques discussed above can in principle be used for *in vivo* measurements also. This however may require positioning of appropriate fiber probes in the tissue to be investigated. For clinical applications a noninvasive approach will clearly be more appropriate. A great deal of effort is being put in to exploit the diffuse reflectance from a tissue for this purpose. Though, both spatially integrated and spatially resolved diffused reflectance measurements have been used the latter are usually more convenient in practice. The basic arrangement for spatially resolved measurements involves illuminating a small area of the sample by a monochromatic light. The relative radiance  $R(r)$  (defined as the ratio of the detected radiance to the incident radiant flux) is determined, as a function of distance  $r$  between the centres of the spot of illumination and detection, using appropriate fiber probes. The measurements can be made in steady state or time resolved mode. Both have been used for measurements of tissue parameters. The rationale for the use of  $R(r, t)$  in tissue parameter measurements is straightforward. Both the spatial and temporal distribution of the diffuse radiance are influenced by  $\mu_a$  and  $\mu_s$ . The lower the value of  $\mu_s'$ , larger will be the spatial extent over which photons will be distributed and consequently the steady state relative radiance curve  $R(r)$  will be less steep. Similarly with increasing absorption the radiance at larger distances will be affected more than at shorter distances leading to a lower and steeper  $R(r)$  curve. Mismatched boundaries lead to surface reflection because of which

the  $R(r)$  curve becomes less steep. Similar considerations apply to temporal broadening of an incident light pulse due to multiple scattering. For  $r \gg 1/\mu_s'$ , a relationship between  $R(r, t)$  and  $\mu_a, \mu_s'$  is provided by Patterson *et al.*<sup>17</sup> using time-dependent diffusion theory for a semi-infinite optically homogenous medium. It also follows from this theory that

$$\mu_a = -\frac{n}{c} \lim_{t \rightarrow \infty} \frac{\partial \ln R(\mathbf{r}, t)}{\partial t}$$

where  $n$  is the average refractive index for tissue. Thus the final slope of local reflectance time curve gives  $\mu_a$  directly. However, for finite geometries the slope also depends on the tissue geometry and source-detector separation. The time resolved measurements can be done in both time and frequency domain. The time domain measurements have the potential to yield  $\mu_a$  and  $\mu_s'$  directly. However, since time resolution of tens of ps is required, sophisticated and expensive lasers are needed for pursuing this approach. Frequency domain measurements by themselves and in combination with steady state measurements have also been explored for determination of  $\mu_a, \mu_s'$  (ref. 12).

*In vivo* measurements of tissue parameters using the steady state spatial radiance profile is receiving a lot of attention. This is motivated by the fact that this approach, due to the simpler technology involved, holds considerable promise for the design of a low cost, portable equipment. This approach was first elaborated by Groenhuis *et al.*<sup>18,19</sup> who also provided an expression for  $R(r)$  using diffusion theory. The parameters  $\mu_s'$  and  $\mu_a$  could be estimated using diffusion theory when applicable and Monte-Carlo simulations when necessary. It has also been shown<sup>20</sup> that the slope of the  $\ln R(r)$  versus  $r$  curve is strongly correlated to the reduced transport coefficient  $\mu_t' = \mu_a + \mu_s'$  for smaller values of  $r$  and to the effective attenuation coefficient  $\mu_{\text{eff}}$  for larger values of  $r$ . This provides a convenient approach to measure  $\mu_a$  and  $\mu_s'$ . The sensitivity, defined as the ratio between a relative variation of the measured quantity, i.e. the slope of  $\ln |R(r)|$ , and a relative variation of a tissue parameter ( $\mu_{\text{eff}}$  or  $\mu_s'$ ) when the other is kept constant, depends on the value of  $r$  at which measurements are made<sup>21</sup>. For good sensitivity in the measurement of  $\mu_s'$ , slope of  $\ln |R(r)|$  should be measured as close to the point of illumination as possible. Another advantage of small fiber separations is that it is expected to enhance sensitivity to high-angle scattering. This is because photons must turn around by way of high-angle scattering events to get detected. It has been shown<sup>22</sup> that high-angle scattering can lead to better differentiation of morphological features of the tissue. However, for the validity of the similarity principle, the separation between the detector and the point of illumination should be greater than

$1/\mu_s'$ . To improve the sensitivity of  $\mu_{\text{eff}}$ , the second measurement position should be selected as far away as possible from the point of illumination. The maximum distance that can be used in practice will be limited by the signal to noise ratio and the size of the probe. Design considerations for a practical system have been investigated<sup>21,23</sup>. *In vivo* clinical measurements of tissue optical parameters during endoscopic procedures in hollow organs, have been reported using this approach<sup>21</sup>. A large variation was observed in the estimated values of  $\mu_{\text{eff}}$  and  $\mu_s'$  for human esophagus from *in vivo* measurements on 11 patients<sup>21</sup>. While this may represent real variance in tissue optical properties, measurement errors, in particular, those induced by tissue inhomogeneities are also expected to contribute.

It is pertinent to note here that for modelling light transport in tissue, usually a homogenous tissue is assumed. However, many tissues of interest, especially skin, cannot be considered homogeneous and are in fact multilayered. Application of semi-infinite homogeneous algorithms to a layered tissue architecture can introduce serious artifacts in the measured optical properties<sup>24</sup>. The artifacts result from forcing the algorithm to fit data, which correspond primarily to the upper layer for smaller values of  $r$  and to the lower layer for larger values of  $r$ , to a model that uses the same optical properties at all distances. Therefore, while for some applications the averaged information provided by the homogeneous single layer model may be sufficient, more demanding applications require multilayered photon propagation models. Efforts are therefore being made to develop such algorithms<sup>24,25</sup>. Clinical applications also require rapid estimation of optical parameters from the measured reflectance profile. This aspect is also being addressed to<sup>23,26</sup>.

### Representative clinical applications

Measurement of tissue optical properties and determination of light transport in a tissue can be of immense value for several clinical applications. As an example, for any phototherapy, the induced effect will depend on the chromophore concentration and the light flux at the target site. The determination of these parameters is therefore crucial for the success of any phototherapy. Similarly, a change in biochemical composition or morphology of tissue will result in a change in the spectral dependence and magnitude of  $\mu_a$  and  $\mu_s$ , respectively. Such changes also get reflected in the inelastic scattering (fluorescence/Raman) from the tissue. Measurements on tissue optical parameters and inelastic scattering, can therefore be used to discriminate a diseased tissue from a normal one as well as for *in situ* monitoring of metabolic activity<sup>27</sup>. The differences in the optical parameters of a normal tissue and tumour are also being exploited for optical imaging of tumours embedded in

soft tissue. Very encouraging results have been reported on optical mammography, a noninvasive imaging modality that employs visible and near infrared light to detect breast cancer<sup>28</sup>. The application of tissue optics for imaging is discussed elsewhere in this issue. Here, we discuss briefly two representative applications of tissue optics in (i) photodynamic therapy and (ii) laser induced fluorescence diagnosis of cancer.

### Photodynamic therapy

Photodynamic therapy (PDT) is a promising approach for cancer therapy. It involves systemic administration of a drug like haemotoporphyrin derivative (HPD) which over a period of two to three days is excreted by the healthy tissue but is selectively retained by the tumour. The drug is inert in dark but when photoexcited at an appropriate wavelength, it leads to generation of singlet oxygen which is toxic to the host tissue cell. Selective destruction of cancerous tissue with minimal effect on healthy tissue can thus be achieved. The technique is now being used for treatment of lung, endobronchial, esophageal cancer and superficial bladder cancer<sup>29</sup>. Its use in other cancerous conditions is also being actively researched.

The therapeutic effect at the tumour site depends on the drug concentration and the radiant energy density at the site which together determine the energy absorbed per unit volume at the target site. Knowledge of these two parameters is therefore required in determining light dose for safe and effective treatment. Tissue optics methods have been developed for this purpose and are being constantly refined to meet clinical requirement<sup>30-32</sup>. A convenient dosimetry model for PDT is based on the assumption<sup>3</sup> that tumour eradication requires the absorption of a minimum energy density ( $w^*$ ) by the localized drug in every region of the tumour. The energy density absorbed by the photosensitizer localized at position  $\mathbf{r}$  for an exposure time  $t$  equals  $\gamma_d c_{d0} \phi(\mathbf{r})t$ . Here  $\gamma_d$  is the specific absorption coefficient of the drug at the irradiation wavelength,  $c_{d0}$  is the drug concentration and  $\phi(\mathbf{r})$  the diffuse energy fluence rate. This is under the assumption that  $\phi(\mathbf{r})$  remains constant during PDT and the drug concentration is uniform throughout the tumour and constant in time. The PDT dosimetry condition is taken as  $w(\mathbf{r}_n) > w^*$  where  $\mathbf{r}_n$  is the tumour location where PDT induces necrosis. The corresponding energy fluence threshold  $q^* = \phi(\mathbf{r}_n)t$ . Thus knowing  $\phi(\mathbf{r})$ , the depth of necrosis can be worked out. The value of  $\phi(\mathbf{r})$  will depend on the mode of light delivery. For the typical irradiation geometries used, dosimetry relations, which relate the depth of necrosis to the power delivered at the tissue surface and the optical parameters of the tissue are provided by Grossweiner<sup>3</sup>.

Generally the light dose and the drug dose do not show reciprocity, i.e. to achieve the same PDT response halving the drug dose requires more than twice the light dose<sup>3</sup>. Therefore, *in vivo* measurements of the localized drug concentration are also highly desirable. The drug concentration can be estimated by determining  $\mu_a$  for the target tissue wherein it is localized, by following the principle of added absorber method discussed earlier. This will require knowledge of the native tissue optical parameters, the extinction coefficient of the drug in tissue environment and the assumption that localization of drug does not affect tissue scattering. *In vivo* estimation of drug concentration can also be made from quantitative measurement of drug fluorescence. The uncertainty in these estimates can result from the fact that the fluorescence quantum yield is a strong function of the local microenvironment. Such measurements have also to contend with the problem of multiple scattering to be discussed next in the article.

### *Laser induced fluorescence diagnosis for cancer*

The use of laser induced fluorescence for discriminating malignant tissue from benign tumour or normal tissue is receiving considerable attention<sup>27</sup>. This is because it offers the promise of a sensitive, *in situ*, near real time diagnosis without any adverse side effects, making it particularly attractive for mass screening. Most often diagnosis is done exploiting the differences in the steady state spectra of normal and diseased tissues. Some of the observed differences are expected to be due to the biochemical changes in tissue that are associated with the onset and progression of the disease. However, the measured spectra also has artifacts due to wavelength-dependent absorption and scattering of excitation and emission photons during their propagation through the tissue. For example, significant differences have been observed in the 337 nm excited fluorescence intensity in the blue spectral region from malignant and normal human tissues from breast<sup>33</sup> and oral cavity<sup>34</sup>. These can be caused by several factors like changes in the contribution of blood absorption owing to changes in neovascularization of the tissue, changes in tissue morphology or due to change in nicotinamide adenine dinucleotide fluorescence<sup>27,33,34</sup>. Although excitation/emission spectroscopy can provide some understanding of the likely causes<sup>35</sup>, extraction of true fluorescence spectrum from the observed spectrum is required to quantify these effects. Several studies have been made with this objective<sup>36-38</sup>. Extraction of true fluorescence spectra will not only generate biochemical information on the tissue but also help in the design of systems with enhanced sensitivity to the specific biochemical features of the tissue.

### Conclusions

One of the cherished dreams of mankind has been to develop techniques to 'peep' inside the body noninvasively and with no ill effects. The persistent march towards this objective has seen the development of a wide variety of biomedical imaging techniques such as computed tomography, magnetic resonance imaging etc. which have in turn resulted in a substantial improvement in the quality of health care. The latest step in this endeavour is the exploration of the use of lasers and optical techniques for the realization of the challenging goal. The other dream is to correct for, with a high selectivity and precision, any potential risk factor detected during routine periodic health checkup. One strategy that has a lot of promise in this respect is the use of drugs that are activated by light. Because these drugs are inert until photoexcited by radiation with the right wavelength, the clinician can target the tissue selectively by exercising the control on light exposure (only the tissue exposed to both drug and light will be affected). A good example is the fast developing photodynamic therapy of cancer. There are indications that selective photoexcitation of native chromophores in the tissue may also lead to therapeutic effects<sup>39</sup>. Tissue optics has to play a crucial role in the realization of both the dreams. An understanding of light transport in tissue and the information content of the elastically or inelastically scattered light from tissues is mandatory for a successful realization of the potential of these optical approaches for achieving quality health care.

1. See for example Caro, R. C. and Choy, D. S. J. (Guest eds) *Optics and Photonics News*, Special issue on Optics and Light in Medicine, October 92, pp. 9-44; Servick-Muraca, E. and D. Benaron (eds), *OSA Trends in Optics and Photonics on Biomedical Optical Spectroscopy and Diagnostics*, Optical Society of America, Washington DC, 1996, Vol. 3; Gupta, P. K., in *Medical Physics for Human Health Care* (eds Bhatnagar, P. K., Pradhan, A. S. and Reddy, A. R.), Scientific Publishers, Jodhpur, 1997, pp. 143-161; Wagnieres, G. A., Star, W. M. and Wilson, B. C., *Photochem. Photobiol.*, 1998, **68**, 603-632.
2. Ishimaru, A., *Wave Propagation and Scattering in Random Media*, Academic Press, New York, 1978, Vol. 1.
3. Grossweiner, L. I., *The Science of Phototherapy*, CRC Press, Tokyo, 1994.
4. Schmitt, J. M. and Kumar, G., *Appl. Opt.*, 1998, **37**, 2788-2797.
5. Nilsson, A. M. K., Sturesson, C., Liu, D. L. and Andersson-Engles, S., *Appl. Opt.*, 1998, **37**, 1256-1267.
6. Mourant, J. R., Freyer, J. P., Hielscher, A. H., Eick, A. A., Shen, D. and Johnson, T. M., *Appl. Opt.*, 1998, **37**, 3586-3593.
7. Perelman, L. T., Backman, V., Wallace, M., Zonios, G., Manoharan, R., Nusrat, A., Shields, S., Seiler, M., Lima, C., Hamano, T., Itzkan, I., Dam, J. V., Crawford, J. M. and Feld, M. S., *Phys. Rev. Lett.*, 1998, **80**, 627-630.
8. Welch, A. J. and Gemert, M. J. C. van (eds), *Optical Thermal Response of Laser Irradiated Tissue*, Plenum Press, New York, 1995. This volume provides a comprehensive account of different aspects of tissue optics.

9. Chandrasekhar, S., *Radiative Transfer*, Oxford University Press, Oxford, 1960.
10. Contini, D., Martelli, F. and Zaccanti, G., *Appl. Opt.*, 1997, **36**, 4587–4599.
11. Yoo, K. M., Liu, F. and Alfano, R. R., *Phys. Rev. Lett.*, 1990, **64**, 2647–2649; 1990, **65**, 2210.
12. Wilson, B. C., in *Optical Thermal Response of Laser Irradiated Tissue* (eds Welch, A. J. and Gemert, M. J. C. V.), Plenum Press, New York, 1995, pp. 233–274.
13. Yoo, K. M., Liu, F. and Alfano, R. R., *J. Opt. Soc. Am.*, 1990, **B7**, 1685–1693.
14. Yoon, G., Roy, D. N. G. and Straight, R. C., *Appl. Opt.*, 1993, **32**, 580–585.
15. Anantha Ramakrishna, S., Rao, K. D. and Gupta, P. K., *Proc. Natl. Laser Symp.*, 10–12 December 1997, pp. 273–274.
16. Ghosh, A. K., Nagarkar, M. M. and Gupta, P. K., *Proc. Natl. Laser Symp.*, 10–12 December 1997, pp. 269–270, and unpublished results.
17. Patterson, M. S., Chance B. and Wilson, B. C., *Appl. Opt.*, 1989, **28**, 2331–2336.
18. Groenhuis, R. A. J., Ferwerda, H. A. and Bosch, J. J. T., *Appl. Opt.*, 1983, **22**, 2456–2462.
19. Groenhuis, R. A. J., Bosch, J. J. T. and Ferwerda, H. A., *Appl. Opt.*, 1983, **22**, 2463–2467.
20. Wilson, B. C. and Patterson, M. S., in *Future Directions and Applications in Photodynamic Therapy*, (ed. Gomer, C. J.), *Proc. Soc. Photo-opt Instrum. Eng.*, 1990, **1506**, 219–231.
21. Bays, R., Wagnieres, G., Robert, D., Braichotte, D., Savary, J. F., Monnier, P. and Bergh, H. V. D., *Appl. Opt.*, 1996, **35**, 1756–1766.
22. Mourant, J. R., Fusellier, T., Boyer J., Johnson, T. M. and Bigio, I. J., *Appl. Opt.*, 1997, **36**, 949–957.
23. Dam, J. S., Anderson, P. E., Dalggaard, T. and Fabricius, P. E., *Appl. Opt.*, 1998, **37**, 772–778.
24. Farrell, T. J., Patterson, M. S. and Essenpreis, M., *Appl. Opt.*, 1998, **37**, 1958–1972.
25. Kienle, A., Patterson, M. S., Dognitz, N., Bays, R., Wagnieres, G. and Bergh, H. V. D., *Appl. Opt.*, 1998, **37**, 779–791.
26. Pifferi, A., Taroni, P., Valentini, G. and Andersson-Engels, S., *Appl. Opt.*, 1998, **37**, 2774–2780.
27. Richards-Kortum, R. and Sevick-Muraca, E., *Annu. Rev. Phys. Chem.*, 1996, **47**, 555–606.
28. Fantini, S., Walker, S. A., Franceschini, M. A., Kaschke, M., Schlag, P. M. and Moesta, K. M., *Appl. Opt.*, 1998, **37**, 1982–1988.
29. Fisher, A. M. R., Murphree, A. L. and Gomer, C. J., *Lasers Surg. Med.*, 1995, **17**, 2–31.
30. Star, W. M., Wilson, B. C. and Patterson, M. S., in *Photodynamic Therapy: Basic Principles and Clinical Applications* (eds Henderson, B. W. and Dougherty, T. J.), Dekker, New York, 1992, pp. 335–368.
31. Svaasand, L. O., Wyss, P., Wyss, M. T., Tadir, Y., Tromberg, B. J. and Berns, M. W., *Lasers Surg. Med.*, 1996, **18**, 139–149.
32. Bays, R., Wagnieres, G., Robert, D., Braichotte, D., Savary, J. F., Monnier, P. and Bergh, H. V. D., *Lasers Surg. Med.*, 1997, **20**, 290–303.
33. Gupta, P. K., Majumder, S. K. and Uppal, A., *Lasers Surg. Med.*, 1997, **21**, 417–422.
34. Majumder, S. K., Gupta, P. K. and Uppal, A., *Laser Life Sci.*, 1999, **8**, 211–227; See also in *Optical Diagnostics of Biological Fluids III* (ed. Priezzhev, A. V.), *Proc. Soc. Photo-Opt. Instrum. Eng.*, 1998, **3252**, pp. 158–168; and in *Proc. Natl. Laser Symp.*, 10–12 December 1997, pp. 284–285.
35. Majumder, S. K., Gupta, P. K., Jain, B. and Uppal, A., *Laser Life Sci.*, 1999, **8**, 249–264; See also in *Optical Diagnostics of Biological Fluids III* (ed. Priezzhev, A. V.), *Proc. Soc. Photo-Opt. Instrum. Eng.*, 1998, **3252**, pp. 169–178, and in *Proc. Natl. Laser Symp.*, 10–12 December 1997, pp. 286–287.
36. Durkin, A. J., Jaikumar, S., Ramanujam, N. and Richards-Kortum, R., *Appl. Opt.*, 1994, **33**, 414–423.
37. Welch, A. J., Gardner, C., Richards-Kortum, R. E., Criswell, G., Pfefer, J. and Warren, S., *Lasers Surg. Med.*, 1997, **21**, 166–170.
38. Avriillier, S., Tinet, E., Ettori, D., Tualle, J. M. and Gelebert, B., *Appl. Opt.*, 1998, **37**, 2781–2787.
39. Baxter, G. D., *Therapeutic Lasers*, Churchill Livingstone, Edinburgh, 1994.

ACKNOWLEDGEMENTS. I thank N. Ghosh and S. K. Majumder for their help in the preparation of the manuscript.

# Moonstones

M. S. Giridhar and S. K. Srivatsa

Raman Research Institute, C. V. Raman Avenue, Sadashivanagar, Bangalore 560 080, India

Moonstones are gems that appear to have a ghostly, shimmering glow floating around inside the material, often bluish in colour. Ancient Romans thought that a moonstone was made of moonlight, hence the name. The characteristic shimmering reflection is called 'adularescence' or the 'schiller effect' and arises due to the optical heterogeneity in the moonstone (Figure 1). A moonstone is made up of crystallites of three different feldspars. They are present in different moonstones to different extents. Generally the most dominant component is the monoclinic potash feldspar (orthoclase). The next important component is the triclinic soda feldspar (albite). Incidentally these two feldspars are similar in chemical composition though they have different crystal structures. The third component that exists in very small amounts is the triclinic lime feldspar (anorthite). It may be mentioned here that this feldspar is an isomorph of soda feldspar. In a moonstone these three feldspar crystallites are interwoven inside the medium.

The spectacular schiller effect is best seen at a particular setting of the stone. At this setting, the direction

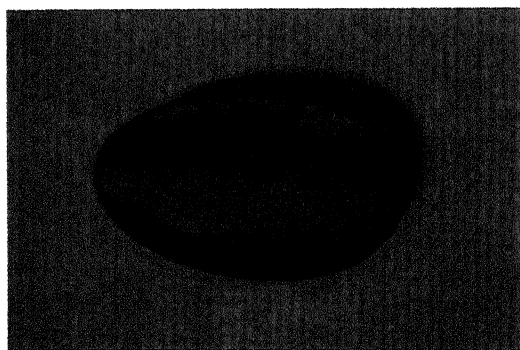


**Figure 1.** An example of a moonstone exhibiting schiller. The large bright elliptical patch seen in the middle of the stone is due to the schiller effect.

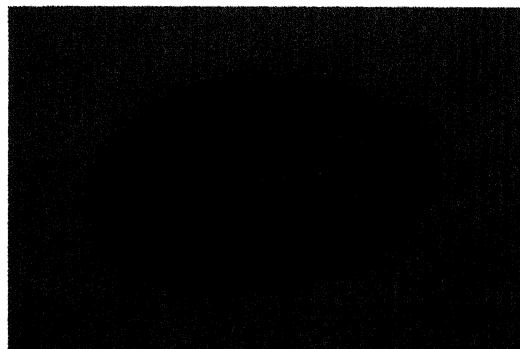


**Figure 2.** A cut and polished yellow labradorite.

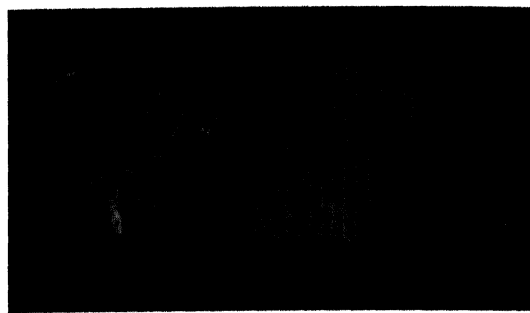


**Figure 3.** An uncut labradorite exhibiting a brilliant deep blue colour.

of the incident light and the direction of observation make equal angles with a particular direction in the stone which is often called the schiller axis. Further, these three directions are in one plane. When either the stone or the direction of incident light is altered the direction in which schiller is most conspicuous also shifts. The schiller is in the nature of a diffusion of light spread over a very wide range of angles. It is largely due to scattering from particles smaller in size compared to the wavelength of light. It is not due to Bragg reflection from a set of planes perpendicular to the schiller axis. It has been suggested that the scattering particles are crystallites of soda feldspar segregating from potash feldspar principally along the 100 planes of the potash feldspar crystal. In this plane, the crystallites spread more along the *c*-axis than along the *b*-axis. Thus the moonstone is a single crystal with the schiller axis perpendicular to the (100) plane of potash feldspar. Generally we see schiller as an elliptical patch of blue light. When the moonstone is rotated this pattern rotates with it.

Interestingly, labradorites (Figure 2) are also made of the same three feldspars. Like moonstones they also exhibit diffusion of incident light over a wide range of angles about what appears to be the direction of reflection. The important difference when compared to moonstones is in the rich variety of colours scattered by it. The colour of the strongly scattered light varies from material to material. There are labradorites with colours from deep blue to red (Figure 3). It is worth recalling here that soda and lime feldspars are isomorphous and hence can form solid solutions. Studies indicate that in labradorites the basic host structure is the lime-soda feldspar solid solution with segregation of potash feldspar crystallites in the form of platelets.

## Photonic crystals

G. S. Ranganath

Nothing captures the eye more than the flutterings of colourful butterflies or a foliage of leaves and flowers. In their presence we forget the noisy and dull world we live in. But why are these coloured the way they are? It is natural to ascribe colours of leaves, fruits and flowers to the presence of specific chemicals, called pigments, in them. For instance, the green colour of the leaves is due to absorption of light by chlorophyll. This pigment absorbs weakly in the green but strongly at all other wavelengths of the white light spectrum. That there could be a physical origin for colours seen in nature was first pointed out in 1801 by Thomas Young, the proponent of the wave theory of light. He argued that a multilayer stack of two alternating dielectric plates exhibits a near total reflection in a band of wavelengths. In literature a dielectric multilayer is also called a *photonic crystal*. Photonic crystals come in all sorts of shapes and structures and one very active area of current research in optics has been their discovery and the fabrication. Here we look at some new and interesting photonic crystals that surfaced in literature during 1998.

Since the time of Young a constant search has been going on to identify and establish this physical mechanism in the manifestation of colours seen in a variety of situations. Many examples have been found not only in the inanimate world of minerals and gems but also in the world of animals like fishes, insects and birds. Recent investigations have revealed that this process operates in plants too<sup>1</sup>. It now appears that feathers of birds are also in this class. Generally the blue colour of the feathers of birds is attributed to the Rayleigh scattering from the air pockets in the feather. It was shown by Prum *et al.*<sup>2</sup> that this explanation is wrong. These authors studied in detail scattering of light from the blue feather barbs of the plum-throated cotinga. Their analysis indicates that the cavities are not only of same size but they are also arranged three-dimensionally in space, like the atoms or molecules of a crystal. Further, they

found that the spacing between the cavities is smaller than the wavelength of light. Thus, Rayleigh scattering cannot account for the blue coloration. Detailed calculations based on the model of a periodic array of air vacuoles support the observed reflection spectra. The authors suggest that possibly the same mechanism is operating in producing the green, blue and violet colours found in other feather barbs. In short, the feathers of birds hide in them photonic crystals.

It is exhilarating to discover such a photonic crystal in nature. But a greater pleasure lies in making it in the laboratory. Eight years ago Yablonovitch *et al.*<sup>3</sup> fabricated such a crystal. They drilled holes in a block of a dielectric such that the criss-crossing of the drilled holes produced a crystal with the connectivity of a diamond-like structure. This process by its very nature is not easy to execute if we want to design a photonic crystal of desired specificity. Another way of making hollow crystals has been suggested recently by Zakhdov *et al.*<sup>4</sup>. These authors synthesized what they call *inverse opals*. These are interesting variations of the opal structure. By a slow crystallization (over ten months) of monodispersed aqueous colloid of SiO<sub>2</sub> spheres they made opal crystals. This was later sintered to get a packing of SiO<sub>2</sub> spheres with voids. By means of a chemical technique these voids were later filled up with carbon to result in a continuous interconnected carbon structure. Later they removed chemically, the SiO<sub>2</sub> spheres. Interestingly, these authors have made structural inverses of not only natural opals but also those of diamond, graphite and glassy carbon. These carbon inverse structures strongly diffract light and exhibit optical opalescence. Instead of filling with carbon, inverse structures filled with titanium oxide have also been made. This has spherical cavities surrounded by a titanium oxide scaffolding. This structure was reported a few months earlier by Holland *et al.*<sup>5</sup>. So it appears that we can imitate nature in fabricating photonic crystals of air.

In a conventional multilayer dielectric, it is impossible to achieve total reflection at all angles of incidence. This is due to the fact that light polarized in the plane of incidence will simply go through if it is incident at the Brewsterian angle corresponding to the interlayer boundary. Thus we expect for this polarisation, a 'hole' in the reflection spectrum which will exist at all wavelengths. Recently, Fink *et al.*<sup>6</sup> overcame this problem in a clever way. It is easy to see that when the angle of incidence varies from 0° to 90° the corresponding angle of refraction at the first dielectric slab will be decided by the Snell's law of refraction. Therefore, we can so choose the materials that the maximum angle of refraction inside the multilayer is less than the Brewster angle for the multilayer. This will completely avoid the 'hole' in the reflection spectrum. Thus this is a total reflector for all angles of incidence from 0° to 90°. In short, it is an omnidirectional one-dimensional photonic crystal. These authors have fabricated such a system with alternating layers of polystyrene and tellurium. This reflects strongly in the wavelength band of 10 to 15 micrometers.

We now come to our last example of a photonic crystal which is very different from the normal ones. In fact, it could be called a photonic fibre as it has been designed to act as an optical fibre. Light is guided in normal fibres by total internal reflection which arises from the fact that the refractive index of the central core is greater than that of the surrounding cladding. Recently Knight *et al.*<sup>7</sup> fabricated a totally different type of optical fibre. Effectively it has a core of a lower refractive index compared to that of the cladding. In this sense it is an inverse structure. Also the mechanism that guides light through the fibre is entirely different. Light is guided in these structures by exploiting the properties of a photonic crystal. The fibre is essentially a periodic array of holes, of nearly 75 nanometers diameter running through the length of the fibre. These holes are arranged on a honeycomb lat-

tice with a near neighbour spacing of 1.9 micrometers. Further, instead of being a perfect lattice of holes the fibre has a large extra hole of 0.8 micrometers at the centre of the fibre. Light is sent down this central hole. For wavelengths within the band gap of the surrounding periodic structure light will not leak out due to Bragg reflection and thus gets guided through the central hole. In this case only light of wavelengths in the band 458 to 528 nanometers (obtained from an argon-ion laser) could be guided through the central hole of the fibre. At other wavelengths light 'fills' the entire fibre. Another extraordinary property of this fibre is its strong birefringence. The velocity for linearly polarized light is different for any two orthogonal azimuths. Hence, light, as it propagates

through the fibre, will retain its linear polarization even in the presence of twists and bends in the fibre.

Nature in all her grandeur and cleverness has come up with any number of tricks to paint herself in different hues and shades. And scientists are not far behind in following her. Here we dwell upon only one of these tricks namely synthesis of photonic crystals. Even in this game there exists a variety that would baffle anyone. We have learnt a lot about these photonic crystals by observing nature. This has not only enriched our understanding of nature but has also led to the fabrication of unusual photonic crystals with surprising optical properties.

1. Lee, D. W., *Nature*, 1991, **349**, 260–262.

2. Prum, R. O., Torres, R. H., Williamson, S. and Dyck, J., *Nature*, 1998, **396**, 28–29.
3. Yablonovitch, E., Gmitter, T. J. and Leung, K. M., *Phys. Rev. Lett.*, 1991, **67**, 2295–2298.
4. Zakhidov, A. A., Baughman, R. H., Iqbal, Z., Cui, C., Khayrullin, I., Dantas, S. O., Marti, J. and Ralchenko, V. G., *Science*, 1998, **282**, 897–901.
5. Holland, B. T., Blanford, C. F. and Stein, A., *Science*, 1998, **281**, 538–540.
6. Fink, Y., Winn, J. N., Fan, S., Chen, C., Michel, J., Joannopoulos, J. D. and Thomas, E. L., *Science*, 1998, **282**, 1679–1682.
7. Knight, J. C., Broeing, J., Birks, T. A. and Russel, P. J., *Science*, 1998, **282**, 1476.

---

*G. S. Ranganath is in the Raman Research Institute, C. V. Raman Avenue, Sadashivanagar, Bangalore 560 080, India.*

# Turmeric – Nature's precious gift

N. M. Khanna

*Turmeric (Curcuma longa) is a well-known indigenous herbal medicine. Its major constituents, curcumin, various curcuminoids, curcuma oil – particularly dl-ar-turmerone – exhibit a wide range of biological activities, e.g. anti-bacterial, anti-inflammatory, hypolipidemic, hepatoprotective, lipoxygenase, cyclooxygenase, protease inhibitory effects, besides being effective active oxygen species scavengers and lipid peroxidase inhibitors.*

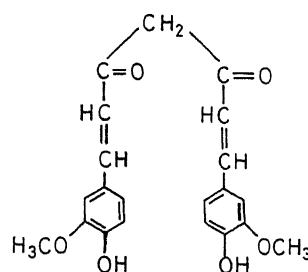
*A Persian physician came to India to confer with the Hindu pandits. Together they studied the Charak Samhita and all other medical texts. They realized that the medical texts are like an ocean and they were like pearl divers who plunged into the ocean to grasp the pearls.*

*From Kavi Taranga, 1703 A.D.*

THE herbal renaissance has produced a profound effect on the Western medicine which is now trying to acknowledge methods of healing that have existed for millenia in the traditional medicine throughout the world, especially Asia. The surge in research on drugs from natural sources is now moving out of the herbalists' shop away from the core texts into the drugs research laboratories. India's herbal tradition is as old as China's. We have rich resources but we have been complacent. In the present day world with numerous challenges facing us, particularly those relating to intellectual property rights, we must brace ourselves up and focus on areas of potential competitive advantage to emerge as winners. The grant of a patent to two non-resident Indian doctors in USA who claimed that they were the first to use turmeric (*Curcuma longa*) and its extract in powder form for healing wounds is yet another example of blatant plagiarism and an attempt to obtain exclusive rights over a traditional medicine that Indians and Chinese have known for centuries. It is a case that pits East against the West. This article is an attempt to put the record straight in respect of one of the most versatile and benign medicine given by God/Nature (or luck as you may call it), namely turmeric (*Curcuma* species especially *C. longa*, Haldi). Since the future is likely to be replete with such examples, the information given here should be helpful to research scientists, physicians, health officials and the public to take a firm stand and safeguard this and other precious gifts of nature that are part of our traditional medicine and heritage.

In the indigenous system of medicine, turmeric enjoys the reputation as a stomachic, blood purifier, useful in common cold, leprosy, intermittent fevers, affections of

the liver, dropsy, purulent ophthalmia, otorrhea, indolent ulcers, pyogenic affections, wound healing and inflammation. A review of literature reveals that turmeric is useful in treating a variety of ailments and metabolic disorders. Turmeric roots are known<sup>1-3</sup> to be antiseptic and aromatic. Its paste is used in cleansing and disinfecting the skin and skin ulcers without drying out its natural oils. The bactericidal properties of turmeric have been proved by clinical testing to have a greater medicinal effect than being merely cosmetic. *In vitro* evaluation of the antibacterial potency of *C. longa* constituents – curcumin, other curcuminoids (Scheme 1)



Curcumin

and the essential oil showed them to be active. The sodium salt of curcumin inhibits *Micrococcus pyogenus* var *aureus* in 1 in 1 million dilution<sup>4</sup>. The inhibitory concentration against *Staphylococcus aureus* was 1:640,000 (refs 5, 6). One of the constituents of the volatile oil, *p*-tolyl methyl carbinol and its isomer phenylethyl carbinol have a strong action against *B. coli* commune<sup>7</sup>. The oil kills *Paramecium caudatum* in 10 to 30 min in dilutions of 1 in 30,000 (ref. 8), *S. aureus* and *S. albus* in 1:5000. Curcumin and other curcuminoids inhibit growth of *S. aureus*, *S. paratyphi*, *Trichophyton gypseum*, *Mycobacterium tuberculosis* in concentrations varying from 1 in 20,000 to 1 in 640,000 (ref. 9). The essential oils show marked anti-microbial activity against gram negative (*Vibrio cholerae*, *Salmonella typhi*, *Klebsiella [enterobacter] aerogenes*, *B. coli*) and gram-positive organisms (*Corynebacterium diphtheriae*, *β-hemolytic streptococci*)<sup>10-15</sup>.

N. M. Khanna lives at 21/26, Tilak Marg, Near Moti Mahal East, Lucknow 226 001, India.

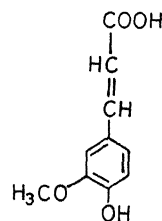
## GENERAL ARTICLE

The essential oil fractions from *C. longa* rhizomes of various habitats exhibit fungistatic activity<sup>16,17</sup> particularly against *Aspergillus niger* *in vitro* and *Physalospora tucumanensis*, *Ceratocystis paradoxa*, *Sclerotium solfsii*, *curvularia lunata*, *Helminthosporium sacchari*, *Fusarium moniliforme* vaz. Subglutinans and *cephalosporium sacchari*.

Turmeric powder significantly increases the mucus content in gastric juices and Indian cuisine lays emphasis on turmeric's therapeutic effect against gastric disorders. Curcuma oil, curcumin and its alkali salts prevent histamine induced gastric ulceration<sup>18,19</sup>. While proving the non-toxicity of turmeric extract before recommending its use as a colouring agent for hydrogenated oils, it was observed<sup>20-22</sup> that liver cholesterol levels were lower in rats fed with hydrogenated groundnut oil containing turmeric extracts. Curcumin and the essential oils of *C. longa* particularly sodium curcuminatate differentially affect the individual constituents of bile<sup>23</sup>. Though the concentrations of the solids decrease in the bile flow stimulated by it, this is compensated by the increased volume of bile excreted. Absolute values for the entire period of choleresis indicate increased total excretion of bile salts, bilirubin and cholesterol. The fatty acid content remains almost constant. Sodium curcuminatate stimulates the flow of bile, the degree and duration of activity depends upon the dosage administered. In conditions where hydrocholagogic effect is desired, it may be found useful. Increased bile salt excretion in higher doses favours the use of curcumin in digestive disorders of fat metabolism. The increased cholesterol secretion may be clinically useful in atherosclerosis and other conditions involving cholesterol metabolism and bilirubin secretion in hastening the recovery from jaundiced conditions. Curcumin seems to combine the choleric and hydrocholagogic action with the antiseptic property and probably would be an ideal therapeutic agent in conditions of suspected staphylococcal infections. The low toxicity and absence of adverse pharmacodynamic action of curcumin also favour its clinical use. The relaxation of intestines while maintaining the spontaneous contractions would probably assist thorough digestion of the food and complete absorption of the digested material. Other active constituents of *C. longa* and a synthetically derived constituent of turmeric manifest useful therapeutic choleric and cholagogic action in humans<sup>24-28</sup>. In rats fed with cholesterol and curcumin, an important constituent of turmeric, levels of serum and liver cholesterol decreased to one-half or one third of those in rats fed with cholesterol alone<sup>29</sup>. Deposition of cholesterol was found to be high in liver sections from rats fed with cholesterol and least in specimens from animals concurrently fed with curcumin. Curcumin increased fecal excretion of bile acids and cholesterol both in normal and hypercholesterolemic rats. This biliary drainage is a plausible explanation for

the reduction of tissue cholesterol on curcumin feeding.  $\alpha$ -Lipoprotein and  $\beta$ -lipoprotein in blood plasma were affected by addition of curcumin and the imbalance in these two lipoproteins brought about by cholesterol feeding was nearly corrected by simultaneous feeding of curcumin. The above beneficial effects of curcumin were about the same with 0.1% or 0.5% of the drug in the diet suggesting that the effective level of curcumin may even be lower than 0.1%. All levels of curcumin maintained body and liver weights, correcting the ill-effects in this respect caused by ingested cholesterol. The effect of curcumin in keeping down cholesterol in conditions which otherwise induced hypercholesterolemia was not through alterations in cecal microflora which are known to dismutate and utilize bile acids in the gut. In hypercholesterolemic rats, 0.05% dietary curcumin decreased serum and hepatic cholesterol within four weeks<sup>30</sup>. Ar-turmerone, the active constituent of curcuma oil also exhibits significant cholagogic activity<sup>31</sup>.

Extracts of *C. longa* rhizomes exhibit good preventive activity against carbon tetrachloride induced liver injury *in vivo* and *in vitro*<sup>32</sup>. After fractionation, the curcuminoids showed significant anti-hepatotoxic action. Ferulic



Ferulic acid

acid, *p*-coumaric acid and their respective analogs (probable metabolites of curcuminoids) also possess marked liver protective effects. In rats, oral administration of paracetamol (100, 200 and 400 mg/kg) caused increase in serum glutamic pyruvic transaminase (SGPT), serum alkaline phosphatase and serum cholesterol. The two higher doses of paracetamol caused vascular changes with scattered areas of necrosis in liver tissue. Pretreatment of rats one hour before with curcumin protected them from paracetamol-induced lesions<sup>33,34</sup>. The induction of gastric ulcers in guinea pigs by intramuscular injection of 5-hydroxytryptamine (serotonin) creatinine sulphate (20 mg/kg) was inhibited by curcumin (5-20 mg/kg orally)<sup>19</sup>.

Curcumin inhibits intestinal gas formation<sup>35</sup> by *Clostridium perfringens* at 0.05% concentration. Its effect was evaluated at 0.005, 0.013, 0.025 and 0.05% on gas formation by *C. perfringens* of intestinal origin. Gas formation decreased gradually as the curcumin concentration increased and there was no gas when curcumin

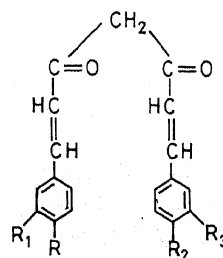
concentration was 0.05%, the level at which bacterial growth was inhibited completely.

Oral administration of curcumin and curcuminoids (750 mg/kg) has been reported<sup>36</sup> to prevent the formation and dissolution of urinary calculi.

In the indigenous system of medicine turmeric (*C. longa*) rhizomes are widely used for treatment of various inflammatory conditions. The use of turmeric paste with or without slaked lime and/or onion juice is a household remedy<sup>37,38</sup> for reducing pain and swelling due to sprains, wound injuries and various types of inflammation. *C. longa* total extracts, its active constituents the curcuminoids and the oil have been extensively investigated<sup>39-50</sup> for anti-inflammatory activity in acute and chronic models of inflammation in experimental animals and were found to exhibit significant anti-inflammatory activity. Of these, curcumin is currently under Phase-2 clinical trials<sup>50</sup>. In curcumin and other curcuminoids, the regression line paralleled with that of cortisone but not with phenylbutazone which is another anti-inflammatory agent. The anti-inflammatory effect of curcumin was significantly less in adrenalectomized rats which suggested an indirect mechanism of action. Curcumin inhibited chemically-induced acute edema in mice as well as subacute arthritis in rats. It inhibited cotton pellet-induced granuloma formation in rats. It had no side-effects on the central nervous system nor any effect on the cardiovascular system of anaesthetized cats up to a dose of 10 mg/kg administered intravenously. Curcumin prevented the increase in serum glutamic oxalacetic transaminase and glutamic pyruvic transaminase seen in inflammation. It had a lower ulcerogenic index than phenylbutazone and had no analgesic, antipyretic effects in mice and rats. The volatile oil also gave protection against injection of talc in the left intratarsal joint in pigeons<sup>42</sup> and was effective against both early and late inflammation. The early protective effect may be due to antihistaminic activity while the late effect may be a result of activation of the adrenohypophyseal axis. Using a newly developed combination of prostaglandin synthesizing cyclooxygenase system from sheep seminal vesicles and an HPLC separation technique for the metabolites of arachidonic acid, curcuma oil and curcumin exhibited significant activity as inhibitors of prostaglandin biosynthesis. Inflammation induced by carrageenin in mice was accompanied by an increase in the *in vitro* formation of lipid peroxides by liver. Pretreatment of mice with curcumin (500 mg/kg p.o.) prevented both edema development and lipid peroxide formation.<sup>51</sup> Curcumin inhibits *in vitro* lipoxygenase and cyclooxygenase activities in mouse epidermis. Topical application of curcumin markedly inhibits TPA and arachidonic acid, induced epidermal inflammation (ear edema) in mice<sup>52</sup>. *In vitro* addition of 3, 10, 30 or 100  $\mu$ M curcumin to cytosol from homogenates of mouse epidermis inhibited the metabolism of arachidonic acid to 5-

hydroxyeicosatetraenoic acid (5 HETE) by 40, 60, 66 or 83%, respectively and the metabolism of arachidonic acid to 8 HETE was inhibited by 40, 51, 77 and 85%, respectively (IC<sub>50</sub>, concentration needed for 50% inhibition: 5–10  $\mu$ M). The metabolism of arachidonic acid to prostaglandin E<sub>2</sub>, prostaglandin F<sub>2x</sub> and prostaglandin D<sub>2</sub> epidermal microsomes was inhibited approximately 50% by the *in vitro* addition of 5 to 10  $\mu$ M curcumin. The inhibitory effect of curcumin on TPA-induced tumor promotion in mouse epidermis parallels its inhibitory effect on TPA-induced epidermal inflammation and epidermal lipoxygenase and cyclooxygenase activities.

Turmeric powder, extracts and curcumin exhibit antioxidant property<sup>53,54</sup> as observed by the induction period and oxygen absorption of coconut, groundnut, safflower, sesame, mustard, cotton seed oils and ghee at 95°C to 220°C for periods up to 144 h. In food, the antioxidant property of turmeric was effective in preventing peroxide development<sup>55</sup>. *C. longa* extract also protects the oil in water emulsion against oxygen absorption<sup>56</sup>. Curcumin at 10<sup>-6</sup> M showed anti-oxidative activity<sup>57</sup> to linoleic acid. Five antioxidative components of turmeric (*C. longa*) oleoresin were detected and identified by comparing with authentic compounds on TLC and HPLC and studied by a TLC fluorescent method developed to separate and evaluate the activity of the individual antioxidative components. Curcumin, demethoxy curcumin and bis-demethoxy curcumin were the major antioxidative components<sup>58</sup>. Curcumin markedly antagonized the lipid peroxide in homogenates of brain, heart, spleen, liver and kidney of NIH mice<sup>59</sup>. The antioxidant activity was dose-dependent with the range of 0.128–20.4 mg/100 ml of curcumin. In a study of the diethyl ether extracts of 23 spices, turmeric extract proved to be the second most active<sup>60</sup>. Turmeric extract was separated into basic, strongly acidic, weakly acidic and neutral fractions. The antioxidative activity was detected in the weakly acidic fraction. To isolate the active compounds C<sub>18</sub> reversed phase HPLC, C<sub>8</sub> preparative HPLC and high performance TLC (RP-8) were employed. Besides



Other curcuminoids:

R = R<sub>1</sub> = R<sub>2</sub> = R<sub>3</sub>: Dicinnamoyl methane

R = R<sub>1</sub> = OH; R<sub>2</sub> = R<sub>3</sub> = H: Bis-demethoxy-curcumin

R = R<sub>1</sub> = OH, R<sub>2</sub> = OCH<sub>3</sub>, R<sub>3</sub> = H: Demethoxy curcumin

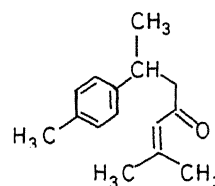
## GENERAL ARTICLE

the main component curcumin, six other compounds were found, one of which was identified as dicinnamoyl methane. In a study of the anti-oxidative activity of curcumin and related compounds, structure-activity relationship was determined<sup>61</sup> for the inhibition of lipid peroxide formation in rat brain homogenates. Demethylated derivatives of curcumin and trans-ferulic acid, e.g. bis(3,4-dihydroxy trans-cinnamoyl) methane ( $1.03 \times 10^{-6}$  –  $1.03 \times 10^{-3}$  M) and trans-caffeic acid ( $1.03 \times 10^{-6}$  –  $1.03 \times 10^{-3}$  M) were potent. Complete methylation abolished antioxidant activity. The OH group in the benzene ring had to be in the para position.

Anti-oxidants are the frontline of defence against free radicals. They are able to neutralize free radicals and put an end to the destructive chain reactions. The anti-oxidant action of curcumin, other curcuminoids and curcuma oil works in many ways. Probably the most important activity as antioxidant is the vital role in the antioxidant enzyme superoxide dismutase (SOD). SOD is a primary defender against free radicals and is so important to survival that it is the fifth most prevalent protein (of more than 100,000 in the body). SOD eliminates destructive superoxide molecules, a common free radical produced in the body<sup>61,62</sup>. SOD apparently blocks the oxidation of harmful LDL cholesterol, thereby inhibiting the initial stages of atherosclerosis. Liver cells produce a free radical known as malondialdehyde (MDA) while human neutrophils (a type of white blood cell) produce superoxide. Active oxygen species (AOS) including superoxide, hydrogen peroxide, hydroxyl and ferryl radicals are considered to be generated or formed subsequent to reduction of molecular oxygen in living organisms. The hydroxyl radical and the ferryl radical, a complex of oxygen radical and iron are the most reactive and thought to be the major species responsible for oxidative injury of enzymes, lipid membranes and DNA in living cells and tissues, a process which causes much damage and contributes to cancer, atherosclerosis, heart attacks and stroke. Nerve cell damage can be caused by free radicals generated by/from breakdown of certain proteins, oxidative stress resulting from increased free radical production and/or defects in antioxidation defences could be central to the degenerative processes. Cells and tissues are protected from attack by AOS under normal conditions by certain enzymes – SOD, catalase, peroxidase, etc. and some low molecular weight substances such as ascorbic acid, tocopherol which exhibit mild AOS scavenging effect. Caffeic acid also inhibits<sup>63</sup> 5-lipoxygenase and lipid peroxidation. Turmeric (*C. longa*) extracts and its constituents – curcumin, the other curcuminoids and curcuma oil are highly effective antioxidants, inhibitors of lipid peroxidation, leukotriene biosynthesis, 5-lipoxygenase, cyclooxygenase,<sup>64,65</sup> AOS scavengers<sup>65</sup> and are able to prevent increased free radical generation or accumulation in the body. They fight free radicals by

competing with peroxidant metals (iron and copper) for cell binding sites which decreases the possibility of free radical formation. Further, they appear to protect against free radical damage by defending sulfhydryl groups against oxidation. In the body sulfhydryl groups are a common part of many molecules and are easily oxidized forming free radicals. These unique properties make turmeric and its constituents useful as hypolipidemics,<sup>66,67</sup> anti-inflammatory, anti-allergy, antimicrobial agents particularly wound healers including bed sores<sup>68</sup>, liver injury, certain forms of cancer and treatment of various metabolic disorders and other degenerative processes.

Like curcumin and other curcuminoids considered to be derived from two caffeic acid molecules combined through a methylene bridge, ar-turmerone the main constituent of curcuma oil also has an  $\alpha$ - $\beta$ -unsaturated keto system in its molecular framework which is an important pharmacophore for most biological activities<sup>66,69</sup>. Curcuma oil too is an effective inhibitor of 5-lipoxygenase, cyclooxygenase, leukotriene biosynthesis, lipid peroxidation and AOS scavenger. For pharmaceutical purposes curcuma oil can be easily standardized on the basis of its ar-turmerone content.



DL-ar-turmerone

Curcumin (30 mg/kg) prevents hypertrophy and other inflammatory changes in the rat uterus induced by IUCD<sup>70</sup>.

Curcuma oil is an effective mosquito repellent<sup>71</sup> and compares favourably with dimethyl phthalate in its repellent action against mosquitoes, the time of protection being 282 min compared to 240 for dimethyl phthalate. Curcuma oil has a quick knock-down effect on housefly (*Musca nebulosa*)<sup>72</sup> nearly comparable with Lethane 384 and Thanite.

Many plant phenolics especially the curcuminoids possess anti-carcinogenic property due to their oxygen radical scavenging property<sup>73</sup>. Turmeric extracts and curcumin reduced the expression of papillomas in mouse skin induced by 7,12-dimethylbenz(a) anthracene followed by croton oil promotion. Curcumin also inhibited tumour formation induced by 20-methylcholanthrene. Curcumin, curcuminoids and curcuma oil derived from turmeric may, therefore, be anti-carcinogens. Evaluation of anti-cancer activity of turmeric rhizomes<sup>74</sup> *in vitro* using tissue culture methods and *in vivo* in mice using

Dalton's lymphoma cells grown as ascites showed that turmeric extract inhibited cell growth in Chinese hamster ovary (CHO) cell culture at a concentration of 4 µg/ml and was cytotoxic to lymphocytes and Dalton's lymphoma cells at the same concentration. Cytotoxic effect was found within 30 min at room temperature. The active cytotoxic constituent was curcumin. Other curcuminoids and the oil also showed promise. Turmeric extracts and curcumin reduce the development of tumours in animal. Plant phenolics including caffeic, ferulic acids at levels of 4% in diet for one week prior to challenge by benzo[a]pyrene (100 mg/kg body weight) inhibited<sup>75</sup> the nuclear damage (micro nuclei, pyknotic nuclei, karyorrhectic bodies) in colonic epithelial cells of C57BL/8J mice. A cytotoxic sesquiterpene active against L 1210 cells was isolated from the roots of *C. domestica* and identified as  $\beta$ -sesquiphellandrene. The cytotoxicity potentiating substance was identified as (+) ar-turmerone<sup>76</sup>. Turmerone potentiated the cytotoxicity of  $\beta$ -sesquiphellandrene 5-fold in ED<sub>50</sub> value. It also potentiated the cytotoxic activities of Me CCNO (10-fold) and cyclophosphamide (10-fold). Although all the effective cytotoxic substances possess relatively good lipophilicity, no relationship between their structure and increase of cytotoxicity by turmerone was found. Curcumin and its derivatives inhibit HIV protease<sup>77</sup>. Derivatives containing boron had enhanced inhibitory activity and one of them irreversibly inhibited the HIV 1 protease. DNA polymerase and human immunodeficiency virus and avian myeloblastosis virus reverse transcriptase inhibition has also been reported<sup>78</sup>.

Curcumin and other 3,4-dihydroxylated compounds structurally related to trans-cinnamic acid inhibit the binding of [<sup>125</sup>I] bovine TSH to human thyroid membrane<sup>79</sup>.

Curcumin inhibits ADP epinephrine and collagen-induced platelet aggregation in monkey plasma<sup>80</sup> and may be preferable in patients requiring antiarthritic therapy who are prone to vascular thrombosis. Curcumin protects<sup>81</sup> mice against thrombotic challenge, the anti-thrombotic activity being dose-related and its inhibitory effect on mouse platelet TXB<sub>2</sub> and cyclooxygenase; the latter indicated by the inhibition of synthesis of malondialdehyde. Anti-coagulant activity of curcumin, *p*, *p'*-dihydroxy dicinnamoyl methane and *p*-hydroxy cinnamoyl ferulyl methane isolated from turmeric rhizomes (*C. longa*) has also been reported<sup>82</sup>. During the isolation process, plasma recalcification time in mice was used to follow the anti-coagulant activity of the compounds. Drug compositions for treating hyperlipidemia, inhibiting blood platelet aggregation and metabolic disorders, comprising curcumin<sup>83,84</sup> and curcuma oil<sup>66,67</sup> along with other plant-based constituents which enhance the biological activity are also known<sup>67</sup>.

1. Naveen Patnaik, in *The Garden of Life*, Double day, New York, 1993, p. 137.
2. Chopra, R. N., Chopra, I. C., Handa, K. L. and Kapur, L. D., in *Indigenous Drugs of India*, U. N. Dhar and Sons, Calcutta, 1958, p. 325.
3. Schraufstatter, E. and Deutsh, F., *Z. Naturforsch. B*, 1948, **3**, 430; 1949, **4**, 276.
4. Prasad, C. R. and Sirsi, M., *J. Sci. Ind. Res. C*, 1957, **15**, 239–241.
5. Schraufstatter, E. and Deutsch, S., *Z. Naturforsch. B*, 1948, **3**, 163–171 (C.A. 1949, **43**, 5446).
6. Rinderknecht, H., Ward, J. L., Bergei, F. and Morrison, A. L., *Biochem. J.*, 1947, **41**, 463.
7. Supniewski, J. V. and Hano, J., *Ber. Ges. Physiol. Exp. Pharmacol.*, 1935, **95**, 119 (C.A. 1938, **32**, 9297).
8. Chopra, R. N., Gupta, J. C. and Chopra, G. S., *Indian J. Med. Res.*, 1941, **29**, 769–772 (C.A. **3b**, 6242).
9. Schraufstatter, E. and Bernt, H., *Nature*, 1949, **164**, 456–457; *Arch. Dermatol. u. Syphilis*, 1949, **188**, 250 (C.A. **43**, 3488, 5446).
10. Sreenivasmurthy, V. and Krishnamurthy, K., *Food Sci.*, 1959, **8**, 284–288 (C.A. **54**, 1764).
11. Rao, B. G. V. and Nigam, S. S., *Indian J. Med. Res.*, 1970, **58**, 627–633.
12. Rao, B. G. V. and Nigam, S. S., *Flavour Ind.*, 1970, **1**, 725–729 (C.A. **74**, 553–559).
13. Lutomski, J., Kedzia, B. and Debska, W., *Planta Med.*, 1974, **26**, 9 (C.A. **81**, 100070).
14. Shankar, T. N. B. and Murthy, V. S. *Indian J. Exptl. Biol.*, 1979, **17**, 1363–1366 (C.A. **92**, 88520).
15. Shankar, T. N. B. and Murthy, V. S., *J. Food Sci. Technol.*, 1978, **15**, 152–153.
16. Rao, B. G. N. and Joseph, P. L., *Riechst., Aromen, Koerper-flegem*, 1971, **21**, 405–406, 408–404 (C.A. **76**, 81621).
17. Sawada, T., Yamahara, J., Shimazu, S. and Ohta, T., *Shoyakugaku Zasshi*, 1911, **2**, 11–16 (C.A. 1972, **76**, 218–238).
18. Bhatia, A., Singh, G. B. and Khanna, N. M., *Indian J. Exp. Biol.*, 1963, **2**, 158–160.
19. Sinha, M., Sikdar, S. and Das Gupta, S. R., *Indian Med. Gaz.*, 1975, **15**, 318–319; *Indian J. Pharmacol.*, 1974, **6**, 87; 1975, **7**, 98.
20. Bhuvneshwaran, C., Kapur, O. P., Sriramachari, S., Jayaraj, A. P., Srinivasan, M. and Subramanyan, V., *Food Sci.*, 1963, **12**, 182.
21. Bhuvneshwaran, C., Sriramachari, S., Jayaraj, A. P. and Srinivasan Subramanyan, V., *Food Sci.*, 1963, **12**, 185.
22. Srinivasan, M., Aiyar, A. S., Kapur, O. P., Kokutnur, M. G., Subba Rao, D., Sreenivasan, A. and Subramanyan, K., *Indian J. Exp. Biol.*, 1964, **2**, 104.
23. Prasad, C. R. and Sirst, M., *J. Sci. Ind. Res. C*, 1956, **15**, 202; 1957, **160**, 108.
24. Kohlstedt, E., *Pharmazie*, 1947, **2**, 529–536 (C.A. **42**, 3143).
25. Sebert, W., *Dent. Med. Wochschr.*, 1941, **67**, 679–682 (C.A., **37**, 4800).
26. Grabe, F., *Arch. Exp. Pathol. Pharmacol.*, 1935, **176**, 673.
27. Rumpel, W., *Arch. Exp. Pathol. Pharmacol.*, 1954, **287**, 350–352 (C.A., **51**, 13186).
28. Robbers, H., *Arch. Exp. Pathol. Pharmacol.*, 1936, **181**, 328 (C.A. 1936, **30**, 6822).
29. Subba Rao, D., Chandrasekhara, N., Satyanarayanam, M. N. and Srinivasan, M., *J. Nutr.*, 1970, **100**, 1307–1316.
30. Palit, T. N. and Srinivasan, M., *Indian J. Exp. Biol.*, 1971, **9**, 167.
31. Mima, H., *Yakugaku Zasshi*, 1959, **79**, 644 (C.A. **53**, 164–171).
32. Kiso, Y., Suzuki, Y., Watanabe, N., Oshima, Y. and Hikino, H., *Planta Med.*, 1983, **49**, 185–187.

33. Sen Gupta, M., Das, J., Sikdar, S. and Mitra, N. K., *Calcutta Med. J.*, 1976, **73**, 119-123.
34. Denatus, I. A. and Sardijoke, V., *Biochem. Pharmacol.*, 1990, **39**, 1869-1875 (C.A. 1990, **113**, 914-915).
35. Bhavanishankar, T. N. and Murthy, V. S., *Nutr. Rep. Int.*, 1985, **32**, 1285-1292 (C.A. 1986, **104**, 50272).
36. Leskover, P., German Patent, 3,046,580; *Chem. Abstr.*, 1982, **97**, 120487.
37. Sathye, B. V., *Jeevaniya*, 1990, p. 48.
38. Sarin, J. P. S. and Khanna, N. M., *Jeevaniya*, 1990, 49.
39. Arora, R. B., Basu, N. and Jain, A. P., Proceedings Second Indo-Soviet Symp. on Natural Products, New Delhi, 1970, p. 170.
40. Arora, R. B., Basu, N., Kapoor, V. and Jain, A., *Indian J. Med. Res.*, 1971, **59**, 10.
41. Mukhopadhyaya, A., Basu, N., Ghatak, N., Singh, K. P. and Gujral, P. D., *Proc. Int. Union of Physiol. Sci.*, 1974, **11**, 241.
42. Chandra, D. and Gupta, S. S., *Indian J. Med. Res.* 1972, **60**, 138-142.
43. Rao, T. S., Basu, N. and Siddiqui, H. H., *Indian J. Med. Res.*, 1982, **75**, 574.
44. Ghatak, N. and Basu, N., *Indian J. Exp. Biol.*, 1972, **10**, 235.
45. Wagner, H., Wierer, M. and Bauer, R., *Planta Med.*, 1986, **3**, 184.
46. Rao, T. S., Basu, N., Seth, S. D. and Siddiqui, H. H., *Indian J. Physiol. Pharmacol.*, 1984, **28**, 211-215.
47. Srimal, R. C., Khanna, N. M. and Dhawan, B. N., *Indian J. Pharmacol.*, 1971, **3**, 10.
48. Srimal, R. C. and Dhawan, B. N., *J. Pharm. Pharmacol.*, 1973, **25**, 447-452.
49. Srivastava, R. and Srimal, R. C., *Biol. Mem.*, 1985, **10**, 66-69.
50. Clinical Pharmacological and Toxicological Data on Diferuloyl Methane (Curcumin), a Non-steroidal Anti-inflammatory Agent: Dossier, submitted (by CDRI Lucknow) to Drugs Controller, India, September 1973.
51. Sharma, S. C., Mukhtar, H., Sharma, S. K. and Krishnamurty, C. R., *Biochem. Pharmacol.*, 1972, **21**, 1210-1214.
52. Huang, M. T., Lysz, T., Ferraro, T., Abidi, T. F., Laskin, J. D. and Conney, A. H., *Cancer Res.*, 1991, **51**, 813-819.
53. Ramaswamy, T. S. and Banerjee, B. N., *Ann. Biochem. Exp. Med.*, 1948, **8**, 55-68.
54. Sethi, S. C. and Agarwal, J. S., *J. Sci. Ind. Res.*, 1952, **118**, 468-470.
55. Chipault, J. R., Mizuno, G. R. and Lundberg, W. O., *Food Technol.*, 1956, **10**, 209-211 (C.A., 1956, **50**, 12340).
56. Chipault, J. R., Mizuno, G. R. and Lundberg, W. O., *Food Res.*, 1955, **20**, 443-448 (C.A. 1956, **50**, 6704).
57. Tokuda, K., *Kaseigaku Zasshi*, 1978, **29**, 52-54 (C.A. 1978, **89**, 1972-1973).
58. Chou, J. W. and Chang, H. W., *Chung Kuo Nung Yeh Hua Hsueh Hui Chih*, 1983, **21**, 97-103 (C.A. 1984, **101**, 109152).
59. Xu, S., Tang, X. and Lin, Y., *Zhongcaoyao*, 1991, **22**, 264-265 (C.A. 1991, **115**, 174596).
60. Yoshioka, M., *Seikatsu Kagaku Kenyusho Kenkyu Hokoku (Miyagi gakun Joshi Daigaku)*, 1990, 1-8, (C.A. 1990, **113**, 189969).
61. Zhao, B., Lix, HeR, Cheng, S. and Xin, W., *Cell Biophys.*, 1989, **14**, 175-185.
62. Lehr, H. A. and Becker, M., *Arteriosclerosis Thromb.*, 1992, **12**, 824-829.
63. Sharma, O. P., *Biochem. Pharmacol.*, 1976, **25**, 1811-1812.
64. Teennesen, H. H., *Int. J. Pharmacol.*, 1989, **50**, 67-69.
65. Kunchandy, E. and Rao, M. N. A., *Int. J. Pharm.*, 1990, **58**, 237-240.
66. Khanna, N. M., Sarin, J. P. S., Singh, S., Pal, R., Seth, R. K. and Nityanand, S., Indian Patent 162441 dated 26 December 1984 (A process for obtaining hypolipidemic, hypocholesterolemic fraction from curcuma species).
67. Khanna, N. M. *et al.* Indian Patent application (pending) (A process for making polyherbal hypolipidemic, metabolic disorders preventing pharmaceutical preparations).
68. Basu, P. K., Krishnan, R. and Khanna, N. M. (Results to be published).
69. Khanna, N. M., Shukla, V. K., Dwivedi, A. K., Sarin, J. P. S., Setty, B. S. and Kamboj, V. P., Indian Patent Appl. No. 1134/Del/88.
70. Srivastava, K. and Mehrotra, P. K., *Indian J. Pharmacol.*, 1978, **10**, 21-25.
71. Dixit, R. S., Perte, S. L. and Agarwal, P. N., *Labdev*, 1965, **3**, 273-274.
72. Dixit, R. S. and Perti, S. L., *Bull. Res. Lab. Jammu*, 1963, **1**, 169-172 (C.A. 1964, **60**, 11312).
73. Soudamini, K. K. and Kuttan, R., *J. Ethnopharmacol.*, 1989, **27**, 227.
74. Kuttan, R., Bhanumatty, P., Nirmala, K. and George, M. C., *Cancer Lett.*, 1985, **29**, 197-202.
75. Wargovich, M. J., Eng, V. W. and Newmark, H. L., *Food Chem. Toxicol.*, 1985, **23**, 47-49 (C.A. 1985, **102**, 144557).
76. Ahn, B. Z. and Lee, J. H., *Saengyak Hachoechi*, 1989, **20**, 223-226 (C.A. 1990, **113**, 70809).
77. Suiz, Luj., Craik, C. S. and Oritz de Montanello, P. R., Proc. 205 ACS National Meeting, Denver, Colorado, 28 March - 2 April, Am. Chem. Soc. Med. Chem. Div. 1993.
78. Take, Y., Inouye, H., Nakamura, S., Alauddin, H. S. and Kuba, A., *J. Antibiot.*, 1989, **42**, 107-115 (C.A. 1989, **110**, 147191).
79. Aufinkolk, M., Amir, S. M. and Ingtar, S. H., *Endocrinology*, 1985, **116**, 1677-1686 (C.A. 1985, **103**, 16403).
80. Srivastava, R., Puri, V., Srimal, R. C. and Dhawan, B. N., *Arznei Forsch.*, 1986, **36**, 715-717.
81. Srivastava, R., Dikshit, M., Srimal, R. C. and Dhawan, B. N., *Thromb. Res.*, 1985, **40**, 413-417.
82. Kosuge, T., Ishida, H. and Yamazaki, H., *Chem. Pharm. Bull.*, 1985, **33**, 1499-1502 (C.A. 1985, **103**, 47978).
83. Liu, Y., US Patent, 4,842,859; *Chem. Abstr.*, 1984, **111**, 162000.
84. Srinivasan, M. and Satyanarayana, J., *Biosci.*, 1987, **12**, 143-152.

Received 2 March 1999; accepted 6 March 1999

# Improvement in nitrogen use efficiency: Physiological and molecular approaches

Yash P. Abrol\*, Sukumar R. Chatterjee, P. Ananda Kumar and Vanita Jain

Division of Plant Physiology, Nuclear Research Laboratory and National Research Centre for Plant Biotechnology, Indian Agricultural Research Institute, New Delhi 110 012, India

**Nitrogen deficiency in agricultural systems is a world-wide problem. It is true of the Indian scenario as well. The utilization efficiency of nitrogenous fertilizers under field conditions is poor. This results in loss of a costly input and accentuates the environmental degradation. In this paper, the present status of our knowledge on physiological and molecular approaches to improve nitrogen utilization efficiency at the level of its uptake, assimilation and relationship to photosynthesis, a major factor determining biomass and grain yield, is discussed. The work done in the authors' laboratory for over a decade is summarized. It is hoped that better understanding will help to apply the tools of molecular biology to genetically manipulate the crop plants so as to enhance yields at low inputs of nitrogen.**

NITROGEN deficiency in agricultural systems is a world-wide problem<sup>1</sup>. It is true of the Indian scenario as well. Soils of more than two hundred districts have been reported to be poor in nitrogen status<sup>2</sup>. To increase crop productivity per unit area and agricultural production to meet the demand of the ever-increasing population which may touch the 1.3 billion mark by 2025 AD, millions of tonnes of nitrogenous fertilizers are applied to the soil. These are accompanied by other major and minor nutrients depending on the health status of the soils. Their use has increased from 0.7 mt in 1950 to around 13.5 mt in 1996–1997 (ref. 3). Two crops viz. wheat and rice, which form the staple diet of teeming millions, consume 70 per cent of the fertilizers. There is likelihood of change in this pattern of utilization due to diversification of crops, export orientation and emphasis on agro-processing<sup>4</sup>. For wheat and rice, the utilization efficiency of nitrogenous fertilizers under field conditions is around 50 and 25–30 per cent, respectively<sup>5</sup>. This poor efficiency is of great concern for a number of reasons: (i) even if the efficiency of nitrogenous fertilizers remains at the present level, the losses will increase enormously as their consumption is expected to double within the next 25–30 years; (ii) their manufacture involves high-cost technology requiring a whole range of

feed stocks, the major one being naphtha, a petroleum product. Its import results in drainage of foreign exchange reserves of the country<sup>6</sup>; (iii) this leads to environmental problems, namely,  $\text{NO}_3^-$  pollution of the ground water and surface water run off and emission of  $\text{NO}_x$  ( $\text{N}_2\text{O}$ ,  $\text{NO}$ ,  $\text{NO}_2^-$ ) which have positive radiative forcing characteristics.  $\text{NO}_2^-$  is involved in stratospheric ozone depletion as well<sup>7</sup>. Their excessive and injudicious use, as reported from a number of regions, further accentuates the environmental degradation of these nitrogenous fertilizers besides affecting the quality of crops, human and animal health, and causes lodging in cereals which may affect crop yields and quality<sup>3,8</sup>. In surface water, presence of high N results in growth of algae and plants, thus accelerating eutrophication, and consequently affect water quality and usage. Incidence of stomach cancer in humans, particularly in infants, and of non-Hodgkin's lymphoma due to intake of water contaminated with nitrate have been reported<sup>9,10</sup>. Nitrosamines produced from nitrite are reported to be carcinogenic; and (iv)  $\text{NH}_3$  gas is a pollutant because of its corrosive nature and through the formation of ammonium salts<sup>8</sup>.

A number of management strategies to improve the efficiency of utilization of nitrogenous fertilizers include application of different types of fertilizers, their mode of application, avoiding runoff, mitigation of losses from soil and plants, use of slow-release fertilizers, nitrification inhibitors; use of organic manures, green manuring; use of legumes in cropping systems; correction in their imbalanced use and integrated nutrient management<sup>3,5,11</sup>.

During the recent past, investigations at the physiological and molecular levels, which relate to acquisition and utilization of nitrogen, were conducted. These are related to understanding of the regulation of uptake and the assimilatory processes, redistribution within the cell and balance between storage and current use at the cellular and whole plant level. It is expected that an understanding of these processes will make it possible to apply the tools of molecular biology to genetically manipulate the plant to improve its nitrogen use efficiency (NUE) and thus contribute to precision management<sup>12</sup>.

\*For correspondence.

In our laboratory, detailed investigations have been conducted over the last two decades on the above-referred aspects. These studies have been primarily confined to wheat (*Triticum aestivum* L.) and barley (*Hordeum vulgare* L.). Salient features of the findings along with the present status of our knowledge and molecular approaches to possibly improve nitrogen use efficiency are discussed.

The predominant form of nitrogenous fertilizer applied to the soil is urea<sup>5</sup>. Under the semi-aerobic conditions prevailing in the field, it is converted to nitrate. The nitrate is taken up by the plant and assimilated by a well-documented assimilation pathway which involves the enzymes nitrate reductase and nitrite reductase. The end product,  $\text{NH}_4^+$  is incorporated into amino acids via the GS/GOGAT pathway<sup>13</sup> (Figure 1). On senescence, the proteins are degraded and mobilized to the sequentially formed foliage and finally to the grains where the storage proteins serve as a source for human consumption<sup>11,14</sup>.

## Nitrate uptake

The first step involved in acquisition of nitrogen is the uptake system which is mediated by transporters located on the plasma membrane of the epidermal and cortical cells<sup>15-17</sup>. Two such transport systems; low affinity

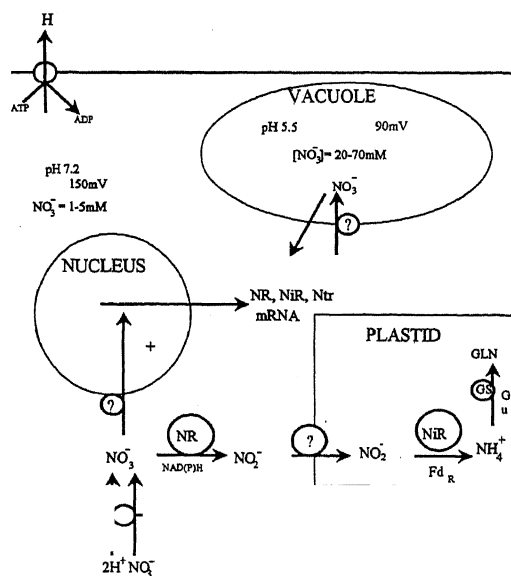


**Figure 1.** Schematic diagram of nitrate assimilation pathway. The  $\text{H}^+$ -ATPase in the plasma membrane pumps protons out of the cell, producing pH and electrical ( $\Delta\Psi$ ) gradients. The nitrate transporters (Ntr) cotransports two or more protons per nitrate into the cell. Nitrate can be transported across the tonoplast and stored in the vacuole. Nitrate in the cytosol is reduced to nitrite, which enters the plastid and is reduced to ammonia. Ammonia is fixed into glutamate (Glu) to produce glutamine (GLN) by the action of glutamine synthetase (GS). Nitrate also acts as a signal to increase the expression of nitrate reductase (NR), nitrite reductase (Nir) and *Ntr* genes (Crawford<sup>13</sup>).

transport systems (LATS), and high affinity transport systems (HATS) have been postulated on the basis of kinetic studies. Initial studies using fungi and algae have shown that low affinity transporter is constitutive in nature, and possibly has a signalling role rather than a nutritional one. It admits enough nitrate into the cell to induce the expression of transporter and assimilatory genes, and presumably plays a physiological role in the nitrate uptake only above a certain threshold. Both the HATS – constitutive HATS and inducible HATS – become active when the concentration of nitrate in the soil/medium is low, i.e. below 1 mM. Both these high affinity uptake systems are upregulated in response to nitrate. Constitutive HATS provide a high affinity, low capacity pathway for nitrate entry in uninduced plants<sup>17</sup> but their activity become three-fold on exposure to nitrate. Inducible HATS have been extensively studied and are known to be induced by nitrate or nitrite. In all the above-mentioned systems, each ion of nitrate is co-transported with two or more protons. A low affinity nitrate carrier has been identified in *Arabidopsis thaliana*<sup>18,19</sup> and rice<sup>20</sup>. Recent kinetic studies indicate the presence of low affinity constitutive nitrate transporter in wheat, rye and triticale<sup>21</sup> and it has been suggested that in maize roots, two plasma membrane polypeptides of 61 and 39 kDa may be the most likely candidates for a role in the transport system<sup>22</sup>.

The genes coding for LATS and HATS have been identified in fungi, algae and more recently, in higher plants<sup>16</sup>. The genes in higher plants appear to be root specific. Two different but homologous genes were isolated from a root hair-specific tomato cDNA library. Of these, while *Ntr1:1Le* is expressed in root hairs as well as other root tissues under all nitrogen treatments and may correspond to a constitutively expressed LATS, *Ntr1:2Le* mRNA accumulation is restricted to root hairs that had been exposed to nitrate. Recently, a full length cDNA, *Ntr2:1Np*, was isolated from a dicot, *Nicotiana plumbaginifolia*<sup>16</sup>. The expression of this gene is root specific, nitrate inducible, and is negatively regulated by nitrogen metabolites. The physiological and biochemical characterization of plants, transgenic or otherwise, that specifically overexpress or underexpress these genes will be of great interest.

Nitrogenous fertilizers (along with other nutrients), as per the management package, are invariably applied at early growth stages of the crop. Accordingly, the nitrogen concentration in the soil at this stage is 100 mM which declines subsequently because of its utilization and losses due to leaching and other processes<sup>23,24</sup>. The concentration may become as low as 10  $\mu\text{M}$  during flag laminae emergence, flowering, and grain development. Thus, it is likely that while both the low and high affinity transporters are functional during the early stages of growth, the high affinity systems are operative at later stages too, when the soil N concentration is low. These

systems offer great potential for future detailed studies on the mechanisms of transport function, particularly when combined with specific site-directed mutagenesis.

It seems, however, that excessive influxes are usually accompanied by rising effluxes. Taking analogy from the studies with Pi and  $\text{SO}_4^{2-}$ , where an excessive uptake of ions across the plasma membrane may on its own do little to improve the nutrition, the improvement would have to be co-ordinated at the very least with corresponding increase in influxes across the tonoplast where ions can be safely stored. The storage of vacuolar nitrate however seems to be for a short period. For example, it has been shown in barley and tomato that stocks of nitrate in vacuoles of both roots and leaves were virtually eliminated in 48 h, while growth continued for ten days by remobilization of protein N (ref. 25).

A few approaches to improve NUE, however, may be worthy of investigation. (i) It is likely that over-expression of high affinity transporter operative at later stages of growth, when soil nitrogen concentrations are low and the potential nitrate assimilatory activity is not fully utilized due to lack of availability of nitrate (see later section), will be beneficial to the plant. Nitrogen acquired at this stage seems to help in improving the grain protein content and the number of fully developed grains<sup>23</sup>. (ii) Constitutive expression of nitrate transporter in the root cells of transgenic plants will circumvent the problem of repression and may result in continuous uptake (see Figure 2). Expression of low affinity transporter gene in *Arabidopsis* and rice resulted in enhanced nitrate uptake<sup>18,20</sup>. Such an enhancement can be coupled to an increase in xylem loading of nitrate by constitutively expressing another gene involved in nitrate translocation<sup>26</sup>. (iii) A considerable amount of variation in  $C_{\min}$  (lowest concentration at which roots can extract ions from the soil solution) at species level has been reported. Screening of cultivars for low  $C_{\min}$  may be helpful in identifying the ones which have higher influx of nitrate as compared to efflux<sup>27</sup>.

At the whole plant level, the rate of nitrate uptake matches the growth of the plant. Its demand increases when there is an internal deficiency. It seems to be regulated by specific amino acids<sup>28</sup>. When plants are adequately supplied with nitrogen, transport processes are down-regulated so that only a small fraction of the potential for transport is expressed. Over-expression of the transporter genes for increased nitrate transport may be feasible if (i) the feedback inhibition of the transport system by amino acids is relaxed, and (ii) adequate storage of nitrate in organs like the shoot were possible. It appears doubtful whether over-expression for increased transport will be a feasible approach. However, manipulating storage capacity of organs may be possible. In wheat and barley, nitrate, whose concentration is high in the soil, is taken up by the plant and stored in the inter-

nodes and assimilated subsequently by the upper laminae which show sub-optimal activity (Table 1) (ref. 29). Similar observations have been reported in maize<sup>30</sup>. In spinach, it was shown by Steingrover *et al.*<sup>31</sup> that the petioles contain 3–4-fold higher concentration of nitrate than the laminae.

## Nitrate assimilation

A series of investigations are being conducted to understand the structure, function and regulation of the enzymes involved in nitrate assimilation. Particular emphasis is on the enzyme nitrate reductase (NR), which is the key enzyme involved in nitrate assimilation showing low affinity for nitrate, is susceptible to stress, and is unstable under *in vitro* conditions<sup>32</sup>. The studies relate to regulation at transcriptional and post-transcriptional levels, interaction with environmental factors e.g. light, substrate availability, moisture stress, carbohydrate supply, phytohormones, phytochrome and covalent modifications<sup>13,14,23,33–40</sup>. Studies to elucidate the molecular structure of the enzyme have led to the identification of gene products that regulate its expression. Three different isoforms of NR: inducible NADH:NR; constitutive NADH:NR and NAD(P)H: NR have been purified from different plant sources. The predominant form, inducible NADH:NR in higher plants, is mostly present as a homodimer with molecular weight ranging from 200 to 230 kDa and sub-unit molecular weight ranging from 110 to 115 kDa. The three prosthetic groups, namely, FAD, cytochrome  $b_{557}$  and molybdenum cofactor (MoCo) present in 1:1:1 stoichiometry are 23, 10, and 90 kDa, respectively. Three functional domains of NR are joined to each other by the hinge regions. On these functional domains are also the active sites where the enzyme's partial and main reactions take place. Cloning and sequencing of higher plant NRs show that amino acid sequences present at the active site are well-conserved. Two cysteine residues corresponding to cys-191 and cys-245 in *Arabidopsis* are found conserved in higher plant NRs studied so far. The residues are proposed to be involved in forming an interchain disulphide bridge during sub-unit association. Histidine residues act as ligands for binding of heme prosthetic group of higher plant NRs. A lys-731 and a

**Table 1.** Total nitrate content ( $\mu\text{mol}/\text{plant part}$ ) in stem, sheath and laminae after ear emergence in barley (*Hordeum vulgare* L.) cv. Jyoti S

| Days after sowing | Stem            | Sheath         | Laminae        |
|-------------------|-----------------|----------------|----------------|
| 98                | 23.1 $\pm$ 0.44 | 8.5 $\pm$ 0.21 | 5.4 $\pm$ 0.40 |
| 105               | 25.4 $\pm$ 0.19 | 9.2 $\pm$ 0.23 | 3.9 $\pm$ 0.21 |
| 111               | 20.5 $\pm$ 0.32 | 6.4 $\pm$ 0.17 | 3.6 $\pm$ 0.11 |

From: Chatterjee *et al.*<sup>29</sup>

cys-889 are found to be conserved in all higher plant NRs. The amino acids may be essential for NADH binding. However, six amino acids, gly-pro-pro-promet-ile, upstream of cys-889 determine the relative affinity for either NADH or NADPH. In birch NR, two proline residues are replaced by alanine and serine which perhaps allows it to bind either NADH or NADPH equally well<sup>41</sup>. Arginine residues are also implicated in binding of NADH (ref. 42). On the other hand, histidine residues may be involved in electron transfer from the reduced FAD to the heme-iron protein of the cytochrome domain of NR (ref. 43). Furthermore, ser-543 present at hinge 1 region, preceding the MoCo domain appears to be involved in phosphorylation-dephosphorylation<sup>44</sup>. Site-directed mutation of ser-543 to asp in *Arabidopsis* NR prevents phosphorylation, modification, and inactivation of NR (refs 38, 45). In brief, once various roles of the different amino acids in the NR molecule have been elucidated, site-directed mutagenesis could be used to modify the activity of the enzyme at will.

*Nia* gene, which encodes NR in higher plants, is conserved among plants and is present in multiple copies per haploid genome. The stimulatory effect of nitrate on NR gene transcription is mediated by a constitutively expressed nitrate-sensor protein. This protein either binds to nitrate-responsive promoter of the *nia* gene in higher plants or activates *nit-2*-like transacting DNA-binding protein in the presence of nitrate and allows enhanced transcription of NR mRNA. The exact mechanism is worth investigation. Light induces *nia* gene transcription by some still unknown mechanism. Light induction of *nia* mRNA is also mediated via phytochrome. Over-expression of NR is found in transgenic tobacco plants transformed with oat *phyA* gene<sup>38</sup>.

In one of the earlier hypotheses put forward by Hageman and his group<sup>32</sup>, a relationship between activity of the enzyme, NR, and grain yield and various other characteristics was suggested. It was postulated that since the enzyme was rate limiting, any increase in its content/activity will be beneficial and thus improve nitrogen utilization. Recent molecular studies with mutants and transgenics of *Arabidopsis* and *Nicotiana*, however, tell a different story<sup>35</sup>. Transgenic plants expressing NR activity at a level five- to six-times of the wild type obtained by transformation of the E23 *nia* mutant with tobacco *nia 2* cDNA under the control of the 35S promoter, showed no differences in chlorophyll, proteins or amino acid accumulation. Plants do not seem to benefit from excess NR activity. It needs to be investigated if *in vitro* NR activity reflects the *in vivo* situation<sup>35,46</sup>. *A. thaliana* mutants affected in *nia 2* gene, and barley mutants which express only 10 per cent of the wild type NR activity, did not show any decline in the nitrogen content and biomass under greenhouse growth conditions<sup>35</sup>. Interestingly enough, it was observed that higher

NR activity in *Nicotiana* resulted in lower  $\text{NO}_3^-$  content compared to the wild ones<sup>47</sup>. Similar relationship between the NR activity and nitrate content, which have been reported to show two- to three-fold variations in wheat cultivars was observed. There was 30 to 56 per cent reduction in nitrate content of high NR cultivars as compared to low NR ones<sup>48</sup> (Table 2). The findings have a bearing on the improvement in the nutritional quality of the leafy vegetables, particularly the ones grown under low light conditions. It may be mentioned here that over-expression of the enzymes of ammonia assimilation (GS and GOGAT) in transgenic tobacco resulted in an enhancement in total protein content under nitrogen deprivation. The plants also had higher carbon dioxide assimilation capacity<sup>49</sup>.

An interesting approach, which has implications to improve the NR enzyme potential and thus possibly improve NUE, was postulated. According to this, the reconstitution of chloroplasts of higher plants with cyanobacterial type NR would make the organelle self-containing and independent in terms of N metabolism. Cyanobacterial-NR derives its energy from reduced ferredoxin through photosynthetic electron transport (Figure 2). The enzyme is small (80 kDa) and the gene

**Table 2.** Nitrate concentration ( $\mu\text{mol g}^{-1}$  dry wt) in the laminae at various growth stages in high (cv. Shera) and low (cv. Pusa Lerma) nitrate reductase (NR) activity wheat cv

|         | Days after sowing |       |       |
|---------|-------------------|-------|-------|
|         | 16                | 23    | 30    |
| High NR | 267.7             | 151.5 | 159.7 |
| Low NR  | 380.3             | 218.2 | 245.8 |

From: Ramraj *et al.*<sup>48</sup>.

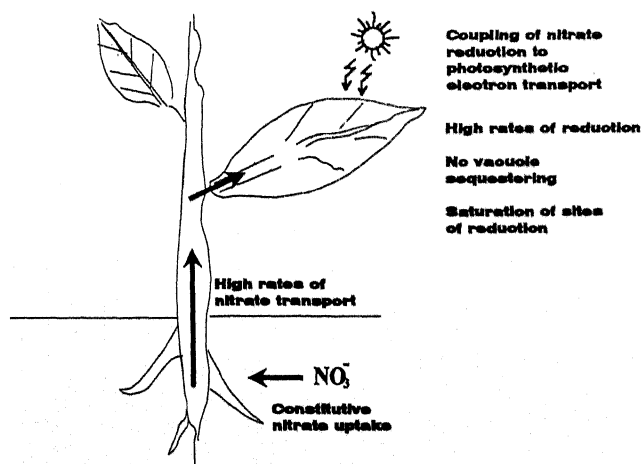


**Figure 2.** Diagrammatic representation of the possible approaches to improve nitrate uptake and its utilization by the plants.

encoding for it was isolated and characterized from *Synechococcus*<sup>50</sup>. There are two possible approaches to introduce *Synechococcus* NR in higher plant chloroplasts: (i) Engineer the chloroplast genome by inserting the NR gene into it and, (ii) Synthesize the enzyme in cytosol and transport it to the organelle with the aid of transit peptide sequences. Nucleotide sequence encoding pea Rubisco small subunit transit peptide was fused translationally to the *Synechococcus* NR gene<sup>51</sup>. The chimeric gene was used to synthesize fusion protein *in vitro* using rabbit reticulocyte system. The translation product with the transit peptide was translocated into the isolated pea chloroplasts and kinetics of transport were studied. The fusion protein was processed completely and NR protein was found to be localized in the stromal compartment of the chloroplast. The chimeric gene was cloned in a binary *Agrobacterium* vector carrying a CaMV 35S promoter to express the foreign gene constitutively. Transgenic tobacco plants have been developed and the analysis of cyanobacterial-NR expression is in progress in our laboratory.

## Field studies

To identify the genotypes and management strategies by which efficient use of nitrogenous fertilizer can be made, a series of field-based experiments with the various cultivars were conducted. These involved a complete analysis of the nitrogen uptake, assimilation of nitrate, storage and, mobilization of nitrogen throughout growth and development<sup>52-58</sup>. A brief summary of major findings is given below.

### Pattern of nitrate assimilation

Following the prevalent management practices, nitrate assimilation is high in the first-formed laminae and declines in the subsequently formed ones (Figure 3). This suggests either a lack of availability of substrate at later stages of growth<sup>52,57</sup> (refer to earlier section) or reduction in the capacity to take up and/or assimilate nitrate. Measurements of soil nitrate concentrations throughout the growth period and feeding nitrate to the excised laminae from field-grown plants showed that it was the lack of availability of substrate viz. nitrate at the later stages<sup>55</sup>. At early stages of growth, however, the laminae are saturated and one can say that the nitrate assimilatory pathway, as per the present management practices, is rate limiting. In fact, it was observed that at the optimal level, as determined by agronomic experiments, there is reduction in NR activity compared to the activity at sub-optimal levels. This may possibly be related to toxicity<sup>23,56</sup>.

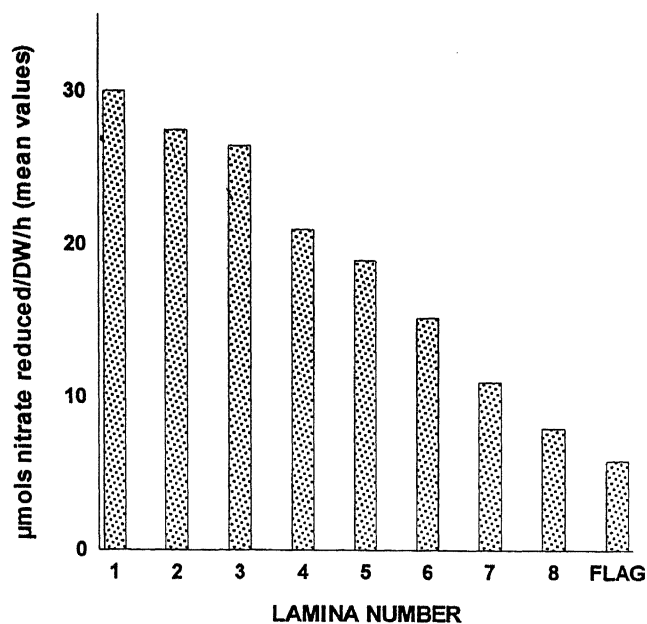


Figure 3. Mean *in vivo* NR activity of the laminae on the main shoot. Each value is a mean of 3 values at full expansion (Abrol<sup>23</sup>).

### Nitrate assimilation by different plant parts

In wheat and barley, while the laminae contribute approximately 65 to 70 per cent of the total nitrate assimilated, roots, stem (leaf sheaths + internodes), and reproductive parts reduce the rest of the amount equally<sup>52</sup>. Maximum nitrate reduction takes place during the flag laminae emergence. During the post-flowering phase, ear components make significant contribution<sup>29</sup> (Figure 4). Amongst the laminae, the upper ones, despite their low NR activity, reduce major amount of the nitrate taken up by the plant. This supports the observation mentioned earlier that nitrate acquired at earlier stages is stored in the internodes (see section Nitrate uptake).

### Differential response of the various cultivars

Response of the wheat cultivars which differed two- to three-fold in NR activity, revealed that (i) there was more than 100 per cent increase in activity in upper laminae of the high NR cv. when they were placed in Hoagland's solution containing nitrate. The magnitude of increase was much less in the upper laminae of low NR cultivars, (ii) major amount of the nitrate was reduced by the upper laminae, which is because of their larger size as compared to the lower ones, and (iii) at optimal doses of nitrogenous fertilizer application, as recommended by the agronomic studies, high as well as

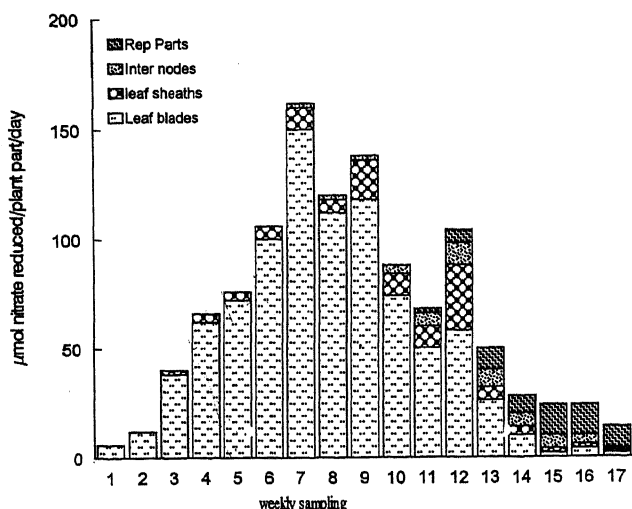


Figure 4. Nitrate reductase activity (*in vivo*) in individual plant parts expressed as  $\mu\text{mol nitrate reduced plant part}^{-1} \text{ day}^{-1}$  (Chatterjee *et al.*<sup>29</sup>).

low NR cultivars, reduce much less nitrate compared to their total reduction potential<sup>23,54</sup>

#### Split application of nitrogenous fertilizer

Application of the same amount of nitrogen in more than two splits under field conditions increases the nitrogen availability at later stages of growth so that the suboptimal activity of the upper laminae can be exploited. It was observed that there was a significant improvement in the nitrate assimilatory activity of the upper laminae<sup>23</sup> (Figure 5) and enhancement in the total N harvest and grain protein content (Table 3). The magnitude of enhancement was higher in the high NR cv. compared to the low NR ones. Application of the additional nitrogen at later stages of growth was also useful, as has been demonstrated by a number of studies. It needs to be mentioned that high NR cv. show better response than the low NR cv. at low soil N levels as well<sup>59</sup>.

#### Nitrogen and photosynthesis

Physiologically speaking, efficiency of nitrogen use is evaluated in terms of development of efficient photosynthetic machinery involving biosynthesis of proteins which mediate the various metabolic steps in the chloroplast and especially the enzyme Rubisco, which is involved in the primary step of carbon dioxide fixation. The other aspects of NUE are the overall leaf growth, canopy development, light interception and contribution to total photosynthesis. All these eventually determine the biomass.

In this context, few approaches which are being followed and need further investigations are: (i) why much

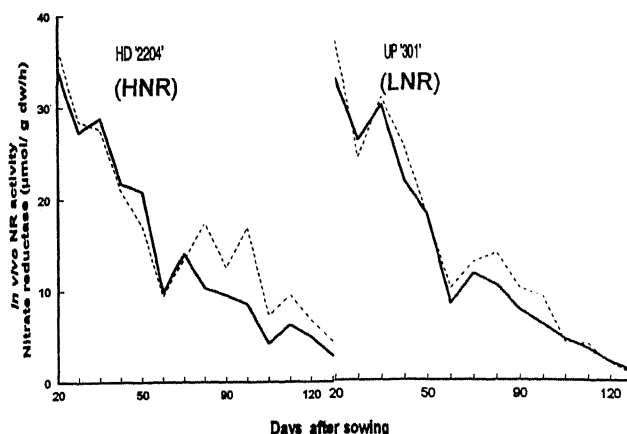


Figure 5. *In vivo* nitrate reductase activity ( $\mu\text{mol g}^{-1} \text{ dw h}^{-1}$ ) in the fully expanded laminae (pooled) at different intervals during the ontogeny of the field grown wheat [High (HD 2204) and low NR (UP 301) cv.] The nitrogen was applied in two (solid lines) splits, i.e. 60 kg N each at 0 and 28 days after sowing, and four (dotted lines) splits, viz. 30 kg N each at 0, 28, 54 and 76 days after sowing (Abrol<sup>23</sup>).

Table 3. Additional nitrogen accumulated as a result of increasing the splitting frequency of the nitrogen application

| Cultivar   | mg additional N in |        |                          |
|------------|--------------------|--------|--------------------------|
|            | Whole plant        | Grains | % additional N in grains |
| Low NR     |                    |        |                          |
| Pusa Lerma | 32.7               | 29.7   | 90.8                     |
| UP 301     | 17.8               | 15.1   | 84.8                     |
| High NR    |                    |        |                          |
| HD 2177    | 57.4               | 42.4   | 73.8                     |
| HD 2204    | 43.8               | 40.0   | 91.3                     |

From: Abrol<sup>23</sup>.

more Rubisco protein is present in the laminae than is actually needed for fixing carbon dioxide? The studies have shown that at ambient irradiance and with good supply of nitrogen, there is excess investment in Rubisco. Lawlor *et al.*<sup>60</sup> observed that there is a linear relationship between the photosynthetic rates and Rubisco amount up to a certain level. Thereafter, the relationship does not hold good. This has been confirmed by lowering the Rubisco content in tobacco plants expressing Rubisco genes in anti-sense orientation. As much as 43 per cent of the wild-type Rubisco could be lost without any negative effect on photosynthesis. It was calculated that there is about 15 per cent more investment in Rubisco in wild type, which is absent in transformed tobacco, resulting thereby in corresponding gain in nitrogen use efficiency<sup>61</sup>. In this context, some of the observations of interest are that at elevated carbon dioxide levels there is sparing effect on Rubisco content<sup>62</sup>. It is

postulated that in future, under carbon dioxide-enriched scenario, the NR overexpressors may perform much better than the wild types<sup>63</sup>, especially under N-limiting conditions, (ii) how to enhance the storage of N in Rubisco and in other vegetative storage proteins at early stages, when soil N is high? This would decrease NUE in the shorter term, but there could be long-term benefits. These storage proteins can be mobilized when deficiency occurs at later stages. Our study with sequentially developed foliage shows that maximum Rubisco content is accumulated in the upper laminae<sup>64</sup>. Is Rubisco already serving as a storage protein by being subsequently mobilized to the grains? and (iii) why various wheat cvs differ in nitrogen responsiveness to photosynthesis and laminae growth<sup>64-66</sup>. An understanding of the mechanism may help in evolving cultivars which are able to maintain the high photosynthetic activity and lamina area at limiting soil-N levels.

This paper has briefly summarized the present status of our knowledge pertaining to nitrogen uptake and its utilization by crop plants. Better understanding at the cellular level and regulation at the whole plant level, coupled with various agronomic management practices specific to agroecological regions may help to improve the utilization of nitrogenous fertilizers, which are one of the major inputs in Indian agriculture.

1. Subba Rao, N. S., in *A Treatise on Dinitrogen Fixation - Agronomy and Ecology* (eds Hardy, R. W. F. and Gibson, A. H.), J. Wiley and Sons, New York, 1977, Section IV, pp. 3-32.
2. Tandon, H. L. S., *Fertilizers, Organic Manures, Recyclable Wastes and Bio-fertilizers*, Fertilizer Development and Consultation Organization, New Delhi, 1992, p. 148.
3. Kanwar, J. S. and Katyal, J. C., *Plant Nutrient Needs, Supply, Efficiency and Policy Issues: 2000-2025*, National Academy of Agricultural Sciences, New Delhi, p. 329.
4. Anonymous, *Scientists' Perception for Agriculture-2020*, National Academy of Agricultural Sciences, New Delhi, June 4-5, 1998, p. 40.
5. Prasad, R., *Curr. Sci.*, 1998, **75**, 677-683.
6. Ramarathnam, K. V., *Fertilizer News*, 1980, **25**, 25-29.
7. Houghton, J. J., Meiro Filho, L. G., Callander, B. A., Harris, N., Kattenberg, A. and Maskell, K. (eds), *Climate Change, The Science of Climate Change*, Cambridge University Press, 1995, p. 875.
8. Bockman, O. C., Kaanstad, O., Lie, O. H. and Richards, I., *Agriculture and Fertilizers*, Agricultural Group, Norsk Hydro a.s., Oslo, p. 243.
9. Hill, M. J., Hawksworth, G. and Tatterstall, G., *Br. J. Cancer*, 1973, **28**, 562-567.
10. Weisenburger, D. D., in *Nitrate Contamination: Exposure Consequences and Control* (eds Bogorad, I. and Kuzerka, R. D.), NATO ASI Series G: Ecological Sciences 30, Springer Verlag, Berlin, 1991, pp. 309-331.
11. Abrol, Y. P. (ed.), *Nitrogen-Soils, Physiology, Biochemistry, Microbiology, Genetics*, Indian National Science Academy, New Delhi, 1993, spl.vol., p. 285.
12. Gadgil, S., Abrol, Y. P. and Seshagiri, A., *Curr. Sci.*, 1999, **76**, 548-556.
13. Crawford, N. M., *Plant Cell*, 1995, **7**, 859-868.
14. Abrol, Y. P. (ed.) *Nitrogen in Higher Plants*. J. Wiley and Sons, NY, 1990, p. 492.
15. Daniel-Vedele, F. and Caboche, M., *CR Acad. Sci. (Paris)*, 1996, **319**, 961-968.
16. Daniel-Vedele, F., Filleur, S. and Caboche, M., *Curr. Opin. Plant Biol.*, 1998, **1**, 235-239.
17. Crawford, N. M. and Glass, A. D. M., *Trends Plant Sci.*, 1998, **3**, 389-395.
18. Tsay, Y.-F., Schroeder, T. I., Feldman, K. A. and Crawford, N. M., *Cell*, 1993, **72**, 705-712.
19. Quesada, A., Krapp, A., Trueman, L., Daniel-Vedele, F., Fernandez, E., Forde, B. and Caboche, M., *Plant Mol. Biol.*, 1997, **34**, 265-267.
20. Lin, C. M., Lee, H. T., Tsai, Y.-L., Yu, S.-M. and Tsay, Y.-F., 5th International Congress on Plant Mol. Biol., Singapore, 1997, Abst. 311.
21. Verma and Chatterjee, S. R. Unpublished data.
22. Ageorgis, A., Morer, M. H. and Grouzis, J. P., *Plant Physiol. Biochem.* 1996, **34**, 863-870.
23. Abrol, Y. P., in *Plant Nutrition-Physiology and Applications* (ed. van Buischem, M. L.), Kluwer Academic Publishers, Dordrecht, 1990, pp. 773-778.
24. Redinbaugh, M. G. and Campbell, W. H., *Physiol. Plant.* 1991, **82**, 640-650.
25. Chapin, F. S., Walker, G. H. S. and Clarkson, D. T., *Planta*, 1988, **173**, 352-356.
26. Kuo, H. F., Liang, Shih-yi and Tsay, Y. F., 5th International Congress on Plant Mol. Biol., Singapore, 1997, Abst. 91.
27. Marschner, H., in *Mineral Nutrition of Higher Plants*, Academic Press, London, 1995, p. 889.
28. Ismande, J. and Touraine, B., *Plant Physiol.*, 1994, **105**, 3-7.
29. Chatterjee, S. R., Pokhriyal, T. C. and Abrol, Y. P., *J. Exptl. Agric.* (Oxford), 1981, **31**, 1-11.
30. Schroeder, L. E., in *Nitrogen in the Environment*. (eds Nielsen, D. R. and MacDonald, J. E.), Academic Press, NY, 1978, vol. 2, pp. 101-141.
31. Steingrover, E., Oosterhuizen, R. and Wieringer, R., *Z. Pflanz. physiol.*, 1982, **107**, 97-102.
32. Hageman, R. H. and Below, F. E., in *Nitrogen in Higher Plants* (ed Abrol, Y. P.), J. Wiley and Sons, NY, 1990, pp. 313-334.
33. Naik, M. S., Abrol, Y. P., Rama Rao, C. S. and Nair, T. V. R., *Phytochem.*, 1982, **21**, 409-412.
34. Abrol, Y. P., Sawhney, S. K. and Naik, M. S., *Plant Cell Environ.*, 1985, **6**, 595-600.
35. Hoff, T., Truong, N. H. and Caboche, M., *Plant Cell Environ.*, 1994, **17**, 489-506.
36. Oaks, A., *Can. J. Bot.*, 1994, **72**, 739-750.
37. Pattanayak, D. and Chatterjee, S. R., *Plant Physiol. Biochem.*, 1997, **24**, 1-9.
38. Pattanayak, D. and Chatterjee, S. R., *Indian J. Exp. Biol.*, 1998, **36**, 644-650.
39. Chandok, M. R. and Sopory, S. K., *Phytochem.*, 1992, **31**, 2255-2258.
40. Chandok, M. R. and Sopory, S. K., *Mol. Gen. Genet.*, 1996, **251**, 599-605.
41. Schondrat, T. and Hachtel, W., *Plant Physiol.*, 1995, **108**, 203-210.
42. Baijal, M. and Sane, P. V., *Phytochem.*, 1988, **27**, 196-202.
43. Pattanayak, D. and Chatterjee, S. R., *J. Plant Biochem. Biotech.*, 1998, **7**, 73-78.
44. Macintosh, C., Douglas, P. and Lillo, C., *Plant Physiol.*, 1995, **107**, 451-457.
45. Su, W., Huber, H. C. and Crawford, N. M., *Plant Cell*, 1996, **8**, 519-527.
46. Foyer, C. H., Lefebvre, C., Provot, M., Vincent, M. and Vaucheret, H., *Aspects Appl. Biol.*, 1993, **34**, 137-145.

## REVIEW ARTICLE

47. Quillere, I., Dufosse, C., Roux, Y., Foyer, C. H. and Caboche, M., *J. Exp. Bot.*, 1994, **45**, 1205-1211.
48. Ramraj, V. M., Guru, S. K. and Abrol, Y. P., *Curr. Sci.*, 1999, **76**, 29-30.
49. Chickova, S., Fuentes, S. I., Arellano, J., Svoboda, S., Lopez, A. V. and Hernandez, G., *5th Intl. Cong. Plant Mol. Biol.*, Singapore, 1997, Abst. 90.
50. Andriesse, X., Bakker, H. and Weisbeck, P., in *Inorganic Nitrogen in Plants and Micro-organisms* (eds Ullrich, W. R., Rigand, C. Fuggi, A. and Aparicio, P. J.), Springer-Verlag, Berlin, 1994, pp. 303-307.
51. Kumar, P. A., Krusse, E., Andriesse, X., Weisbeck, P. and Kloppstech, *Eur. J. Biochem.*, 1993, **214**, 533-547.
52. Abrol, Y. P., Kaim, M. S. and Nair, T. V. R., *Cereal Res. Commun.*, 1976, **4**, 431-440.
53. Nair, T. V. R. and Abrol, Y. P., *J. Agric. Sci. (Cambridge)*, 1979, **93**, 473-484.
54. Abrol, Y. P., Kumar, P. A. and Nair, T. V. R., *Adv. Cereal Sci. Tech.*, 1984, **6**, 1-48.
55. Abrol, Y. P. in Platinum Jubilee Lecture series (82nd), Indian Science Congress, Calcutta, 1995, pp. 49-60.
56. Chatterjee, S. R., Kaim, M. S., Pandey, H. C., Lal, M. and Nair, T. V. R., *Plant Physiol. Biochem.*, 1992, **19**, 75-84.
57. Pokhriyal, T. C., Sachdev, M. S., Grover, H. L., Arora, R. P. and Abrol, Y. P., *Physiol. Plant.*, 1981, **48**, 477-481.
58. Abdin, M. Z. and Abrol, Y. P., in *Plant Nutrition - From Genetic Engineering to Field Practice* (ed. Barrow, M. J.), Kluwer Academic Publishers, The Netherlands, 1993, pp. 529-932.
59. Abrol, Y. P., in Proc. Annual Seminar: Fertiliser Use Efficiency. Fertiliser Association of India, New Delhi, 1981, **11**, 1-20.
60. Lawlor, D. W., Kontturi, M. and Young, A. T., *J. Exp. Bot.*, 1989, **40**, 43-52.
61. Clarkson, D. T. and Hawkesford, M. J., in *Plant Nutrition - From Genetic Engineering to Field Practice* (ed. Barrow, M. J.), Kluwer Academic Publishers, The Netherlands, 1993, pp. 23-33.
62. Theobald, J. C., Mitchell, R. A. C., Parry, M. A. J. and Lawlor, D. W., *Plant Physiol.*, 1998, **118**, 1-11.
63. Foyer, C. H., Lescure, J. C., Lefebvre, C., Morot-Gaudry, J.-F., Vincentz, M. and Vaucheret, H., *Plant Physiol.*, 1994, **104**, 171-178.
64. Sivasankar, A., Lakkineni, K. C., Jain V., Ananda Kumar, P. and Abrol, Y. P., *J. Agron. Crop Sci.*, 1998, **181**, 65-70.
65. Sivasankar, A., Lakkineni, K. C., Jain, V., Ananda Kumar, P. and Abrol, Y. P., *J. Agron. Crop Sci.*, 1998, **181**, 21-27.
66. Jain, V., Guru, S. K. and Abrol, Y. P., in Proceedings of XIth International Congress on Photosynthesis, August 17-23, 1998, Budapest, Hungary, in press.

Received 15 November 1998; revised accepted 1 March 1999

# Expression of anthocyanin pigmentation in wheat tissues transformed with anthocyanin regulatory genes

H. S. Chawla<sup>†\*</sup>, Leslie A. Cass and J. A. Simmonds

Agriculture and Agri-Food Canada, Eastern Cereal and Oilseed Research Centre, Building 21, Central Experimental Farm, Ottawa, Ontario, K1A 0C6, Canada

<sup>†</sup>Present address: Genetics and Plant Breeding Department, G. B. Pant University of Agriculture and Technology, Pantnagar 263 145, India

**Screening of transgenic tissue on the basis of the anthocyanin pigmentation has been studied in wheat. Cell-autonomous anthocyanin pigmentation, controlled by *B* and *C1* anthocyanin regulatory genes under the control of constitutive CaMV35s promoter (pBC1-7), was obtained in scutellum of immature embryos by biolistic procedures with or without a herbicide resistance gene (pAct1bar). Anthocyanin production as red/purple pigmented cells could be visualized 24 h after bombardment. Bialaphos herbicide resistant calli/plants generated transgenic sectors which showed light-dependent anthocyanin pigmentation. The pigmentation was suppressed in regenerating shoots but expressed in the ovary and pericarp of developing seeds. Transgenic shoots were obtained following selection of cultures co-bombarded with a selectable herbicide resistance gene. Southern analysis showed that transgenes were present as multiple copy insertions in high molecular weight DNA. The results obtained showed that anthocyanin marker could be used for tracking transformed tissue on the basis of anthocyanin pigment formation whose potential is realized by environmental factors particularly light.**

THE microprojectile bombardment technique developed by Sanford *et al.*<sup>1</sup> for the introduction of DNA into plant cells has shown considerable versatility in the production of transgenic plants and gene regulation studies<sup>2</sup>. Using this method, the first transgenic wheat plants were generated from embryogenic suspension cultures<sup>3</sup>. Current protocols favour the use of embryogenic callus derived from the scutellum of immature embryos for the production of transgenic wheat<sup>4-7</sup>.

Transformation efficiency is, to a large extent, dependent on the regeneration efficiency of the target tissue and on the efficacy of selectable genes to capture transformed tissues. These limitations are particularly significant in cereal transformation where the generally low level of *in vitro* responses of agronomically impor-

tant genotypes have restricted application of transformation technologies<sup>8</sup>. The use of biochemical agents such as antibiotics and herbicides for *in vitro* selection protocols further impair the regenerative response. A reporter system, that would not require the application of selectable agents or external substrates for isolation or detection of transgenic cells, utilizes the *C1*, *B* and *R* genes which code for trans acting factors that regulate the anthocyanin biosynthetic pathway in maize<sup>9</sup>. The introduction of these regulatory genes under the control of constitutive promoters induces cell-autonomous pigmentation and allows for direct visualization of transformed cells and tissues *in vivo* in maize<sup>9</sup>. Potentially, transgenic lines could be isolated physically, obviating the need for the introduction of selectable markers.

Introduction of a plasmid encoding the maize *R* and *C1* transcriptional factors, each under the control of a separate 35s promoter with maize *Adh1* intron, into immature wheat embryos resulted in the production of anthocyanin expressing cells<sup>10</sup>. Pigmented cells were observed in callus derived from these embryos for up to one month after bombardment, but these cells appeared to be the original cells, which had failed to proliferate. In a similar study, in which suspension cells of wheat were co-transformed with an anthocyanin marker and a selectable marker, anthocyanin expressing callus was isolated<sup>11</sup>.

Anthocyanin pigmentation is subject to controls other than the presence of the regulatory proteins. It has been reported that *R* gene although under the control of constitutive promoter showed restricted expression either due to the action of *C1/P1* gene or light, thus indicating that constitutive expression of an *R/B* type protein alone was not sufficient for expression of anthocyanin pigmentation<sup>9,12</sup>.

We report here the conditions required for the expression of anthocyanin as a visual marker with and without the use of selectable markers for isolation of transgenic tissue in wheat. We also report our observations on the developmental stages in which the pigment is expressed.

\*For correspondence. (email: ag@gbpuat.ernet.in)

## Materials and methods

### Plant material and culture conditions

*Triticum aestivum* L. cv. Chris plants were grown in greenhouse or controlled environment cabinets maintained in a 16 h photoperiod with light intensity of ~ 3000 lux, in a 25°C day/20°C night regime. Caryopses were collected 10–14 days post-anthesis, surface sterilized in 20% (v/v) bleach (1% active chlorine) for 10 min followed by 4 rinses with sterile distilled water. Immature embryos (1.0–1.2 mm long) were excised aseptically and placed with scutellum side up on MS2 embryo induction medium (Murashige and Skoog salts<sup>13</sup>, 3% sucrose, supplemented with 2 mg/l 2,4-D, 200 mg/l casein hydrolysate, 100 mg/l glutamine and solidified with 0.8% phytagar). Cultures were kept in the dark at 25°C. After 4 to 6 weeks, embryos were regenerated by transferring the cultures to RM1 medium (MS, 3% sucrose, 5 mg/l zeatin, 0.4 mg/l NAA) in a 16 h photoperiod with light intensity of ~ 3000 lux and maintained at 25°C. Plants were rooted on RM2 medium (1/2 strength MS, 1% sucrose), transferred to soil and grown to maturity in the greenhouse in a 16 h photoperiod, 25°C day/20°C night regime.

### Selection and screening protocols

In preparation for bombardment, embryos were cultured for 1 day on MS2 medium and were then transferred, 25 per dish, to MS2 medium supplemented with 0.4 M mannitol for 1 day prior to bombardment. Scutellum cultures, 2 d post-bombardment, were transferred from MS2 mannitol medium to MS2 medium for 2 weeks for somatic embryogenesis. For selection of herbicide-resistant embryos, the calli were transferred to MS2-S selection medium (MS2 without glycine or glutamine and supplemented with bialaphos) for 3 weeks in the dark at 25°C. The first cycle of selection was at 2 mg/l bialaphos for 3 weeks and this was followed by either 1 or 2, three-week cycles at 5 mg/l bialaphos and a final three-week cycle at 20 mg/l bialaphos. Resistant calli were transferred to RM1-S medium (RM1 without glycine or glutamine and supplemented with 5 mg/l bialaphos) in a 16 h photoperiod for plant development. For rooting, the cultures were grown on RM2 with 2 mg/l bialaphos. For visual screening of transgenic tissue on the basis of anthocyanin pigmentation, scutellum cultures, 2 days post-bombardment, were transferred to MS2 medium and processed without selection as described above in plant materials. Any calli or developing shoots showing anthocyanin pigmentation were isolated for plant production and establishment.

### Herbicide application

Young leaves of bialaphos were selected and control plants at 3–4 leaf stage were brushed with a solution of 0.4% L-phosphinothricin (L-PPT) containing 0.1% (v/v) Tween 20. L-PPT was applied on both sides of a sector of the leaf, twice at an interval of 30 min. Plants were assessed for damage one week after herbicide application.

### Biolistic procedures

Scutellum cultures were bombarded with DNA-coated gold particles (1.6 µm diameter) using a helium driven Bio-Rad PDS-1000/He biolistic delivery device. Plasmid DNA (1 µg/µl), was precipitated onto gold particles by the procedure of Klein<sup>14</sup>. For co-bombardment of visual and selectable marker genes, a 1:1 ratio of DNAs was used. Bombardment parameters were optimized for transient expression using purple spots of anthocyanin expression obtained by pBC1-7 plasmid expression vector activity.

### Plant expression vectors

Plasmid pBC1-7 (a gift from Ted Klein, DuPont, Agricultural Products, Wilmington, Delaware, USA) contains cDNAs of *Bperu*<sup>15</sup> and *C1*<sup>16</sup> anthocyanin regulatory genes each under the control of the CaMV35S promoter with the maize *adh1* intron for constitutive expression in monocots (Figure 1a). The plasmid pAct1Bar contains the selectable *bar* herbicide resistance gene under the control of rice *actin1* promoter and *actin1* intron<sup>17</sup> (Figure 1b).

### DNA isolation and Southern blot hybridization

Genomic DNA was isolated from leaves of wheat and maize (for positive control of *B* regulatory gene) according to a modification of the method of Junghans and Metzlaff<sup>18</sup>. 25 µg of wheat DNA were digested with *XbaI/XhoI* to release a 1.7 kb fragment containing the *bar* gene and with *XbaI* to release a 3.5 kb fragment containing the *Bperu* gene. pBC1-7 is a complex plasmid and any restriction enzyme found to linearize the construct was inefficient at digesting wheat genomic DNA. For the positive controls, maize genomic DNA (5 µg) was digested with *BglII* which released 2 fragments (7.6 and 9.0 kb) of *Bperu* homologous DNA. DNA was separated in 0.7% agarose gel, transferred to Hybond N membrane (Amersham Life Science) and analysed by Southern hybridization using standard techniques. PCR-generated probes were labelled with DIG-11-dUTP (Boehringer Mannheim) according to the

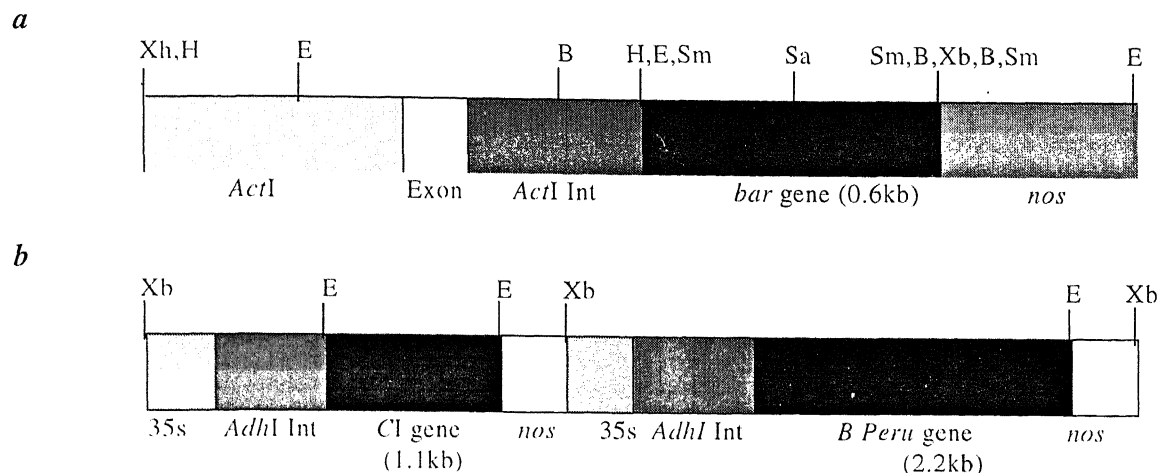


**Figure 1.** Schematic representation of plasmids used for transformation. *a*, pBC1-7; *b*, pAct1bar. B, *Bam*HI; E, *Eco*RI; H, *Hind*III; Sm, *Sma*I; Xb, *Xba*I; Xh, *Xho*I.

method of Feinberg and Vogelstein<sup>19</sup>. The following PCR primers were used to generate probes: for *Bperu* 1: 5'-GCCGCGAGGAGCATCAACTG-3' (position on *Bperu* 217 → 236) and *Bperu* 2: 5'-TGACGTGGTTCT-TGGCGCCG-3' (position on *Bperu* 1281 ← 1300); for *Bar* 1: 5'-GAGACCAGTTGAGATTAGGCC-3' (position on *Bar* 20 → 40) and *Bar* 2: 5'-ATCGGGT-AACTGGCCTAAC-T-3' (position on *Bar* 533 ← 553). Membranes were washed in 0.2 × SSC at 65°C, and detection was with lumigen-PPD chemiluminescent substrate (Boehringer Mannheim).

## Results

### *Transient expression of anthocyanin regulatory genes*

In transient expression assays for pBC1-7 activity (containing *CI* and *B* regulatory genes), anthocyanin pigmented cells could be seen 24 h after bombardment when the scutellum cultures were kept either in the dark or in continuous light. Bombardment parameters for transformation studies were standardized on the basis of production of pigmented cells that were observed 48 h post-bombardment. Each shot produced, on an average, 70 to 80 pigmented foci per scutellum (Figure 2*a*). Anthocyanin pigmented cells were visible for up to a week, with maximum intensity on the 2nd and 3rd day post-bombardment. After one week in culture, the pigmented foci had been overgrown by the developing callus tissue.

### *Anthocyanin pigmentation in herbicide selected transgenic tissue*

To observe the pattern of anthocyanin expression in developing transgenic tissue, scutellum cultures were co-

bombarded with the selectable herbicide resistance gene (pAct1Bar) and the anthocyanin regulatory genes (pBC1-7). After 9 to 12 weeks of selection on bialaphos media in continuous darkness, putative transgenic calli were transferred to RM1-S medium and maintained in a 16 h photoperiod to induce plant regeneration. At this time anthocyanin pigmentation was never observed in the cultures. However, after exposure to light for only 48 h, pigmentation could be observed in pBC1-7 bombarded cultures. This occurred in cultures that were maintained on the embryo induction medium as well as in cultures transferred to plant regeneration medium. During the next 7 to 14 days in culture, pigmentation increased in intensity. As green shoots started developing from the embryogenic nodular callus, production of anthocyanin pigmented structures were suppressed and eventually only an occasional leaf with anthocyanin pigment or streaks of purple pigment on the leaf were observed (Figure 2*b, c*). The green shoots established and rooted in soil. Anthocyanin pigmentation was not observed during vegetative development, but unique patterns of anthocyanin pigmentation were detected in the ovary wall and in the pericarp of developing seeds which were exposed to light by removing the lemma (Figure 2*d*).

The selection protocol resulted in 4 bialaphos resistant plants from 944 bombarded embryos (overall frequency of 0.42%). These bialaphos selected *T*<sub>0</sub> plants were resistant to herbicide application and Southern analyses showed that both *bar* and anthocyanin regulatory genes were present as multiple copy insertions in high molecular weight DNA, indicating integration of transgenes, into the wheat genome (Figure 3). Earlier reports of gene integration by microprojectile bombardment technique in the hexaploid genome of wheat also showed multiple copy insertion and the bands formed were not of expected sizes indicating that multiple rearrange-

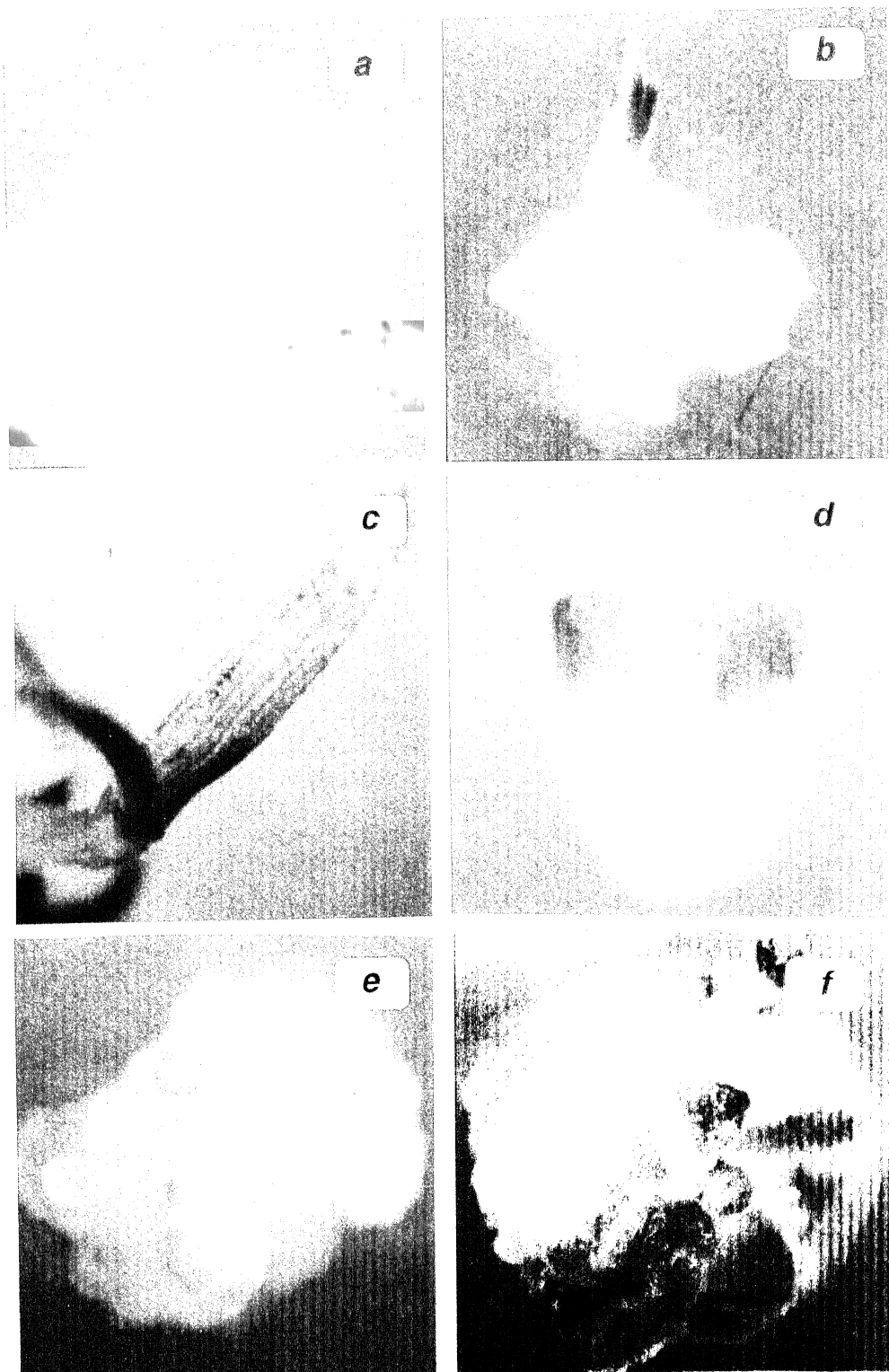


**Figure 2a-f.** Anthocyanin pigmentation following transformation with pBC1-7. *a*, Transient expression of anthocyanin in the scutellum of immature wheat embryos 48 h post-bombardment; *b-d*, Effect of light on anthocyanin production in herbicide selected embryogenic cultures after 9 weeks of selection in darkness; *b*, After 3 weeks in light green shoots with some purple colour at the base predominate ( $\times 6$ ); *c*, Purple streaks on leaf ( $\times 10$ ); *d*, Developing caryopsis, 10 days post-pollination, showing anthocyanin pigmentation in the pericarp ( $\times 3$ ); *e, f*, Anthocyanin pigmentation in non-herbicide screened embryogenic cultures after 6 weeks in dark; *e*, 4 days in light after 6 weeks in darkness ( $\times 6$ ); *f*, Same culture as *e* after 9 days of light ( $\times 4$ ).

ments have occurred to alter the size of the fragment<sup>4,5</sup>. The seeds on these plants did not develop to maturity as the embryo aborts.

#### *Anthocyanin pigmentation in non-herbicide screened tissues*

To screen pigmented transgenic tissue without imposing selection pressure, the cultures were bombarded with pBC1-7 alone. After bombardment the cultures were grown on MS2 embryo induction medium for 6 weeks in the dark. The embryogenic callus was then transferred to RM1 regeneration medium in a 16 h photoperiod. It was seen that within 48 h the putative transgenic tissue started showing purple colour and the intensity of colour increased for another 4 to 5 days. Microscopic observations were made daily for development of anthocyanin pigmentation. Observation on one such callus over a two-week period, showed pigmentation development after 48 h exposure to light and pigmented somatic embryos were observed by day 4 (Figure 2c), followed by a rapid expansion of the pigmented sector by day 9 (Figure 2f). This was arrested over the course of the next week as regenerating green shoots became predominant. Forty-six pigmented sectors were isolated from cultures established from 1024 bombarded embryos. The pigmented tissues grew relatively slowly and plants regenerated from the calli were green with occasional presence of pigments in the leaf base or streaks of purple pigment on the leaf. Five plants were regenerated from the calli and grown to maturity. At the seed development stage, the lemma was removed and variable pattern of purple colour on the developing seeds were observed again on exposure to light. The expression of anthocyanin on callus, leaf and on developing seeds was similar in both non-herbicide and herbicide selected cultures.

#### *Growth and development of isolated anthocyanin containing tissues*

Pigmented callus isolated from these cultures selected on herbicide media or those obtained by visual screening grew relatively slowly in the light and could not be maintained for more than 4 weeks. Calli which were non-pigmented, when cultured in the light grew vigorously, developed chlorophyll and prolific number of shoots. These cultures could be multiplied for several months without loss of vigour. Calli with both red and green pigmented sectors could be maintained in light for longer periods than the isolated red calli; but once the areas of anthocyanin became intense they ceased to expand, developing green shoots with the relative proportion of anthocyanin expressing callus diminished.

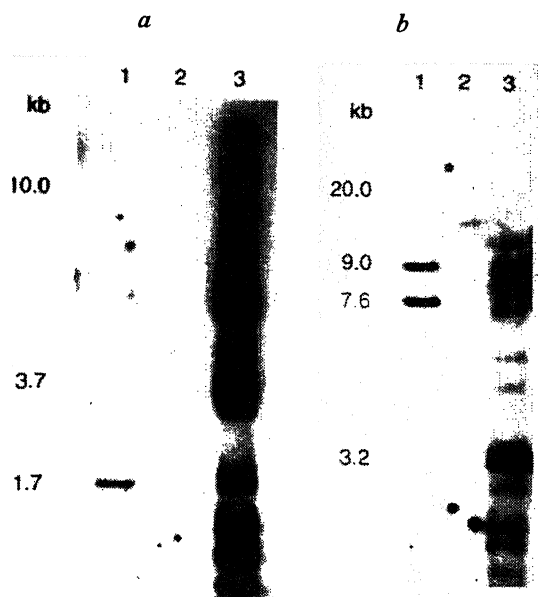


**Figure 3.** Southern blot analysis of pBC1-7 transformed wheat. *a*, Genomic DNA probed with 0.5 kb *Bar* fragment. Lane 1, positive control, pAct1*Bar* digested with *Xba*I/*Xho*I to release 1.7 kb *Bar* fragment. Lane 2, negative control, untransformed wheat DNA digested with *Xba*I/*Xho*I. Lane 3, transformed wheat DNA digested with *Xba*I/*Xho*I showing incorporation of rearranged *Bar* gene in high molecular weight genomic DNA. *b*, Genomic DNA probed with 1.1 kb *Bperu* fragment. Lane 1, positive control, maize genomic DNA digested with *Bgl*II to release 7.6 and 9.0 kb fragments of *Bperu* homologous DNA. Lane 2, negative control, untransformed wheat DNA digested with *Xba*I. Lane 3, transformed wheat DNA digested with *Xba*I showing incorporation of rearranged pBC1-7 in high molecular weight genomic DNA.

#### Discussion

Different reporter genes have been used in cereal transformation but no single gene meets all the critical requirements. The use of anthocyanin regulatory genes from maize, which control the biosynthetic pathway of anthocyanin, may however, meet some of the requirements more satisfactorily. The anthocyanin regulatory genes, *B* and *C1*, under the control of constitutive promoters (pBC1-7) induced pigmentation in wheat scutellum cultures 24 h after bombardment when cultures were incubated either in dark or light. Bombardment conditions were standardized using purple spots of anthocyanin as a visual marker for transient events because the target tissue can be studied in the same position of plating and is not moved or sacrificed. Transient expression of anthocyanin in both epiblast and scutellar tissues of wheat had been reported earlier<sup>10</sup>. But, anthocyanin pigmented cells could not be tracked after 16 days of growth, as the growth of these foci was overwhelmed by the growth of non-pigmented cells, suggesting a strong growth disadvantage for pigmented cells.

Bialaphos herbicide selected calli, which were kept in the dark never showed any anthocyanin purple pigmentation, but when transferred to light for regeneration revealed pigmentation. Dhir *et al.*<sup>11</sup> used different selectable markers in co-bombardment with anthocyanin genes and selected resistant calli, which showed occasionally anthocyanin pigment in regenerating shoots. Our experiments clearly showed that if calli are selected in dark for more than 6 weeks and subsequently brought under light regime, dark red or purple colour foci start appearing within 48 to 72 h and the whole tissue shows a purple colour.

Cell-specific expression of anthocyanin pigmentation occurs at several developmental stages in maize. In aleurone tissue, pigmentation is independent of light, but seedling pigmentation that requires either light or *P1*, a regulatory factor that determines pigmentation in the absence of light<sup>12</sup> is suppressed in darkness. This suppression of seedling pigmentation was not specific to regulation of promoter activity of the regulatory gene because in transient expression assays the induction of cell-autonomous anthocyanin pigmentation by the regulatory gene *Lc*, fused to a constitutive promoter, also responded like an endogenous gene, i.e. aleurone pigmentation was independent of *P1* or light, whereas seedling pigmentation required one of these factors<sup>9</sup>.

Regenerating shoot cultures in which anthocyanin pigmentation was suppressed were identified, but subsequently, late in development, unique patterns of pigmentation were shown to be light-induced in non-chlorophyllous tissues of the ovary and pericarp. Regenerated anthocyanin pigmented shoots could not be maintained without the cross-feeding support of numerous green shoots, some of which contained the anthocyanin transgenes but in which pigmentation might have been suppressed.

Transgenic shoots confirmed by Southern hybridization were mainly obtained following selection of cultures co-bombarded with a selectable herbicide resistance gene. Presumably in the absence of selection the transformed anthocyanin cells are at a comparative disadvantage with non-transformed cells resulting in the generation of only terminally expressing chimeric sectors. It may be possible that anthocyanin regulatory genes which result in accumulation of pigment, may also be responsible for terminating the continued development of transformed cells. There is evidence which suggests that over-expression of these trans acting factors in cereal cells can be debilitating<sup>20</sup>. Further experimental

tion is needed to find out whether the expression of anthocyanin genes was lethal.

1. Sanford, J. C., Klein, T. M., Wolf, E. D. and Allen, N., *J. Plant Sci. Technol.*, 1987, **5**, 2-7.
2. Goff, S. A., Klein, T. M., Roth, B. A., Fromm, M. E., Cone, K. C., Radicella, J. P. and Chandler, V., *EMBO J.*, 1990, **9**, 2517-2522.
3. Vasil, V., Castillo, A. M., Fromm, M. E. and Vasil, I. K., *BioTechnology*, 1992, **10**, 667-674.
4. Weeks, J. T., Anderson, O. D. and Blechl, A. E., *Plant Physiol.*, 1993, **102**, 1077-1084.
5. Becker, D., Brettschneider, R. and Lorz, H., *Plant J.*, 1994, **6**, 299-309.
6. Nehra, N. S., Chibbar, R. N., Leung, N., Caswell, K., Mallard, C., Steinhauer, L., Baga, M. and Kartha, K. K., *Plant J.*, 1994, **5**, 285-297.
7. Blechl, A. E. and Anderson, O., *Nat. Biotechnol.*, 1996, **14**, 875-879.
8. Maheshwari, N., Rajyalakshmi, K., Baweja, K., Dhir, S. K., Chowdhry, C. N. and Maheshwari, S. C., *Crit. Rev. Plant Sci.*, 1995, **14**, 147-178.
9. Ludwig, S. R., Bowen, B., Beach, L. and Wessler, S. R., *Science*, 1990, **247**, 449-450.
10. McKinnon, G. E., Abedinia, M. and Henry, R. J., *Plant Tissue Culture Biotechnol.*, 1996, **2**, 24-32.
11. Dhir, S. K., Pajean, M. E., Fromm, M. E. and Fry, J. E., in *Improvement of Cereal Quality by Genetic Engineering* (eds Henry, J. R. and Ronalds, J. A.), Plenum Press, New York, 1994, pp. 71-75.
12. Coe, E. H., Neuffer, M. G. and Hoisington, D. A., in *Corn and Corn Improvement* (eds Sprague, G. F. and Dudley, J. W.), American Society of Agronomy, Madison., 1988, pp. 81-268.
13. Murashige, T. and Skoog, F., *Physiol. Plant*, 1962, **15**, 473-497.
14. Klein, T. M., Roth, B. A. and Fromm, M. E., *Proc. Natl. Acad. Sci. USA*, 1989, **86**, 6681-6685.
15. Chandler, V. I., Radicella, J. P., Robbins, T. P., Chen, J. and Turks, D., *Plant J.*, 1989, **1**, 1175-1183.
16. Paz-Ares, J., Ghosal, D., Wienand, U., Peterson, P. and Saedler, H., *EMBO J.*, 1987, **6**, 3353-3558.
17. McElroy, D., Zhang, W., Cao, L. and Wu, R., *Plant Cell*, 1990, **2**, 163-171.
18. Junghans, H. and Metzlaiff, M., *Biotechniques*, 1990, **8**, 176.
19. Feinberg, A. P. and Vogelstein, B., *Anal. Biochem.*, 1983, **132**, 6-13.
20. McElroy, D. and Brettell, R. I. S., *Trends Biotechnol.*, 1994, **12**, 62-68.

ACKNOWLEDGEMENTS. We thank Meiji Seika Kaisha Ltd., Japan for a gift of bialaphos, Dr R. Wu, Cornell University, for providing the plasmid pActBar and Dr T. Klein, DuPont, Delaware for the plasmid pBC1-7. H. S. C. is grateful to Department of Biotechnology, Govt. of India, for fellowship assistance during this study.

Received 20 October 1998; revised accepted 2 March 1999

# Quantum signature of the classical chaos in the field-induced barrier crossing in a quartic potential\*

P. K. Chattaraj<sup>†</sup>, S. Sengupta and A. Poddar

Department of Chemistry, Indian Institute of Technology, Kharagpur 721 302, India

**The quantum domain behaviour of a classical double-well oscillator which exhibits chaos in the presence of an external monochromatic field has been studied using Bohmian mechanics. The classical Kolmogorov–Arnol'd–Moser (KAM) tori break down in the presence of an external perturbation for which the corresponding quantal phase portrait exhibits regular islands owing to the quantum suppression of the classical chaos. It has also been observed that the classical chaos generally enhances the quantum fluctuations.**

THERE has been a recent upsurge of interest in the study of the quantum dynamics of classically chaotic systems<sup>1–14</sup>. It has been shown<sup>1–14</sup> that the quantum nonclassical effects suppress the classical stochasticity. An integrable classical system or a system in the presence of a weak perturbation is characterized by invariant KAM tori. The phase space begins to appear chaotic when the amplitude of the external destabilizing field is increased<sup>15</sup>. The KAM tori in this case break down into cantori<sup>16</sup> which help in stabilizing the corresponding quantum system<sup>13,14</sup>. In order to understand these aspects better we study the quantum domain behaviour of a quartic oscillator in the presence of an external monochromatic field. This problem is considered to be important in several areas of chemical dynamics<sup>17</sup> and has been studied in detail<sup>13–15</sup> in recent years. It has been observed<sup>13,14</sup> that the classical chaos and quantum tunneling occur simultaneously in this case to give rise to the coherent oscillatory nature of the quantum diffusion between two stable KAM tori.

Quantum potential based approaches<sup>1,18–20</sup> offer a good quantum description of classically chaotic systems. In quantum fluid dynamics (QFD)<sup>18</sup>, the overall motion of the system is mapped onto the motion of a 'probability fluid' having density  $\rho(\mathbf{r}, t)$  and velocity  $\mathbf{v}(\mathbf{r}, t)$  under the influence of the external classical potential augmented by a quantum potential. The basic equations of QFD comprise an equation of continuity and an Euler-type equation of motion. It has been shown<sup>9</sup> that these equations can be written in the form of

Hamilton's equations of motion with a Hamiltonian functional properly defined for this purpose and by considering  $\rho(\mathbf{r}, t)$  and  $(-\chi(\mathbf{r}, t))$  as canonically conjugate variables, where  $\chi(\mathbf{r}, t)$  is the velocity potential. Chaotic dynamics of a quantum Hénon-Heiles oscillator has been studied<sup>9</sup> using QFD, in terms of  $\rho$  versus  $(-\chi)$  plots and time evolution of several time-dependent density functionals like Shannon entropy, density correlation and macroscopic kinetic energy. Another quantum potential-based theory is the quantum theory of motion (QTM)<sup>1</sup> in the sense of classical interpretation of quantum mechanics as developed by de Broglie<sup>19</sup> and Bohm<sup>20</sup>. In QTM<sup>1</sup>, the overall motion of a physical system is understood in terms of both wave and particle pictures. The pertinent time-dependent Schrödinger equation (TDSE) governs the wave motion. This wave guides a point particle whose motion is described in terms of forces originating from the classical as well as quantum potentials. In QTM, important insights into quantum domain chaotic dynamics are obtained<sup>10,11</sup> in terms of the phase space distance between two initially close Bohmian trajectories and the associated Kolmogorov–Sinai (KS) entropy. Quantum standard map<sup>11</sup>, Weigert's quantum cat map<sup>11</sup>, Rydberg atoms in external fields<sup>10</sup> and a quantum Hénon-Heiles oscillator<sup>10</sup> have been studied successfully using QTM. Possibility of a QTM for many-electron systems is being explored<sup>21</sup> within a quantum fluid density functional framework<sup>22</sup>.

In the present work, we apply QTM in analysing the quantum analogue of the classical domain chaotic dynamics associated with the penetration of a barrier in a double-well potential in the presence of a monochromatic external field with increasing amplitude.

The classical Hamiltonian of a double-well oscillator under the influence of an external oscillating driving force is given by:

$$\mathcal{H} = \frac{p^2}{2m} + ax^4 - bx^2 + c \cos(\omega_0 t). \quad (1)$$

For a given set of parameter values, the classical Hamilton's equations of motion can be solved<sup>13,14</sup> to generate the stroboscopic plots of various trajectories. Depending on the choice of the initial position and momentum values one may obtain stable regions in phase space bounded by KAM surfaces or a chaotic sea extended over the whole phase space.

In order to get a quantum mechanical description of this problem, the classical Hamiltonian (eq. (1)) is directly quantized and the pertinent TDSE has been written as:

$$\begin{aligned} \hat{H}\psi(x, t) &= \left[ -\frac{1}{2} \frac{d^2}{dx^2} + ax^4 - bx^2 + c \cos(\omega_0 t) \right] \psi(x, t) \\ &= i \frac{\partial \psi(x, t)}{\partial t}. \end{aligned} \quad (2)$$

\*This paper is based on a seminar talk delivered by P. K. Chattaraj at the International Conference on Nonlinear Dynamics: Integrability and Chaos, at the Centre for Nonlinear Dynamics, Bharathidasan University, Tiruchirapalli in February 1998.

<sup>†</sup>For correspondence. (email: pkcj@hijli.iitkgp.ernet.in)

## RESEARCH COMMUNICATIONS

Atomic units are used throughout unless otherwise specified. The complete description of a physical system involves both wave and particle pictures in QTM<sup>1</sup>. While the wave motion is governed by the TDSE, the motion of a point particle guided by this wave is characterized by its velocity as given by:

$$\dot{\mathbf{x}} = \nabla \chi(x, t)|_{x=x(t)}, \quad (3)$$

where  $\chi$  is the velocity potential expressed as the phase of the wavefunction in its polar form as follows:

$$\psi(x, t) = \rho^{1/2}(x, t) \exp[i\chi(x, t)]. \quad (4)$$

An assembly of initial positions will constitute an ensemble of particle motions guided by the same wave, and the probability that the particle be present between  $x$  and  $x + dx$  in this ensemble at time  $t$  is given by  $\rho(x, t)dx$ . Solution of eq. (3) with various initial positions would yield the so-called 'Bohmian trajectories'. A phase space distance function can be defined as follows<sup>10,11</sup> in order to study the quantum signature of chaos through sensitive dependence on initial conditions,

$$D(t) = \{(x_1(t) - x_2(t))^2 + (p_{x_1}(t) - p_{x_2}(t))^2\}^{1/2}, \quad (5)$$

where  $(x, p_x)$  refers to a point in phase space.

A generalized quantum Lyapunov exponent has also been defined as<sup>11</sup>:

$$\Lambda = \lim_{\substack{D(t) \rightarrow 0 \\ t \rightarrow \infty}} \frac{1}{t} \ln \left[ \frac{D(t)}{D(0)} \right]. \quad (6)$$

The corresponding KS entropy is given by<sup>11</sup>:

$$H = \sum_{\Lambda_i > 0} \Lambda_i. \quad (7)$$

Chaotic quantum dynamics is characterized by a positive KS entropy<sup>11</sup>.

The phase space volume is defined as<sup>12</sup>:

$$V_{ps}(t) = [(\langle x - \langle x \rangle \rangle^2) \langle p_x - \langle p_x \rangle \rangle^2]^{1/2}. \quad (8)$$

A sharp increase in  $V_{ps}(t)$  implies a chaotic motion<sup>10,12</sup>. This quantity is same as the associated uncertainty product which can be used as a measure of quantum fluctuations<sup>14</sup>. Classical chaos generally enhances quantum fluctuations<sup>10,12,14</sup>.

The double-well potential used in the present problem is given by:

$$V(x) = ax^4 - bx^2 + c \cos(\omega_0 t), \quad (9)$$

where the parameter values are taken as follows<sup>13</sup>:  $a = 0.5$ ,  $b = 10.0$ ,  $c = 10.0$  and  $\omega_0 = 6.07$ . Classical phase-portraits and their QTM counterparts are generated for two different initial conditions,  $(x, p_x)|_{t=0}$ , viz. (a)  $(-2.0, 0.0)$  and (b)  $(2.0, 0.0)$ . For the given set of parameter values the classical motion is regular for case (a) and chaotic for case (b) although both the cases correspond to the same value of the unperturbed energies of the double-well oscillator.

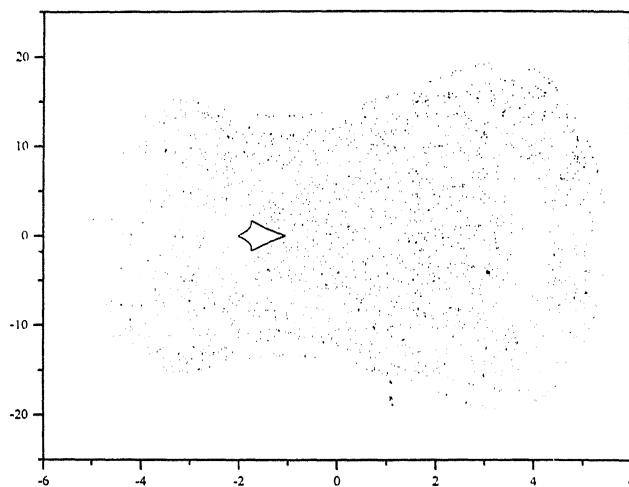


**Figure 1.** Classical phase space trajectories for a double-well oscillator in the presence of an external field with  $c = 10$  and two different initial conditions: (a)  $(x_0 = -2.0, p_0 = 0.0)$ ; (b)  $(x_0 = 2.0, p_0 = 0.0)$ .

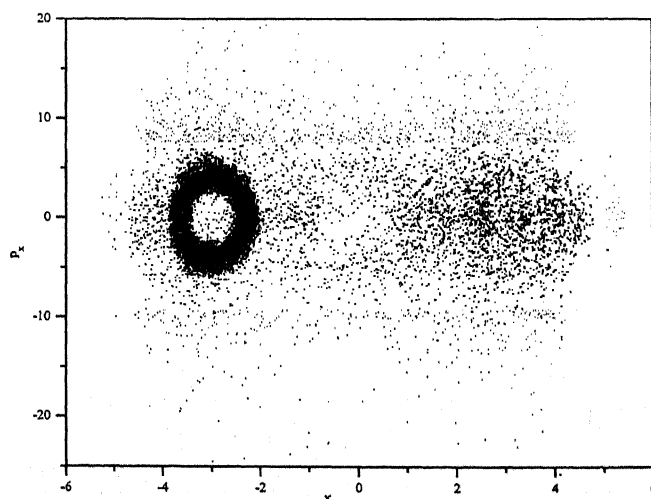


**Figure 2.** Quantal phase space trajectories for a double-well oscillator in the presence of an external field with  $c = 10$  and two different initial conditions: (a)  $(x_0 = -2.0, p_0 = 0.0)$ ; (b)  $(x_0 = 2.0, p_0 = 0.0)$ .

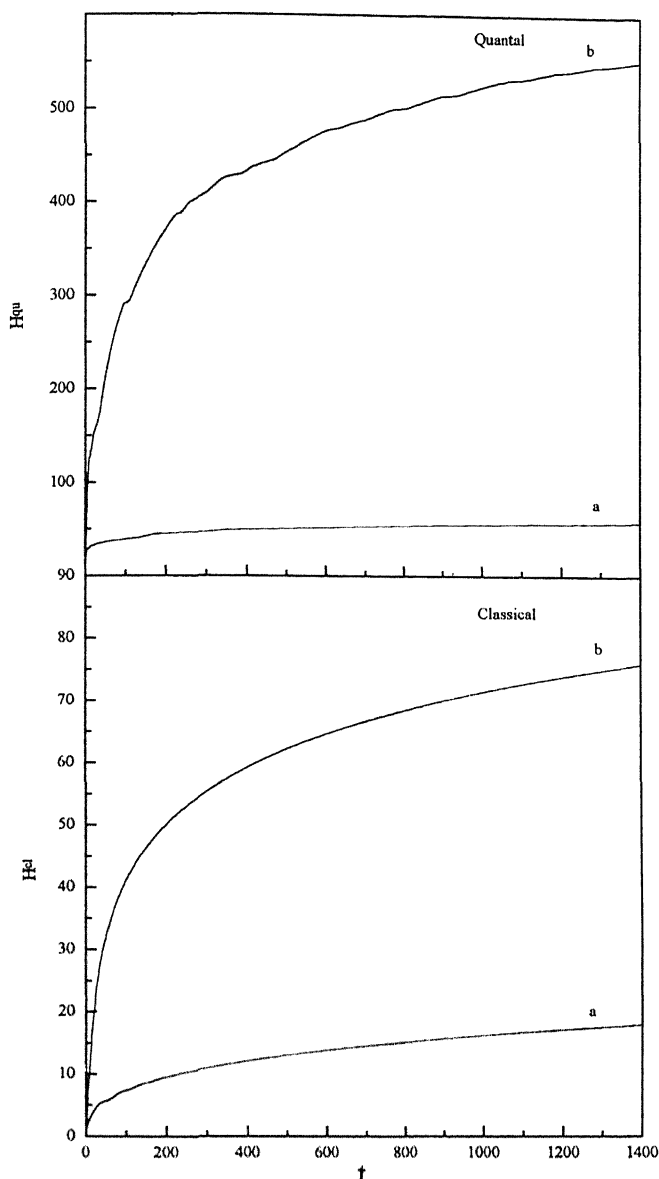


**Figure 3.** Time evolution of the KS entropy associated with the classical motion ( $H^c$ ) and quantal motion ( $H^q$ ) for a double-well oscillator in the presence of an external field with  $c = 10$  and two different initial conditions: (a) ( $x_0 = -2.0, p_0 = 0.0$ ); (b) ( $x_0 = 2.0, p_0 = 0.0$ ).

To understand the classical regular/chaotic motion associated with the field-induced barrier penetration in a quartic potential we solve the relevant classical Hamilton's equations of motion using a fourth order Runge-Kutta method. In order to study the corresponding quantum signatures we generate the respective Bohmian trajectories. For this purpose, the numerical solution is launched with the propagation of a Gaussian wavepacket under the influence of the quartic potential (eq. (9)). The details of the numerical solution are available elsewhere<sup>10,23</sup>. Mesh sizes adopted are  $\Delta x = 0.1$  and  $\Delta t = 0.02$ . Calculation is carried out for  $-15 \leq x \leq 15$  and for  $10^5$  time-steps. It may be noted that the classical phase space

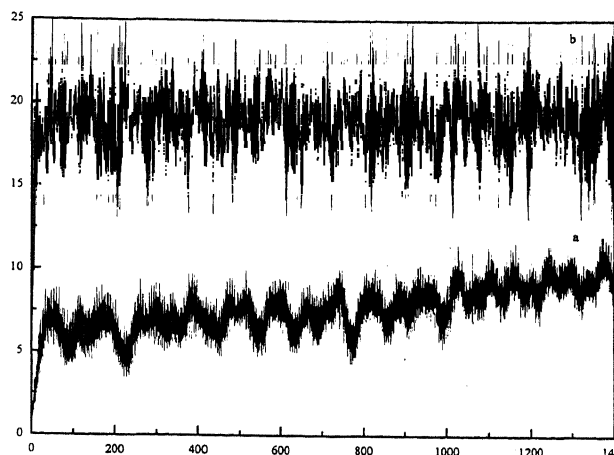


**Figure 4.** Time evolution of the phase space volume  $V_{ps}$  associated with the quantal motion for a double-well oscillator in the presence of an external field with  $c = 10$  and two different initial conditions: (a) ( $x_0 = -2.0, p_0 = 0.0$ ); (b) ( $x_0 = 2.0, p_0 = 0.0$ ).

for this problem is three-dimensional ( $x, p, t$ ) and hence possesses the minimum number of phase space degrees of freedom to exhibit the possible chaotic behaviour. However, momentum is not a 'true variable' in the case of the corresponding quantum system. In the present study, like others<sup>9-14</sup>, we are interested in the signature of the classically chaotic motion, if any, in the associated quantum dynamics.

Once we know  $\psi(x, t)$ , we can rewrite eq. (3) as:

$$\dot{x} = \nabla \chi(x, t)|_{x=x(t)} = \text{Re} \left[ -\frac{i \nabla \psi}{\psi} \right], \quad (10)$$

which has been solved with two different initial conditions (cases (a) and (b)) to obtain the Bohmian trajectories. A second-order Runge-Kutta method is used for this purpose.

In order to understand the breakdown<sup>15</sup> of KAM tori with increasing amplitude of the external field and a possible quantum suppression of the classical chaos, the calculation for case (a) is repeated for two other values of  $c$ , viz. 20, 40.

Figure 1 depicts the classical phase space trajectories (stroboscopic plots) for the double-well oscillator in the presence of an external field for two different initial conditions (cases (a) and (b)). While case (a) corresponds to a regular island, case (b) gives rise to the chaotic sea. The KAM torus is surrounded by the following phase-space points, ( $x, p_x$ ), in this case:  $(-2.00, 0.00)$ ,  $(-1.05, 0.00)$ ,  $(-1.72, -1.65)$  and  $(-1.72, 1.65)$ .

Corresponding quantal phase portraits generated through the respective Bohmian trajectories are presented in Figure 2. The quantal behaviour properly mimicks the underlying classical dynamics, viz. a regular island for case (a) and a chaotic sea for case (b). It

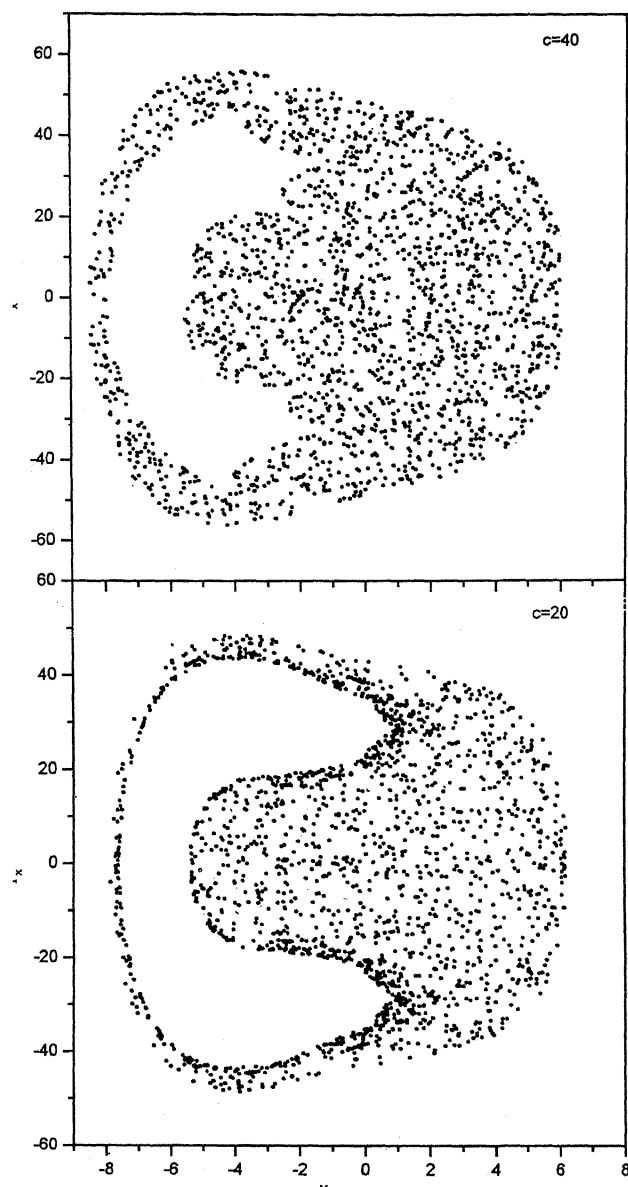


**Figure 5.** Classical phase space trajectory for a double-well oscillator in the presence of an external field with  $c = 20$  and  $c = 40$  with initial condition:  $(x_0 = -2.0, p_0 = 0.0)$ .

appears that a cantorus-like structure<sup>16</sup> is a quantum equivalent of the classical KAM torus. The cantorus is 'bounded' by the following phase-space points:  $(-3.90, 0.00)$ ,  $(-2.00, 0.00)$ ,  $(-3.00, 5.00)$  and  $(-3.00, -5.00)$ . It is important to note that although the initial conditions associated with classical regular/chaotic behaviour give rise to quantal regular/chaotic behaviour, the size and the position of the classical KAM torus are not necessarily the same as those of the quantal cantorus.

Figures 3 and 4 present respectively the classical ( $H^{cl}$ ) and quantal ( $H^{qu}$ ) KS entropies and the phase space

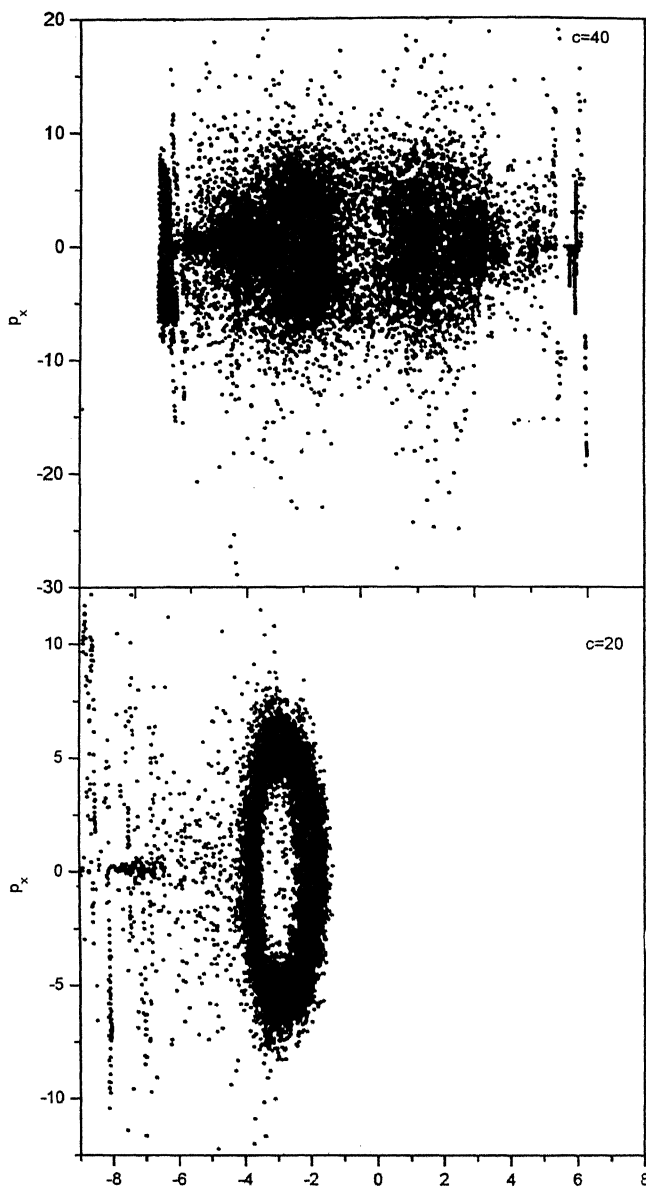


**Figure 6.** Quantal phase space trajectory for a double-well oscillator in the presence of an external field with  $c = 20$  and  $c = 40$  with initial condition:  $(x_0 = -2.0, p_0 = 0.0)$ .

volume ( $V_{ps}$ ). It may be noted that the orders of magnitude of  $H^{cl}$  and  $H^{qu}$  are not the same. It is, however, transparent in these plots that the classical stochasticity enhances quantal fluctuations.

In order to investigate the breakdown of the KAM torus<sup>15</sup> (case (a)) when the strength of the perturbation is increased as well as any possible quantum suppression<sup>1-14</sup> of the classical chaos, we study the behaviour of the double-well oscillator in the presence of the external field with two other amplitudes, viz.  $c = 20$  and  $40$ , and the same initial conditions as in case (a) which corresponds to a regular motion for  $c = 10$ .

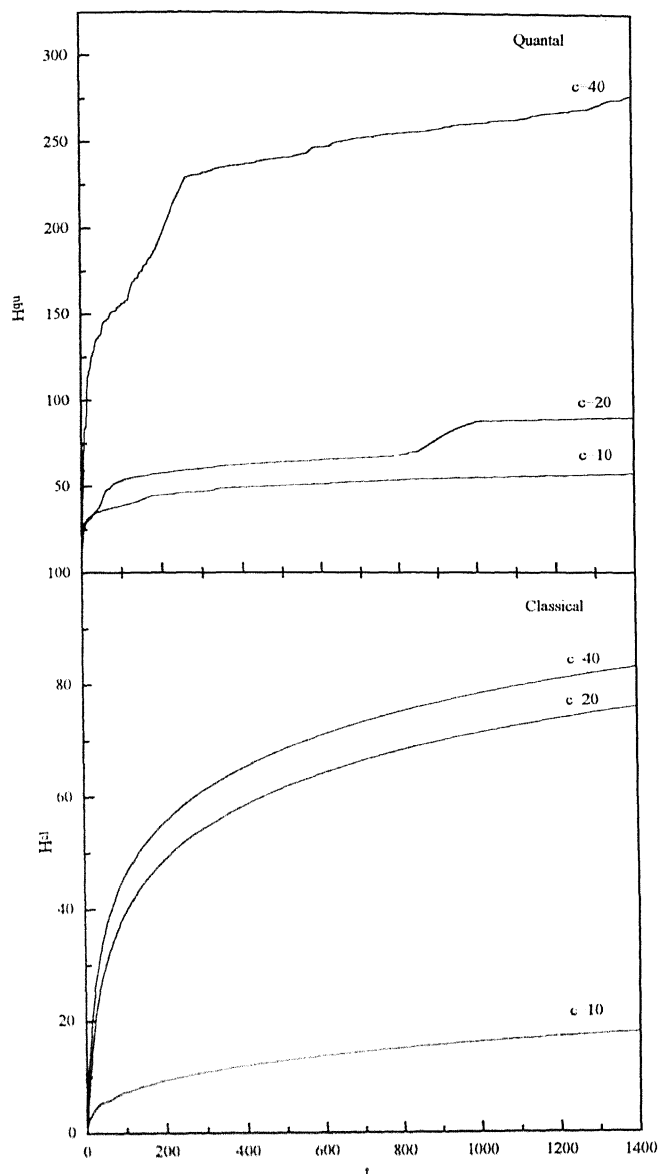


Figure 7. Time evolution of the KS entropy associated with the classical motion ( $H^I$ ) and quantal motion ( $H^{III}$ ) for a double-well oscillator in the presence of an external field with  $c = 10, 20$  and  $40$  respectively, with initial condition: ( $x_0 = -2.0, p_0 = 0.0$ ).

Figure 5 presents the stroboscopic plots of the classical trajectories for case (a) corresponding to  $c = 20$  and  $c = 40$ , respectively. It is transparent in these plots that the regular island ( $c = 10$ ) is destroyed and the phase space appears to be completely chaotic, more pronounced for the higher  $c$  value. Similar plots for the respective quantal motion are given in Figure 6. It is quite clear that a 'cantorus-like' island still persists for  $c = 20$  which, however, breaks down for  $c = 40$ . This fact provides an unmistakable signature of the quantum suppression of chaos. The size and the position of the

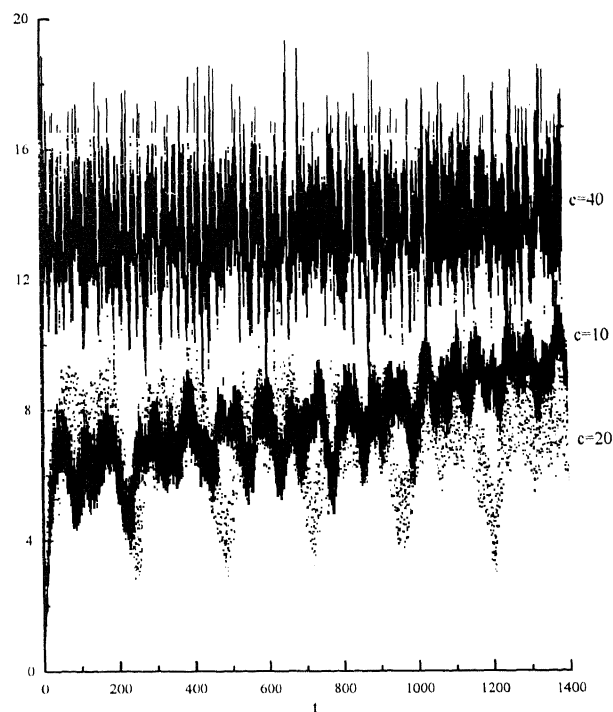


Figure 8. Time evolution of the phase space volume  $V_{ps}$  associated with the quantal motion for a double-well oscillator in the presence of an external field with  $c = 10, 20$  and  $40$  respectively, with initial condition: ( $x_0 = -2.0, p_0 = 0.0$ ).

cantorus ( $c = 20$ ) remain more or less the same as in the case of  $c = 10$ .

Figure 7 depicts  $H^{I1}$  and  $H^{III}$  while Figure 8 presents  $V_{ps}$  for the above mentioned cases. These quantities mimic all the trends and strengthen the above inference. For the classical case,  $H^{I1}$  remains small for  $c = 10$  but increases rapidly for the other two  $c$  values. For  $c = 10$  and  $20$ ,  $H^{III}$  values are relatively much smaller when compared to the corresponding value for  $c = 40$ . When the cantorus breaks down ( $c = 40$ ), very large quantum fluctuations are clearly revealed by the  $V_{ps}$  plots while the  $V_{ps}$  values are comparable for  $c = 10$  and  $20$ .

To summarize, important insights into the quantum manifestations of the classical regular and chaotic motions of a double-well oscillator in the presence of an external field with different amplitudes have been obtained in terms of the corresponding Bohmian trajectories. Two quantum systems which exhibit regular and chaotic motions respectively in the classical domain can be differentiated with the help of the quantum theory of motion. It has been demonstrated for the first time in terms of stroboscopic plots within a Bohmian mechanical framework that the classical chaos enhances the quantum fluctuations and quantum nonclassical effects suppress the classical stochasticity. The KS entropy and phase space volume support this result.

1. Holland, P. R., in *The Quantum Theory of Motion*, Cambridge University Press, Cambridge, 1993.
2. Gutzwiller, M. C., in *Chaos in Classical and Quantum Mechanics*, Springer, Berlin, 1990.
3. Eckhardt, B., *Phys. Rep.*, 1988, **163**, 205–209.
4. Jensen, R. V., *Nature*, 1992, **355**, 311–317; *ibid*, 1995, **373**, 16.
5. Casati, G., Chirikov, B. V., Shepelyansky, D. L. and Guarneri, I., *Phys. Rev. Lett.*, 1986, **57**, 823–826; Casati, G., Chirikov, B. V., Guarneri, I. and Shepelyansky, D. L., *Phys. Rep.*, 1987, **154**, 77–123; Casati, G., Chirikov, B. V., Izrailev, F. M. and Ford, J., in *Stochastic Behaviour in Classical and Quantum Hamiltonian Systems* (eds Casati, G. and Ford, J.), Springer, Berlin, 1979.
6. de Polavieja, G. G., *Phys. Rev. A*, 1996, **53**, 2059–2061; *Phys. Lett. A*, 1996, **220**, 303. Frisk, H., *Phys. Lett. A*, 1997, **227**, 139; Konkel, S. and Makowski, A. J., *Phys. Lett. A*, 1998, **238**, 95–100.
7. Berry, M. V. and Balazs, N. L., *J. Phys. A*, 1979, **12**, 625–642; Hogg, T. and Huberman, B. A., *Phys. Rev. Lett.*, 1982, **48**, 711; Grempel, D. R., Fishman, S. and Prange, R. E., *Phys. Rev. Lett.*, 1984, **53**, 1212–1216; Chang, S. and Shi, K., *Phys. Rev. Lett.*, 1985, **55**, 269–272.
8. Nakamura, K. and Lakshmanan, M., *Phys. Rev. Lett.*, 1986, **57**, 1661–1664; Nakamura, K. and Thomas, H., *Phys. Rev. Lett.*, 1988, **61**, 247–250; Nakamura, K. and Mikeska, H. J., *Phys. Rev. A*, 1987, **35**, 5294–5297; Nakamura, K., Bishop, A. R. and Shudo, A., *Phys. Rev. B*, 1989, **39**, 12422–12425.
9. Chattaraj, P. K. and Sengupta, S., *Phys. Lett. A*, 1993, **181**, 225–231; Chattaraj, P. K., *Indian J. Pure Appl. Phys.*, 1994, **32**, 101–105; Chattaraj, P. K. and Sengupta, S., *Indian J. Pure Appl. Phys.*, 1996, **34**, 518–527.
10. Sengupta, S. and Chattaraj, P. K., *Phys. Lett. A*, 1996, **215**, 119–127; Chattaraj, P. K. and Sengupta, S., *Curr. Sci.*, 1996, **71**, 134–139; Chattaraj, P. K., Sengupta, S. and Poddar, A., *Curr. Sci.*, 1998, **74**, 758–764.
11. Schwengelbeck, U. and Faisal, F. H. M., *Phys. Lett. A*, 1995, **199**, 281–286; Faisal, F. H. M. and Schwengelbeck, U., *Phys. Lett. A*, 1995, **207**, 31–36.
12. Feit, M. D. and Fleck, Jr. J. A., *J. Chem. Phys.*, 1984, **80**, 2578–2584.
13. Lin, W. A. and Ballentine, L. E., *Phys. Rev. Lett.*, 1990, **65**, 2927–2928.
14. Graham, R. and Hohnerbach, H., *Phys. Rev. A*, 1991, **43**, 3966–3981; *Phys. Rev. Lett.*, 1990, **64**, 637–640; Chaudhuri, S., Gangopadhyay, G. and Ray, D. S., *Indian J. Phys. B*, 1995, **69**, 507–523.
15. Reichl, L. E. and Zhang, W. M., *Phys. Rev. A*, 1984, **29**, 2186–2193.
16. McKay, R. S. and Meiss, J. D., *Phys. Rev. A*, 1988, **37**, 4702–4706; Hanson, J. D., Cary, J. R. and Meiss, J. D., *J. Stat. Phys.*, 1985, **39**, 327–345; Meiss, J. D., *Parti. Accel.*, 1986, **19**, 9.
17. Hanggi, P., in *Activated Barrier Crossing* (eds Fleming, G. R. and Hanggi, P.), World Scientific, Singapore, 1993.
18. Madelung, E., *Z. Phys.*, 1926, **40**, 322–326; Deb, B. M. and Ghosh, S. K., *J. Chem. Phys.*, 1982, **77**, 342–348; Bartolotti, L. J., *Phys. Rev. A*, 1982, **26**, 2243–2244.
19. de Broglie, L., *C.R. Acad. Sci.*, 1926, **183**, 447–448; *ibid*, 1927, **184**, 273–274; *ibid*, 1927, **185**, 380–382.
20. Bohm, D., *Phys. Rev.*, 1952, **85**, 166–179, 180–193; in *Causality and Chance in Modern Physics*, Routledge and Keegan Paul, London, 1957.
21. Chattaraj, P. K., Sengupta, S. and Poddar, A., *Int. J. Quantum Chem., DFT Special Issue*, 1998, **69**, 279–291; in *Nonlinear Dynamics and Computational Physics* (ed. Sheory, V. B.), Narosa, New Delhi, 1999, pp. 45–53.
22. Deb, B. M. and Chattaraj, P. K., *Phys. Rev. A*, 1989, **39**, 1696–1712.
23. Goldberg, A., Schey, H. M. and Schwartz, J. L., *Am. J. Phys.*, 1967, **35**, 177–186; *ibid*, 1968, **36**, 454–455; Galbraith, I., Ching, Y. S. and Abraham, E., *Am. J. Phys.*, 1984, **52**, 60–68.

ACKNOWLEDGEMENT. This article is dedicated to Prof. M. Lakshmanan on his 50th birthday. We thank CSIR, New Delhi for financial assistance. We are grateful to the referee for constructive criticism.

Received 28 December 1998; revised accepted 10 March 1999

## Multicomponent coordinated defence response of rice to *Rhizoctonia solani* causing sheath blight

S. Bera and R. P. Purkayastha

Department of Botany, University of Calcutta, Calcutta 700 019, India

An excellent multicomponent coordinated defence response of rice plants (cv. IET-2233) to fungal attack has been demonstrated and a plausible relationship among them has been proposed. Some selected defence components such as momilactone 'A' (a rice phytoalexin),  $\beta$ -1,3-glucanases and exo chitinases (both pathogenesis related (PR)-proteins) and an enzyme phenylalanine ammonia lyase (PAL) were employed as biochemical parameters for evaluating the degree of response of rice plants to *Rhizoctonia solani* Kühn, a fungus causing sheath blight disease. A systemic fungicide kitazin which reduced disease significantly also concomitantly activated biosynthesis of momilactone A, induced PR-proteins and increased PAL activity in rice. Treatment of rice leaf sheaths with a PR-protein inhibitor (kinetin + NAA) increased disease markedly but inhibited  $\beta$ -1,3-glucanases and exo-chitinase activities in treated plants. Similarly, amino oxyacetic acid (AOA), a PAL inhibitor also enhanced disease intensity and inhibited PAL activity in treated, inoculated plants. Results confirm the coordinated function of various defence components in rice following infection by *Rhizoctonia* and also after abiotic induction of resistance.

USUALLY a plant responds to a pathogen by mobilizing a complex network of active defence mechanisms. The success of the plant in warding-off the pathogenic attack depends upon the coordination among the different defence strategies and the rapidity of the response. It is generally believed that plants defend themselves against pathogenic fungi by producing fungitoxic substances such as phytoalexins, pathogenesis related (PR)-

proteins, oxidized phenols and several other components. But in most cases the role of a single defence component has been reported at a time while working on disease resistance of a host-pathogen system. Hence, an attempt has been made to determine whether a multi-component coordinated mechanism is operative in disease resistance of rice with special reference to sheath blight. Initially, the amount of production/accumulation of rice phytoalexin (momilactone 'A'), PR-proteins and phenylalanine ammonia lyase (PAL) activity in non-infected and *Rhizoctonia solani*-infected rice plants were measured under similar conditions. PAL is important since it is associated with the production of fungitoxic phenolics and some phytoalexins (PA). The activities of defence components (PA, PR-proteins and PAL) were also reassessed after chemical induction and suppression of constitutive resistance in order to demonstrate their coordinated functions. In this communication we have shown the probable relationship among PA, PR-proteins, PAL and disease resistance of rice on the basis of our experimental results.

Rice grains (*Oryza sativa* L. cv. IET-2233) were disinfected, and germinated on moist filter paper in sterilized Petri dishes. Ten days after germination, the seedlings were transplanted to pots (25 cm diam.) containing non-infested soil. Two-month-old plants were inoculated by inserting sclerotia (10-day-old) of *Rhizoctonia solani* in the 2nd leaf sheaths (from the top) of the plants (one/leaf sheath) and covered with moist polythene bags for 48 h to provide adequate humidity at the initial stage of infection. Disease intensity was assessed following the method of Bera and Purkayastha<sup>1</sup>.

Rice phytoalexin momilactone 'A' was extracted and quantified following the method described by Li *et al.*<sup>2</sup>. The infected portions of rice leaf sheaths were boiled in 70% methanol for 3 min. The methanolic extract was evaporated to aqueous phase in a vacuum evaporator at 40°C. The aqueous fraction was extracted with diethyl ether. The ether fraction was evaporated to dryness in a vacuum evaporator and the residue was dissolved in methanol. The methanolic fraction was added to distilled water and applied on a Bond Elut C-18 column and eluted with 80% methanol. The eluate (80% methanolic fraction) was collected, evaporated to dryness at 60°C and dissolved in 0.1 ml methanol (HPLC grade).

Momilactone 'A' content was estimated by a Shimadzu QP<sub>1000</sub> GC-MS-SIM (fitted with a column J & W Scientific DB-5, inner diameter of 0.25 mm with linear He (helium) flow at the rate of 20 ml/min; the column temperature was raised from 250°C to 300°C at the rate of 10°C/min and kept at 300°C for 5 min). A standard solution of momilactone 'A' (2 µl of 100 µg ml<sup>-1</sup> solution) was used as reference.

The leaf sheath tissue (1 g fresh wt) of rice was homogenized with 1 ml of 0.1 M sodium citrate buffer (pH 5.0). The buffer extracts were centrifuged at 9600 g for

20 min at 4°C and the supernatant used for analysis by polyacrylamide gel electrophoresis<sup>3</sup>. Protein extracts were concentrated by using lyophilizer and adjusted to 3 mg ml<sup>-1</sup> following Lowry *et al.*<sup>4</sup> and bovine serum albumin (BSA) as a standard.

SDS-PAGE was carried out according to Laemmli<sup>5</sup> using a 12.5% acrylamide separating gel. The gels were stained overnight with 0.03% coomassie brilliant blue and destained in a methanol:acetic acid:water (40:20:50 v/v) mixture.

The leaf sheath tissue (1 g fresh wt) was homogenized in a prechilled mortar pestle with an appropriate homogenizing buffer (1 ml g<sup>-1</sup>). The homogenate was clarified by centrifugation at 9600 g for 20 min at 4°C. The resultant extracts were used for enzyme assays. Protein contents were measured following the method of Lowry *et al.*<sup>4</sup>.

β-1,3-glucanase was extracted with sodium citrate buffer (0.1 M, pH 5.0) and assayed colorimetrically by measuring the rate of reducing sugar production from laminarin<sup>6</sup>. The assay mixture (12.5 g laminarin in 2.5 ml of 50 mM sodium citrate buffer, pH 5.0) was preincubated for 10 min at 37°C. Subsequently, 20 µl enzyme was added to the assay mixture and incubated for 0, 5, 10 and 15 min. Finally, 0.5 ml aliquot in each case was taken from the assay mixture and mixed with 0.5 ml of Somogyi<sup>7</sup> reagent and the mixture was heated at 100°C for 15 min under water-saturated air. After cooling, 0.5 ml of Nelson's chromogenic reagent<sup>8</sup> was added to 3.5 ml water and absorbance measured at 660 nm. Glucose standards and appropriate controls were included. The glucanase activity nanokatal (nkat) was defined as the enzyme catalysing the formation of 1 nmol glucose equivalent sec<sup>-1</sup>.

Exo-chitinase activity was assayed colorimetrically following the method of Boller *et al.*<sup>9</sup>. The reaction mixture (0.5 ml enzyme, 1 mg colloidal chitin, 0.3 µmol sodium azide and 14 µmol sodium citrate buffer (pH 4.5)) was incubated at 37°C for 4 h. After incubation, 0.1 ml sodium borate buffer (0.8 M, pH 9.1) was added and the mixture was centrifuged at 1000 g for 15 min. *N*-acetyl glucosamine (Glc NAc) was estimated colorimetrically using 0.5 ml supernatant<sup>10</sup>. Standards of

Table 1. Effect of *Rhizoctonia* infection on momilactone 'A' production

| Incubation period (h) | DI/plant | Momilactone 'A' (µg g <sup>-1</sup> fresh wt) |
|-----------------------|----------|---|
| 24                    | 0.15     | 5.83  |
| 48                    | 0.35     | 10.09   |
| 72                    | 0.45     | 8.06  |
| 96                    | 0.78     | 3.74  |

Age of the plant 60 days at the time of inoculation.

No phytoalexin was detected in healthy non-infected leaf sheaths.

DI, Disease index.

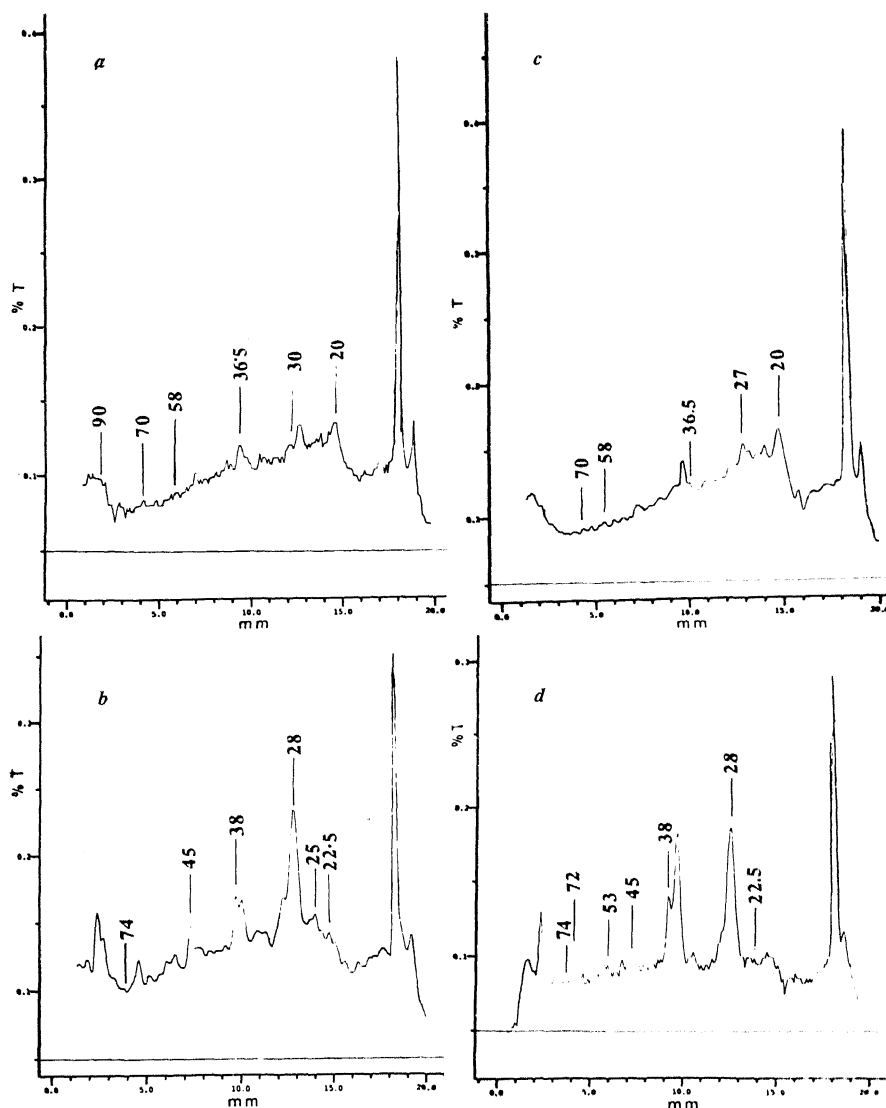


**Figure 1.** Densitometric scanning of SDS-PAGE showing profiles of defence-related proteins in rice leaf sheaths. *a*, Untreated non-inoculated; *b*, Untreated inoculated; *c*, Kitazin-treated non-inoculated; *d*, Kitazin-treated inoculated.

Glc NAc and appropriate blanks (enzyme, substrate) were also maintained. The enzyme activity nkat was defined as the amount of enzyme producing 1 nmol sec<sup>-1</sup> Glc NAc equivalent.

In the case of PAL, the extract was prepared by grinding rice leaf sheath in 50 mM Tris-HCl buffer (pH 8.6) containing 10 mM ascorbic acid (1 ml g<sup>-1</sup> fresh wt). The homogenate was filtered through a cloth, centrifuged at 20,000 g for 20 min at 4°C and the supernatant dialysed against 50 mM Tris-HCl buffer (pH 8.6) for overnight at 4°C.

The PAL activity in 1 ml dialysate (containing 3 mg ml<sup>-1</sup> protein) was assayed spectrophotometrically after adding 1 ml of 30 mM L-phenylalanine dissolved

in 50 mM Tris-HCl (pH 8.6). Absorbance at 290 nm was recorded after 2 h of incubation at 30°C against a control of 10 mM D-phenylalanine<sup>11</sup>. Enzyme activity was expressed as  $\mu\text{M}$  cinnamic acid mg<sup>-1</sup> protein min<sup>-1</sup>.

Leaf sheaths of 60-day-old plants were inoculated, incubated and momilactone 'A' was extracted. Results (Table 1) revealed that *Rhizoctonia*-infected leaf sheaths produced 10.09  $\mu\text{g}$  momilactone 'A' g<sup>-1</sup> (fresh wt) leaf sheaths while no momilactone 'A' was detected in non-inoculated (control) leaf sheaths.

PR-proteins were also extracted from *Rhizoctonia*-infected rice leaf sheaths following the standard method. The details of the extraction, isolation, identification and characterization of the PR-proteins have been

**Table 2.** Effect of *Rhizoctonia* infection and kitazin treatment on sheath blight disease development, glucanase and exo-chitinase activities

| Treatment       | Incubation period (h) | DI/plant <sup>a</sup> | -1,3-glucanase activity <sup>b</sup> | Correlation coefficient (r)          | Exo-chitinase activity <sup>b</sup> | Correlation coefficient (r)         |
|-----------------|-----------------------|-----------------------|--------------------------------------|--------------------------------------|-------------------------------------|-------------------------------------|
| Untreated       |                       |                       |                                      |                                      |                                     |                                     |
| Non-inoculated  | 0                     | 0                     | 0.539                                | <i>r</i> = 0.014 <sup>NC</sup>       | 0.091                               | <i>r</i> = 0.75 <sup>NS</sup>       |
|                 | 24                    | 0                     | 0.235                                |                                      | 0.112                               |                                     |
|                 | 48                    | 0                     | 0.683                                |                                      | 0.115                               |                                     |
|                 | 72                    | 0                     | 0.475                                |                                      | 0.115                               |                                     |
|                 | 96                    | 0                     | 0.477                                |                                      | 0.112                               |                                     |
|                 | 120                   | 0                     | 0.443                                |                                      | 0.119                               |                                     |
| Inoculated      | 24                    | 0.23                  | 3.387                                | <i>r</i> = 0.997<br><i>P</i> < 0.001 | 0.246                               | <i>r</i> = 0.988<br><i>P</i> < 0.01 |
|                 | 48                    | 0.43                  | 4.320                                |                                      | 0.336                               |                                     |
|                 | 72                    | 0.60                  | 5.836                                |                                      | 0.543                               |                                     |
|                 | 96                    | 1.08                  | 7.349                                |                                      | 0.627                               |                                     |
|                 | 120                   | 1.73                  | 8.580                                |                                      | 0.729                               |                                     |
| Kitazin-treated |                       |                       |                                      |                                      |                                     |                                     |
| Non-inoculated  | 24                    | 0                     | 4.526                                | <i>r</i> = 0.983<br><i>P</i> < 0.01  | 0.279                               | <i>r</i> = 0.965<br><i>P</i> < 0.01 |
|                 | 48                    | 0                     | 5.664                                |                                      | 0.367                               |                                     |
|                 | 72                    | 0                     | 7.345                                |                                      | 0.474                               |                                     |
|                 | 96                    | 0                     | 7.575                                |                                      | 0.462                               |                                     |
|                 | 120                   | 0                     | 9.391                                |                                      | 0.582                               |                                     |
| Inoculated      | 24                    | 0.08                  | 10.573                               | <i>r</i> = 0.988<br><i>P</i> < 0.01  | 0.504                               | <i>r</i> = 0.986<br><i>P</i> < 0.01 |
|                 | 48                    | 0.15                  | 12.259                               |                                      | 0.706                               |                                     |
|                 | 72                    | 0.20                  | 14.303                               |                                      | 0.909                               |                                     |
|                 | 96                    | 0.35                  | 15.494                               |                                      | 0.960                               |                                     |
|                 | 120                   | 0.55                  | 16.336                               |                                      | 1.153                               |                                     |

<sup>a</sup>Average of 10 plants/treatment.

Age of the plant 60 days at the time of inoculation.

<sup>b</sup>nkat mg<sup>-1</sup> protein sec<sup>-1</sup>; 3 replicates/treatment.NS, not significant ( $P > 0.05$ ); NC, not correlated.

published earlier<sup>12</sup>. Comparison of the protein profiles of healthy and infected leaf sheaths (Figure 1a, b) revealed that inoculated leaf sheaths produced more protein bands (16) than their corresponding non-inoculated leaf sheaths (11 bands).  $\beta$ -1,3-glucanases (known PR-protein, involved in defence reactions of plants) were extracted from the inoculated and non-inoculated rice leaf sheaths. The activity of  $\beta$ -1,3-glucanase was lower (Table 2) in untreated, non-inoculated leaf sheaths than in *Rhizoctonia*-infected leaf sheaths. Approximately 19-fold increase in glucanase activity was observed over the untreated non-inoculated control after 120 h of inoculation. Chitinase (exo-form) activity was relatively low in the untreated, non-inoculated control leaf sheaths, which however, increased 2-fold within 24 h after inoculation and the same activity increased with time up to 120 h (Table 2).

PAL activity of untreated and non-inoculated leaf sheaths was measured after 12, 24, 48, 72 and 96 h of inoculation. A 5-fold increase in PAL activity was observed in inoculated leaf sheaths after 24 h of inoculation (Table 3), which decreased with increase in incubation time.

Fiftysix-day-old plants were sprayed twice at an interval of 2 days separately with different concentrations of kitazin (25 and 480  $\mu\text{g ml}^{-1}$ ). Kitazin (480  $\mu\text{g ml}^{-1}$ ) was effective (72, 69, 65 and 46% reduction in disease index (DI)/plant after 7, 12, 21 and 28 days, respectively) in controlling sheath blight disease significantly (Figure 2f). It also induced maximum (14.58  $\mu\text{g g}^{-1}$ ) and minimum (5.85  $\mu\text{g g}^{-1}$ ) amount of momilactone 'A' in inoculated and non-inoculated leaf sheaths respectively (Table 4).

Kitazin-treated, inoculated leaf sheaths showed greater number of PR-proteins compared to non-inoculated kitazin treated leaf sheaths (Figure 1c, d). Time course study also confirmed that  $\beta$ -1,3-glucanase activity was higher in kitazin-treated inoculated leaf sheaths than in kitazin-treated non-inoculated ones (Table 2). Exo-chitinase activity was also relatively lower in kitazin-treated non-inoculated leaf sheaths than in kitazin-treated inoculated leaf sheaths (Table 2). Kitazin enhanced PAL activity more in treated inoculated plants than in untreated, non-inoculated control (Table 3).

## RESEARCH COMMUNICATIONS

**Table 3.** Effect of *Rhizoctonia* infection and kitazin treatment on disease development and PAL activity

| Treatment       | Incubation period (h) | DI/plant <sup>a</sup> | Specificity activity <sup>b</sup><br>( $\mu\text{mol cin mg}^{-1}$<br>protein $\text{min}^{-1}$ ) |
|-----------------|-----------------------|-----------------------|---|
| Untreated       |                       |                       |   |
| Non-inoculated  | 0                     | 0                     | 0.38  |
|                 | 12                    | 0                     | 0.40  |
|                 | 24                    | 0                     | 0.38  |
|                 | 48                    | 0                     | 0.36  |
|                 | 72                    | 0                     | 0.39  |
|                 | 96                    | 0                     | 0.46  |
| Inoculated      | 12                    | 0                     | 1.49  |
|                 | 24                    | 0.25                  | 2.03  |
|                 | 48                    | 0.81                  | 1.25  |
|                 | 72                    | 0.92                  | 0.99  |
|                 | 96                    | 1.38                  | 0.77  |
| Kitazin-treated |                       |                       |   |
| Non-inoculated  | 12                    | 0                     | 1.49  |
|                 | 24                    | 0                     | 1.71  |
|                 | 48                    | 0                     | 1.23  |
|                 | 72                    | 0                     | 1.06  |
|                 | 96                    | 0                     | 0.77  |
| Inoculated      | 12                    | 0                     | 2.46  |
|                 | 24                    | 0.10                  | 2.70  |
|                 | 48                    | 0.17                  | 2.32  |
|                 | 72                    | 0.25                  | 1.98  |
|                 | 96                    | 0.48                  | 1.52  |

<sup>a</sup>Average of 12 plants/treatment.

Age of plants 60 days at the time of inoculation.

<sup>b</sup>3 replicates/treatment.

Leaves of 56-day-old rice plants were sprayed twice at an interval of 2 days with a mixture of Kinetin + NAA (1:7.6), a PR-protein inhibitor and inoculated as stated earlier. Healthy, treated and inoculated leaf sheaths were collected after 24, 48, 72 and 96 h, DI/plant was calculated,  $\beta$ -1,3-glucanase and exo-chitinase activities were measured. Although NAA and NAA + kinetin treatment increased sheath blight disease (Figure 2 c), there was no marked change in DI for kinetin-treated plants (Table 5).  $\beta$ -1,3-glucanase activity also increased significantly after inoculation in all cases, except NAA + kinetin-treated leaf sheaths where no significant difference in glucanase activity was observed before and after inoculation. The activity slowly decreased in NAA + kinetin-treated, non-inoculated plants with time up to 96 h of incubation.

The results showed that PAL activity increased after inoculation as well as kitazin treatment and that disease intensity decreased in kitazin-treated plants. This suggests that PAL may play a role in the reduction of disease. Hence, an attempt was made to ascertain whether suppression of PAL could alter the disease reaction in rice leaf sheaths. The plants (56-day-old) were sprayed with AOA (amino oxyacetic acid,  $500 \mu\text{g ml}^{-1}$ ) twice at an interval of 48 h and inoculated after another 48 h.

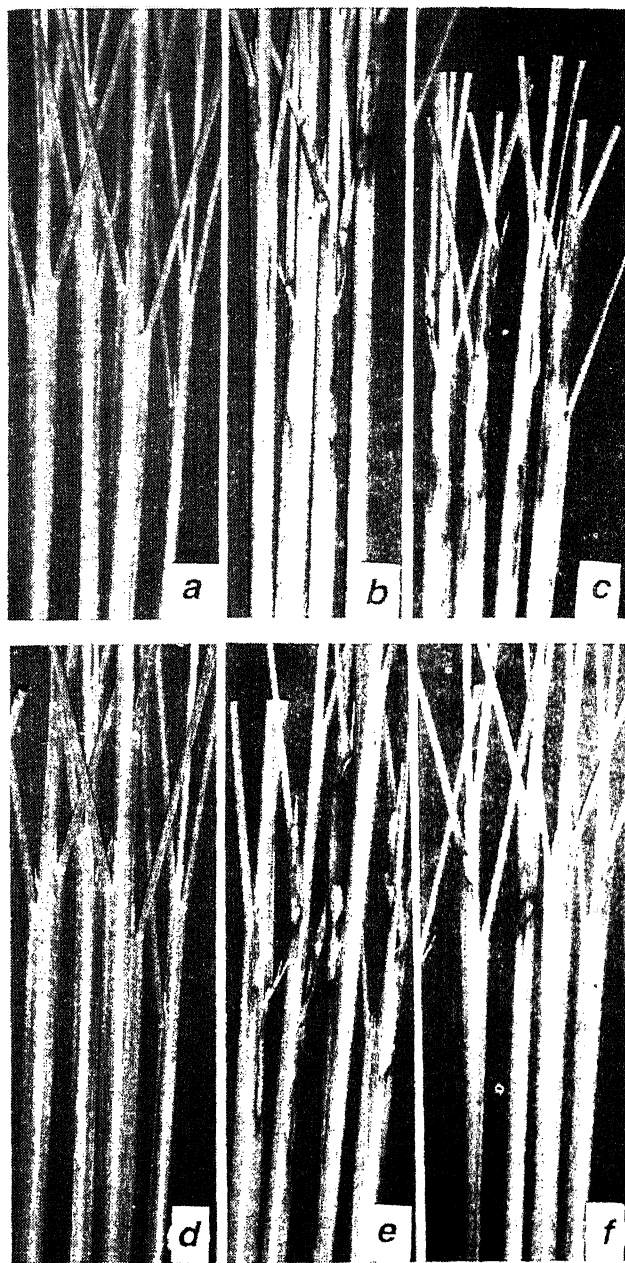


**Figure 2.** Inducer and inhibitor of PR-proteins affecting development of sheath blight of rice. a, d, Untreated non-inoculated leaf sheaths; b, e, Untreated inoculated leaf sheaths; c, Inhibitor (kinetin + NAA)-treated inoculated leaf sheaths showing increase in disease intensity; f, Inducer (kitazin)-treated inoculated leaf sheaths showing reduction in disease intensity (restricted lesions only).

Healthy untreated, healthy treated, untreated inoculated and treated inoculated leaf sheaths were collected and DI/plant and PAL activity were measured (Table 6). AOA treatment enhanced disease and also reduced PAL expression. However, the enzyme activity was relatively higher in inoculated than in non-inoculated leaf sheaths.

**Table 4.** Effect of kitazin on the production of momilactone 'A'

| Treatment       | Momilactone A*<br>( $\mu\text{g g}^{-1}$ fresh wt) |
|-----------------|--|
| Untreated       |  |
| Non-inoculated  | 0  |
| Inoculated      | 10.7   |
| Kitazin-treated |  |
| Non-inoculated  | 5.85   |
| Inoculated      | 14.58  |

\*48 h after inoculation.

PAL activity and incubation time showed negative correlation for all combinations excepting for untreated non-inoculated leaf sheaths. Results strongly support the involvement of PAL in disease reaction in rice.

Any drastic change in the basic physiology of a plant could influence the development of a disease. In the present communication multicomponent coordinated defence response of rice plants to *Rhizoctonia* infection has been reported for the first time. At the outset, pathogenicity of *R. solani* was tested on 6 rice cultivars of which IET-2233 was the most susceptible and hence an

**Table 5.** Effect of PR-protein inhibitor (NAA + kinetin) on  $\beta$ -1,3-glucanase and exo-chitinase activities

| Treatment             | Incubation period (h) | DI/plant <sup>a</sup> | $\beta$ -1,3-glucanase activity <sup>b</sup> | Correlation coefficient ( <i>r</i> ) | Exo-chitinase activity <sup>b</sup> | Correlation coefficient ( <i>r</i> ) |
|-----------------------|-----------------------|-----------------------|--|--------------------------------------|-------------------------------------|--------------------------------------|
| Untreated             |                       |                       |  |                                      |                                     |                                      |
| Non-inoculated        | 0                     | 0                     | 0.605  | <i>r</i> = 0.503 <sup>NS</sup>       | 0.081                               | <i>r</i> = 0.17 <sup>NC</sup>        |
|                       | 24                    | 0                     | 0.669  |                                      | 0.112                               |                                      |
|                       | 48                    | 0                     | 0.624  |                                      | 0.111                               |                                      |
|                       | 72                    | 0                     | 0.774  |                                      | 0.081                               |                                      |
|                       | 96                    | 0                     | 0.657  |                                      | 0.088                               |                                      |
| Inoculated            | 24                    | 0.15                  | 2.901  | <i>r</i> = 0.981<br><i>P</i> < 0.05  | 0.445                               | <i>r</i> = 0.865 <sup>NS</sup>       |
|                       | 48                    | 0.40                  | 3.973  |                                      | 0.529                               |                                      |
|                       | 72                    | 0.58                  | 4.868  |                                      | 0.552                               |                                      |
|                       | 96                    | 1.17                  | 6.532  |                                      | 0.550                               |                                      |
| Kinetin-treated       |                       |                       |  |                                      |                                     |                                      |
| Non-inoculated        | 24                    | 0                     | 0.661  | <i>r</i> = 0.157 <sup>NC</sup>       | 0.089                               | <i>r</i> = 0.809 <sup>NS</sup>       |
|                       | 48                    | 0                     | 0.785  |                                      | 0.098                               |                                      |
|                       | 72                    | 0                     | 0.716  |                                      | 0.093                               |                                      |
|                       | 96                    | 0                     | 0.660  |                                      | 0.139                               |                                      |
| Inoculated            | 24                    | 0.21                  | 2.624  | <i>r</i> = 0.886 <sup>NS</sup>       | 0.304                               | <i>r</i> = 0.830 <sup>NS</sup>       |
|                       | 48                    | 0.42                  | 3.877  |                                      | 0.293                               |                                      |
|                       | 72                    | 0.69                  | 4.264  |                                      | 0.320                               |                                      |
|                       | 96                    | 1.33                  | 4.281  |                                      | 0.425                               |                                      |
| NAA-treated           |                       |                       |  |                                      |                                     |                                      |
| Non-inoculated        | 24                    | 0                     | 0.677  | <i>r</i> = -0.948 <sup>NS</sup>      | 0.082                               | <i>r</i> = 0.124 <sup>NC</sup>       |
|                       | 48                    | 0                     | 0.677  |                                      | 0.082                               |                                      |
|                       | 72                    | 0                     | 0.595  |                                      | 0.069                               |                                      |
|                       | 96                    | 0                     | 0.545  |                                      | 0.089                               |                                      |
| Inoculated            | 24                    | 0.21                  | 2.490  | <i>r</i> = 0.986<br><i>P</i> < 0.05  | 0.237                               | <i>r</i> = 0.720 <sup>NS</sup>       |
|                       | 48                    | 0.50                  | 2.943  |                                      | 0.372                               |                                      |
|                       | 72                    | 0.79                  | 3.986  |                                      | 0.359                               |                                      |
|                       | 96                    | 1.25                  | 4.445  |                                      | 0.359                               |                                      |
| NAA + kinetin-treated |                       |                       |  |                                      |                                     |                                      |
| Non-inoculated        | 24                    | 0                     | 0.535  | <i>r</i> = -0.973<br><i>P</i> < 0.05 | 0.037                               | <i>r</i> = -0.246 <sup>NC</sup>      |
|                       | 48                    | 0                     | 0.413  |                                      | 0.088                               |                                      |
|                       | 72                    | 0                     | 0.376  |                                      | 0.057                               |                                      |
|                       | 96                    | 0                     | 0.207  |                                      | 0.031                               |                                      |
| Inoculated            | 24                    | 0.35                  | 0.629  | <i>r</i> = -0.982<br><i>P</i> < 0.05 | 0.075                               | <i>r</i> = 0.507 <sup>NS</sup>       |
|                       | 48                    | 0.69                  | 0.541  |                                      | 0.044                               |                                      |
|                       | 72                    | 1.20                  | 0.488  |                                      | 0.101                               |                                      |
|                       | 96                    | 2.21                  | 0.450  |                                      | 0.088                               |                                      |

<sup>a</sup>Average of 12 plants/treatment.

Age of the plant 60 days at the time of inoculation.

<sup>b</sup>nkat  $\text{mg}^{-1}$  protein  $\text{sec}^{-1}$ ; 3 replicates/treatment.NS, not significant ( $P > 0.05$ ); NC, not correlated.

## RESEARCH COMMUNICATIONS

**Table 6.** Effect of amino oxyacetic acid on disease development and PAL activity

| Treatment                     | Inocubation period (h) | DI/ plant <sup>a</sup> | Specific activity <sup>b</sup> | Correlation coefficient (r)    |
|-------------------------------|------------------------|------------------------|--------------------------------|--------------------------------|
| Untreated                     |                        |                        |                                |                                |
| Non-inoculated                | 0                      | 0                      | 0.26                           | $r = 0.65^{\text{NS}}$         |
|                               | 12                     | 0                      | 0.22                           |                                |
|                               | 24                     | 0                      | 0.30                           |                                |
|                               | 48                     | 0                      | 0.27                           |                                |
|                               | 72                     | 0                      | 0.26                           |                                |
|                               | 96                     | 0                      | 0.35                           |                                |
| Inoculated                    | 12                     | 0                      | 1.48                           | $r = -0.913$<br>( $P < 0.05$ ) |
|                               | 24                     | 0.21                   | 1.61                           |                                |
|                               | 48                     | 0.58                   | 1.13                           |                                |
|                               | 72                     | 0.69                   | 1.09                           |                                |
|                               | 96                     | 0.90                   | 0.58                           |                                |
| Amino oxyacetic acid-treated* |                        |                        |                                |                                |
| Non-inoculated                | 12                     | 0                      | 0.27                           | $r = -0.0345^{\text{NC}}$      |
|                               | 24                     | 0                      | 0.26                           |                                |
|                               | 48                     | 0                      | 0.26                           |                                |
|                               | 72                     | 0                      | 0.23                           |                                |
|                               | 96                     | 0                      | 0.28                           |                                |
| Inoculated                    | 12                     | 0                      | 0.72                           | $r = -0.843^{\text{NS}}$       |
|                               | 24                     | 0.25                   | 0.86                           |                                |
|                               | 48                     | 0.69                   | 0.73                           |                                |
|                               | 72                     | 0.88                   | 0.53                           |                                |
|                               | 96                     | 1.04                   | 0.40                           |                                |

<sup>a</sup>Average of 12 plants/treatment.

<sup>b</sup> $\mu\text{mol cin mg}^{-1} \text{ protein min}^{-1}$ ; 3 replicates/treatment.

\*500  $\mu\text{g ml}^{-1}$ .

NS, not significant ( $P > 0.05$ ); NC, not correlated.

attempt was made to control sheath blight disease by a systemic fungicide kitazin. Although kitazin reduced the disease, it also induced phytoalexin momilactone 'A' in rice leaf sheaths. However, the accumulation of phytoalexin was always more in treated inoculated leaf sheaths than in non-inoculated ones. Induction of phytoalexin by a fungicide is not unusual since Reilly and Klarman<sup>13</sup> tested 27 fungicides of which 15 induced detectable quantities of phytoalexin (hydroxyphaseollin) in soybean plants. These results suggest that reduction of disease by some fungicides may be associated with induction of phytoalexin, a known defence component. Apart from phytoalexins, role of PR-proteins in plant defence has also been suggested<sup>14-16</sup>. Therefore, it is not unreasonable to speculate that a relationship might exist between the production of phytoalexins and PR-proteins since both are defence components and are regulated by host genes. To trace the relationship between phytoalexins and PR-proteins, PAL may be considered as an important factor. PAL plays an active role in the biosynthesis of cinnamic acid from phenylalanine; cinnamic acid is closely associated with biosynthetic pathways of some isoflavonoid phytoalexins<sup>17</sup>. Salicylic acid, an inducer of PR-proteins, is also synthesized from cinnamic acid via benzoic acid<sup>18</sup> and the accumulation of salicylic acid may induce production of PR-proteins. The results of the present study showed that kitazin not only reduced sheath blight but also induced both PR-proteins and rice phytoalexin (RPA). Precursors of RPA can be derived

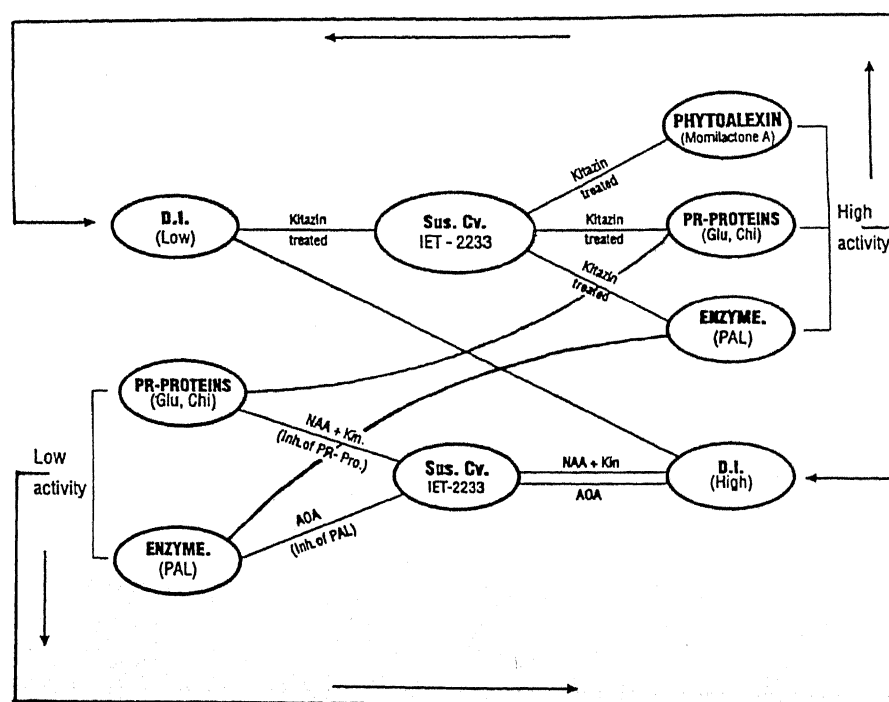


**Figure 3.** Schematic diagram showing involvement of different defence components in rice plants during development of sheath blight disease. Sus. cv., Susceptible cultivar; Glu- $\beta$ , 1,3-glucanase; Chi, chitinase; PAL, phenylalanine ammonia lyase; NAA, naphthaleneacetic acid; AOA, amino oxyacetic acid; DI, disease index; kin, kinetin.

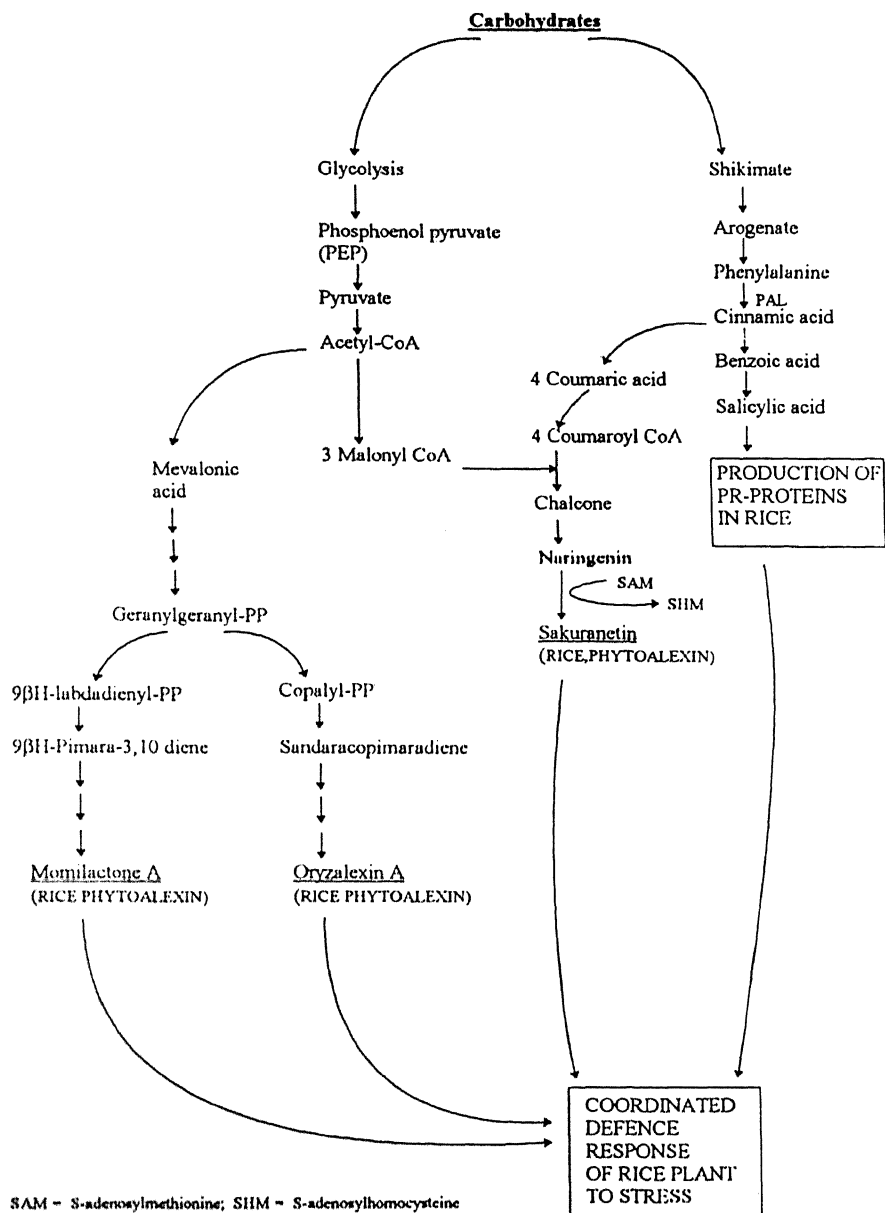


Figure 4. Probable relationship among phytoalexins, PR-proteins, PAL activity and defence response of rice against stress (biotic or abiotic).

from one of the three biosynthetic pathways (i.e. shikimate, acetate-malonate and acetate-mevalonate) or a combination of 2 or 3 pathways. Several key enzymes such as PAL, cinnamate-4-hydroxylase, 4-coumarate coenzyme A, chalcone synthase and chalcone isomerase of phytoalexin biosynthesis may be coordinately regulated. Usually phytoalexin accumulation after infection or treatment with inducers is consistent with mRNA production and enzyme activity<sup>19</sup>. Thus, it is likely that kitazin influences the biosynthetic pathways of RPA and PR-proteins (Figures 3, 4). A relationship between the two has been proposed. To confirm this, rice leaf

sheaths were treated with a mixture of kinetin + NAA (1:7.6), which inhibits both glucanase and chitinase. The results showed a significant increase in DI and concomitant decrease in glucanase and chitinase activities. These findings are in sharp contrast with that of inducer (kitazin)-treated rice plants where reduction in disease intensity and increase in glucanase and chitinase activities were noted.

Any host cv. resistant or susceptible has its natural defence to pathogens and as such occurrence of multicomponent defence response of a susceptible rice cv. is not unnatural. But why is this rice cv. IET-2233 susceptible

to the disease in spite of the coordinated defence response? It is likely that the speed of defence response of a susceptible cv. is usually slow or weak and the production of defence components is not sufficient for the total inhibition of growth of the pathogen or the syntheses of certain critical components of defence are not activated by the infection process. The delay in recognition of the pathogen and induction of the defence response, in this case, are also not unlikely. It has been possible to enhance the speed of response to some extent by kitazin which is evident from the higher production of phytoalexin, PR-proteins and higher activity of PAL in treated than in untreated plants.

Multicomponent, coordinated defence response of tobacco was reported earlier by Oelofse and Dubery<sup>20</sup>. The tobacco cells in cultures were treated with heat released soluble cell wall elicitors from mycelial walls of the pathogen (*Phytophthora nicotianae*). The experiments reported here suggest that a multicomponent, coordinated defence mechanism is also operative in rice plants after *Rhizoctonia solani* infection. Since there are practically no known sources of resistance against *R. solani* in the rice germplasm it would be worthwhile to identify potent inducers of multicomponent defence which could be exploited in the control of sheath blight.

1. Bera, S. and Purkayastha, R. P., in *Detection of Plant Pathogens and their Management* (eds Verma, J. P., Varma, A. and Kumar, D.), Angkor Publishers (P) Ltd., New Delhi, 1995, pp. 305–314.
2. Li, W. X., Kodama, O. and Akatsuka, T., *Agric. Biol. Chem.*, 1991, **55**, 1041–1047.
3. Vogeli, U., Meins, F. Jr. and Boller, T., *Planta*, 1988, **174**, 364–372.
4. Lowry, O. H., Rosenbrough, N. J., Farr, A. L. and Randall, R. J., *J. Biol. Chem.*, 1951, **193**, 265–275.
5. Laemmli, U. K., *Nature*, 1970, **227**, 680–685.
6. Fischer, W., Christ, U., Baumgartner, M., Erismann, K. H. and Mosinger, E., *Physiol. Mol. Plant Pathol.*, 1989, **35**, 67–83.
7. Somogyi, M., *J. Biol. Chem.*, 1952, **195**, 19–23.
8. Nelson, N., *J. Biol. Chem.*, 1944, **153**, 257–262.
9. Boller, T., Gehri, A., Mauch, F. and Vogeli, U., *Planta*, 1988, **157**, 22–31.
10. Reissig, J. L., Strominger, J. L. and Loloir, L. F., *J. Biol. Chem.*, 1955, **217**, 959–966.
11. Smith, C. J., Mittow, J. M. and Williams, J. M., in *Handbook of Phytoalexin Metabolism and Action* (eds Daniel, M. and Purkayastha, R. P.), Marcel Dekker, Inc., New York, 1995, pp. 405–433.
12. Bera, S. and Purkayastha, R. P., *Indian J. Exp. Biol.*, 1997, **35**, 644–649.
13. Reilly, J. J. and Klarman, W. L., *Phytopathology*, 1972, **62**, 1113–1115.
14. Christ, W. and Mosinger, E., *Physiol. Mol. Plant Pathol.*, 1989, **35**, 53–65.
15. Ahl Goy, P., Felix, G., Metraux, J. P. and Meins, F. Jr., *Physiol. Mol. Plant Pathol.*, 1992, **41**, 11–20.
16. Alexander, D., Goodman, R. M., Gut Rella, M., Glascock, Weymann, K., Friedrich, L., Maddox, D., Ahl Goy, P., Luntz, T., Ward, E. and Ryals, J., *Proc. Nat. Acad. Sci. USA*, 1993, **90**, 7327–7331.
17. Lamb, C. and Dixon, R. A., *Annu. Rev. Plant Physiol. Mol. Biol.*, 1997, **48**, 251–275.
18. Silverman, P., Seskar, M., Karder, D., Schweizer, P., Metraux, J. P. and Raskin, I., *Plant Physiol.*, 1995, **108**, 633–639.
19. Kuc, J., *Annu. Rev. Phytopathol.*, 1995, **33**, 275–297.
20. Oelofse, D. and Dubery, I. A., *Int. J. Biochem. Cell Biol.*, 1996, **28**, 295–301.

ACKNOWLEDGEMENTS. We thank to Prof. Osamu Kodama, Laboratory of Bioorganic and Pesticide Chemistry, Ibaraki University, Japan for helping us to quantify momilactone 'A'. The financial assistance received from UGC is gratefully acknowledged.

Received 15 October 1998; revised accepted 18 February 1999

## Characterization of tobacco mosaic virus isolated from tomato in India

Shoba Cherian<sup>†</sup>, Jomon Joseph<sup>†</sup>,  
V. Muniyappa\* and H. S. Savithri<sup>†,‡</sup>

<sup>†</sup>Department of Biochemistry, Indian Institute of Science, Bangalore 560 012, India

\*Department of Plant Pathology, University of Agricultural Sciences, GKVK, Bangalore 560 065, India

Tomato mosaic tobamovirus (ToMV) differs from the type strain of tobacco mosaic virus (TMV) in producing local lesions instead of systemic infection on *Nicotiana glauca*. An isolate collected from Kolar district of Karnataka which produced this differential host reaction was propagated in the greenhouse on *N. tabacum* cv. Samsun and purified. The virus is a rigid rod shaped particle with a coat protein of molecular weight 18 kDa and genomic RNA of size 6.3 kb. A cDNA library was constructed using a specific primer designed based on the conserved nucleotide sequence at the 3' non coding region of tobamoviruses. The cDNA library was screened for recombinant clones and the recombinant clone 82 with an insert of size 1.04 kb was sequenced in both directions. This sequence was compared with the genomic sequence of TMV and ToMV which showed 93.1 and 73.7 per cent identity, respectively. The sequence encompassed the 3' non coding region, the complete coat protein ORF and 467 nucleotides of the movement protein. The deduced amino acid sequence of the coat protein was compared with that of TMV and ToMV. This sequence was nearly identical to TMV with nine amino acid changes whereas thirty-two changes were observed with ToMV. This suggests that the virus under study is a strain of TMV and therefore we have named it as tobacco mosaic virus tomato strain from Karnataka, India (TMV(Tom-K)).

KARNATAKA is a major producer of tomatoes in India. Several tomato hybrids are grown all round the year.

<sup>‡</sup>For correspondence. (e-mail: bchss@biochem.iisc.ernet.in)

Tomato grown in Karnataka is distributed to other states in India and also exported to the Middle East. Tobacco mosaic virus (TMV) and tomato mosaic tobamovirus (ToMV) are two tobamoviruses known to naturally infect tomato and cause yield losses<sup>1,2</sup>. Field surveys conducted during 1994–95 to determine the natural distribution and prevalence of the virus in tomato revealed that 688 of 1228 samples tested in enzyme linked immunosorbent assay (ELISA) and on local lesion host (*Nicotiana glutinosa*) were infected with TMV/ToMV (ref. 3). However, none of the isolates of tobamoviruses from India have been characterized with respect to the genomic sequence thus far.

In the current paper we report the purification and characterization of a tobamovirus infecting tomato from India, the second most prevalent virus after tomato leaf curl geminivirus on tomato.

A tobamovirus causing mosaic on tomato collected from a naturally infected tomato field in Kolar district of Karnataka was maintained on *N. tabacum* cv. Samsun by sap inoculation in an insect-proof glasshouse.

The virus under study was purified from infected *N. tabacum* cv. Samsun leaves using the method of Asselin and Zaitlin<sup>4</sup>. Purified viral samples applied on carbon-coated grids were stained with 1% uranyl acetate and examined under a JEOL 100CX transmission electron microscope.

The viral coat protein was analysed by SDS-PAGE as described by Laemmli<sup>5</sup>. The gel was stained with coomassie blue. Molecular weights were determined by plotting log molecular weight against migration distance using a set of marker proteins (Dalton Mark VII – L, SDS – 7, Sigma).

Viral RNA was isolated from purified virus essentially by the method of Murant *et al.*<sup>6</sup>. Purified virus was incubated with an equal volume of RNA extraction buffer (0.1 M Tris, 0.01 M EDTA, 2% SDS, pH 7.5) at 55°C for 10 min. Following phenol–chloroform extraction, RNA was precipitated by adding 1/10 volume of sodium acetate and 0.8 volume of isopropyl alcohol. The isolated RNA was then run on a 1% agarose gel. Physalis mottle virus RNA of 6 kb and Sesbania mosaic virus RNA of 4.5 kb were used as markers.

Antisera were produced in rabbits against purified virions of the virus under study by giving three intramuscular injections in Freund's incomplete adjuvant at weekly intervals and one intravenous injection without the adjuvant in the fourth week. Serum was collected every week starting a week after the last injection. Antiserum titre was determined by ELISA. Double antibody sandwich ELISA (DAS–ELISA) was performed as follows.

Next, the procedure of Clark and Adams<sup>7</sup> was employed and the concentration of the protein ( $\gamma$ -globulin) was adjusted to 1 mg/ml (A 280 nm = 1.4) and then conjugated with penicillinase (from Hindustan Antibiotics

Ltd.) at an enzyme: globulin ratio of 2:1 in the presence of 0.06% glutaraldehyde.

Flat-bottomed polystyrene micro titre plates (Corning, Sigma) were pre-coated with 100  $\mu$ l (100 ng) of  $\gamma$ -globulin in carbonate buffer pH 9.6. After 3h, the plates were blocked with 5% dried milk powder in PBS, coated with antigen from infected leaves (1 g/10 ml) extracted in phosphate buffered saline tween-20-poly vinyl pyrrolidone-ovalbumin (PBST–PVP–OA). Following overnight incubation and washing, the antigen was detected using penicillinase conjugated globulins of homologous antiserum at 1:1000 dilution. The substrate (2 mg sodium penicillin-G/ml bromothymol blue + 0.2 M NaOH, pH 7.2) was added and the disappearance of the blue colour at 620 nm was monitored.

The polyclonal antiserum to the virus was also used for penicillinase-based direct antigen coating ELISA (DAC–ELISA) which was done as described by Sudarshana and Reddy<sup>8</sup>. Micro titre plates were coated with antigen (infected leaf extract 1 g/10 ml) extracted in carbonate buffer pH 9.6 and diluted to 1:10. Following overnight incubation at 4°C, the plates were coated with crude antiserum diluted in PBST–PVP–OA cross-adsorbed with healthy leaf extract.  $F_c$ -specific anti-rabbit penicillinase conjugate was then added followed by the addition of the substrate (2 mg sodium penicillin-G/ml of bromothymol blue + 0.2 M NaOH, pH 7.2).

Using a specific primer synthesized corresponding to the 24 bases at the 3' end of TMV RNA (3' GGG CC/AT/A TGG GGG CCA A/TCC CCG GGT 5') the first strand cDNA was synthesized essentially following the protocol described by Sambrook *et al.*<sup>9</sup>. This first strand cDNA was then used as a template for the second strand synthesis.

Following gel filtration, the cDNA fractions were cloned in the *Hinc*II site of pUC 19 cloning vector. After ligation, the DNA was transformed in competent DH 5 $\alpha$  cells and spread on LB–Amp–X gal–IPTG plates. The colonies were initially screened by blue/white selection and later by plasmid isolation and restriction digestion with *Xba*I and *Hind*III.

Initially, the sequencing of the clone was performed manually by Sanger's dideoxy chain termination method<sup>10</sup>. The clone was later sequenced using a Perkin–Elmer ABI Prism DNA sequencer.

Nucleic acid and deduced amino acid sequences were analysed using the 'GCG' program package at the Bioinformatics Centre, IISc. The viral sequence determined was compared and aligned with the other tobamoviral sequences in the GenBank and EMBL data base using the 'FASTA' and 'GAP' programs.

The program 'CLUSTALW' was used to generate multiple alignment<sup>11</sup>. The aligned sequences were analysed with the 'PHYLIP' package of programs<sup>12,13</sup> to infer phylogenies and to place a confidence limit on the phylogeny. The program 'SEQBOOT' was used to

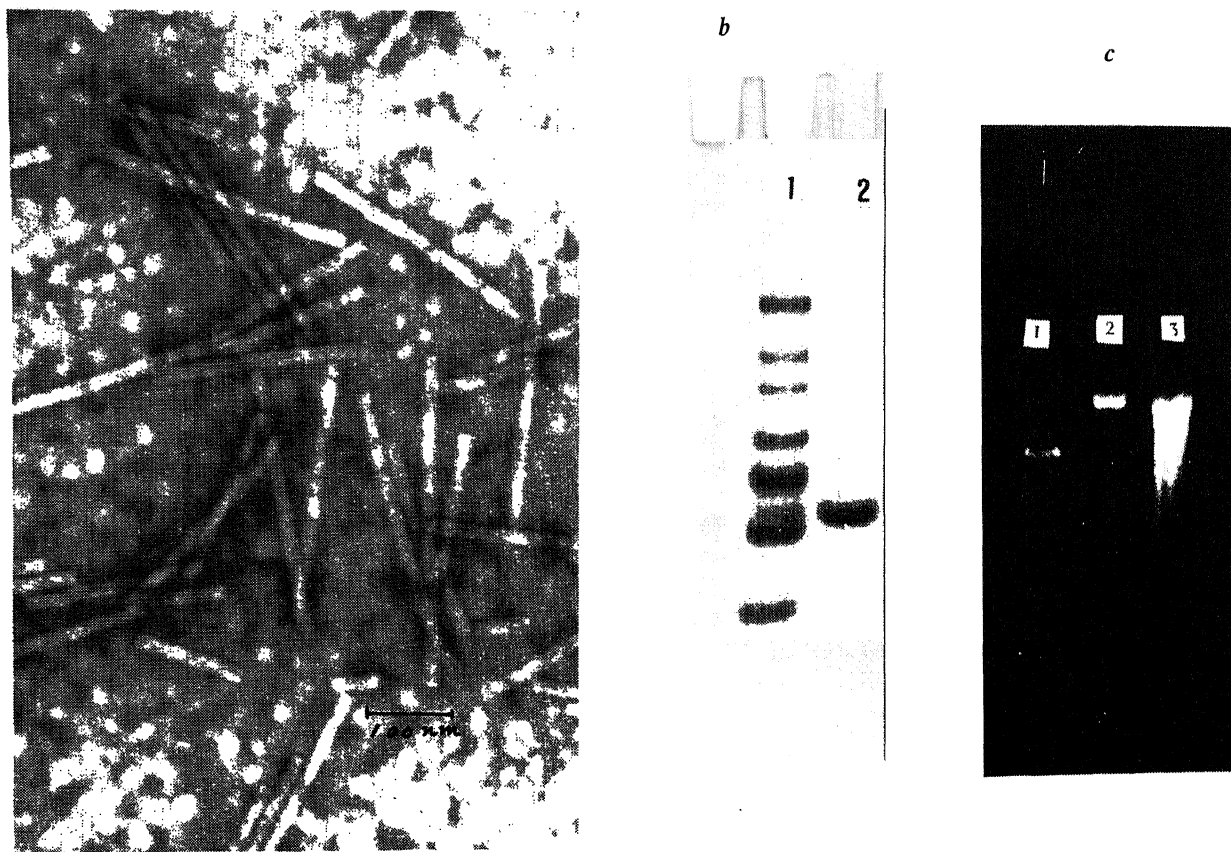


**Figure 1.** *a*, Electron micrograph of purified TMV (Tom-K) particles visualized by negative staining with 1% w/v uranyl acetate; *b*, Electrophoresis of the TMV (Tom-K) coat protein in 10% SDS-polyacrylamide gel stained with coomassie brilliant blue. Lane 1: Markers Type VII-L (Sigma) from top to bottom – bovine albumin (66,000); albumin egg (45,000), glyceraldehyde 3 – phosphate dehydrogenase (36,000); carbonic anhydrase (29,000); trypsinogen (24,000); trypsin inhibitor (20,100) and lactalbumin (14,200); Lane 2: Coat protein of TMV (Tom-K); *c*, Electrophoresis of TMV (Tom-K) RNA in 1% agarose gel stained with ethidium bromide. Lane 1: Sesbania mosaic virus RNA (4.5 kb). Lane 2: TMV (Tom-K) RNA. Lane 3: Physalis mottle virus RNA (6.2 kb).

produce 100 bootstrap<sup>14</sup> replacement sequence alignments from the original 'CLUSTALW' aligned sequences. The bootstrapped samples were analysed by the maximum parsimony method using the program 'PROTPARS'. The trees produced by 'PROTPARS' were analysed by the program 'CONSENSE' to deduce a consensus tree. The unrooted phylogenetic tree was drawn using the program 'DRAWTREE'.

The virus under study was transmitted mechanically from tomato to tomato and tobacco with an efficiency of 100%. It induced mild to severe form of mosaic in tomato. Infected tobacco leaves showed light and dark green mottling, together with distortion and smaller size. The virus produced necrotic local lesions on *Datura metel*, *D. stramonium*, *Gomphrena globosa*, *Nicotiana tabacum* cvs. White Burley, Riwaka-1, L-1158, CTRI special, *N. glutinosa* and *N. sylvestris*. It produced chlorotic local lesions on *Chenopodium amaranticolor*. It may be noted that TMV gives systemic infection of *N. sylvestris* whereas ToMV produces necrotic lesions<sup>15,16</sup>.

**Table 1.** Comparison of DAC-ELISA with local lesion assay for detection of the virus causing mosaic on tomato

| Antigen dilution | Absorbance readings <sup>a,b</sup> | Lesions/cm <sup>2</sup> on <i>N. glutinosa</i> |
|------------------|------------------------------------|--|
| Infected 10-1    | 1.139                              | 7.37   |
| 10-2             | 1.130                              | 5.45   |
| 10-3             | 1.118                              | 4.15   |
| 10-4             | 1.117                              | 2.30   |
| 10-5             | 0.856                              | 0.43   |
| 10-6             | 0.215                              | 0.06   |
| 10-7             | 0.054                              | 0.00   |
| 10-8             | 0.005                              | 0.00   |
| Healthy 10-1     | 0.011                              | 0.00   |

<sup>a</sup>Mean absorbance values of five wells at 620 nm obtained after deducting the mean absorbance value of buffer control.

<sup>b</sup>Absorbance values were considered positive if they yielded OD values twice greater than the mean optical density of wells coated with healthy plant extracts.

When the same inoculum of the virus under study obtained from *N. tabacum* cv. Samsun was inoculated to

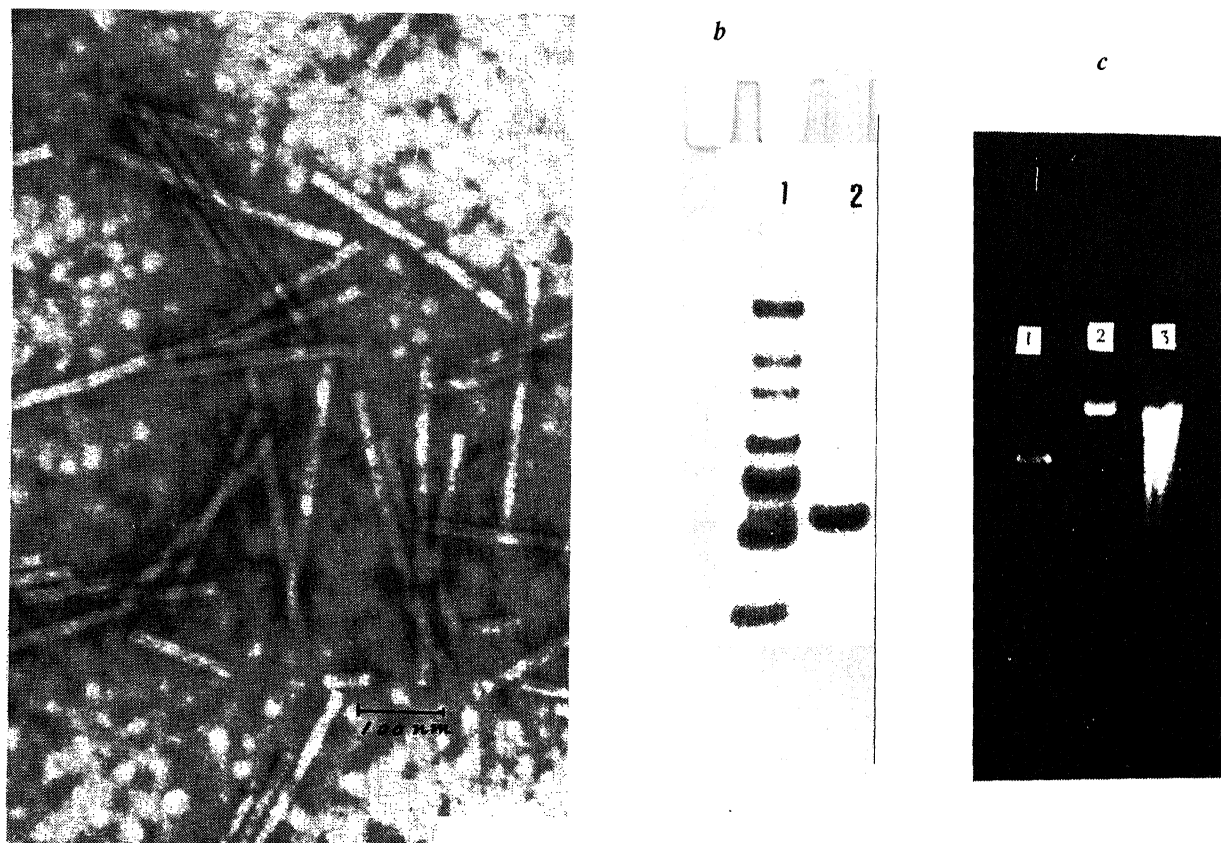


**Figure 1.** *a*, Electron micrograph of purified TMV (Tom-K) particles visualized by negative staining with 1% w/v uranyl acetate; *b*, Electrophoresis of the TMV (Tom-K) coat protein in 10% SDS-polyacrylamide gel stained with coomassie brilliant blue. Lane 1: Markers Type VII-L (Sigma) from top to bottom – bovine albumin (66,000); albumin egg (45,000); glyceraldehyde 3 – phosphate dehydrogenase (36,000); carbonic anhydrase (29,000); trypsinogen (24,000); trypsin inhibitor (20,100) and lactalbumin (14,200); Lane 2: Coat protein of TMV (Tom-K); *c*, Electrophoresis of TMV (Tom-K) RNA in 1% agarose gel stained with ethidium bromide. Lane 1: Sesbania mosaic virus RNA (4.5 kb). Lane 2: TMV (Tom-K) RNA. Lane 3: Physalis mottle virus RNA (6.2 kb).

produce 100 bootstrap<sup>14</sup> replacement sequence alignments from the original 'CLUSTALW' aligned sequences. The bootstrapped samples were analysed by the maximum parsimony method using the program 'PROTPARS'. The trees produced by 'PROTPARS' were analysed by the program 'CONSENSE' to deduce a consensus tree. The unrooted phylogenetic tree was drawn using the program 'DRAWTREE'.

The virus under study was transmitted mechanically from tomato to tomato and tobacco with an efficiency of 100%. It induced mild to severe form of mosaic in tomato. Infected tobacco leaves showed light and dark green mottling, together with distortion and smaller size. The virus produced necrotic local lesions on *Datura metel*, *D. stramonium*, *Gomphrena globosa*, *Nicotiana tabacum* cvs. White Burley, Riwaka-1, L-1158, CTRI special, *N. glutinosa* and *N. sylvestris*. It produced chlorotic local lesions on *Chenopodium amaranticolor*. It may be noted that TMV gives systemic infection of *N. sylvestris* whereas ToMV produces necrotic lesions<sup>15,16</sup>.

**Table 1.** Comparison of DAC-ELISA with local lesion assay for detection of the virus causing mosaic on tomato

| Antigen dilution | Absorbance readings <sup>a,b</sup> | Lesions/cm <sup>2</sup> on <i>N. glutinosa</i> |
|------------------|------------------------------------|--|
| Infected 10-1    | 1.139                              | 7.37   |
| 10-2             | 1.130                              | 5.45   |
| 10-3             | 1.118                              | 4.15   |
| 10-4             | 1.117                              | 2.30   |
| 10-5             | 0.856                              | 0.43   |
| 10-6             | 0.215                              | 0.06   |
| 10-7             | 0.054                              | 0.00   |
| 10-8             | 0.005                              | 0.00   |
| Healthy 10-1     | 0.011                              | 0.00   |

<sup>a</sup>Mean absorbance values of five wells at 620 nm obtained after deducting the mean absorbance value of buffer control.

<sup>b</sup>Absorbance values were considered positive if they yielded OD values twice greater than the mean optical density of wells coated with healthy plant extracts.

When the same inoculum of the virus under study obtained from *N. tabacum* cv. Samsun was inoculated to

```

1  CTGCGGGTTT CTGTCGCCCT TCTCTGGAGT TTGTGTCGGT ATGTATTGTT
51  TATAGAAATA ACATAAAATT AGGTTTGAGA GAGAAAAATTA CGAGCGTGAG
101 AGACGGAGGG CCCATGGAAT CCACAGAAGA AGTTGTTGAT GAGTTCATGG
151 AAGATGTCCC TATGTCGATA AGGCTTGCAA AGTTTCGATC TCGAACCGGG
201 AAAAAAGAGT ATGTCTTGAA AGCGAAAGTT AGTAGTAATG ATCGGTCGCA
251 GCCCAACAAG AACTATATAA ATGTTTAAGA TTATGGAGGA ATGAGTTTAA
301 AAAAGAATAA TTTAATCGAT GATGATTCGG AGACTTCTGT CGCCCAATCG
      Start codon
351 GATTTCGTTT AAATATGCTT TATAATATCA CTACTCCATC TCAGTTCGTG
401 TTCTTGTCTG CCGCGTGGGC CGACCCGATA GAGTTAATTA ATTTATGTAC
451 TAATGCCCTT GGTATCAGT TCCAAACACA ACAAGCTCGA ACTGTCGTTT
501 AAAGACAATT CAGCGAGGTG TGGAAACCTT CACCACAAGT TACTGTCACT
551 TCCCCTGACA GCGACTTTAA GGTATATAGG TACATTGCGG TATTAGAGCC
601 TCTAGTTACT CGACTATTAG GCGCTTTTGA TACTAGAAAT AGAATAATAG
651 AAGTTGAAAA TCAAGCAAAAC CCCACGACTG CCGAAACGTT AGATGCTACT
701 CGTAGAGTAG AGGACGCAAC GGTGGCCATA AGGAGCGCGA TAAATAATTT
751 AATAGTAGAA TTGATCAGAG GAACTGGATC TTATAATCGG AGCTCTTTCG
      Stop codon
801 AGAGCTCTTC TGGTTTGTTT TGGACCTCTA GTCCGGCAAC TTGAAGTAGT
851 CAAGATGCAT AATAAATAAC GGATTGTGTC CGTAATCACA CGTGGTGCCT
901 ACGATAACGC ATAGTGTGTT TCCCTCCACT TAAATCGAAG GGTGTGTGCT
951 TGGATCGCGC GGGTCAAAAT TATATGGTTA ATATACATCC GTAGGCACGT
      Primer
1001 AATAAAGCGA GGGGTTTCGAA TCCCCTCCGT ACCCCCGGTT GGGGCCGA

```

Figure 2. Nucleotide sequence of the 3' terminal 1048 nucleotides of TMV (Tom-K). The start and stop codons of the coat protein ORF and the sequence of the primer used to generate the cDNA clones are underlined.

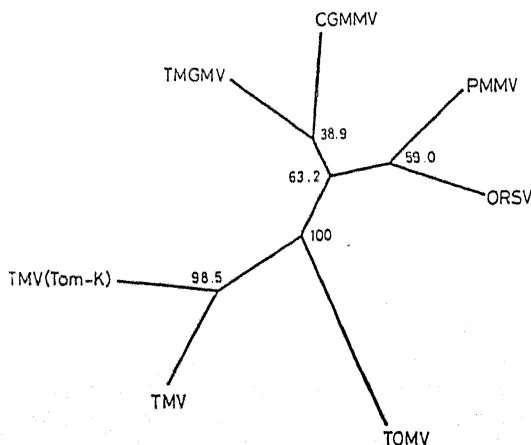


Figure 3. Phylogenetic analysis of tobamovirus coat protein. The dendrogram represents the consensus relationship obtained from 100 bootstrap samples for CP sequences. The number at the branch nodes indicate the number of times a particular branch appeared in all the trees that were used to determine the consensus tree.

*N. glutinosa* leaves of different sizes, they produced widely varying lesion numbers. But mean lesions/cm<sup>2</sup> were similar and varied from 6.09 to 6.88.

TMV (Tom-K) MSYNIITPSQFVFLSSAWADFIELINLCTNALGQFQTQARTVVRQFSEVWKPSPQVT  
 TMV MSYSIITPSQFVFLSSAWADFIELINLCTNALGQFQTQARTVVRQFSEVWKPSPQVT  
 ToMV MSYSITSPSQFVFLSSVWADFIELINLCTNALGQFQTQARTVVRQFSEVWKPFPQST

TMV (Tom-K) VSSPDSDFKVYRYIAVLEPLVTRLLGAFDTRNRIIEVENQANPTTATLDA TRVEDATV  
 TMV VRFPDSDFKVYRYIAVLDPLVTALLGAFDTRNRIIEVENQANPTTATLDA TRVDDATV  
 ToMV VRFPDVTYKVRYIAVLDPLITALLGAFDTRNRIIEVENQGSFTTATLDA TRVDDATV

TMV (Tom-K) AIRSAINNLIVELIRGTGSYNRSSFESSGLVWTSPPAT  
 TMV AIRSAINNLIVELIRGTGSYNRSSFESSGLVWTSPPAT  
 ToMV AIRSAINNLIVELIRGTGLYNQNTFESMSGLVWTSAPAS

Figure 4. Comparison of the deduced amino acid sequence of the coat protein of TMV (Tom-K) with TMV strain vulgare and ToMV. Conservative substitutions are indicated by . or ; ; \* indicates identities.

Purified virion preparations gave an yield of 80 mg/100 g of leaf tissue, assuming an extinction coefficient of 3.1 for a 0.1% solution at 260 nm. The ultra-violet absorption spectrum of the purified virus showed maximum absorption at 260 nm. The A<sub>260</sub>/A<sub>280</sub> ratio of the virus was close to 1.2. Electron microscopy of purified virions of the virus under study showed that the particles were rigid rods measuring 300 × 18 nm in size (Figure 1a). The CP of the virus was shown to have a molecular weight of 18,000 daltons (Figure 1b). The virus was found to consist of a single species of RNA which moved the same distance as physalis mottle virus RNA of molecular weight 2 × 10<sup>6</sup> daltons when subject to agarose gel electrophoresis (Figure 1c). The protein and nucleic acid molecular weights determined for the Kolar viral isolate agree with those reported in literature<sup>17-19</sup>.

The polyclonal antiserum produced against the virus under study reacted with the infected sap and the purified virus to give titres of 1/10,000 and 1/32,000, respectively, in penicillinase-based DAS-ELISA. The penicillinase globulin conjugate had a titre of 1/2000 when tested in DAS-ELISA. Table 1 (ELISA results) shows that the virus can be detected in infected leaf extracts in the dilution range of 10<sup>-1</sup> (1.14) to 10<sup>-7</sup> (0.054) using an antiserum dilution of 1:1000. In comparison, the local lesion host *N. glutinosa* detected the virus in tomato leaf extracts diluted up to 10<sup>-6</sup>.

Among the recombinant clones generated, clone 82 released an insert of size 1.04 kb upon digestion with *Xba*I and *Hind*III. Automated DNA sequencing of this clone in both the directions resulted in the sequence of the 3' terminal 1048 nucleotides of the virus (Figure 2). Comparison of this sequence with other members of the tobamovirus group showed that this sequence aligned at nucleotide 5711 of TMV and ended at 6395, the 3' terminal nucleotide of TMV<sup>20</sup>. It is interesting to note that the sequence obtained matched well with that of TMV (93.1% identity) whereas it had much less homology with ToMV (73.7% identity). This suggests that though this isolate produces local lesion on *N. sylvestris*, it is a

## RESEARCH COMMUNICATIONS

**Table 2.** Per cent identity of the coat protein and 3' non coding region of TMV (Tom-K) with other tobamoviruses

| Virus                                      | Nucleotide sequence of CP | 3' NC | Deduced amino acid sequence of CP | Ref. |
|--|---------------------------|-------|-----------------------------------|------|
| Tobacco mosaic virus strain vulgare (TMV)  | 92.6                      | 97.6  | 94.3                              | 20   |
| Tomato mosaic virus (ToMV)                 | 72.7                      | 77.3  | 78.6                              | 21   |
| Odontoglossum ring spot virus (ORSV)       | 65.8                      | 69.5  | 70.5                              | 22   |
| Pepper mild mottle virus (PMMV)            | 64.5                      | 63.3  | 68.2                              | 23   |
| Tobacco mild green mosaic virus (TMGMV)    | 62.9                      | 35.7  | 66.7                              | 24   |
| Cucumber green mottle mosaic virus (CGMMV) | 45.7                      | 56.0  | 35.8                              | 25   |

strain of TMV and not a strain of ToMV. This is further supported by the data presented in Table 2 which depicts the per cent identity of the coat protein and 3' non-coding region of the present isolate with other tobamoviruses. Figure 3 shows the dendrogram of the tobamoviral CP sequences. Even here TMV (Tom-K) clusters with TMV CP rather than with ToMV CP. Comparison of the CP sequence of TMV (Tom-K) with the TMV strain vulgare<sup>20</sup> showed that there are 9 amino acid changes between TMV CP and that of the Indian isolate (Figure 4). Out of these, 5 of the changes are conservative substitutions. On the other hand, 32 amino acid changes were observed between TMV (Tom-K) and ToMV<sup>21</sup>. Thus the analysis of the 3' terminal nucleotides of the Indian isolate clearly establishes that the isolate is a strain of tobacco mosaic and hence is called tobacco mosaic virus tomato strain (TMV (Tom-K)).

The nucleotide sequence reported in this paper has been submitted to GenBank and assigned the accession number AF 126505.

- Rejinders, L., Aalbers, A. M. J. and Van Kammun, A., *Virology*, 1974, **69**, 515-521.
- Goelet, P., Lomonosoff, G. P., Butter, P. J. G., Akem, M. E., Gait, M. J. and Karn, J., *Proc. Natl. Acad. Sci. USA*, 1982, **79**, 5818-5822.
- Ohno, T., Aoyagi, M., Yamanashi, Y., Saito, H., Ikawa, S., Meshi, T. and Okada, Y., *J. Biochem.*, 1984, **96**, 1915-1923.
- Isomura, Y., Matumoto, Y., Murayama, A., Chatani, M., Inouyee, N. and Ikegami, M., *J. Gen. Virol.*, 1991, **72**, 2247-2249.
- Alonso, E., Garcia-Luque, I., de la Cruz, A., Wicke, B., Avila-Rincon, M. J., Serra, M. T., Castresana, C. and Diaz-Ruiz, J. R., *J. Gen. Virol.*, 1991, **72**, 2875-2884.
- Nejidat, A., Cellier, F., Holt, C. A., Gafny, R., Eggenberger, A. L. and Beachy, R. N., *Virology*, 1991, **180**, 318-326.
- Ugaki, M., Tomiyama, M., Kakutani, T., Hidaka, S., Kiguchi, T., Nagata, R., Sato, T., Motoyoshi, F. and Nishiguchi, M., *J. Gen. Virol.*, 1991, **72**, 1487-1495.

**ACKNOWLEDGEMENTS.** This work was supported by CSIR and DBT, New Delhi, India. We also thank DBT for providing the Bioinformatics and Automated DNA sequencing facilities. We thank Mr P. Elango, Ms Savitha and Ms H. A. Prameela, for all the help rendered.

Received 19 December 1998; revised accepted 12 March 1999

## Serotyping of foot-and-mouth disease virus from aerosols in the infected area

V. V. S. Suryanarayana\*, Pradeep Bist, G. R. Reddy and L. D. Misra

Indian Veterinary Research Institute, Hebbal, Bangalore 560 024, India

**A simple and reliable test was standardized for serotyping foot-and-mouth disease virus from aerosols. The test, which is based on antigen capture-RT/PCR method, detected the serotype of the virus in the air exhaled by a diseased bull. The test has also been successfully used to detect the virus serotype in the aerosols from the containment area where the tissue culture virus was handled. Antibodies raised against recombinant proteins of all the serotype were used in the test to improve the specificity.**

FOOT-and-mouth disease (FMD) is one of the most important diseases of livestock such as cattle, sheep, goat

\*For correspondence. (email: bngivri@kar.nic.in)

- Rao, M. H. P. and Reddy, D. V. R., *Indian Phytopathol.*, 1971, **24**, 672-678.
- Giri, B. K. and Mishra, M. D., *Indian Phytopathol.*, 1990, **43**, 487-490.
- Shoba Cherian and Muniyappa, V., *Indian J. Virol.*, 1998, **14**, 65-69.
- Asselin, A. and Zaitlin, N., *Virology*, 1978, **88**, 191-193.
- Laemmli, U. K., *Nature*, 1970, **227**, 680-685.
- Murant, A. F., Taylor, M., Duncan, G. H. and Raschke, J. H., *J. Gen. Virol.*, 1981, **53**, 321-332.
- Clark, M. F. and Adams, A. N., *J. Gen. Virol.*, 1977, **34**, 475-483.
- Sudarshana, M. R. and Reddy, D. V. R., *J. Virol. Methods*, 1989, **26**, 45-52.
- Sambrook, J., Fritsch, E. F. and Maniatis, T., *Molecular Cloning - A Laboratory Manual*, Cold Spring Harbor Laboratory Press, USA, 1989, 2nd ed. vol. 1-3.
- Sanger, F., Nicklen, S. and Coulson, A. R., *Proc. Natl. Acad. Sci. USA*, 1977, **74**, 5463-5467.
- Thompson, J. D., Higgins, D. G. and Gibson, T. J., *Nucleic Acids Res.*, 1994, **22**, 4673-4680.
- Felsenstein, J., *Annu. Rev. Genet.*, 1988, **22**, 521-565.
- Felsenstein, J., *Cladistics*, 1989, **5**, 164.
- Felsenstein, J., *Evolution*, 1985, **39**, 783.
- VanRegenmortel, M. H. V., in *Handbook of Plant Virus Infections and Comparative Diagnosis* (ed. Krustak, K.), Elsevier, Amsterdam, 1981, p. 541.
- Wang, A. L. and Knight, C. A., *Virology*, 1967, **31**, 101-106.
- Bem, F. and Murant, A. F., *J. Gen. Virol.*, 1979, **44**, 817-826.
- Murant, A. F. and Taylor, M., *J. Gen. Virol.*, 1978, **41**, 53-61.

and pigs. The causative agent, foot-and-mouth disease virus (FMDV) belongs to genus *Aphthovirus* of the family *Picornaviridae*<sup>1</sup>. The virus particle which sediments at 146S consists of a single stranded positive sense RNA molecule of about 8.5 kb (ref. 2) with a molecular weight of  $2.6 \times 10^6$  daltons enclosed in a capsid which is composed of 60 copies each of four structural proteins named VP1, VP2, VP3 and VP4. VP1 is exposed on the surface of the virion and has immunogenic property<sup>3</sup>. India has remained an ideal habitat for the infection to persist, spread and flourish over centuries with its agro-climatic and socio-economic conditions conducive to the perpetuation of the virus. It has mixed farming of different species of livestock, which altogether provides a favourable ecological milieu for the pathogen. Epidemiology of FMD is complex and rather difficult to understand with its changing pattern of frequency, multiplicity of types and variants, ease of transmission and spread and the total number of disease outbreaks that occur over a particular period of time. The disease is endemic to India with four (A, O, C, Asia-1) serotypes in circulation besides numerous field variants. In countries like India, where slaughtering policy cannot be adopted due to various reasons, the disease can only be controlled by regular vaccination supported by early diagnosis, proper disposal of infected animals and restricted animal movement. Since inactivated viral vaccines against FMDV confer short duration of immunity and continued disease outbreaks and variations among circulating viruses are the major problems of control programmes, it is essential to have rapid and sensitive diagnostic tests. Various serological, immunological, and biochemical tests have been developed for specific diagnosis of FMD in field samples. Of late, sensitive tests based on PCR and nucleic acid hybridization have been developed<sup>4-7</sup>. Most of these are related to the major immunogen VP1 as type-specific amino acid sequence variations have been found at the carboxy terminal end of this protein. The homology in this region with respect to the nucleic acid sequence is less than 60% among the various types<sup>6,8,9</sup>. Probes corresponding to this region have been used for FMDV typing<sup>10</sup> and sequence information was used to study the strain variation<sup>11,12</sup>. Application of nucleic acid probes is time consuming and needs trained manpower and cost intensive infrastructure. However PCR based methods are highly sensitive, less time consuming and can be adopted for routine use. The PCR method was modified and used for virus typing. The modified technique termed antigen capture RT/PCR (Ag-RT/PCR) was found to be 100 times more sensitive than ELISA<sup>13</sup>. These tests were conducted routinely on saliva or tongue epithelia collected from the diseased animal. However, collection of these samples for diagnostic purpose is associated with physical handling of the animal and thereby increasing the risk of spreading the virus to the

environment, which is not desirable. In order to avoid this risk, we have a standardized simple method, which uses the aerosol samples for virus type detection by Ag-RT/PCR. The test not only detected the virus type from the aerosol near the affected animal, but also from the area where the virus is handled.

BHK 21 clone 13 passaged FMDV maintained as vaccine virus at the Indian Veterinary Research Institute (IVRI), Bangalore was used as positive control. Ten per cent tongue epithelial extract was prepared in PBS (8 g of NaCl, 0.2 g of KCl, 1.44 g of  $\text{Na}_2\text{HPO}_4$  and 0.24 g of  $\text{KH}_2\text{PO}_4$ , pH 7.4) and used. Air collected near the animals during the recent outbreak of the disease in Bangalore or from the containment area where the cell culture virus was handled, was used as test sample. In the first case, 50 ml of air was drawn from the vicinity (12 cm away) of the affected animals using a sterile plastic syringe without touching the animal, feed or water and bubbled slowly into 200  $\mu\text{l}$  of sterile distilled water in 1.5 ml microcentrifuge tube. Ten  $\mu\text{l}$  of the sample was used for capturing and detection. In the second case, 50 ml air was drawn near the working place (10 feet away from the actual handling spot) and passed into 200  $\mu\text{l}$  of sterile distilled water and 10  $\mu\text{l}$  of the sample was subjected as per the procedure described by Suryanarayana *et al.*<sup>7</sup>, except that antibodies against *E. coli* expressed truncated proteins were used in the test in place of antibodies raised against the whole virus.

Application of Ag-RT/PCR test for virus serotyping was reported<sup>13</sup>. Briefly, a set of microcentrifuge tubes coated with all the four type-specific antibodies (against immuno-reactive recombinant proteins) was used for virus capturing. Ten  $\mu\text{l}$  of the virus solution (either from the aerosol or tissue extracts) was mixed with 100  $\mu\text{l}$  of PBS-Tween 3% BSA and subjected to antigen capture in antibody-coated tubes for 2 h at 37°C. The bound antigen in the tubes were subjected to RT/PCR as described elsewhere<sup>13</sup>. In order to study the use of this test on aerosols for virus typing, the air collected from the containment area before and after handling of FMDV serotype Asia I and A22 (with one day interval in between) was subjected to the assay. There was no amplification of the 330 bp DNA in the air collected before handling of the virus (Figure 1, lanes 2 to 5). Intense DNA bands corresponding to Asia I and A22 were seen in the lanes 9 and 11, respectively. No non-specific amplification of DNA in other heterologous antibody-coated tubes (lanes 6 to 8 and 12 to 14, respectively) were found. When the test was further extended to identify the presence of the virus in the containment area one day after handling of the Asia I virus, the air collected showed the amplified DNAs corresponding to Asia I virus (lane 18) indicating that the test is sensitive enough to detect even a minute quantity of virus in the aerosol. Encouraged with the sensitivity and specificity of the technique of detecting the virus in aerosol sam-

## RESEARCH COMMUNICATIONS

ples, we have tested the method on the air collected (in duplicate) from the vicinity of the diseased animals kept separately in animal sheds. Subsequently, the epithelial extracts of the affected animals were also tested for confirmation of the results from the aerosol (Figure 2). Intense amplified DNA corresponding to Asia I was seen in both the aerosol samples (lanes 5 and 9) and epithelial extract (lane 13) indicating that the virus causing the disease was FMDV serotype Asia I and the released virus particles in the aerosol could be trapped and the specific gene amplified. There was no non-specific amplification as observed by the absence of DNA bands in other lanes (lane 2 to 4, 6 to 8 and 10 to 12).

This test was repeated on several other aerosol samples, which include air samples from guinea pig cages housing infected guinea pigs and laminar floors. In case of FMD, which is highly contagious and spreads rapidly, handling of infected tissue for diagnostic purpose is undesirable. In countries like India where FMD is endemic and FMDV occurs as four serologically distinct serotypes, rapid diagnosis by way of serotyping is essential for successful control of the disease. Initially, FMD was diagnosed by conventional tests like CFT and virus neutralization. Later nucleic acid-based probes have been developed for virus detection in infected animals. With the advent of highly sensitive PCR methods, the

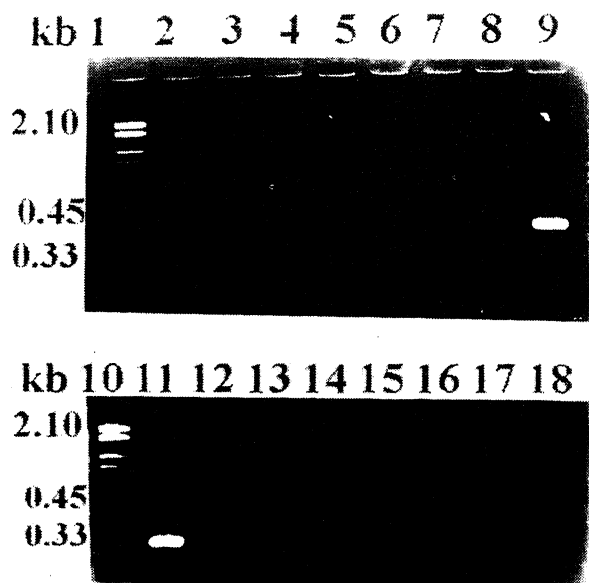


**Figure 1.** Agarose gel electrophoresis of PCR amplified DNA from aerosols. Air was collected, virus captured and subjected to Ag-RT/PCR. The products were analysed by 1.5% agarose gel electrophoresis. Amplified DNA from virus handling room, lane 2-5, before handling; lane 6-9, after handling FMDV type Asia I; lane 11-14, after handling A22 virus; and lanes 15-18, one day after handling Asia I virus. A (2, 6, 11, 15) or O (3, 7, 12, 16) or C (4, 8, 13, 17) or Asia I (5, 9, 14, 18) coated tubes. Lane 1 and 10, molecular weight marker.

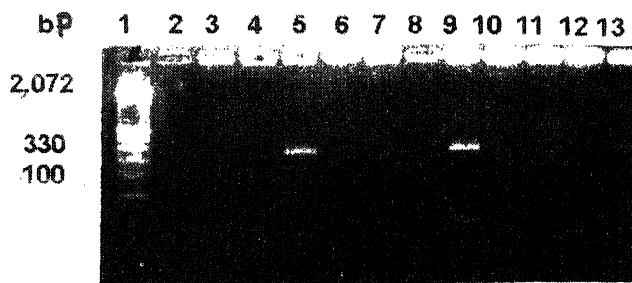


**Figure 2.** Agarose gel electrophoresis of PCR amplified DNAs from aerosols and epithelium. Cattle tongue epithelial extract or aerosol sample collected from the infected area was subjected to Ag-RT/PCR and the amplified products were analysed by agarose gel electrophoresis. The amplified products are: lane 2 to 5, virus captured from cattle tongue epithelial extract; lanes 6 to 9 and 10 to 13, aerosol samples collected in A22 (2, 6, 10), O (3, 7, 11), C (4, 8, 12) and Asia I (5, 9, 13) antibody-coated tubes.

detection of strain variation by sequencing was possible<sup>14</sup>. The Ag-RT/PCR developed by us was found to be highly sensitive for virus typing. Use of antibodies against recombinant proteins further added to the sensitivity and specificity of the test (manuscript under preparation).

We have indicated the scope of this technique in the detection of the virus from contaminated water and aerosols in our earlier studies. This has been found true in the present report, which is the first of its kind. We feel that the test can be adapted regularly for typing the virus released out in the air without physically handling the animal for want of infected tissue. This simple method will avoid unnecessary spread of the virus in the environment. Our studies in the containment area showed that the test may be employed for checking the presence of the virus type in the P3 laboratories or in the air exhausts of the virus handling units or in any other contaminated area.

1. Mathews, R. E. F., *Intervirology*, 1982, 17, 1-15.
2. Fross, S., Strebel, K., Beck, E. and Schaller, H., *Nucleic Acid Res.*, 1984, 12, 6587-6601.
3. Bachrach, H. L., Moore, D. M., McKercher, P. D. and Polantic, J., *J. Immunol.*, 1975, 115, 1636-1641.
4. Saiz, J. C. and Sobrinho, F., *Virology*, 1992, 189, 363-367.
5. Suryanarayana, V. V. S., Sen, A. K., Tratschin, J. D., Kihm, U. and McCullough, Indo-Swiss Seminar on Biotechnology, Bangalore, 1991, p. 23.
6. Suryanarayana, V. V. S., Tyagi, M. and Reddy, G. R., *International Seminar on Virus Cell Interaction, Cellular and Molecular Responses*, Bangalore, 1993, pp. 32-35.
7. Suryanarayana, V. V. S., Banumathi, N. and Reddy, G. R., *International Conference on Virology in Tropics*, Lucknow, 1991, p. 86.
8. Mateu, M. G., Hernandez, J. and Martinez, M. A. *J. Virol.*, 1994, 68, 1407-1417.
9. Strohmaier, K., Franze, R. and Adam, K. H., *J. Gen. Virol.*, 1982, 59, 295-306.

10. Suryanarayana, V. V. S., Tulasiram, P., Prabhudas, K., Mishra, L. D. and Natarajan, C., *Virus Genes*, 1998, **16**, 169–174.
11. Tulasiram, P., Mudit Tyagi, Srinivas, K., Prabhudas, K. S. and Natarajan Suryanarayana, V., *Virus Genes*, 1997, **15**, 247–253.
12. Tulasiram, P. and Suryanarayana, V., *Indian J. Exp. Biol.*, 1998, **36**, 70–75.
13. Suryanayana, V., Madanmohan, B., Pradeep Bist, Natarajan, C. and Tratchin, J. D., *J. Virol. Methods*, 1999 (in press).
14. Reddy, G. R. and Suryanarayana, V. V. S., International Symposium on Virus-Cell Interaction: Cellular and Molecular Responses, 22–24 November 1993, pp. 35–36.

**ACKNOWLEDGEMENTS.** This research work was supported by the Department of Biotechnology, Government of India and Swiss Development Cooperation under Indo-Swiss collaborative project. The authors thank the Director and Joint Director, IVRI Bangalore for facilities to carry out this work.

Received 17 December 1998; revised accepted 15 February 1999.

## Identification of alpha-terthienyl radical *in vitro*: A new aspect in alpha-terthienyl phototoxicity

Manish Nivsarkar

B. V. Patel Pharmaceutical Education and Research Development Centre, Thaltej-Gandhinagar Highway, Thaltej, Ahmedabad 380 054, India

**Alpha-terthienyl, the naturally occurring larvicide from tagetes species, exhibits unique free radical generating property. Besides generating singlet oxygen and superoxide anion radical, it generates alpha-terthienyl radical, when exposed to ultraviolet light. This free radical generating property of alpha-terthienyl can be utilized to understand the mechanism of action against insects; however this use also poses a threat to the non-target species exposed to it.**

LIGHT-activated pesticides are recognized as a new technology with considerable promise in the area of pest control. Erythrosin B has already been registered for housefly control, and a promising photodynamic herbicide based on porphyrin metabolism is under development<sup>1</sup>. Among the most active biocides whose activity is enhanced by light are the naturally occurring thiophenes and biosynthetically-related polyacetylenes which are characteristic secondary plant metabolites of the plant family Asteraceae<sup>1</sup>. For example, alpha-terthienyl ( $\alpha$ -T) (Figure 1) has been extensively studied and evaluated as a larvicide<sup>2</sup>, fungicide<sup>3</sup> and nematocide<sup>4</sup>. Several attempts have been made to examine the phototoxicity of terthienyl and bithienyl analogs<sup>5–8</sup>, which have been moderately successful in improving our understanding of the structure–activity relationship and for improving

efficacy.  $\alpha$ -T gives an absorption peak at 351 nm in ethanol (Figure 2) and generates singlet oxygen<sup>6</sup> and superoxide anion radical both *in vivo*<sup>9,10</sup> and *in vitro*<sup>10,11</sup> under ultraviolet (UV) light.

A stock solution of 2  $\mu$ g/ml of  $\alpha$ -T was prepared in absolute ethyl alcohol. Ten  $\mu$ l of  $\alpha$ -T solution was added to 100  $\mu$ l on *n*-*t*-butyl- $\alpha$  phenyl nitron (PBN) (50 mM, final concentration). The total mixture of 100  $\mu$ l was irradiated with ultraviolet light (320–400 nm) for different time intervals from 1 to 120 s (1, 2, 5, 10, 15, 30, 45, 60, 90 and 120 s). Another tube containing the same reagents was kept in total darkness for 1 h, which served as control. After incubation, 50  $\mu$ l aliquots from each of the above samples were transferred to glass capillary tubes and one end of each capillary tube was flame-sealed.

Electron paramagnetic resonance (EPR) spectra of the PBN free radical adducts formed were then recorded on a Varian E-104 EPR spectrometer (Pal Alto, USA) equipped with a TM<sub>110</sub> cavity, and were compared with the reference spectrum of superoxide radical generated by autoxidation of pyrogallol<sup>12</sup>, which served as a control. Instrument settings were as follows: field set, 3237 G; temperature, 27  $\pm$  5°C; scan range, 10  $\times$  10 G; time constant, 0.5 s; scan time, 4 min; microwave power, 5 mW; microwave frequency, 100 kHz; modulation amplitude, 2 G; modulation frequency, 9.01 GHz; and receiver gain, 1.25  $\times$  10<sup>4</sup>  $\times$  10 (unless otherwise stated).

Figure 3 shows spin-trapping results of free radicals formed by exposure of  $\alpha$ -T to UV light. The EPR signals obtained by ultraviolet irradiation of  $\alpha$ -T for 1, 2, 5, 10, 15, 30 and 40 s (Figure 3 a–g) exhibited an EPR signal with three lines. The line intensities were 1:2:1 (aN = 16 G) which differed from the line intensities of

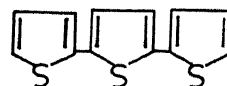


Figure 1. Chemical structure of alpha-terthienyl.

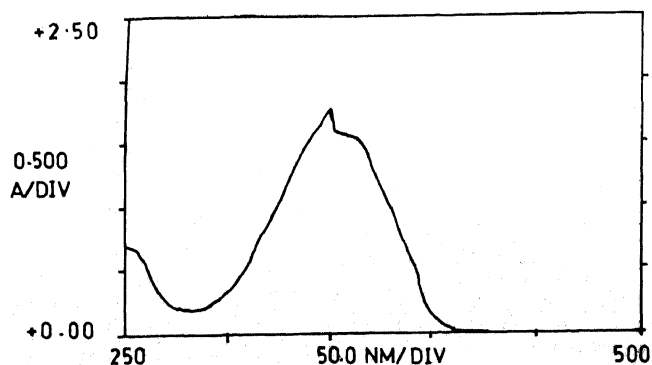
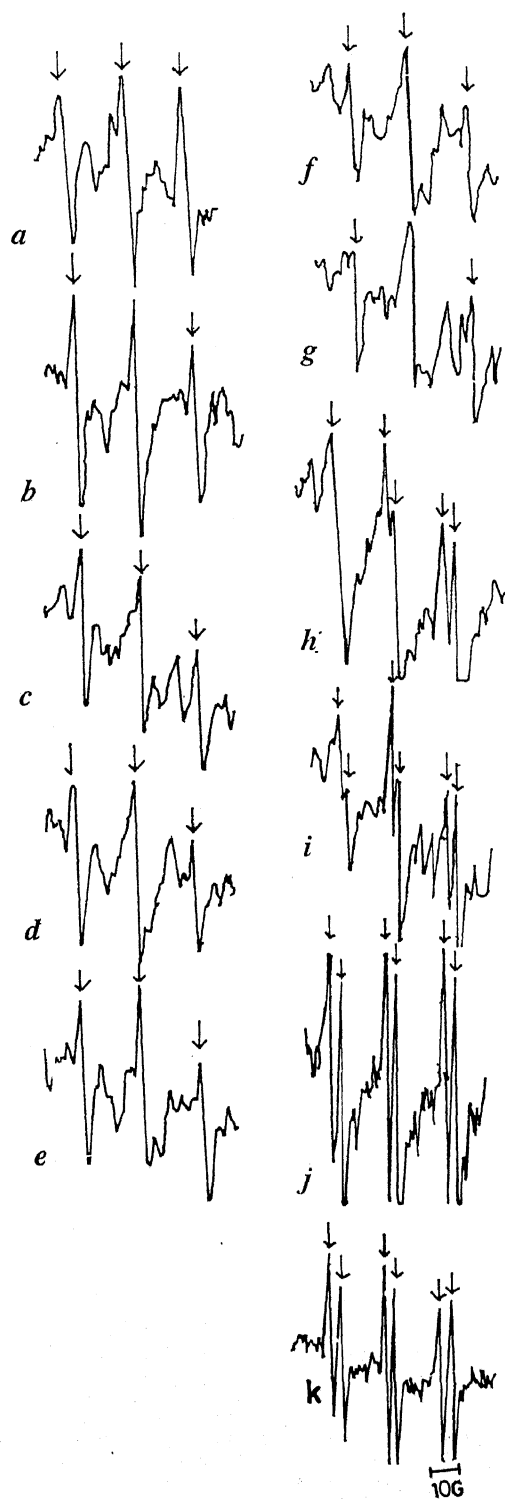


Figure 2. UV-VIS absorption spectrum of alpha-terthienyl showing a sharp absorption peak at 351 nm.

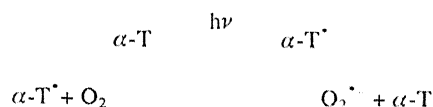


**Figure 3.** *a-g*, Formation of a three-line spectrum of alpha-terthienyl radical-PBN adduct; (indicated by arrows) after illumination of alpha-terthienyl with long wave ultraviolet light for 1, 2, 5, 10, 20, 30 and 45 s; *h-j*, Emergence of three more lines on further illumination of alpha-terthienyl for 60, 90 and 120 s, which is similar to superoxide anion radical; *k*, Reference spectrum obtained using artificially generated superoxide anion radical by pyrogallol autoxidation system (control).

the superoxide anion radical which exhibits a six line adduct with PBN ( $aN = 14.81$  G). An increase in the illumination to 60, 90 and 120 s (Figure 3 *h-j*) showed the emergence of 3 more lines and the spectrum thus obtained corresponded to the superoxide-PBN adduct (Figure 3 *j*); this can then be compared with a reference spectrum of superoxide anion radical (Figure 3 *k*), the control. No signal was obtained from the control samples.

Triplet thiophenes are excellent electron donors both in homogeneous and micellar solutions. Electron transfer from triplet thiophenes to suitable electron acceptors leads to strongly absorbing, rather stable thiophene radical cations, which in nanosecond-microsecond time scale are insensitive to oxygen. The main decay pathways of these radical cations appear to be second-order diffusion controlled reactions, and quenching of thiophene triplet by oxygen leads to only minor yields of the corresponding cation radicals<sup>13</sup>.

Our results provide evidence from EPR studies of the formation of an  $\alpha$ -T radical and its further conversion to a superoxide anion radical (Scheme 1). Studies concerning the cellular target(s) of  $\alpha$ -T have yielded conflicting data. MacRae *et al.*<sup>14</sup> were unable to detect chromosomal aberrations in cultured Syrian hamster cells following treatment with  $\alpha$ -T and UV-A (ref. 14). Kagan *et al.*<sup>15</sup>, on the other hand, reported that both calf thymus DNA *in vitro* and *Candida utilis* DNA *in vivo* were targets of  $\alpha$ -T (ref. 15).



**Scheme 1.** Formation of  $\alpha$ -T and superoxide anion radical.

The substantial effect of this thiophene and UV-A on the inactivation of membrane-bound cholinesterase in human erythrocyte<sup>16</sup> and on *E. coli* membrane proteins<sup>17</sup>, demonstrates the importance of these membrane components as the target of photodynamic attacks. Other reports have also indicated the damage of membranes in the photodynamic action of  $\alpha$ -T. For example, Wat *et al.*<sup>18</sup> demonstrated lesions in the cytoplasmic membrane of human erythrocytes irradiated in the presence of  $\alpha$ -T. This membrane damage might reflect involvement of either the lipid or protein components of the membrane. Experiments with liposomes entrapped with glucose as a membrane model system showed enhanced permeability to glucose and introduced high degree of unsaturation in liposomes involving lipid peroxidation in the presence of this thiophene and UV-A (ref. 19). Thus, a free radical role in these phototoxic effects is suggested.

Free radicals are well-known causes of major damage to biological membranes, resulting in inactivation of membrane-bound proteins, membrane lysis and lipid peroxidation; in turn this damage decreases the membrane fluidity and increases leakiness of the membrane<sup>20</sup>. Formation of free radicals from  $\alpha$ -T may also expose a number of non-target species to a free radical threat. Thus, some irreversible damage to those non-target species seems to be inevitable. Further studies are required to assess the role of  $\alpha$ -T on the non-target species, with special reference to free radicals.

1. Arnason, J. T., Philogene, B. J. R., Morand, P., Imire, K., Iyengar, S., Duval, F., Sovey-Breaw, C., Scaiano, J. C., Werstiuk, N. H., Hasspiller, B. and Downe, A. E. R., *Am. Chem. Soc. Symp. Series*, 1989, **387**, 164–172.
2. Philogene, B. J. R., Arnason, J. T., Berg, C. W., Duval, F. and Morand, P., *Chem. Ecol.*, 1986, **12**, 891–896.
3. DiCosmo, F., Towers, G. H. N. and Lam, J., *Pestic. Sci.*, 1981, **13**, 589–594.
4. Gommers, F. J. and Geerlings, J. W. G., *Nematologica*, 1973, **19**, 389–393.
5. Kagan, J., Prakash, I., Dhawan, S. N. and Jawroski, J. A., *Photochem. Photobiol.*, 1984, **8**, 25–33.
6. McLachlan, D., Arnason, J. T. and Lam, J., *Photochem. Photobiol.*, 1984, **39**, 177–182.
7. McLachlan, D., Arnason, J. T. and Lam, J., *Biochem. Syst. Ecol.*, 1986, **14**, 17–23.

8. Reyftman, J. P., Kagan, J., Santus, R. and Morliere, P., *Photochem. Photobiol.*, 1985, **41**, 1–7.
9. Bakker, J., Gommers, F. J., Nieuwenhuis, I. and Wynberg, H., *J. Biol. Chem.*, 1979, **254**, 1841–1844.
10. Nivsarkar, M., Kumar, G. P., Laloraya, M. and Laloraya, M. M., *Arch. Insect Biochem. Physiol.*, 1992, **19**, 261–270.
11. Arnason, J. T., Chan, C. F. Q., Wat, C. K., Downum, K. R. and Towers, G. H. N., *Photochem. Photobiol.*, 1981, **33**, 821–824.
12. Kim, S. J., Han, D., Moon, K. D. and Rhee, J. S., *Biosci. Biotech. Biochem.*, 1995, **59**, 822–826.
13. Kagan, J., Bazin, M. and Santus, R., *J. Photochem. Photobiol. B*, 1989, **3**, 165–174.
14. MacRae, W. D., Chan, C. F. Q., Wat, C. K., Towers, G. H. N. and Lam, J., *Experientia*, 1980, **36**, 1096–1097.
15. Kagan, J., Gabriel, R. and Reed, S. A., *Photochem. Photobiol.*, 1980, **31**, 465–469.
16. Yamamoto, E., Wat, C. K., MacRae, W. D. and Towers, G. H. N., *FEBS Lett.*, 1979, **107**, 134–136.
17. Downum, K. R., Hancock, R. E. W. and Towers, G. H. N., *Photochem. Photobiol.*, 1982, **36**, 517–523.
18. Wat, C. K., MacRae, W. D., Yamamoto, E., Towers, G. H. N. and Lam, J., *Photochem. Photobiol.*, 1980, **32**, 167–172.
19. MacRae, W. D., Yamamoto, E. and Towers, G. H. N., *Biochim. Biophys. Acta*, 1985, **821**, 448–496.
20. Nivsarkar, M., Kumar, G. P., Laloraya, M. and Laloraya, M. M., *Biochem. Syst. Ecol.*, 1993, **21**, 442–447.

Received 4 July 1998; revised accepted 15 February 1999

## Erratum

### Crystal structure of the peanut lectin–T-antigen complex. Carbohydrate specificity generated by water bridges

R. Ravishankar, M. Ravindran, K. Suguna, A. Surolia and M. Vijayan  
[*Curr. Sci.*, 1997, **72**, 855–861]

In the crystal structure of the complex, it was noticed that O4 in the GalNAc moiety of T-antigen (Gal $\beta$ 1-3GalNAc) was inappropriately positioned. This happened on account of the inadequacy of the geometrical restraints applied to this part of the molecule during refinement. O4 was re-fixed geometrically and 140 cycles of conjugate gradient refinement was carried out using XPLOR<sup>1</sup>. The final R-factor and R-free are 0.175 and 0.251, values identical to those obtained in the earlier refinement. The re-refined coordinates have been deposited in the PDB (code: 2TEP).

Expectedly, there is no significant change in the structure except in the position of O4. The protein carbohydrate interactions in the re-refined structure are listed in Table 1. The only change in them is an additional possible interaction between GalNAc O4 and Leu 212 N. Thus the main difference in interactions between the T-antigen and lactose complexes remains the additional water bridges in the former. Efforts are on to assess the effect of the possible additional interaction.

We thank Dr Remy Loris of Vrije Universiteit Brussel for pointing out this error which is deeply regretted.

1. Brünger, A. T., *X-PLOR Version 3.1 Manual*, Yale University, 1992.

Table 1. Peanut lectin–T-antigen interactions. Lengths in the PNA-lactose interactions are in parenthesis. Distances are in Å

| A. Hydrogen bonds |              |             |             |             |             |
|-------------------|--------------|-------------|-------------|-------------|-------------|
| Sugar atom        | Protein atom | Subunit 1   | Subunit 2   | Subunit 3   | Subunit 4   |
| Gal O3            | Asp83 OD1    | 2.76 (2.67) | 2.62 (2.43) | 2.72 (2.58) | 2.63 (2.49) |
|                   | Gly104 N     | 3.22 (3.08) | 2.99 (2.92) | 2.83 (3.07) | 2.88 (2.81) |
|                   | Asn127 ND2   | 2.76 (2.86) | 2.92 (3.00) | 2.76 (3.12) | 2.96 (3.02) |
| Gal O4            | Asp83 OD2    | 2.73 (2.59) | 2.66 (2.68) | 2.57 (2.64) | 2.91 (2.55) |
|                   | Ser211 OG    | 2.92 (2.62) | 3.24 (2.82) | 2.82 (2.66) | 2.55 (2.76) |
| Gal O5            | Ser211 OG    | 3.03 (3.12) | 2.99 (3.34) | 2.73 (3.09) | 2.96 (3.16) |
| Gal O6            | Asp80 OD2    | 2.85 (3.33) | 2.95 (3.39) | 3.48 (3.36) | 3.13 (2.98) |
| Glycosidic O      | Ser211 OG    | 3.24 (3.38) | 3.34 (3.86) | 3.20 (3.70) | 3.25 (3.81) |
| GalNAc O4         | Ser211 OG    | 3.09 (3.34) | 2.78 (3.31) | 3.07 (3.58) | 3.07 (2.98) |
|                   | Gly213 N     | 2.73 (2.92) | 2.88 (2.98) | 2.78 (3.29) | 2.76 (3.28) |
|                   | Leu212 N     | 3.34 (4.04) | 3.21 (4.08) | 3.01 (4.65) | 3.08 (4.06) |

### B. Water-mediated interactions (distances averaged over four subunits)

|                         |   |
|-------------------------|---|
| GalO2--W1--Glu129 OE1   | [O2--W1 = 3.03 (3.07); W1--OE1 = 3.30 (2.98)] |
| GalO2--W2--Gly104 N     | [O2--W2 = 2.91 (2.67); W2--N = 2.91 (3.15)]   |
| GalNAcO7--W3--Ile101 O  | [O7--W3 = 3.06; W3--O = 2.95]                 |
| GalNAcO7--W4--Leu212 N  | [O7--W4 = 2.78; W4--N = 2.83]                 |
| GalNAcO7--W4--Asn41 ND2 | [W4--ND2 = 2.65]                              |

Water-mediated interactions involving W3 and W4 do not exist in the Lactose complex

### C. Residues less than 4 Å from any sugar atom

Asp80, Ala82, Asp83, Gly103, Gly104, Tyr125, Asn127, Ser211, Leu212, Gly213, and Gly214.

## BOOK REVIEWS

**The Collected Papers of Albert Einstein – Volume 8 – The Berlin Years: Correspondence, 1914–1918.** A. M. Heutschal. English Translation, Princeton University Press, 41 William Street, Princeton NJ 08540, USA. 1998. 714 pp. Price: US \$39.50.

The English version of Volume 8 of Albert Einstein's Collected Papers has, for editorial reasons, been published ahead of Volume 7. This is part of the projected 40 volumes covering all of his work and correspondence. It spans the years 1914–1918, which coincides exactly with the First World War, and is devoted entirely to correspondence.

On the personal front, this period saw the separation from his first wife Mileva Maric, feelings on both sides being often expressed quite acrimoniously. (The divorce came in 1919, followed soon after by Einstein's marriage to his (also divorced) cousin Elsa). Professionally, Einstein had just moved in April 1914 from a Professorship at the Eidgenössische Technische Hochschule (ETH) in Zurich to a research position created specially for him by the Prussian Academy of Sciences in Berlin. And in his science this was the period of the tortuous progress towards the final formulation of his general theory of relativity, completed in November 1915. Later in this period he was to present his ideas on the interaction of radiation and matter leading to the celebrated A and B coefficients; the first application of general relativity to cosmology; and in 1917 a profound study of the quantization rules of the old quantum theory, involving deep topological aspects of classical dynamics.

There are close to 700 letters in this volume of more than 700 pages, covering many personal, professional, public and scientific matters. One can only recall and highlight a few chosen pieces, presenting telling and memorable quotations. Among the major correspondents were Mileva Maric, Elsa Einstein, Hendrik Lorentz, Arnold Sommerfeld, Paul Ehrenfest, Tullio Levi-Civita, David Hilbert, and Willem de Sitter; and following not far behind were Max Born, Max Planck, Hermann Weyl and Felix Klein. One notes that in this phase there were as yet no exchanges with Niels Bohr – that was still in the future.

The letters between Einstein and Mileva are quite painful – they show a relationship gone awry, and plenty of petty squabbling on financial and legal matters. In a memorandum and two letters all dated 18 July 1914, Einstein stipulates very strict rules of conduct to govern social contacts between them, including such conditions as these: '... you must leave my bedroom or office immediately without protest if I so request... you commit yourself not to disparage me either in word or in deed in front of my children...'. After all that has happened, a comradely relationship with you is out of the question... It remains possible that I'll regain a greater degree of confidence in you through proper behaviour on your part...'. So much rancour in separation. At the same time, in intimate and confiding letters to Elsa, he mentions the possibility of a divorce from Mileva, which came through only in 1919. In many letters to Mileva, Einstein details the amount of financial support he has provided for her and their sons, and at what cost to himself; and at one point he insists '... that the money in Prague be transferred to my name. I will have it credited to the children and am convinced that *this* is the safest way for the amount to go to the benefit of the children'.

Through this period, Einstein was deeply absorbed in his quest for the general relativity theory. It is well known that the way to the final result was full of wrong leads and mistaken hypotheses. Einstein had learnt the basic mathematics of Riemannian geometry and the absolute differential calculus from his Zurich classmate Marcel Grossmann, but in a July 1915 letter to Sommerfeld he says categorically that 'Grossmann will never lay claim to being co-discoverer. He only helped in guiding me through the mathematical literature but contributed nothing of substance to the results'. The extensive correspondence with the Italian mathematician Tullio Levi-Civita on the one hand, and with the master theoretical physicist Hendrik Lorentz on the other, are both profound and absorbing. On the mathematical side Levi-Civita was an accomplished master, one of the finest geometers of the Italian school; while Einstein had profound physical intuition and insight. Yet the expression

of the latter in the language of the former was exceedingly difficult, and many steps had to be retraced. It must have been this experience that Einstein had in mind when in a 1933 lecture he said: 'The years of searching in the dark for a truth that one feels but cannot express, the intense desire and the alternations of confidence and misgiving until one breaks through to clarity and understanding are known only to him who has himself experienced them'. In a March 1915 letter to Levi-Civita, Einstein says 'I also cannot help admiring the uncommon sureness with which you make use of a language that is foreign to you'; and in another place he pleads: 'I shall be delighted if next time you write to me in Italian ... even now I still enjoy being able to apply my modest knowledge of the Italian language... you can hardly imagine what a pleasure it gives me to receive such a genuine Italian letter. While reading, the finest memories of my youth come alive'. Through these letters pass claims and counter claims about the alleged tensorial behaviours of various field quantities under given groups of transformations.

One of Lorentz's very lengthy letters deals with Einstein's use of special co-ordinate systems while on the road to the general theory. He even chides the younger man thus: 'Are you not going a bit too far here by presenting a personal view as self-evident?' And in one of his replies Einstein says: 'If anyone had to relive exactly the same struggles here in the considerations on general relativity, I'd ardently wish that it be you'.

It is part of history that towards the end in November 1915, David Hilbert too joined in the race towards the general theory. Claims of priority in this matter have only very recently been settled in favour of Einstein as the first discoverer of the general field equations of gravity. Einstein rightly criticized Hilbert's approach as too closely tied to a specific model for matter (the Mie theory); and in a triumphant 18 November 1915 letter he told Hilbert: 'Today I am presenting to the Academy a paper in which I derive quantitatively out of general relativity, without any guiding hypothesis, the perihelion motion of Mercury discovered by Le Verrier. No gravitation theory had achieved this until now'. Einstein's elation is captured in these well-known lines to

Sommerfeld: '... in the last month I had one of the most stimulating, exhausting times of my life, indeed also one of the most successful. I could not think of writing' (28 November 1915); '... You will be convinced of the general theory of relativity when you have studied it. That is why I am not mentioning a word in its defense' (8 February 1916).

Karl Schwarzschild's exact solution for the field of a gravitating mass came soon after Einstein's work; and the latter's appreciation of the result was thus expressed: 'I would not have expected that the exact solution to this problem could be formulated so simply. The mathematical treatment of the subject appeals to me exceedingly'. This incident really seems a precursor to C. G. Darwin's finding the exact solution to the relativistic wave equation for the electron in a Coulomb field, which Dirac had left undone after discovering the equation itself! Of Hermann Weyl's systematic exposition of the general theory in his book *Space, Time, Matter*, Einstein had this to say: 'I am reading with genuine delight the correction proofs of your book, which I am receiving sheet by sheet. It is like a symphonic masterpiece. Every word has its relation to the whole, and the design of the work is grand. What a magnificent method the infinitesimal parallel displacement of vectors is for deriving the Riemann tensor! How naturally it all comes out' (8 March 1918); 'Busily involved in studying the details of your book, I constantly admire anew the beauty and elegance of your derivations' (18 April 1918).

There is some correspondence with the great Swiss-French writer Romain Rolland (who incidentally was so drawn to India), on matters of war, politics, conscience and the role of the intellectual in trying times. These remind us of the backdrop against which the scientific advances were being made. On 15 September 1915, Einstein wrote to Rolland: 'One of the most disheartening phenomena of this terrible time is that in many cases intellectuals have completely lost their composure'. And in a 23 August 1917 letter Rolland says: '... Evil spreads like a splotch of oil... I am awaiting salvation (if it is meant to come) from other – social – forces; and if it does not come, ... by God! it will not have been the first time that a pow-

erful civilization has crumbled. Life will know very well how to blossom again from the ruins ... The soul is never conquered – except when it consents to it. It is ahead of its times'. In a public appeal to Hilbert and many others on these issues, Einstein proclaims: 'This serious situation places those, who through fortunate intellectual achievements have gained an elevated position among scholars throughout the entire civilized world, before a mission they must not evade: They must make a public declaration that could serve as support and consolation for those who in their solitude have not yet lost their belief in moral progress'.

So many names who have passed into the history of physics and other realms come alive in these pages. For those of an older generation, here is proof that with the current decline in the art of correspondence, the expression and hammering out of profound ideas through such dialogue is likely to suffer. One is also left with a strong impression of a supremely gifted intellect having to concern itself also with the petty and the mundane concerns of life. Grappling with the profoundest questions of nature is no insurance against having to also deal with and resolve personal relationships, and arrange one's material affairs with some degree of satisfaction. A complete, a full life is made up of all of these.

N. MUKUNDA

*Centre for Theoretical Studies and  
Department of Physics,  
Indian Institute of Science,  
Bangalore 560 012, India*

**Annual Review of Plant Physiology  
and Plant Molecular Biology 1998.**  
Annual Reviews Inc., 4139, El Camino  
Way, Palo Alto, CA 94603-0139, USA.  
Vol. 49. 832 pp. Price: Individuals, US  
\$65. Institutions, US \$130.

Like children who look forward to receiving a gift on their birthday, many of us look forward to seeing the new *Annual Review of Plant Physiology and Plant Molecular Biology*.

The present volume has 28 chapters and a prefatory chapter by Sussex on

'Plant Development'. In fact, there are four other chapters that also deal with the same theme. Mandoli discusses the body plan and development in *Acetabularia*, an organism that has fascinated developmental biologists for a long time. This chapter describes in detail the spatial and temporal controls in development and is one among the few chapters in this volume with good explanatory and summary figures. Koonneef *et al.* have summarized the work on flowering, especially its onset and the timing. They clearly emphasize the importance of molecular genetics in understanding this complex developmental process. Figure 2 in this chapter amply demonstrates how different gene products, and their interaction with each other is essential to convert a vegetative meristem to a reproductive one. Gasser *et al.* have described the genetic regulation of ovule development in sexual plant reproduction.

Leon *et al.* have discussed the overriding influence of nucleus in the development of mitochondria and chloroplasts. In fact, during the last few years many new genetic loci have been defined whose function in early chloroplast development is not known. In another chapter, the role and functions of brassinosteroids during plant development is discussed by Clouse and Sasse. Although research on brassinosteroids was started 3 decades ago, and a review on this was published in this series in 1988 by Bhusan Mandava (an Indian scientist working at the USDA, Beltsville), yet it is only during the last few years, through the application of molecular genetics, that the importance of this group of regulators has been convincingly shown in normal plant development. In *Arabidopsis*, brassinosteroids signal transduction has been elucidated and is well described in this chapter.

Besides these topics, there are six more chapters that deal with signal transduction, development and gene expression. Schwechheimer *et al.* deal with plant transcription factors. The mechanism of ABA-mediated signal transduction is covered by Leung and Giraudat. ABA is an important hormone having a role in seed maturation and mediates many stress-related responses. Although ABA receptor is not yet known, the intermediates in ABA-signal

## BOOK REVIEWS

transduction and ABA-responsive *cis*-elements have been well characterized. The chapter on DNA methylation as a mechanism of gene control, by Finnegan *et al.* from Peacock's laboratory, Canberra, clearly brings out the data related to the loss of DNA methylation affecting plant development. It is becoming increasingly clear that in addition to other mechanisms, DNA methylation causes transgene silencing and this aspect too is covered in this chapter. Signalling mechanisms in relation to hormone-induced development in mosses is reviewed by Schumaker and Dietrich. Even in these lower organisms, calcium seems to play an important role in development. In a separate chapter, Zielinski has emphasized the role of calcium as a signal in higher plants and brought out the importance of regulation of calmodulin binding proteins. Argüello-Astorga and Herrera-Estrella provide an interesting review on the evolution of light-regulated plant promoters. Light is one of the important factors affecting plant development and this is achieved via modulating the expression of genes. A detailed analysis of various light regulatory *cis*-elements has been reported for a number of genes. While the evolution of a gene across various phyla has been discussed earlier, in this chapter, with the help of a few studies, the authors have attempted to describe how the promoter functions would have evolved from primitive land plants to an angiosperm ancestor and then diverged to monocot and dicot plants.

There are about a dozen chapters that broadly deal with signal transduction, gene expression and development. Rightly so, the prefatory chapter of this volume is written on 'Themes in Plant Development'. In his concluding remarks, Sussex writes 'there is huge increase in the number of scientists working in the fields that can broadly be defined as developmental plant biology. In my early years, it was rare to find another person working on the same question that I was. Now it is usual to find several labs working on the same genes in the same plant'.

Somewhat related to the area of developmental biology and gene expression, there are three other chapters. One is on plant pre-mRNA splicing mechanism by Brown and Simpson. The other,

which is well-timed, is on *Synechocystis* by Kotani and Tabata. The entire genome of this cyanobacterium has been sequenced and it carries a total of 3168 protein coding genes. All the information about this is available at <http://www.kazusa.or.jp/cyano>. Recently, using this data bank similar genes for two-component signalling system were reported in *Arabidopsis* and tomato. In fact, the translated amino acid sequence of str 0473 was found to be similar to photochrome *c* in higher plants and the gene product has been found to have kinase activity. An analysis of the whole sequence of *Synechocystis* will take time; nevertheless, this is an important chapter to draw the attention of plant biologists to the area of bioinformatics and functional genomics. The chapter by Dawe on meiotic chromosomal organization has brought together various results in this area of research. While there is an increase in research activity towards understanding of mitotic cell cycle controls at the molecular level, yet meiotic programme is still not well worked out in plants. A number of plant homologs of meiotic regulatory and functional genes have been found, but the molecular basis of switching off mitosis and switching on meiosis is hardly known. I am sure that in view of its importance in engineering apomixis in crops, this field will elicit further interest.

A number of chapters deal with photosynthesis, chlorophyll and carotenoids. Merchant and Dreyfuss discuss the assembly of chloroplast iron-sulfur centres, plastocyanin, Mn-centre and cytochromes. Details of photosynthetic cytochrome *c* are given in a review by Kerfeld and Krogmann. The reader is also referred to an article by Suzuki *et al.* on chlorophyll biosynthesis in *Annual Review of Genetics* (1998). Schnell has very nicely reviewed the present concepts of protein targeting to thylakoid membranes. There is a chapter on the regulation of genes of carotenoid biosynthesis by Cunningham and Gantt. It encompasses the structure and function of genes involved in the biosynthesis of carotenoids and also focuses on the possibility of metabolic engineering to modify carotenoid content and composition. This is beautifully reflected in Figure 1 of the chapter where the bacte-

ria were made to write the carotenoid they had accumulated. The other chapters dealing with biosynthesis are those of Benning on sulfolipid sulfoquinovosyl diacylglycerol, plant cell wall proteins by Cassab; lignin biosynthesis by Whetten *et al.* and fatty acid modification by Shanklin and Cahoon. In his article on Plant P-450's, Chappe has listed all the cloned genes encoding Plant P-450-dependent monooxygenases, which are a large group of heme-containing enzymes that generally catalyse NADPH- and O<sub>2</sub>-dependent hydroxylation reactions. It may be relevant to mention that some of the products of P-450 genes are involved in biosynthesis of brassinosteroid and gibberellins which have a major role in regulating plant development. One of the important areas of research in plants is to understand the mechanisms they adopt for their survival under stress conditions. In this context, Noctor and Foyer have discussed the role of ascorbate and glutathione as antioxidants under oxidative stress.

There are a few chapters on ions transport and phytoremediation. The role of boron, a very important element for many plant responses, is reviewed by Blevin and Lukaszewski. The review by Fox and Guerinot takes stock of genes whose products are involved in the transport of K<sup>+</sup>, Ca<sup>2+</sup> and Cu<sup>2+</sup>, Mn<sup>2+</sup> and Zn<sup>2+</sup>. It is now shown that the level of calcium, which as an important second messenger in plants, is regulated by different transport systems. In *Arabidopsis*, 5 genes have been identified which code for calmodulin stimulated Ca<sup>2+</sup>-ATPase, calmodulin insensitive Ca<sup>2+</sup>-ATPase and Ca<sup>2+</sup>/H<sup>+</sup>-Antiporter and these are localized on chloroplast, endomembrane, ER or tonoplast. The review also includes a compilation of a list of genes whose products are involved in micronutrient transport in plants. Most of this work so far seems to be restricted to *Arabidopsis*, barley and rice. In their review, Rea *et al.* have discussed the transport of other substances like sugars, peptides, alkaloids, lipids, etc. It has now been shown that plants do have proteins belonging to the ABC (ATP-binding cassette) superfamily. In this context two classes have been identified, viz. multidrug resistance proteins (MDR) and multidrug associated proteins (MRP). This review

essentially focuses on the role and function of MRPs. Now, the role of MDRs is also being analysed in detail in plants. It is remarkable that certain plants have the ability to take up, concentrate and metabolize toxic heavy metals and organic pollutants in soil and water. The field of phytoremediation is growing for obvious benefits. Research in this will not only provide solutions to environmental and health problems, but will also give an insight into the physiology of these plants that make phytoremediation possible. This and many other related issues are reviewed and discussed by Salt, Smith and Raskin.

As in previous issues, this volume also has a wealth of recent information on important topics. It is becoming absolutely clear that for a deeper understanding of various phenomena, in plant physiology and development, greater input from genetics, molecular biology and recombinant DNA technology will be required. An era of plant genomics has already set in and we look forward to an exciting phase in plant research in the next decade. Presently I recommend that this volume should find a place on the personal book-shelf of all plant biologists.

S. K. SOPORY

*International Centre for Genetic Engineering and Biotechnology,  
Aruna Asaf Ali Marg,  
New Delhi 110 067, India*

**Annual Review of Immunology 1998.**  
William E. Paul (ed.). Annual Reviews Inc., 4139 El Camino Way, Palo Alto, CA 94303-0139, USA. Vol. 16. 714 pp. Price: Individuals, US \$69; Institutions, US \$138.

The 1998 issue of the *Annual Review of Immunology* contains several interesting articles on different areas of active research in immunobiology. These may be grouped under the following headings: cytokines, cell surface receptors, transcription factors, immune response to disease, signal transduction and interactions of T cells with antigen presenting cells (APC).

Reviews on cytokine research covered articles on IL-12, TGF- $\beta$  and the role of IL-1 antagonist. IL-12 is composed of two subunits, p35 and p40, and is important in mediating Th1-mediated responses to pathogens and some diseases. Using mice that lack each subunit, recent evidence points to different effects of individual IL-12 subunits. For example, p35 $^{-/-}$  mice are resistant to infection by *Listeria* whereas p40 $^{-/-}$  mice are susceptible to infection by *Listeria*, suggesting that p40 alone may have independent functions. Mechanisms responsible for the suppression of inflammatory responses are being identified. A review on TGF- $\beta$  discussed the myriad activities mediated by this cytokine as well as the description of a unique population of Th3 type of T cells that secrete TGF- $\beta$ , IL4 and IL-10. Different forms of IL-1 receptor antagonists are found which bind to IL-1 receptors and appear to be important in reducing inflammatory reactions and endotoxin-induced injury.

The importance of CD40-CD154 interactions in B cell responses is well known, and the importance of these interactions in T cell priming and differentiation, enhancing macrophage function, activation of NK cells and controlling infections were highlighted in a chapter by Grewal and Flavell. Levy *et al.* reviewed information on CD81, a cell surface molecule with four transmembrane spanning domains, which is part of the complex that lowers the threshold for activation on B cells. Although different antibodies to CD81 have effects on T cell development, the phenotype of CD81 $^{-/-}$  mice suggests that the primary role of CD81 is in B cell activation but not in T cell development or activation.

Mammals contain large amounts of natural antibodies (i.e. predominantly IgM antibodies produced by the body in the absence of an immune response) that play an important role in innate immunity. Recent data suggest that complement binds to natural antibody immune complexes and plays an important role in determining host resistance to pathogens. On the other hand, Fc receptors bind to IgG immune complexes and play an important role in mediating inflammatory responses. Complement links the innate immune system with adaptive immune system as Ag-complement

complexes are recognized by the complement receptors, CD21 and CD35, which are expressed on follicular dendritic cells (FDCs) and B cells. CD21 is also a part of the B cell receptor (BCR) and responsible for lowering the threshold of B cell activation. This may explain an old observation that antigen complexed to complement is several-fold more immunogenic than antigen alone. Recent data also suggest that complement and its receptors are important in the elimination of self-reactive (autoimmune) B cells.

In a well-written overview on B cell development, recombination of Ig genes, somatic mutation, the significance and roles of different transcription factors were discussed by Henderson and Calame. Some transcription factors, e.g. PU.1, Ikaros, play an important role during development whereas others, e.g. Oct-2, Ets-1, have redundant functions. The transcription factor NFkB plays an important role in the immune response from *Drosophila* to mammals. Two recent discoveries have enhanced interest in this field: first is the discovery of the I $\kappa$ B inhibitor kinase, which phosphorylates I $\kappa$ B in an inducible manner. After phosphorylation, I $\kappa$ B is degraded and NFkB enters the nucleus and activates several immune function-related genes. The second discovery centres around the anti-apoptotic function of NFkB. Most current volumes contain an article on apoptosis and this review is not an exception. The Bcl2 family of molecules which are important in cell death were discussed by Chao and Korsmeyer. It appears that the ratio of molecules that act as death agonists compared to the levels of death antagonists determine susceptibility to death stimulus. There is also interesting data suggesting that Bcl family of proteins belong to a family of pore forming proteins.

Systemic lupus erythematosus (SLE) is caused when the body produces antibodies to host DNA and other self proteins. It is a complex disease and both major histocompatibility complex (MHC) and non-MHC genes are involved in disease progression. Genome wide linkage studies have identified twelve non-MHC disease loci in a mouse model of SLE and the identification of the actual genes will help in understanding the contributions of these

## BOOK REVIEWS

genes in disease. Hodgkin's disease is a common malignant lymphoma; current evidence suggests that these lymphomas predominantly arise due to clonal proliferation of germinal B cells and infection by Epstein-Barr virus (EBV) plays an important role in this process. Genetic variations in human leukocyte antigen (HLA), tumour necrosis factor, chemokine receptors, vitamin D3 and interferon- $\gamma$  receptors have been implicated in affecting progression of several infectious diseases. Whole genome analysis will reveal additional loci of importance and these studies may be important in designing effective protective mechanisms in combating various diseases which is an exciting prospect.

Xenotransplantation, the transplantation of organs/tissues between members of different species, has received attention due to the growing needs for additional organs. Recent progress in making xenotransplantation possible involves the modulation of key molecules responsible for initiating immune responses, the removal of preformed natural antibodies and the use of genetically engineered organs that lack key molecules responsible for hyperacute rejection. Research in this area may increase the chances of xenografts to be

accepted by recipients. Waldmann and Cobbold discuss an interesting research area on the use of non-depleting monoclonal antibodies to different lymphocytic cell surface markers (CD4, CD11a, etc.) to induce tolerance. This strategy has the potential to be used to treat autoimmune diseases and transplantation. Current evidence suggests that regulatory T cells may be induced by these antibodies, resulting in tolerance.

There has been progress in elucidating TCR-MHC structures and role of oligomers of TCRs (minimum number is 3) in stimulating T cells. Mark Davis *et al.* discuss a new model to explain how immunoglobulins and TCR interact with antigens especially with emphasis on the diversity of the CDR3 regions of immunoglobulins and TCRs. Dimerization between proteins occurs in several biological systems, including cell surface receptors (TCRs, BCRs, TGF- $\beta$  receptors) and transcription factors (e.g. BCL-2). Approaches to study the role of dimerization between proteins include the use of CID (chemical inducers of dimerization) which are low molecular weight organic molecules that enter cells and induce dimers of two protein targets – these approaches may help in studying signal transduction pathways *in vitro*.

In addition to the excellent reviews mentioned above, a wide variety of areas ranging from T cell memory, development of a malaria vaccine, Janus family tyrosine kinases (JAKs) and signal transducers and activators of transcription (STATs), MHC class I antigen processing, NK receptors, positive and negative signalling in lymphocytes have been covered. Finally, the autobiographical piece by Metzger makes for compelling reading. He muses over the early influences that shaped his scientific career and foray from protein chemistry to immunology, especially the characterization of IgE and its receptor. He is most optimistic of those who are beginning their scientific career now and says, 'I feel they will have a fantastic voyage and am confident they will not fall off the edge; not because I think the universe of knowledge is round but because I think it is unbounded'. This volume lives up to its reputation and offers plenty of knowledge and interesting reading.

DIPANKAR NANDI

*Department of Biochemistry,  
Indian Institute of Science,  
Bangalore 560 012, India*

---

# Fifth World Conference on Injury Prevention and Control

**5–8 March 2000, New Delhi**

The Fifth World Conference on Injury Prevention and Control will be held in Delhi during 5–8 March 2000. This is the fifth conference in a series of which the first four were held in Stockholm, Atlanta, Melbourne and Amsterdam. About 1,000 professionals from around the world have attended each conference. The conference theme is 'Sharing Experiences: Blending Perspectives'. The conference will adopt a Charter on People's Right to Safety. Twelve satellite meetings are also being organized just before or after the conference. The conference encourages participants to exchange ideas and practical experiences in injury control and safety promotion in the following sectors:

Transportation  
Sports and leisure  
Violence and suicide  
Legislation  
Education and safety promotion

Work place  
Domestic accidents  
Emergency and pre-hospital care  
Environmental changes  
Safe communities

The Indian Institute of Technology, Delhi, is hosting the conference.

Sponsors: World Health Organization, Ministry of Surface Transport, Government of India, National Highway Traffic Safety Administration, USA, Insurance Institute of Highway Safety, USA, Confederation of Indian Industry, Society of Indian Automobile Manufacturers, Government of the State of Uttar Pradesh, India.

LAST DATE for Abstracts: 20 June 1999

## FURTHER INFORMATION:

Ms Arati Walia, CONFER/FIWOCO, D-1 Kalindi Colony, New Delhi 110 065, India  
Tel: ++91 11 691 9377, 684 9399 Fax: ++91 11 684 8343, 692 9541  
E-mail: awconfer@del2.vsnl.net.in Website: <http://www.ciionline.org/fiwoco/>

## B. D. BANGUR AWARD

Indian Carbon Society invites applications from Indian scientists/technologists/engineers who have contributed to the science and technology of carbon materials in India for the 1999 'B.D. Bangur Award' instituted by Graphite India Limited, which is one of the leading manufacturers of graphite products in India.

The award consists of cash amount of Rs 30,000/- and a medal and scroll. The selected person would be required to give a 45-minute lecture during the CARBON'99 conference which is being organized on 28–29 October 1999, by the Indian Carbon Society at New Delhi.

Application forms can be obtained from the office of the Indian Carbon Society, at the address mentioned below. Completed application forms must reach the office of the Society latest by 30 June 1999.

Dr O. P. Bahl  
Indian Carbon Society  
C/o. National Physical Laboratory  
Dr K. S. Krishnan Marg  
New Delhi 110 012  
Phone: 11-5786086  
Fax: 11-5764189 and 11-5752678  
E-mail: opbahl@csnpl.ren.nic.in

# INDIAN SCIENCE CONGRESS ASSOCIATION

## YOUNG SCIENTISTS AWARD PROGRAMME

To encourage young scientists, the Indian Science Congress Association under its above programme introduced a number of awards in January 1981. Each award carries a cash amount of Rs 5,000/- and a certificate of merit.

1. Only members of the Association are eligible for consideration for the award. The upper age limit of the candidates for the award is 32 years (as on 31 December 1988).
2. Two copies of biodata, including full name and address along with the date of birth (duly supported by attested copy of the certificate), membership status and number, research experience (in case of joint authorship, the candidate has to be acknowledged by the other author(s) in terms of a certificate as having made the major contribution) and certification that the work has been carried out in India and has not been submitted for any award, should be appended to the complete paper.
3. Three copies of full papers along with their abstracts in triplicate (not exceeding 100 words) should reach the office of the General Secretary (Head Quarters), Indian Science Congress Association, 14, Dr Biresh Guha Street, Calcutta 700 017, not later than 20 September 1999. At the top of each copy of the paper and its abstract, the name of the Section where the paper is to be presented, should be indicated.
4. A young scientist could present only one paper in only one section (and not a second paper with the same or any other context in any other section) for the year under consideration.
5. Full papers will be assessed for their content and at most 6 young scientists in each section will be invited to make an oral presentation of their papers during the Science Congress Session. They will be provided with admissible travelling and daily allowances by the ISCA (maximum of first class train fare by convenient shortest route to and from residence/Institute to venue and DA as per ISCA rules).
6. The final selection for the awards will be done by a duly constituted committee and will be announced on the last day of the congress.

# INDIAN INSTITUTE OF HORTICULTURAL RESEARCH (ICAR)

## Hessaraghatta Lake Post, Bangalore 560 089

### ADVERTISEMENT NO. 1/99

Applications are invited for the following temporary posts at the Indian Institute of Horticultural Research, Hessaraghatta, Bangalore under the administrative control of ICAR.

1. *Senior Research Fellow* : Two posts  
*Scale of pay* : Rs 5000/- for first two years and Rs 5600/- for 3rd year  
*Qualification* : *Essential*  
M.Sc. in Agri./Hort./Biochem./Molecular Biology/Biotechnology/  
Applied Botany/Genetic Engineering/Life Sciences  
*Desirable:*  
Experience in Molecular biology
2. *Senior Research Fellow* : Two posts  
*Scale of pay* : Rs 5000/- for first two years and Rs 5600/- for 3rd year  
*Qualification* : M.Sc. in Agri./Hort./Biochem./Molecular Biology/Biotechnology/  
Applied Botany/Genetic Engineering/Life Sciences  
*Desirable:*  
Experience in Molecular biology
3. *Senior Research Fellow* : Two posts  
*Scale of pay* : Rs 5000/- for first two years and Rs 5600/- for 3rd year  
*Qualification* : *Essential*  
M.Sc. in Agri./Hort./Biotechnology/Plant Physiology/Botany/Applied  
Botany/Life Science  
*Desirable:*  
Experience in tissue culture
4. *Senior Research Fellow* : One post  
*Scale of pay* : Rs 5000/- for first two years and Rs 5600/- for 3rd year  
*Qualification* : *Essential*  
M.Sc. (Ag) Entomology or M.Sc. Zoology  
*Desirable*  
Knowledge on the rearing of insects and computer operation
5. *Senior Research Fellow* : One post  
*Scale of pay* : Rs 5000/- for first two years and Rs 5600/- for 3rd year  
*Qualification* : *Essential*  
M.Sc. in Biotechnology/Botany Hort./Life Sciences (specialization  
in genetic transformation)

Posts no. 1–3 are sanctioned for a period up to 24 January 2004, under the NATP scheme 'Biotechnological approaches for the improvement of horticultural crops in the centre/Team of

excellence'. Candidates should have aptitude and motivation to carry out research in biotechnology. Selected candidates would be allowed to register for their Ph.D. degree.

Post no. 4 is sanctioned for a period up to 30 June 2001, under the *ad hoc* scheme 'Development of biocontrol technology for the exotic spiralling whitefly in horticultural crops with special reference to guava'.

Post no. 5 is sanctioned for a period up to 5 October 2001, under the *ad hoc* scheme 'Genetic transformation... resistance to pathogens'.

Scale of pay is fixed per month without allowances.

Age: 35 years or below as on the last date for receipt of application (relaxable in case of SC/ST and other exempted categories of candidates to the extent permissible under Rule).

Applicants should have registered their names in the Employment Exchange. Otherwise their applications will not be considered. A separate application should be submitted for each post.

Applications for the above posts may be made on plain paper in the prescribed format given below containing particulars/information duly supported by attested copies of educational/technical experience certificates, etc. The applications for the above posts should reach the Director, Indian Institute of Horticultural Research, Hessaraghatta Lake Post, Bangalore 560 089 within fifteen days from the date of this advertisement.

Incomplete applications and the applications received after the last date will not be considered.

Candidates already in service should send their applications through proper channel.

No TA/DA will be paid to the candidates called for interview.

### FORMAT

Advt No..  
Item No.

Application for the post of

Affix recent  
passport size  
photograph

1. Name in full  
(in capital letters)
2. Father's/husband's name
3. Present postal address
4. Permanent address
5. Place and date of birth
6. Age as on closing date of advertisement

7. Nationality :
8. Sex :
9. Name of the Employment Exchange, Registration no. and date of validation of registration :
10. Whether SC/ST :
11. Qualification: Copies of degree certificates/marks sheets to be enclosed

| Name of the Exam | Name of Board University | Class/ Divn | Percentage | Year of passing | Subjects taken |
|------------------|--------------------------|-------------|------------|-----------------|----------------|
| 1                | 2                        | 3           | 4          | 5               | 6              |

12. Details of experience (if employed)

| Name of the employer | Designation | Pay scale & salary drawn per month | Nature of employment Temp./QP/permanent | Date of joining | Date of leaving |
|----------------------|-------------|------------------------------------|---|-----------------|-----------------|
| 1                    | 2           | 3                                  | 4                                       | 5               | 6               |

13. List of publications :

I hereby declare that all the statements made above are true, complete and correct to the best of my knowledge and belief. I also declare that (i) I have never been punished or debarred from Government (Central/State), Autonomous Organizations and ICAR service (ii) I have not been convicted by a Court of law for any offence. In the event of any information being found false/incorrect/ineligibility being detected at any time before or after the examination/interview, action may be taken against me and I shall be bound by the decision of the employer.

Place:

Date:

Signature of the candidate

**Note:** Candidates who can join duty within one month of the date of issue of appointment order only need apply.

## Transformation Biologists for Monsanto Research Centre, Bangalore

Monsanto Research Centre, Bangalore, is recruiting a Ph D scientist with experience to lead the Transformation Programme in ornamental plants. The position requires constant communication within the group and with various collaborators, particularly the team in St. Louis, USA. Excellent communication and leadership skills are essential. There is also an opening for M Sc level scientist in the area of sugarcane transformation.

Monsanto is a world leader in the discovery and development of agricultural products based on advanced chemistry and biotechnology. Monsanto has recently established a state-of-the-art research centre in Bangalore, which is conducting research on crop protection, genomics and transformation technology. The Centre seeks highly motivated professionals to work in an interactive team-based environment. Successful candidates will be responsible for the development and improvement of transformation systems to generate genetically modified crops.

**Qualifications:** Ph D degree from reputed Universities, in the area of tissue culture/plant transformation/regeneration for position 1 (ornamental plants) and M Sc in biological/life sciences with experience in similar areas as above, for position 2 (sugarcane). The responsibilities include developing, improving and evaluating transformation systems. The ability to work in a team-based environment and interactions with different groups are necessary. Additional consideration will be given to individuals with experience in ornamental crops for position 1 and in sugarcane for position 2.

**Contact:** The Director, R&D, Monsanto Research Centre, Opp: J.N. Tata Auditorium, Indian Institute of Science Campus, Bangalore 560 012. Phone: 080-3460370/4, Fax: 080-3460369, e-mail: k.p.gopinathan@monsanto.com.

## Current Science

### SUBMISSION IN ELECTRONIC FORM

**A**uthors who have been informed of acceptance of their manuscripts may send the final version in electronic form on floppy diskette (3.5" preferred; IBM PC format only, *not* Macintosh). The text of the manuscript only should be supplied as a plain ASCII file with no formatting other than line and paragraph breaks. (Wordstar 5.5 or 7.0 and Microsoft Word for Windows 6.0 are acceptable, but ASCII is preferred.) A hard copy of the text, with all typesetting information (italics, bold, mathematical type, superscripts, subscripts, etc.) must accompany the electronic copy. Tables and figures must be supplied only as hard copy. The diskette must be labelled clearly with the following: manuscript number, file name, file information (ASCII or Wordstar, version number, etc.)

Text may also be transmitted as ASCII only by e-mail to currsci@ias.ernet.in.

We expect that electronic submission will result in quicker processing for publication.

# INDIAN SCIENCE CONGRESS ASSOCIATION

## ANNOUNCEMENT FOR AWARDS: 1999–2000

1. **Professor Hira Lal Chakravarty Awards:** Applications in prescribed forms are invited from Indian scientists, below 40 years of age on 31 December 1998 with Ph.D. degree, having significant contributions in any branch of Botany – either pure or applied. There are two awards, each carries a cash amount of Rs 4000/- and a certificate. The awards are given on original independent published work carried out in India within three years prior to the award. Each awardee will be required to deliver a lecture on the topic of his/her specialization during the Annual Session of the Indian Science Congress in the Section of Botany. Last date for submitting applications is 15 July 1999.
2. **Pran Vohra Award:** Applications in prescribed forms are invited from Indian scientists below 35 years of age on 31 December 1998 with Ph.D. degree in Agricultural Sciences from any University or Institution in India, having made significant research contributions in any branch of Agricultural Sciences. Only research done in India will be considered for the award. The award carries a cash amount of Rs 10,000/- and a certificate. The awardee will be required to deliver a lecture on the topic of his/her specialization during the Annual Session of the Indian Science Congress in the Section of Agricultural Sciences. Last date for submitting applications is 15 July 1999.

For proforma of application forms and necessary information, please write to the General Secretary, Indian Science Congress Association, 14, Dr Biresh Guha Street, Calcutta 700 017.

## NORTH–EASTERN HILL UNIVERSITY

### PERMANENT CAMPUS, SHILLONG 793 022

Applications are invited for the position of Junior Research Fellow (one) in the Department of Atomic Energy sponsored research project titled 'Neutrino Masses and Mixing in Unified Theories' under the supervision of Dr M. K. Parida, Department of Physics, North Eastern Hill University, Shillong 793 022. The candidate should have a Master's degree in Physics with at least 55% marks. Those who have appeared in the final examination and whose results are awaited may also apply. The value of the fellowship is Rs 5000/- p.m. In addition, other allowances as per DAE rules are also admissible. Applications on plain paper giving full details of educational qualifications together with copies of certificates should reach Dr Satish Kumar, Institute of Self-Organizing Systems and Bio-Physics, North Eastern Hill University, Permanent Campus, Shillong 793 002, Meghalaya within one month from the date of publication of this advertisement.

# BIBLIOMETRIC ANALYSIS SERVICES

Indian scientists and researchers contribute nearly 40,000 R&D papers annually, most of them published in more than 700 Indian S&T journals and the rest of foreign origin. The quality of research output of a laboratory or a scientist is based on their research contribution as reflected through their research articles in scientific journals.

Bibliometric analysis service evaluates and analysis the scientific research output of institutions, group of scientists and individual scientists using specialised techniques to rank an organisation or individual scientist and their work.

Citation analysis of research papers is also carried out to know how many times a given paper is cited in the world literature. Get in touch with us for more details.

## INDIAN SCIENCE ABSTRACTS (ISA)

Indian Science Abstracts (ISA) is a semi-monthly abstracting journal reporting scientific work done in India since 1965. Original research articles including short communications, review articles, and informative articles published in scientific and technical periodicals, proceedings of conferences and symposia, monographs and other publications, as well as patents, standards and theses are reported in ISA.

The disciplines covered in ISA are: Agriculture, Anthropology, Architecture, Building Industry, Chemistry, Commerce, Communications, Computers, Engineering, Geography, Geology, Life Sciences, Management, Manufacturing Technology, Mathematics, Medicine, Paleontology, Photography, etc.

The annual subscription to Indian Science Abstracts is Rs 1500/- only.

For further details, **write today:**



Assistant Head  
Marketing and Customer Services Division  
**Indian National Scientific Documentation Centre**  
14-Satsang Vihar Marg, New Delhi 110 067  
Phone: 686 3617, 6560 141 Fax: 686 2228  
E-mail: mcs@sirnetd.ernet.in, mcs@del3.vsnl.net.in

# CURRENT SCIENCE

A fortnightly journal of research

Editors: P. Balaram and S. Ramaseshan

## Editorial Board

- V. H. Arakeri, Departments of Mechanical and Civil Engineering, Indian Institute of Science, Bangalore 560 012
- S. Arunachalam, Department of Humanities and Social Sciences, Indian Institute of Technology, Chennai 600 036
- J. Chandrasekhar, Department of Organic Chemistry, Indian Institute of Science, Bangalore 560 012
- D. Chatterji, Molecular Biophysics Unit, Indian Institute of Science, Bangalore 560 012
- S. G. Dani, School of Mathematics, Tata Institute of Fundamental Research, Mumbai 400 005
- R. Gadagkar, Centre for Ecological Sciences, Indian Institute of Science, Bangalore 560 012
- K. N. Ganeshaiah, Department of Plant Genetics and Breeding, University of Agricultural Sciences, Bangalore 560 065
- V. K. Gaur, Indian Institute of Astrophysics, Bangalore 560 034
- R. M. Godbole, Centre for Theoretical Studies, Indian Institute of Science, Bangalore 560 012
- K. Gopalan, National Geophysical Research Institute, Hyderabad 500 007
- N. V. Joshi, Centre for Ecological Sciences, Indian Institute of Science, Bangalore 560 012
- C. C. Kartha, Division of Cellular and Molecular Cardiology, Sree Chitra Tirunal Institute for Medical Sciences and Technology, Thiruvananthapuram 695 011
- A. V. Khare, Institute of Physics, Bhubaneswar 751 005
- S. S. Krishnamurthy, Department of Inorganic and Physical Chemistry, Indian Institute of Science, Bangalore 560 012
- S. Krishnaswami, Physical Research Laboratory, Ahmedabad 380 009
- S. C. Lakhotia, Department of Zoology, Banaras Hindu University, Varanasi 221 005
- K. Muralidhar, Department of Zoology, University of Delhi, Delhi 110 007
- R. Nityananda, Raman Research Institute, Bangalore 560 080
- T. J. Pandian, School of Biological Sciences, Madurai Kamaraj University, Madurai 625 021
- G. Prathap, Structures Division, National Aerospace Laboratories, Bangalore 560 017
- Y. S. Rajan, Confederation of Indian Industry, New Delhi 110 003
- M. Ramakrishnan, 201, Skyline Surabhi Apartments, Banashankari III Stage, Bangalore 560 085
- A. V. Ramani, T. T. K. Pharma Ltd, Bangalore 560 025
- S. Ranganath, Liquid Crystal Laboratory, Raman Research Institute, Bangalore 560 080
- S. Rangarajan, INSAT Master Control Facilities, Hassan 573 201
- P. N. Shankar, Computational and Theoretical Fluid Dynamics Division, National Aerospace Laboratories, Bangalore 560 017
- S. R. Shetye, Physical Oceanography Division, National Institute of Oceanography, Goa 403 004
- V. Siddhartha, No. 51, Bharati Nagar, New Delhi 110 003
- G. Srinivasan, Raman Research Institute, Bangalore 560 080
- R. Srinivasan, Raman Research Institute, Bangalore 560 080
- R. Uma Shaanker, Department of Crop Physiology, University of Agricultural Sciences, Bangalore 560 065
- K. S. Valdiya, Jawaharlal Nehru Centre for Advanced Scientific Research, Bangalore 560 064
- M. Vidyasagar, Centre for Artificial Intelligence and Robotics, Bangalore 560 001

## Subscriptions effective January 1999

|                                | Personal | Institutions | Industries/<br>Corporate |
|--------------------------------|----------|--------------|--------------------------|
| India (one year)               | Rs 200   | Rs 500       | Rs 700                   |
| India (two years)              | Rs 350   |              |                          |
| SAARC (one year)               | US \$10  | US\$ 30      | US\$ 50                  |
| All other countries (one year) | US \$50  | US \$200     | US\$ 200                 |

(Air Mail)

Single copies other than special issues: Rs 75/US \$15

All overseas addresses are served by Air Mail.

Send subscriptions to: Circulation Department, Indian Academy of Sciences, C. V. Raman Avenue, P.B. 8005, Bangalore 560 080, INDIA (NOT to Current Science). Allow four weeks from subscription realisation for shipments to begin.

Payment method: Demand Drafts or Cheques payable to **Indian Academy of Sciences, Bangalore** (NOT to Current Science).

Cheques drawn in Indian Rupees must be payable on a Bank in India, and must add bank charges of Rupees 15.

**Editorial Office:** CURRENT SCIENCE, C. V. Raman Avenue, P. B. 8001, Bangalore 560 080, India  
Telephone: 91-80-334 2310, Fax: 91-80-334 6094  
email: currsci@ias.ernet.in

Website : <http://tejas.serc.iisc.ernet.in/~currsci/index.html>  
<http://ces.iisc.ernet.in/curscinev>

**Editorial staff:** Chandrika Ramesh, G. Madhavan, Manjuli Maheshwari, C. S. Ravi Kumar, N. Subashini, M. S. Venugopal

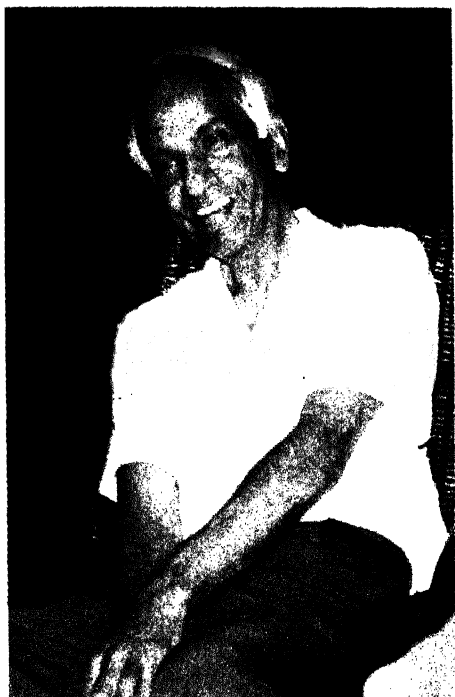
**Circulation and Accounts:** Peter Jayaraj, Ranjini Mohan, B. Sethumani, Shanthi Bhaskar, B. K. Shivaramiah, R. Shyamala

## Working Committee, Current Science Association

- N. Balakrishnan, Indian Institute of Science, Bangalore
- P. Balaram, Indian Institute of Science, Bangalore
- R. Chidambaram, Department of Atomic Energy, Mumbai
- C. M. Gupta, Central Drug Research Institute, Lucknow
- K. Kasturirangan, Department of Space, Bangalore
- N. Kumar, Raman Research Institute, Bangalore (*Vice-President*)
- N. V. Madhusudana, Raman Research Institute, Bangalore (*Secretary*)
- R. A. Mashelkar, Council of Scientific and Industrial Research, New Delhi (*Vice-President*)
- N. Mukunda, Indian Institute of Science, Bangalore
- A. E. Muthunayagam, Department of Ocean Development, New Delhi
- R. Narasimha, National Institute of Advanced Studies, Bangalore
- R. Ramachandran, The Institute of Mathematical Sciences, Chennai
- P. Rama Rao, Atomic Energy Regulatory Board, Mumbai
- S. Ramaseshan, Raman Research Institute, Bangalore (*Treasurer*)
- M. S. Valiathan, Manipal Academy of Higher Education, Manipal (*President*)

*Current Science*, founded in 1932, is published by the Current Science Association in collaboration with the Indian Academy of Sciences. The journal is also intended as a medium for communication and discussion of important issues that concern science and scientific activity. All articles published in *Current Science*, especially editorials, opinions and commentaries, letters and book reviews, are deemed to reflect the individual views of the authors and not the official points of view, either of the Current Science Association or of the Indian Academy of Sciences.

## Chandrasekhar Memorial Issue



### Contents

|  |                      |
|--|----------------------|
| Stars: their structure and evolution   | G. Srinivasan        |
| Neutron Stars before 1967 and my debt to Chandra   | E. E. Salpeter       |
| The Stellar-Dynamical Oeuvre   | James Binney         |
| Radiative Transfer   | George B. Rybicki    |
| The Negative Ion of Hydrogen   | A. R. P. Rau         |
| Chandrasekhar and Magnetohydrodynamics   | E. N. Parker         |
| The Viral Method and the Classical Ellipsoids  | Norman R. Lebovitz   |
| Stability Theory of Relativistic Stars   | John L. Friedman     |
| Making the Transition from Newton to Einstein: Chandrasekhar's Work on the Post-Newtonian Approximation and Radiation Reaction | Bernard F. Schutz    |
| Chandrasekhar, Black Holes and Singularities   | Roger Penrose        |
| Chandra and his Students at Yerkes Observatory   | Donald E. Osterbrock |

THE INDIAN ACADEMY OF SCIENCES has brought out a Special Publication (of the *Journal of Astrophysics and Astronomy*) in honour of the late **Subrahmanyan Chandrasekhar**. In this Memorial Issue several very distinguished physicists and astrophysicists have critically analysed and commented upon Chandra's monumental contributions to many diverse fields.

This volume is approximately 250 pages, includes several photographs, and has been printed using very high quality paper. The cost per volume is a modest Rs 250 (inclusive of postage). The Academy has printed about 200 extra copies of this important publication for sale to individuals on a 'first-come-first-served' basis. If you are interested in purchasing a copy for yourself please contact:

### INDIAN ACADEMY OF SCIENCES

C. V. Raman Avenue  
Post Box No. 8005  
Bangalore 560 080.

FAX: +91-80-334 6094

e-mail: office@ias.ernet.in